AD-A187 016 BEACH EROSION CONTROL STUDY HOMER SPIT ALASKA(U) 1/2
COASTAL ENGINEERING RESEARCH CENTER VICKSBURG MS
Y CHU ET AL SEP 87 CERC-87-15

UNCLASSIFIED F/G 8/3 NL

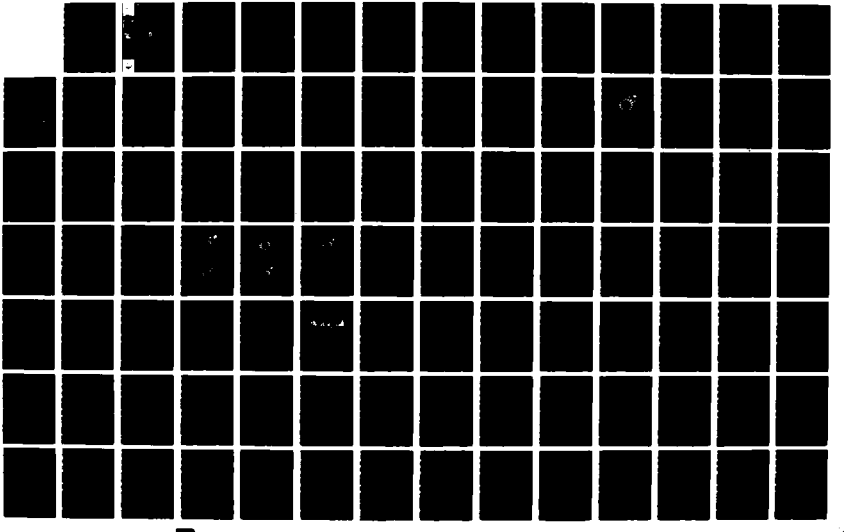

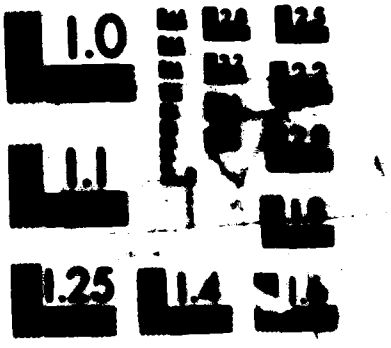

MISCELLANEOUS PAPER CERC-87-15

BEACH EROSION CONTROL STUDY HOMER SPIT, ALASKA

by

Yen-hsi Chu, Mark B. Gravens, Jane M. Smith
Laurel T. Gorman, H. S. Chen

Coastal Engineering Research Center

DEPARTMENT OF THE ARMY
Waterways Experiment Station, Corps of Engineers
PO Box 631, Vicksburg, Mississippi 39180-0631

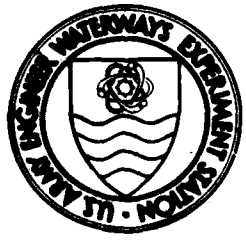

September 1987
Final Report

Prepared for US Army Engineer District, Alaska
PO Box 898, Anchorage, Alaska 99506-0898

Under Intra-Army Order for Reimbursable Services,
No. E86864030

When this report is no longer needed return it to the originator.

The findings in this report are not to be construed as an official Department of the Army position unless so designated by other authorized documents.

The contents of this report are not to be used for advertising, publication, or promotional purposes. Citation of trade names does not constitute an official endorsement or approval of the use of such commercial products.

Unclassified
SECURITY CLASSIFICATION OF THIS PAGE

AD-A187016

REPORT DOCUMENTATION PAGE

Form Approved
OMB No 0704-0188
Exp. Date: Jun 30, 1986

1a. REPORT SECURITY CLASSIFICATION Unclassified	1b. RESTRICTIVE MARKINGS
2a. SECURITY CLASSIFICATION AUTHORITY	3. DISTRIBUTION/AVAILABILITY OF REPORT Approved for public release; distribution unlimited.
2b. DECLASSIFICATION/DOWNGRADING SCHEDULE	
4. PERFORMING ORGANIZATION REPORT NUMBER(S) Miscellaneous Paper CERC-87-15	5. MONITORING ORGANIZATION REPORT NUMBER(S)
6a. NAME OF PERFORMING ORGANIZATION USAEWES, Coastal Engineering Research Center 6b. OFFICE SYMBOL (If applicable)	7a. NAME OF MONITORING ORGANIZATION
6c. ADDRESS (City, State, and ZIP Code) PO Box 631 Vicksburg, MS 39180-0631	7b. ADDRESS (City, State, and ZIP Code)
8a. NAME OF FUNDING/SPONSORING ORGANIZATION See reverse 8b. OFFICE SYMBOL (If applicable) CENPA	9. PROCUREMENT INSTRUMENT IDENTIFICATION NUMBER Intra-Army Order for Reimbursable Services, No. E86864030
8c. ADDRESS (City, State, and ZIP Code) PO Box 898 Anchorage, AK 99506-0898	10. SOURCE OF FUNDING NUMBERS PROGRAM ELEMENT NO. / PROJECT NO. / TASK NO. / WORK UNIT ACCESSION NO.
11. TITLE (Include Security Classification) Beach Erosion Control Study, Homer Spit, Alaska	
12. PERSONAL AUTHOR(S) Chu, Yen-Hsi; Gravens, Mark B.; Smith, Jane M.; Gorman, Laurel T.; Chen, H. S.	
13a. TYPE OF REPORT Final report 13b. TIME COVERED FROM _____ TO _____	14. DATE OF REPORT (Year, Month, Day) September 1987 15. PAGE COUNT 179
16. SUPPLEMENTARY NOTATION Available from National Technical Information Service, 5285 Port Royal Road, Springfield, VA 22161.	

17. COSATI CODES		
FIELD	GROUP	SUB-GROUP

18. SUBJECT TERMS (Continue on reverse if necessary and identify by block number)
Beach erosion
Spits (Geomorphology)
Erosion control
Homer Spit (Alaska)

19. ABSTRACT (Continue on reverse if necessary and identify by block number)

The US Army Engineer Waterways Experiment Station Coastal Engineering Research Center was requested by the US Army Engineer District, Alaska (CENPA) to provide technical assistance in engineering analysis and assessment of various structure alternatives for flood mitigation and erosion control at the southeast coastline of Homer Spit, Alaska. Study elements included are wave climatology and wave transformation analysis, coastal geomorphological study, tidal circulation analysis, shoreline change numerical modeling analysis, and structure elements design. This report details the study and provides final recommendations to CENPA.

Spectrally-based deepwater wave heights, peak periods, and peak directions were calculated from Homer Spit wind distributions based on the usable wind data of February 1965 to February 1986. The deepwater wave statistics were then transformed by applying the Regional

(Continued)

20. DISTRIBUTION/AVAILABILITY OF ABSTRACT ☒ UNCLASSIFIED/UNLIMITED ☐ SAME AS RPT ☐ DTIC USERS	21. ABSTRACT SECURITY CLASSIFICATION Unclassified
22a. NAME OF RESPONSIBLE INDIVIDUAL	22b. TELEPHONE (Include Area Code) / 22c. OFFICE SYMBOL

DD FORM 1473, 84 MAR — 83 APR edition may be used until exhausted. All other editions are obsolete.

SECURITY CLASSIFICATION OF THIS PAGE
Unclassified

8a. NAME OF FUNDING/SPONSORING ORGANIZATION (Continued).

US Army Engineer District, Alaska

19. ABSTRACT (Continued).

Coastal Processes Wave finite difference model to the breaking points near the Spit shoreline as the data base for nearshore sediment transport analysis. The shoreline response to various structure alternatives was analyzed by using the shoreline change model. Five options--including without project, revetment extension, revetment extension with beach fill, beach fill, and offshore breakwater--with various design alternatives were simulated by the modeling study. The final recommendations were formulated based on the model simulation results along with engineering judgments derived from the other study elements of the project.

PREFACE

Authority for the Coastal Engineering Research Center (CERC) of the US Army Engineer Waterways Experiment Station (WES) to conduct this study was granted by the Office, Chief of Engineers. Funding was provided by the US Army Engineer District, Alaska (CENPA), in the form of an Intra-Army Order for Reimbursable Services, No. E86864030, dated 14 May 1986, and subsequent correspondence which extended the 14 May 1986 scope of work.

The study was conducted by an interdisciplinary team of engineers and scientists at CERC in conjunction with cooperative efforts of CENPA staff. Key members of the CERC team, who also authored this report, are as follows: Dr. Yen-hsi Chu, Principal Investigator, Research Hydraulic Engineer, Coastal Design Branch (CW-D), Wave Dynamics Division (CW); Ms. Jane M. Smith, Hydraulic Engineer, and Dr. H. S. Chen, Research Hydraulic Engineer, Coastal Oceanography Branch (CR-O), Research Division (CR); and Ms. Laurel T. Gorman, Physical Scientist, and Mr. Mark B. Gravens, Hydraulic Engineer, Coastal Processes Branch (CR-P), CR, CERC. Special recognition is due Dr. Nicholas C. Kraus, Research Physical Scientist, CR, for his effort in reviewing the manuscript and his technical assistance in developing the shoreline change model. The supporting effort of Ms. Karen R. Wood, CW-D, in typing this report is gratefully acknowledged. Technical editing by Ms. Shirley A. J. Hanshaw and drafting support by the staff of the Information Technology Laboratory, WES, are appreciated also.

Cooperative efforts of the following individuals of the CENPA staff are gratefully acknowledged: Messrs. Ted Bales, Carl Stormer, Stanley Brust, and Carlson Davenport, and Ms. Tyare Roelofs. Constructive comments and suggestions throughout this study from Messrs. Harvey N. Smith and Murph O'Brien, Alaska State Department of Transportation and Public Facilities, are gratefully acknowledged as well.

The interdisciplinary team at CERC served under general supervision of Dr. James R. Houston and Mr. Charles C. Calhoun, Jr., Chief and Assistant Chief, CERC, respectively; and under direct supervision of Mr. C. Eugene Chatham, Chief, CW; Dr. Fred E. Camfield, Chief, CW-D; Mr. H. Lee Butler, Chief, CR; Dr. Edward F. Thompson, Chief, CR-O; and Dr. Steven A. Hughes, Chief, CR-P.

During report publication COL Dwayne G. Lee, CE, was Commander and Director of WES. Dr. Robert W. Whalin was Technical Director.

CONTENTS

CONVERSION FACTORS, NON-SI TO SI (METRIC) UNITS OF MEASUREMENT

Non-SI units of measurement used in this report can be converted to SI (metric) units as follows:

Multiply	By	To Obtain
cubic feet per foot	0.0929	cubic metres/metric
cubic yards	0.7646	cubic metres
fathoms	1.8288	metres
feet	0.3048	metres
foot-pounds per second per foot	4.448225	joules per second per metre
miles (US statute)	1.6093	kilometres
yards	0.9144	metres

BEACH EROSION CONTROL STUDY
HOMER SPIT, ALASKA

PART I: INTRODUCTION

1. Homer Spit is a prominent landmark lying immediately southeast of the City of Homer on the Kenai Peninsula in Alaska. The Spit is a narrow peninsula, 100 to 500 yards* wide, extending approximately 4-1/2 miles from northwest to southeast into Kachemak Bay which opens to lower Cook Inlet in south central Alaska. At the tip of the Spit are a small-boat harbor and a city dock that are used for year-round shipping activities. Homer Spit has been intermittently used as a landing by vessels for two centuries, but most heavy development on the outer portion for commercial and recreational activities occurred in the past 25 years. A single two-lane roadway leads from Homer to these developments following the southwestern shore of the Spit.

Background

2. Since its construction in 1927, the inshore half of the two-lane roadway has been a continual source of maintenance problems. Severe storms accompanied by high water levels and wave action have overtopped and washed out stretches of the roadway causing the road to be closed for major repairs on several occasions. Various means, including the installation of groins, revetments, and bulkheads have been attempted to control the erosion at the southwestern beach facing outer Kachemak Bay and to mitigate damages to the roadway during extreme storm events. Results of these efforts have not been satisfactory, and all shoreline structures, except the rubble revetment, have suffered damage of various degrees.

3. The US Army Engineer Waterways Experiment Station Coastal Engineering Research Center (CERC) was authorized by the US Army Engineer District, Alaska (CENPA), in May 1984 to provide technical assistance in identifying the cause of coastal erosion along Homer Spit and to recommend potential long-term

---

* A table of factors for converting non-SI units of measurement to SI (metric) units is presented on page 3.

means of erosion control. The engineering analysis of beach erosion at Homer Spit conducted by CERC (Smith et al. 1985) included:

a. Field data collection and field investigation program.

b. Wind and nearshore wave analysis.

c. Coastal geology and littoral transport analysis.

d. Preliminary engineering plan formulation.

Two variations of protective beach design and an extension of existing rubble revetment were recommended for further evaluation.

Scope

4. During the feasibility study phase, CENPA requested CERC to further refine the engineering analysis and quantitatively assess the various structure alternatives for erosion control. Specifically, the work elements to be performed included:

a. Wave climatology and wave transformation analysis.

b. Coastal geomorphological study.

c. Tidal circulation analysis.

d. Shoreline change numerical modeling analysis.

e. Structure elements design.

This report summarizes study results from each of the above tasks and associated recommendations of the CERC specialists. Detailed descriptions of each task and study results are provided in Appendixes A-F.

PART II: EXISTING CONDITION AND BEACH SURVEYS

5. From August 1984 to August 1986, four beach surveys were conducted at Homer Spit by the Alaska Department of Transportation and by CENPA (Figures 1 and 2). These surveys followed about 60 preselected transects for the purpose of establishing a data base for long-term beach erosion assessment. However, during the interim a preliminary evaluation of the obtained data was performed to assist in formulation of beach erosion protection plans and to assess volumetric profile changes in the vicinity of the sheet-pile seawall, located between midway of beach profile (BP) -49 and BP-50 and BP-46 (Figures 3 and 4*), where severe beach erosion and structural damage had occurred.

6. Table 1 summarizes results of 22 profiles that were analyzed. Changes in cross-sectional areas are shown as "cut" and "fill" that represent, respectively, erosionary and accretionary changes. From August 1984 to August 1985 the southwestern beach generally experienced an accretionary process, while this process was reversed during the 1985-86 period. For the 3.4-mile stretch of shoreline from BP-20 to BP-60 (Figure 1), net erosion during the 1985-86 period was estimated to be 390,000 cu yd compared to a net accretion of 304,000 cu yd during the 1984-85 period. The net result for the 1984-86 period is 86,000 cu yd of erosion, which is a moderate amount in view of the accelerated beach erosion processes which had occurred since the 1964 Alaska earthquake. These numbers also illustrate the large magnitude of year-to-year fluctuations in beach erosion and the dynamic nature of littoral processes at the Spit. Figure 2 shows the variation of accretion/erosion estimates for the 2-year study period along the southwestern shoreline. In general, erosion occurred along the lower half of the Spit near the distal end, while accretion occurred at the upper half near the Spit base. The 2-year survey result is not consistent with the long-term processes discussed in Part V of this report.

7. The nearshore bathymetry (Figures 3 and 4) of the project area was derived from beach survey data. Figures 3 and 4 suggest the presence of standing waves in front of the sheet-pile seawall and rubble revetment. Standing waves are the result of partial reflection of incident wave energy

---

* Contour depths in Figures 3, 4, and 19 are referred to mean lower low water (MLLW).

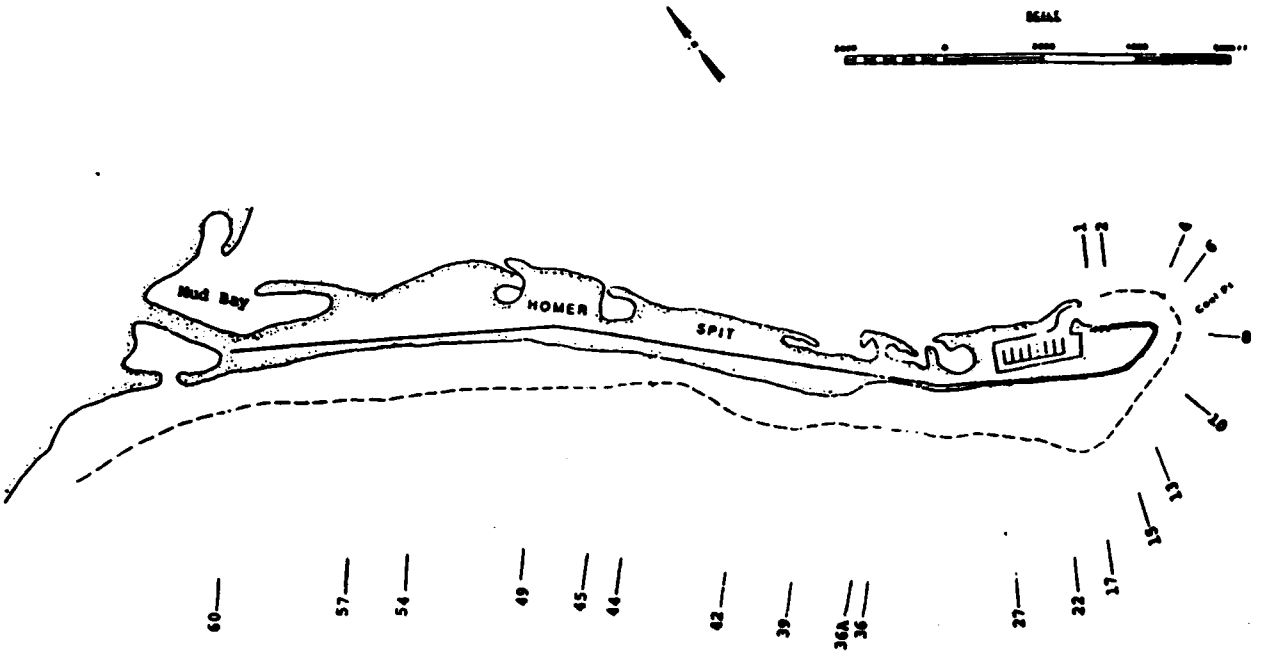

Figure 1. Beach profiling locations for 1984-86 beach surveys, Homer Spit, Alaska

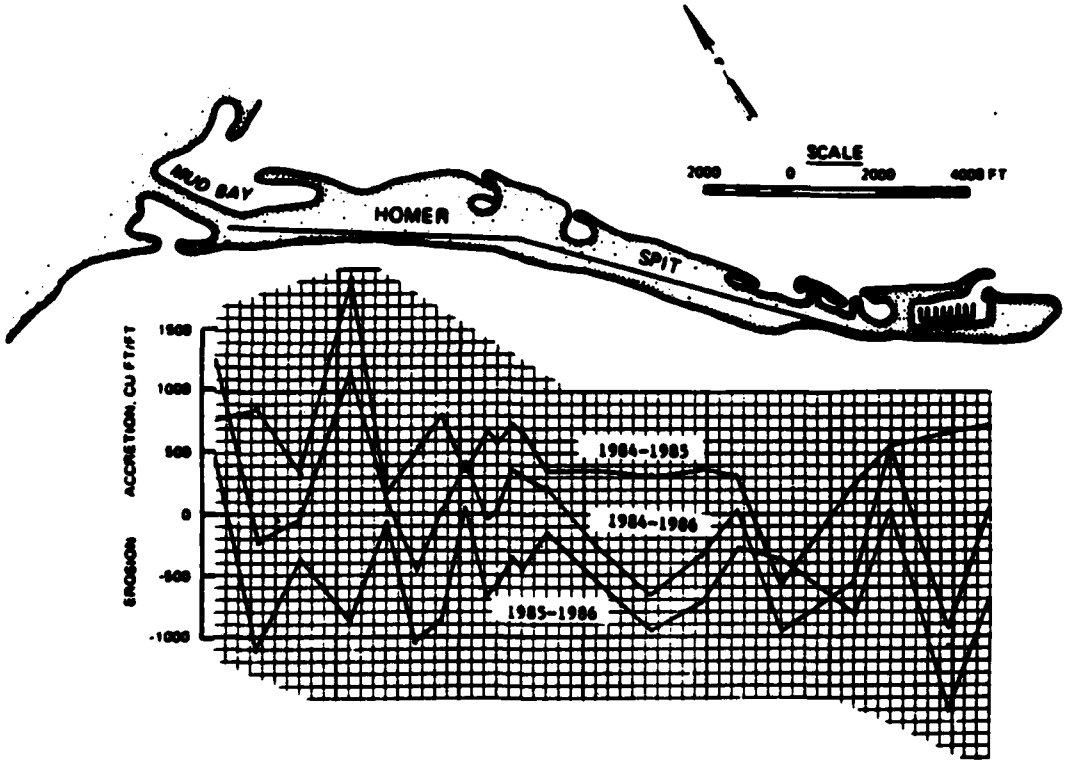

Figure 2. Beach cross-sectional change, 1984-86, Homer Spit, Alaska

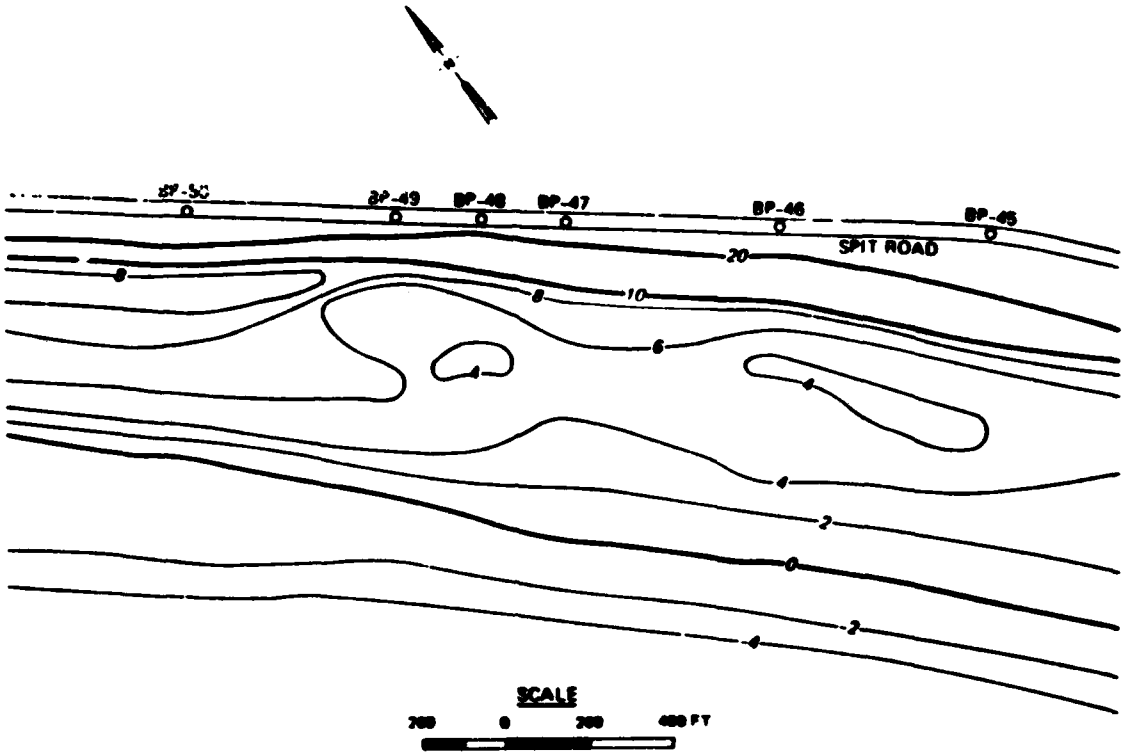

Figure 3. Bathymetry of the project site, August 1985

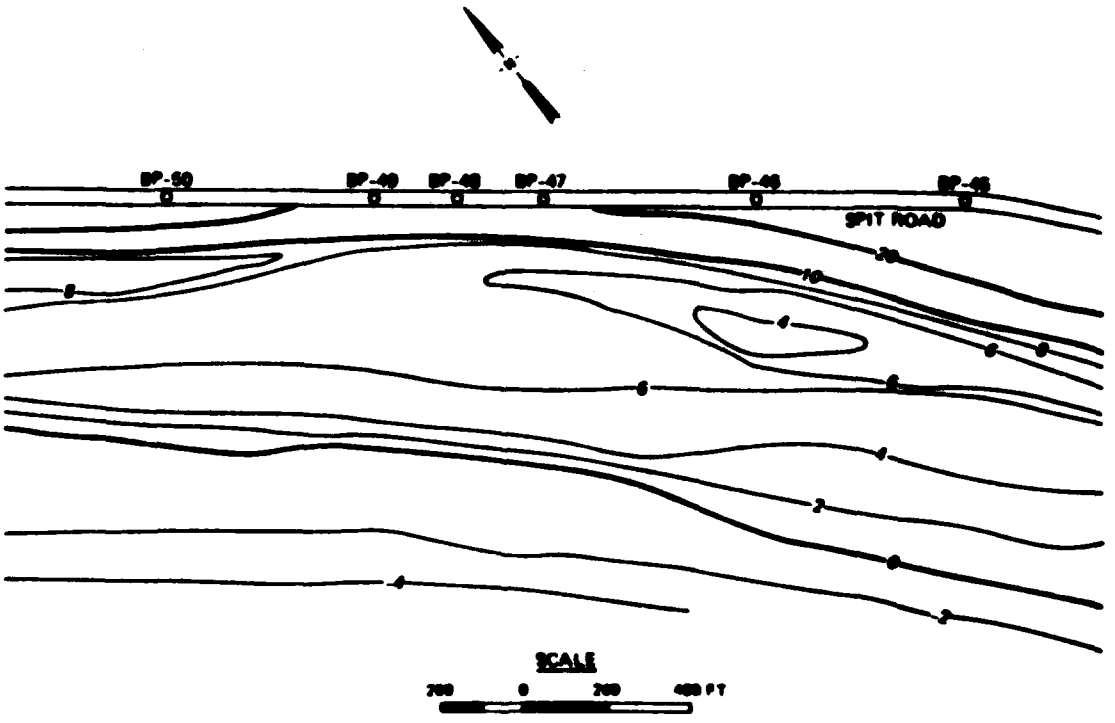

Figure 4. Bathymetry of the project site, August 1986

Table 1

Summary of Beach Profiles Comparison

Profile	Station No.	Quantity, cu ft/ft					
		1984-85		1985-86		1984-86	
		Cut	Fill	Cut	Fill	Cut	Fill
BP-20	13700.6	85	824	1,154	437	757	780
BP-25	14700.6	324	998	1,693	120	1,556	639
BP-31	15721.2	341	917	525	537	523	1,112
BP-34	16721.2	461	708	1,175	348	1,048	468
BP-38	18366.1	1,070	478	700	316	1,412	440
BP-40	19366.1	181	495	686	392	697	718
BP-42	20438.5	122	501	847	133	468	132
BP-43	21597.5	424	736	1,014	59	755	111
BP-44	22797.5	260	624	751	195	516	291
BP-46	23997.5	314	668	402	251	432	635
BP-47	24497.5	270	932	1,203	745	498	788
BP-48	24697.5	439	1,162	1,089	737	443	827
BP-49	24897.5	463	1,059	1,145	574	611	658
BP-50	25397.5	269	954	982	311	332	310
BP-51	25897.5	566	922	515	569	276	674
BP-52	26397.5	339	1,143	1,174	288	263	285
BP-53	26897.5	394	942	1,334	298	715	227
BP-54	27586.2	700	893	765	693	300	422
BP-56	28359.3	406	2,324	1,127	267	79	1,251
BP-58	29539.5	568	895	960	590	360	317
BP-59	30539.6	276	1,160	1,246	135	435	208
BP-60	31539.6	67	852	457	932	195	1,455

Note: All three surveys used for analysis were conducted during August. "Cut" and "Fill" quantities are measured in cubic feet per foot of shore and are interpreted as erosion and accretion, respectively. Calculations of changes for each profile were made from base points to points approximately 1,400-1,800 ft offshore.

caused by the shoreline structures. The resulting higher wave amplitude and water particle velocities in front of the seawall may further aggravate the situation of wave overtopping, roadway flooding, and local scouring of beach material during storm events. Minimizing the standing wave amplitude and occurrence at the project area by promoting wave breaking and reducing wave reflection appears to be a logical engineering solution to the present problem at the Spit.

PART III: TIDES AND CURRENTS

8. Astronomical tides at the Kachemak Bay area are semidiurnal having a pronounced diurnal inequality. Observed and estimated tidal elevations at Homer Spit are:

Tide Level	Elevation, ft
Estimated Extreme High Water	23.3
Mean Higher High Water	18.1
Mean High Water	17.3
Mean Tide Level	9.5
Mean Low Water	1.6
MLLW	0.0 (datum)
Estimated Extreme Low Water	-5.5

9. A numerical simulation of water elevations and tidal currents of Kachemak Bay, with special attention to the water along the southwest coast of the Spit, was conducted under the present study program, including a multilayer finite element mathematical model based on the mass and momentum conservation equations. The four-layer finite element mesh system for Kachemak Bay, containing 637 elements and 409 nodes, is shown in Figure 5. In shallow water, such as along the southwestern shoreline of the Spit, the model is limited to only one layer. A lumped finite element technique using the Galerkin weighted residual formulation is employed for numerical solutions. The task of simulation was contracted to the University of Mississippi and was closely supervised by CERC specialists.

10. The simulated maximum ebb- and flood-tidal circulations for a tidal range of 26 ft are shown in Figures 6 and 7. These results clearly exhibit the longshore currents existing along the Homer Spit coastline. Figure 8 shows the tidal elevation and current pattern at the project location where the maximum ebb current was 0.61 fps and maximum flood current 0.86 fps. At the tip of the Spit, the maximum ebb-tidal current was 1.65 fps, and the maximum flood current 1.78 fps. The maximum currents were found to be lowered proportionally at lower tidal ranges. At Homer Spit, the mean tidal range is 15.7 ft, and the diurnal range is 18.1 ft.

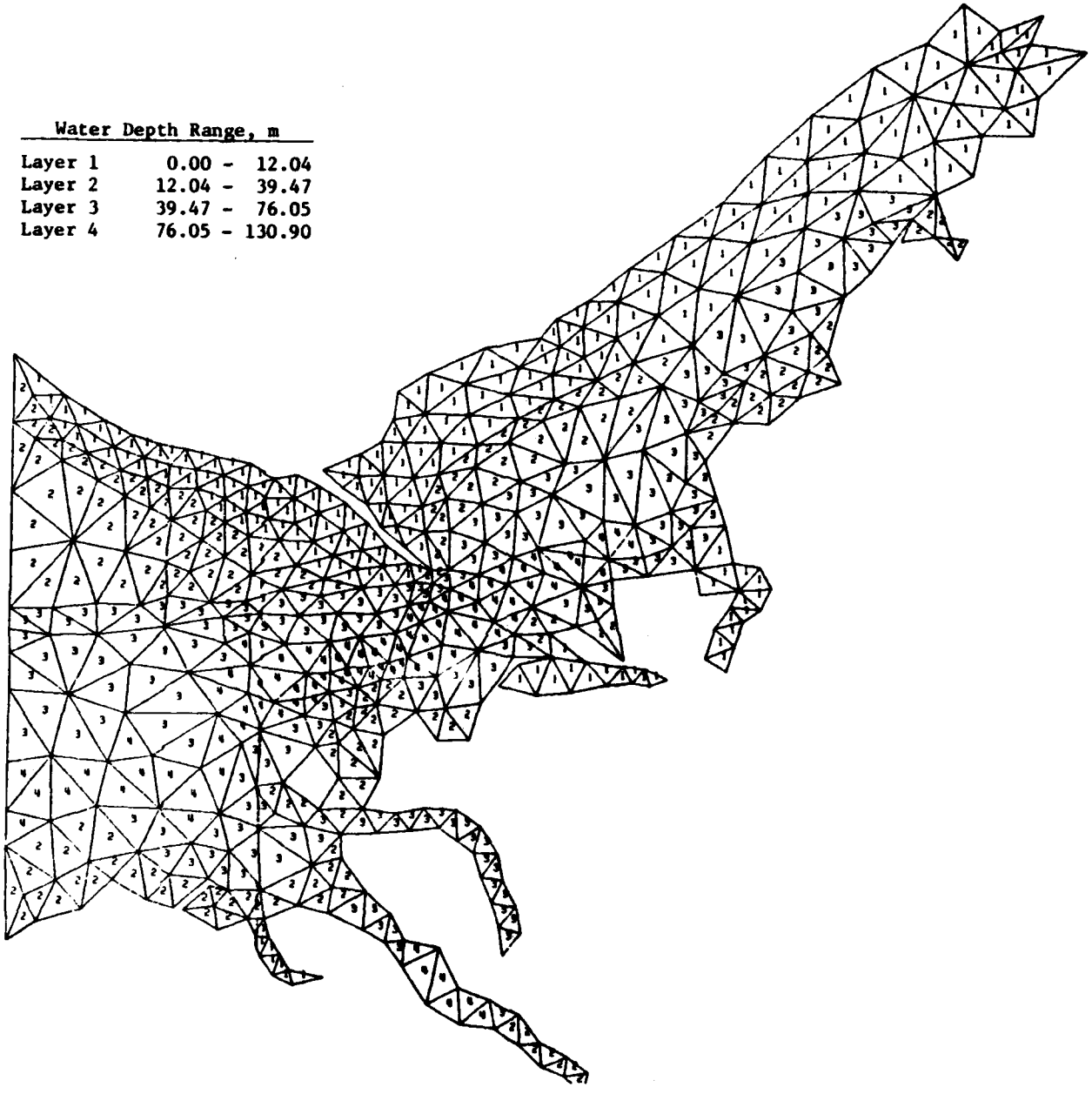

Figure 5. Finite element mesh system for Kachemak Bay model

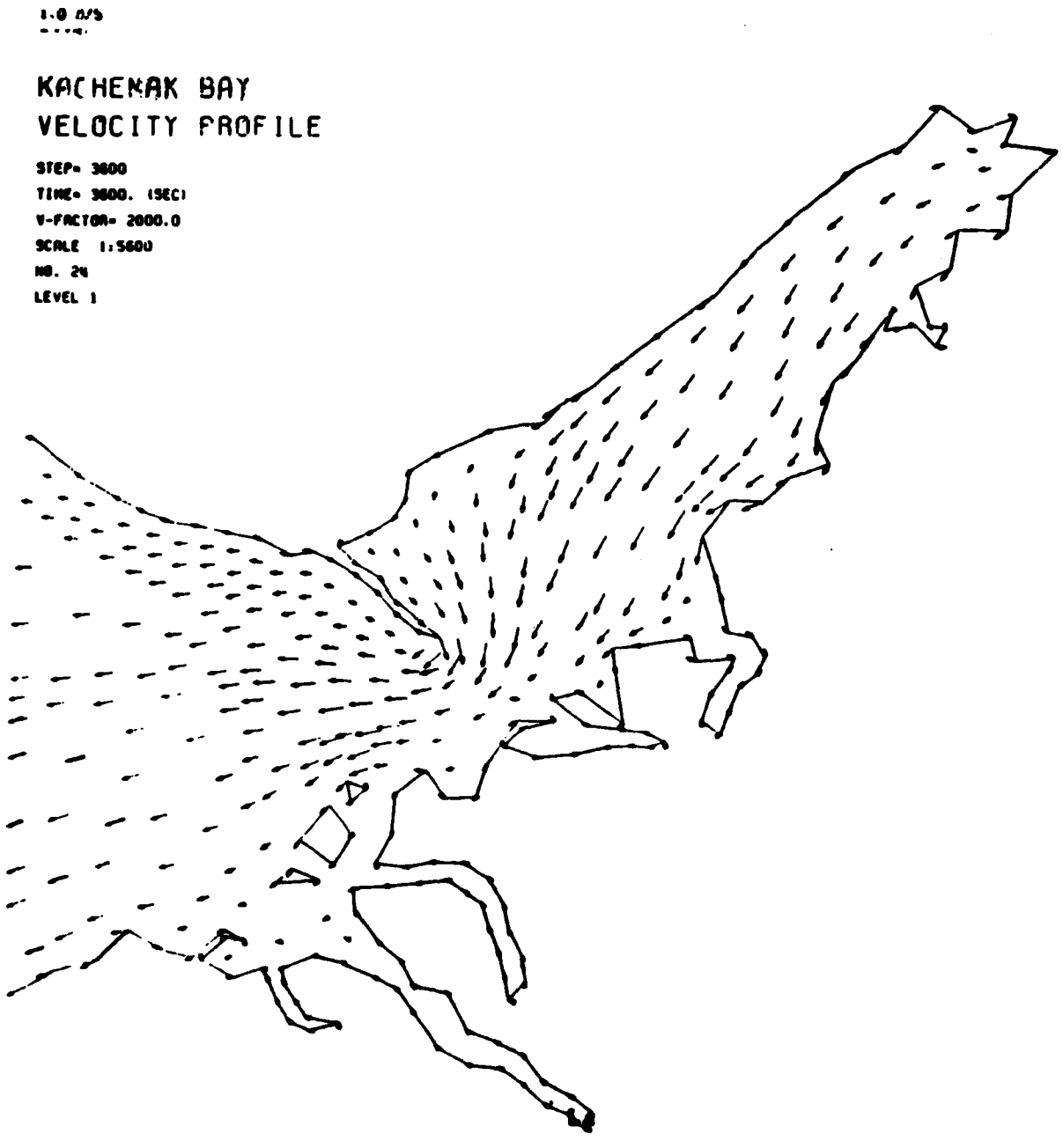

Figure 6. Ebb-tidal circulation in layer 1, tidal range = 7.9 m

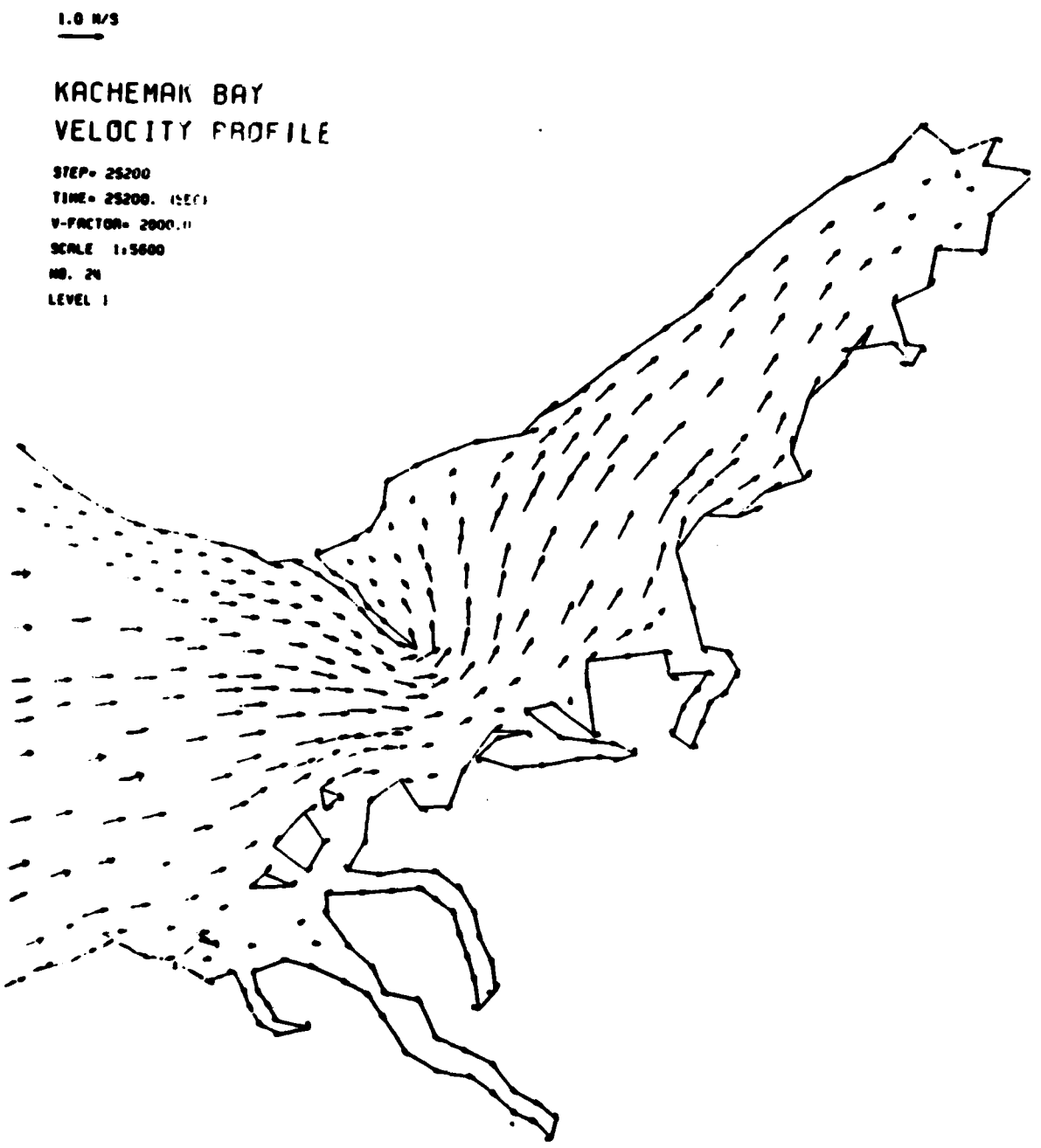

Figure 7. Flood-tidal circulation in layer 1, tidal range = 7.9 m

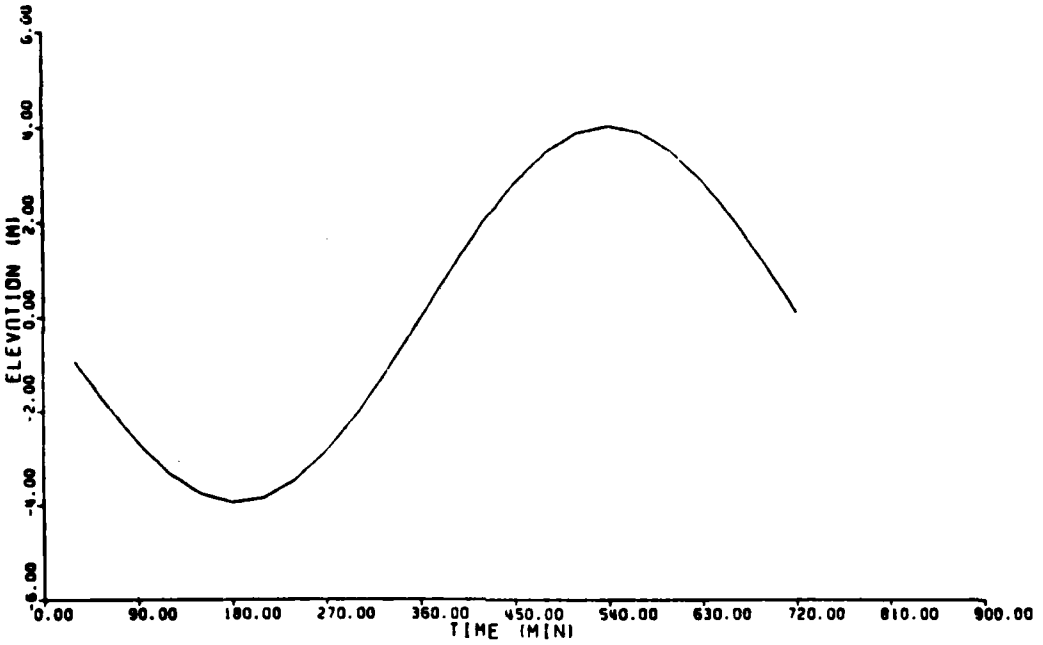

KACHEMAK BAY

a. Tidal elevation

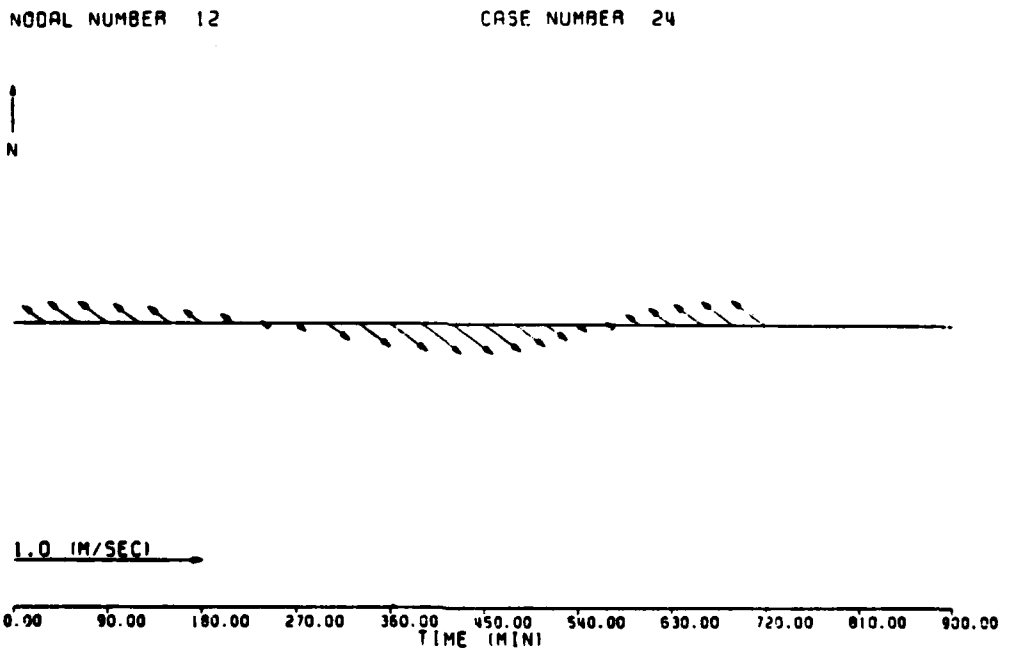

KACHEMAK BAY VELOCITY VECTORS

NODAL NUMBER 12 CASE NUMBER 24

b. Current pattern

Figure 8. Tidal elevation and velocity at node 12, tidal range = 7.9 m

PART IV: WAVE CLIMATOLOGY

Wind Data Analysis

11. Because of the lack of a long-term wave record at the project area, a hindcast of deepwater waves based on local wind data was the only alternative means to generate information on wave climate at Kachemak Bay near the Spit. During the reconnaissance level study, wind records measured by anemometers at the harbor master's office near the tip of the Spit, and at Homer Airport, were used for wave hindcasting. Further study found that the quality of airport data was inferior to that of Spit data with respect to use in wave hindcasting. The Spit wind data, therefore, were used for the present feasibility level study. The adjusted hourly wind speed and direction distribution are shown in Figure 9.

Deepwater Wave Hindcast

12. Spectrally-based deepwater wave heights, peak periods, and peak directions were calculated from Homer Spit wind distribution based on 6-hr wind averages using the fetch-limited Joint North Sea Wave Project equation from the Shore Protection Manual (1984). Table 2 presents the deepwater wave statistics in terms of cumulative probabilities for various wave height and period categories. The assumption of wind homogeneity over the entire water body covering outer Kachemak Bay for wave hindcasting could result in overestimation of local wave heights near the Spit since the winds well offshore from the Spit are generally not blowing toward it. Measured wave data from Kachemak Bay (59° 36.36' N, 151° 32.39' W) and concurrent wind data from the Spit anemometer for July 1984 through February 1986 were used to assess the validity of the applied hindcast technique. Wave heights were calculated from the 6-hr averaged wind data and then compared to the measured wave data (Figure 10). It was concluded that the present methodology and the concept of locally generated waves at the project area are reasonable. Long-period swells from remote sources may reach the Spit. However, the energy content and the statistical significance associated with the long-period swells are believed to be negligible.

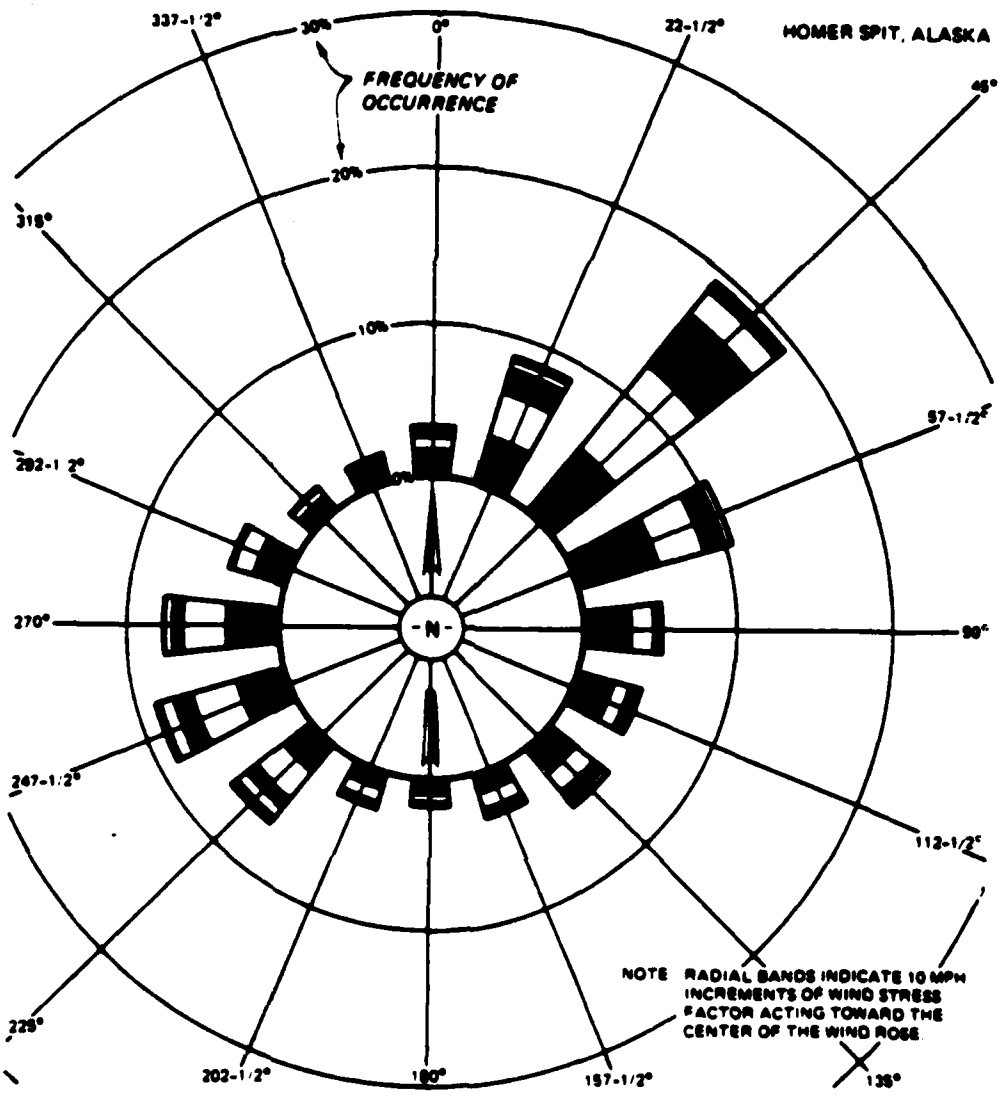

Figure 9. Wind rose for Homer Spit anemometer

Wave Transformation Analysis

13. The Regional Coastal Processes Wave (RCPWAVE) model (Ebersole, Cialone, and Prater 1986) was used to transform the hindcast deepwater waves over the outer Kachemak Bay bathymetry to breaking points near the Spit shoreline. The model employs an iterative, finite difference scheme including full refraction and diffraction effects produced by the sea bottom. Two types of results were obtained from the wave transformation analysis. A potential longshore sediment transport rate (Figure 11) was calculated by using the breaking wave data (height and breaking angle). Figure 11 exhibits the

Table 2

Deepwater Wave Statistics Versus Cumulative Probabilities

Wind Stress Factor, mph	Wave Height ft	Wave Period sec	Cumulative Probabilities occurrence per year
	Wave angle = -35.5 deg (relative to grid x-axis)		
2.5	0.10	0.93	0.1008
7.5	0.91	2.78	0.0833
12.5	2.54	4.63	0.0535
17.5	4.64	6.19	0.0306
22.5	5.97	6.73	0.0183
27.5	7.30	7.27	0.0136
32.5	8.62	7.61	0.0085
37.5	9.95	7.98	0.0055
42.5	11.28	8.32	0.0036
47.5	12.60	8.64	0.0020
52.5	13.93	8.93	0.00095
57.5	15.26	9.21	0.00014
	Wave angle = -58.0 deg (relative to grid x-axis)		
2.5	0.10	0.93	0.0559
7.5	0.91	2.78	0.0424
12.5	2.54	4.63	0.0244
17.5	4.14	5.74	0.0121
22.5	5.33	6.24	0.0057
27.5	6.51	6.67	0.0034
32.5	7.70	7.06	0.0023
37.5	8.88	7.40	0.0011
42.5	10.06	7.72	0.00085
47.5	11.25	8.01	0.00071
52.5	12.43	8.28	0.00043
57.5	13.62	8.53	0.00030
	Wave angle = -69.25 deg (relative to the grid x-axis)		
2.5	0.10	0.93	0.0267
7.5	0.91	2.78	0.0189
12.5	2.54	4.63	0.0091
17.5	3.60	5.23	0.0054
22.5	4.63	5.68	0.0025
27.5	5.66	6.08	0.0014
32.5	6.69	6.42	0.00081
37.5	7.71	6.74	0.00054
42.5	8.74	7.03	0.00013

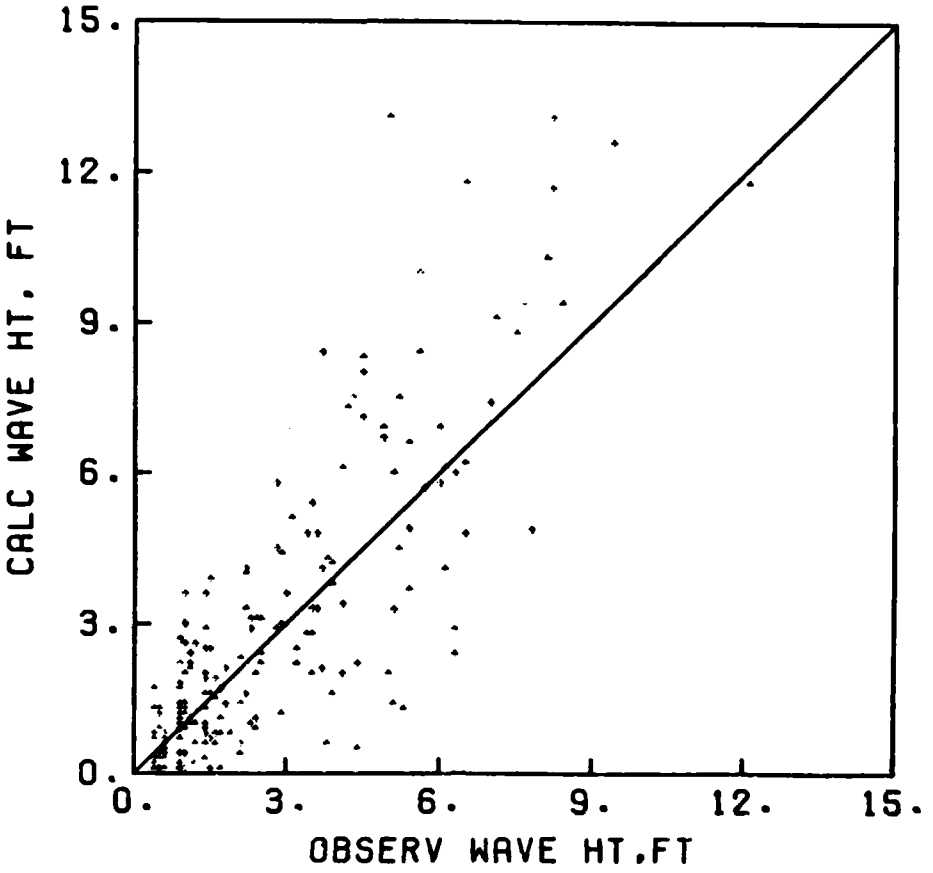

Figure 10. Comparison of calculated wave heights versus observed wave heights at Kachemak Bay off Homer Spit, Alaska

characteristics of longshore wave energy flux and potential sediment transport rates along the shoreline from Bluff Point, Alaska, to the tip of Homer Spit. The transport directions are predominantly from northwest to southeast with only minor direction reversals. Also, a representative 1-year time series of nearshore wave conditions was assembled and later used as input to the shoreline change model to assess the performance of various structure alternatives.

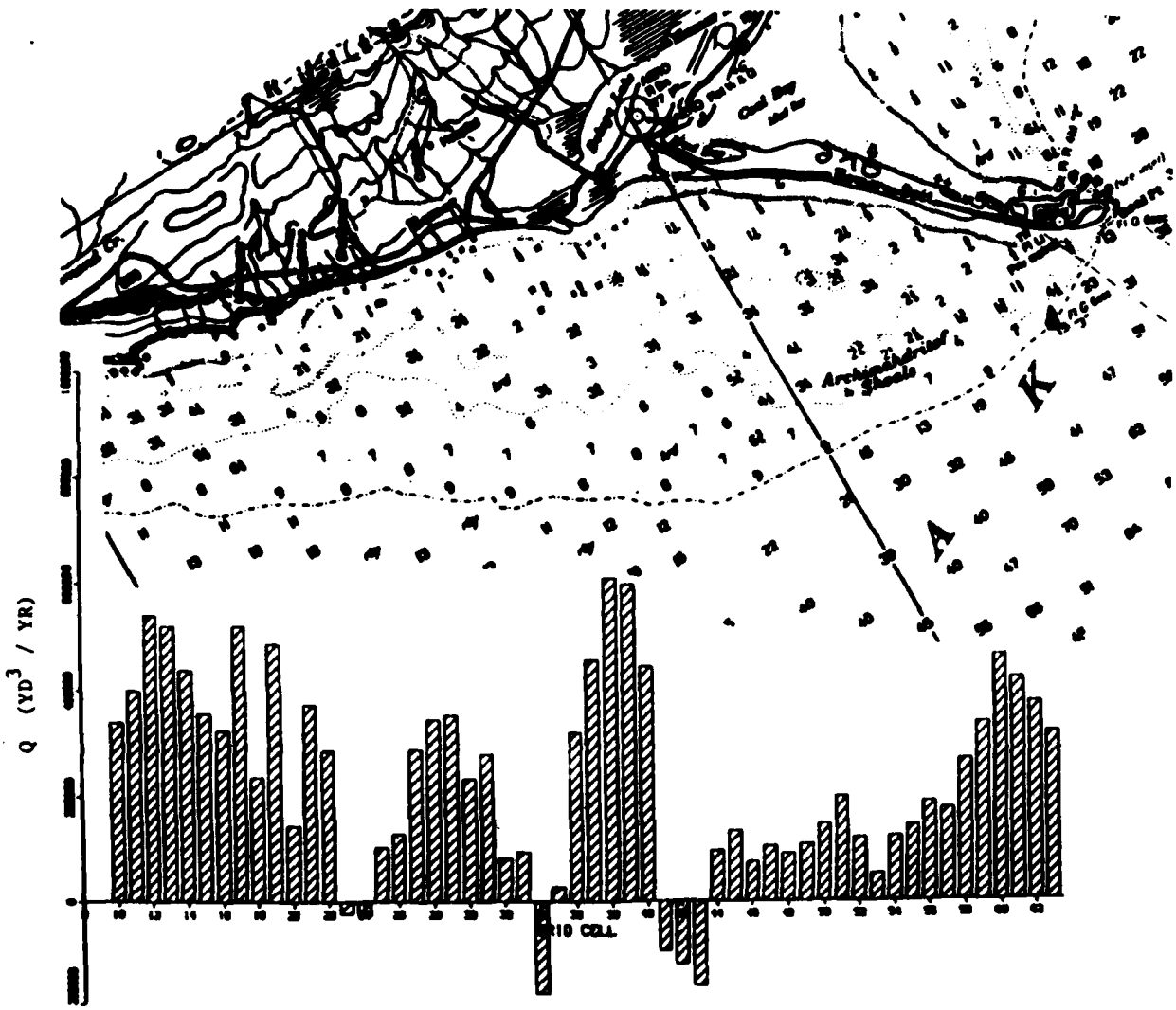

Figure 11. Potential longshore sediment transport rate

PART V: GEOMORPHOLOGICAL ANALYSIS

14. Shoreline trends were analyzed using four historical and recent maps that date from 1918 through 1985. The shoreline data were evaluated as two separate data bases which include the pre-1964 earthquake shorelines of 1918 and 1961 and the post-1964 earthquake shorelines of 1968 and 1985. Several other maps of Homer Spit were not included in the data bases because of a lack of reference points or questionable data accuracy. These shoreline data were digitized and formatted into a Cartesian coordinate system, and shoreline positions were recorded at 100-ft intervals along the southwestern shoreline of the Spit. Figures 12 and 13 show the average shoreline movement for 1918-61 and 1968-85, respectively. Both figures show that beach erosion and shoreline recession occurred at the project area before and after the 1964 Alaska earthquake. Between BP-9 and BP-60 (Figure 1) the net recession is 0.7 ft/year for 1918-61 and 7.7 ft/year for 1968-85, a more than ten-fold increase at the project area after the earthquake. The effects of this earthquake on morphodynamic processes have been discussed and documented by Waller (1966), Stanley (1966), Woodward-Clyde (1980), Nottingham, Drage, and Gilman (1982), and Gronewald and Duncan (1965). The pre-earthquake shoreline was relatively stable. The following tabulation compares shoreline movement pre- and post-1964 by the mean rate in ft/year calculated for four segments.

Segment	Mean rate, ft/year 1918-61	1968-85
Northwest of BP-60	+1.8	-11.8
BP-50 to BP-60	-0.7	-19.2
BP-38 to BP-50	-0.8	-7.4
BP-9 to BP-38	+1.1	+2.7

Positive rates indicated above imply shoreline advance; whereas negative values imply shoreline recession.

15. The accelerated beach erosion and shoreline recession experienced at the Spit can be attributed also to the two tidal inlets northwest from BP-60. The opening at the entrance to Beluga Lake has a deltaic feature covered with boulders and cobbles that is believed to trap sediment and prevent littoral drift from nourishing the downdrift beaches along the main body of the Spit. The second inlet feature, located immediately north of BP-60, is

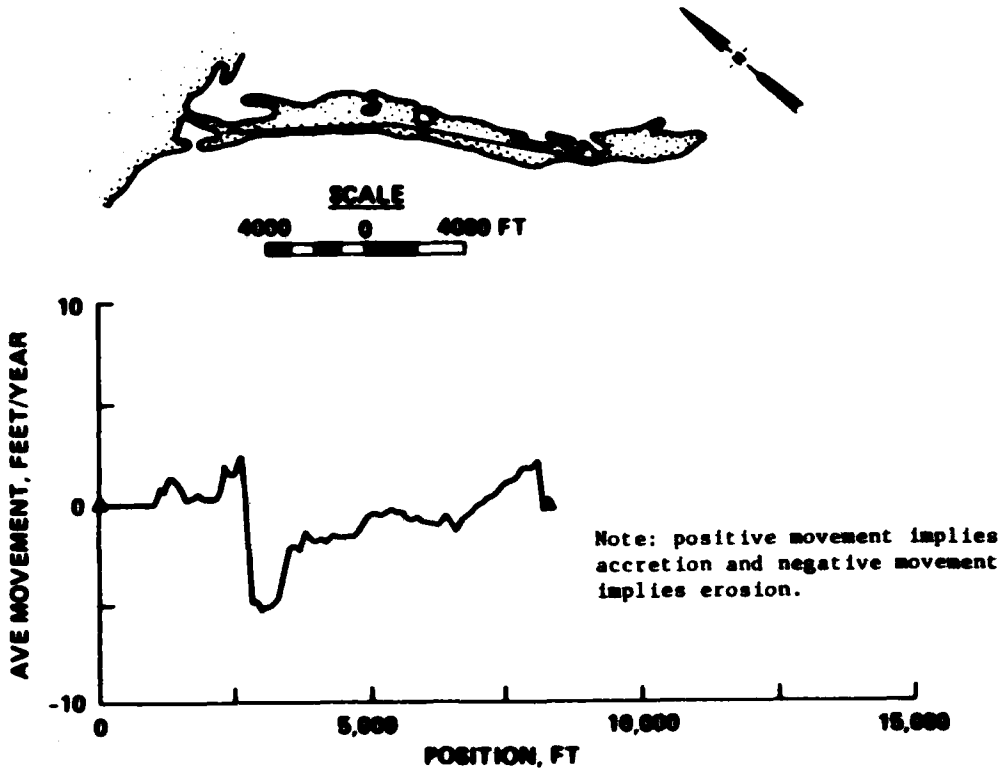

Figure 12. Shoreline movement, 1918-61, Homer Spit, Alaska

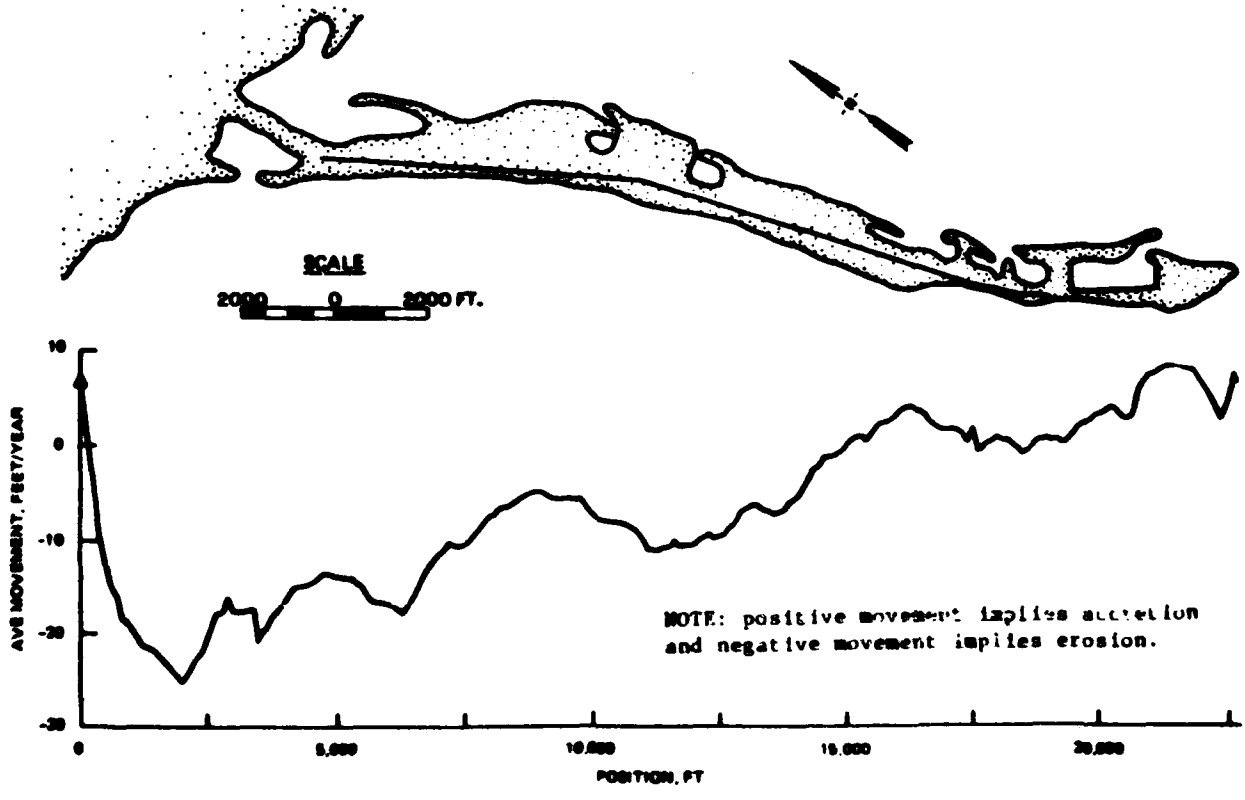

Figure 13. Shoreline movement, 1968-85, Homer Spit, Alaska

also a sediment sink where sand and silt are migrating into the tidal entrance.

PART VI: EVALUATION OF EROSION CONTROL ALTERNATIVES

Shoreline Change Model

16. A numerical shoreline change model was used to evaluate the relative merits of alternative plans for erosion control and storm damage reduction. The model was a modified version of the GENEralized model for SImulating Shoreline change (GENESIS) recently developed at CERC. The modification involved incorporation of a method of simulating the large tidal range and the observed variability in mean sediment grain size with depth along the beach profile. GENESIS is an integrated set of computer programs prepared to calculate wave refraction and diffraction under simplified conditions (breaking wave height and direction, longshore sediment transport rates, and shoreline changes). The shoreline change portion of GENESIS is classified as a one-line model in which it is assumed that beach contours remain parallel over the simulation period. Therefore, one contour or one line, if taken as the shoreline, can be used to characterize beach planform change. The fundamental assumptions of the one-line model are:

a. Nearshore bottom contours move in parallel.

b. A depth of closure exists beyond which longshore sediment transport is insignificant.

c. The volume of beach material is conserved.

d. Longshore sediment transport is dominated by wave action.

Grid and Model Boundary

17. Calculation of the shoreline position was accomplished through discretization of the sediment conservation equation. The longshore axis was set parallel to the trend of the southwest shoreline of Homer Spit and denoted as the "x-axis." The axis orthogonal to the longshore axis, pointing positive offshore, was denoted as the "y-axis." The longshore grid spacing in GENESIS was set at 200 ft, and the grid was extended beyond the project area on both sides to obtain termination points that would provide appropriate boundary conditions. The southeast model boundary was placed midway between BP-34 and BP-36 (Figure 14), and the northwest boundary was placed at the base of the Spit, off Beluga lake.

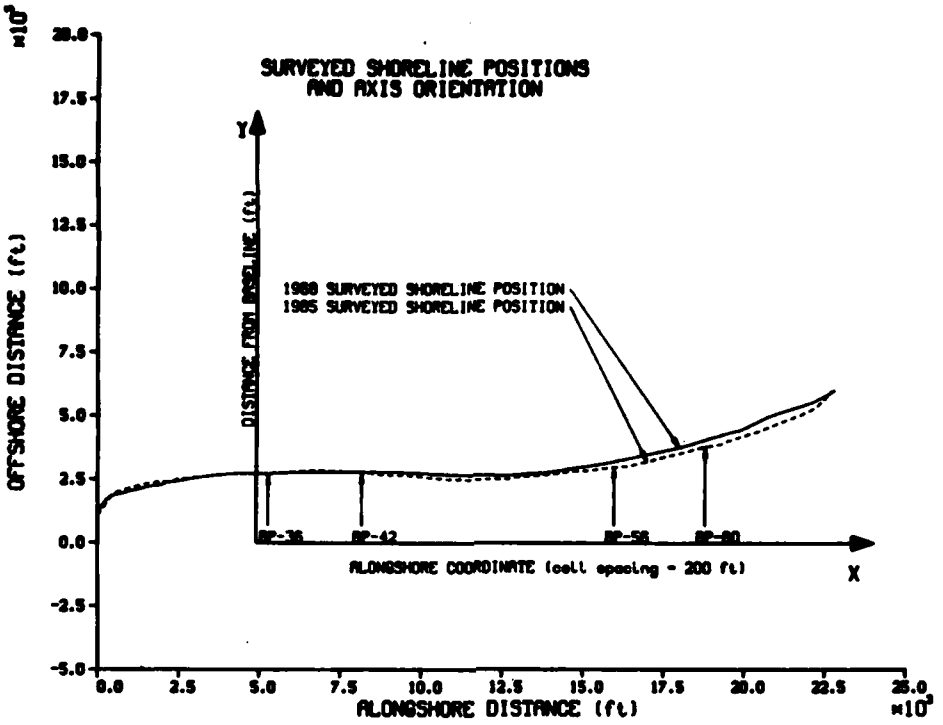

Figure 14. Shoreline positions and model boundary

Representative Wave Conditions

18. The input wave data used in GENESIS was obtained from the hindcast wave record. Although wind data were available for approximately 11 years, the longest continuous record was only 7 months. Therefore, a representative 1-year time series of wave conditions at 6-hr intervals was assembled from the available data. Comparison between the selected and the available wave data were made with seasonally averaged wave height as follows:

	Average Wave Height, ft	
Time Period	Available Data	Selected Data
Winter	0.46	0.51
Spring	0.99	1.17
Summer	0.96	0.66
Fall	0.57	0.42
One Year	0.72	0.69

In the above tabulation, winter months include December, January, and February; spring months include March, April, and May; summer months include June, July, and August; and fall months include September, October, and November.

It is believed that the selected 1-year time series adequately represents the wave climate at Homer Spit based on examination of available data.

Alternative Selected for Erosion Control

19. A total of five alternative options (some options including several variations) was analyzed using the shoreline change model. The options simulated were:

a. Without-project.

b. Revetment extension.

c. Revetment extension with beach fill.

d. Beach fill.

e. Offshore breakwater.

20. The without-project option represents existing conditions at Homer Spit and corresponds to shoreline change, that is, assuming no remedial actions for erosion control and shoreline protection are taken. The revetment extension option was executed to examine the effect of extending the existing revetment 2,000 ft longshore toward the tip of the Spit. Several variations of beach fill, by varying fill locations and volume of the borrow material, were considered along with the revetment extension in the third option. The variations of beach fill without revetment extension were studied in the fourth option. For options requiring beach fill, renourishment was assumed for all the alternatives at the end of the fifth year. The final option studied the shoreline responses to several arrangements of segmented offshore breakwaters at the problem area.

21. A total of 19 alternative erosion control measures was modeled and studied. One best alternative from each of the general design options was selected for the comparative study. A plot of the shoreline positions for each of the selected alternatives at the end of simulated 5- and 10-year intervals is given in Figures 15 and 16. Three of the alternatives shown indicate considerable erosion both at the 5- and 10-year intervals and are not recommended for implementation. These alternatives are the without-project option, the revetment extension option, and the offshore breakwater option. The remaining two alternatives are the revetment extension with beach-fill option and the beach-fill option. Model results clearly indicate that nourishment of the existing beach is required to control the coastal erosion

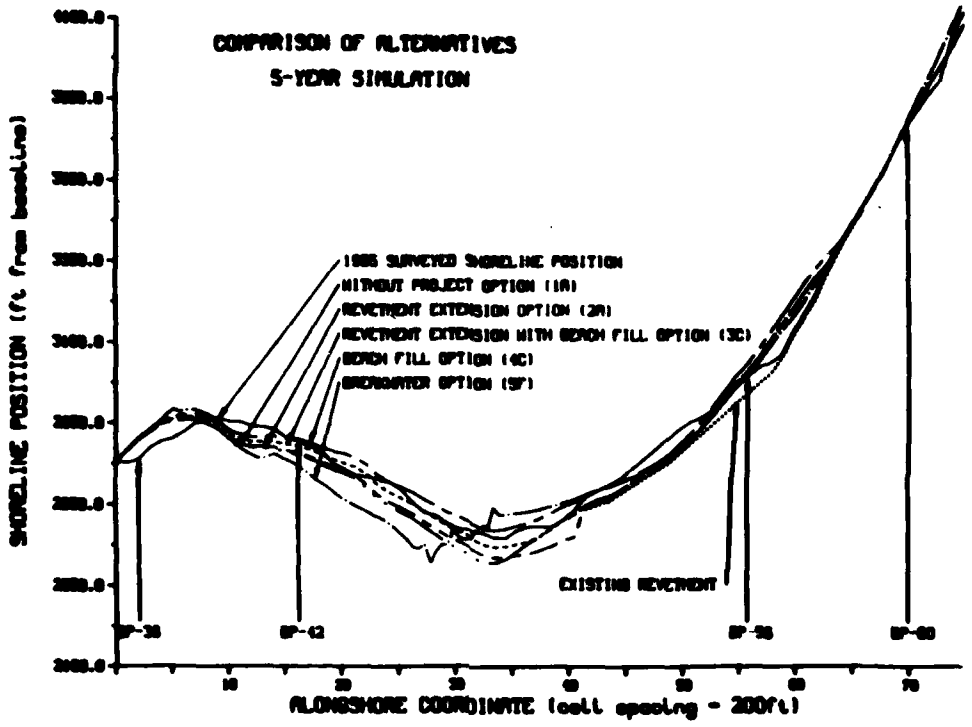

Figure 15. Comparison of alternatives after 5-year simulation

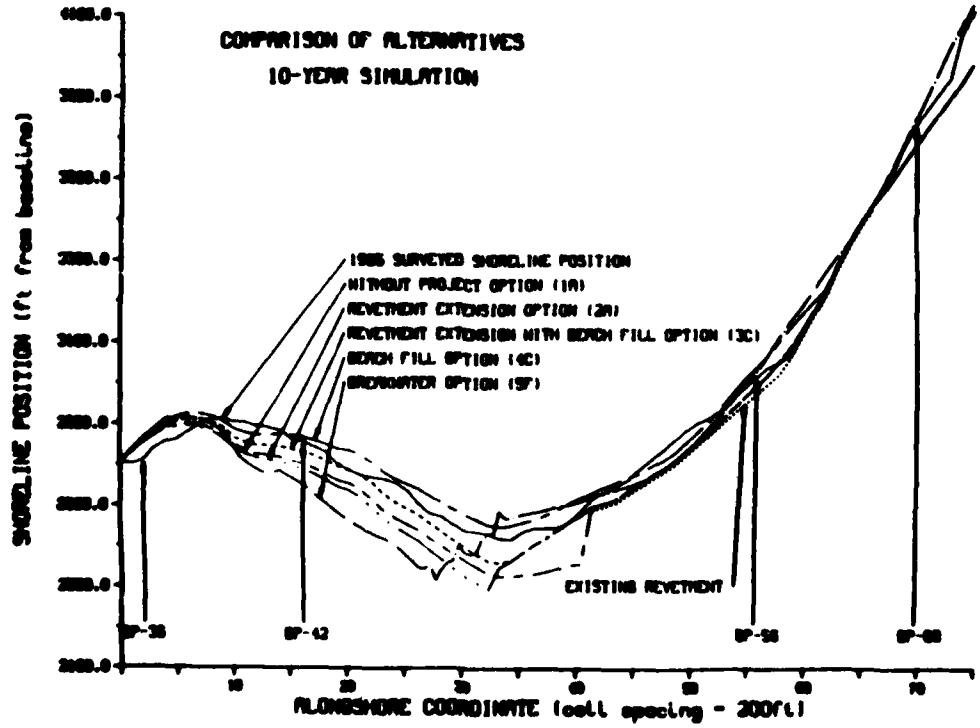

Figure 16. Comparison of alternatives after 10-year simulation

problem at Homer Spit. Since revetment extension is required to protect the roadway during periods of high tide and storms, beach fill, along with extended revetment, is considered as the most effective means for erosion control and storm damage reduction at the project area.

PART VII: ENGINEERING DESIGN AND ANALYSIS

Revetment Design

22. A rubble revetment at the front of the existing sheet-pile seawall is a necessary feature to protect the roadway from flooding and to protect the sheet-pile seawall. With the assumption that the beach fill will raise the beach elevation at the revetment to 16.0 ft MLLW, a depth-limited breaking wave height of 9.6 ft was used to determine the size of armor stone unit. Figure 17* shows the structural arrangement of the revetment which extends 1,100 ft from the existing revetment toward the tip of the Spit to protect the reach of roadway where severe flooding has occurred in the past.

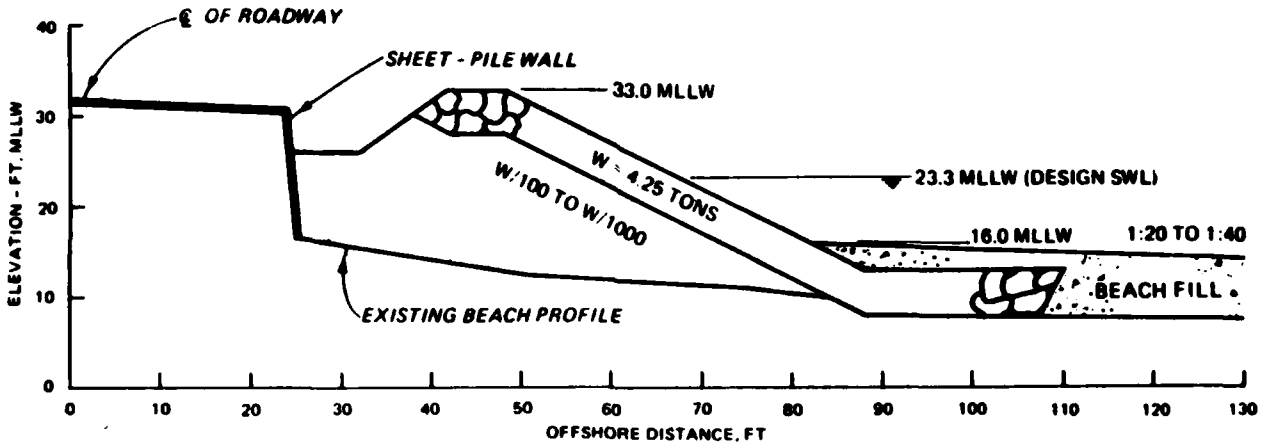

Figure 17. Beach fill and revetment design at BP-48, Homer Spit, Alaska (swl = still-water level)

Beach-Fill Engineering

23. Alternative 3C (see Figures 15 and 16), conducted by the shoreline change model simulation study, is the basic plan recommended for engineering design. It requires that 150,000 cu yd of borrow material be placed in front of the existing seawall and the recommended revetment. It is understood that the more fill material applied at the beach the better the shoreline stability. Selection of alternative 3C is based on the assumption that erosion

---

* All elevations cited herein are given relative to MLLW.

at the project area has slowed in recent years, and an extensive fill as suggested in alternative 4C may not be needed. If this assumption is proven false, then more material may be placed later in the renourishment period. The borrow material should be placed approximately 500 ft offshore or to an elevation of 5 ft MLLW, as shown in Figure 18. Figure 19 shows the bathymetry at the project area after the beach fill (which can be compared to Figures 3 and 4 showing bathymetries before the beach fill). Model simulation assumes the borrow material has the same gradation distribution characteristics of the native material. It was concluded that a 5-year renourishment of the project beach is needed. If the borrow material is more stable than the native beach material, the renourishment period may be increased. Four alternative borrow sites--Martin River, Anchor Point, Archimandritof Shoals, and Beluga Shoals--were considered for renourishment analysis. Results are summarized in the following tabulation:

Site	D_{50}, mm	Renourishment Factor	Renourishment Period, years
Homer Spit	4.1	1.00	5
Martin River	9.5	0.45	11
Anchor Point	5.0	0.53	9
Archimandritof Shoals	4.0	0.80	7
Beluga Shoals	5.7	0.56	9

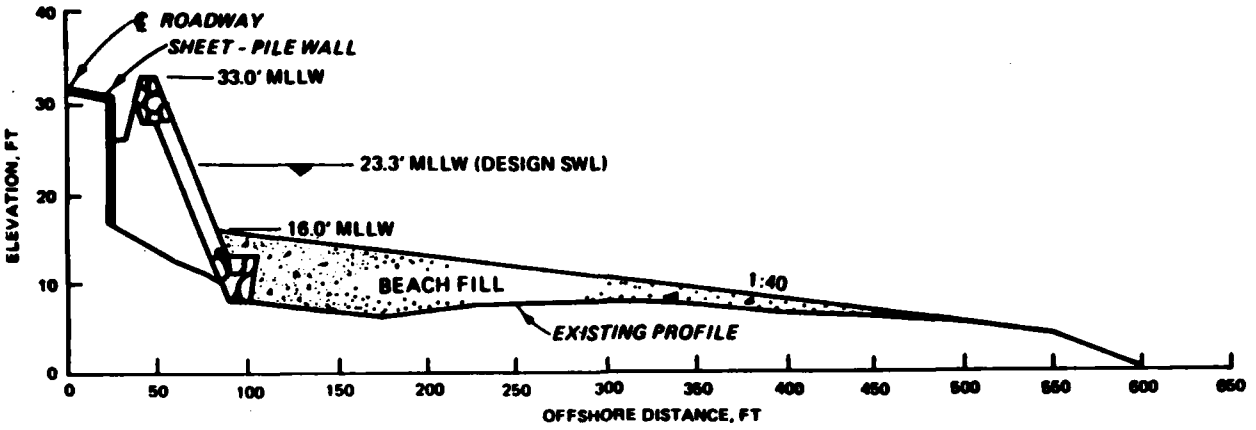

Figure 18. Cross-sectional beach profile at BP-48 after beach fill, Homer Spit, Alaska

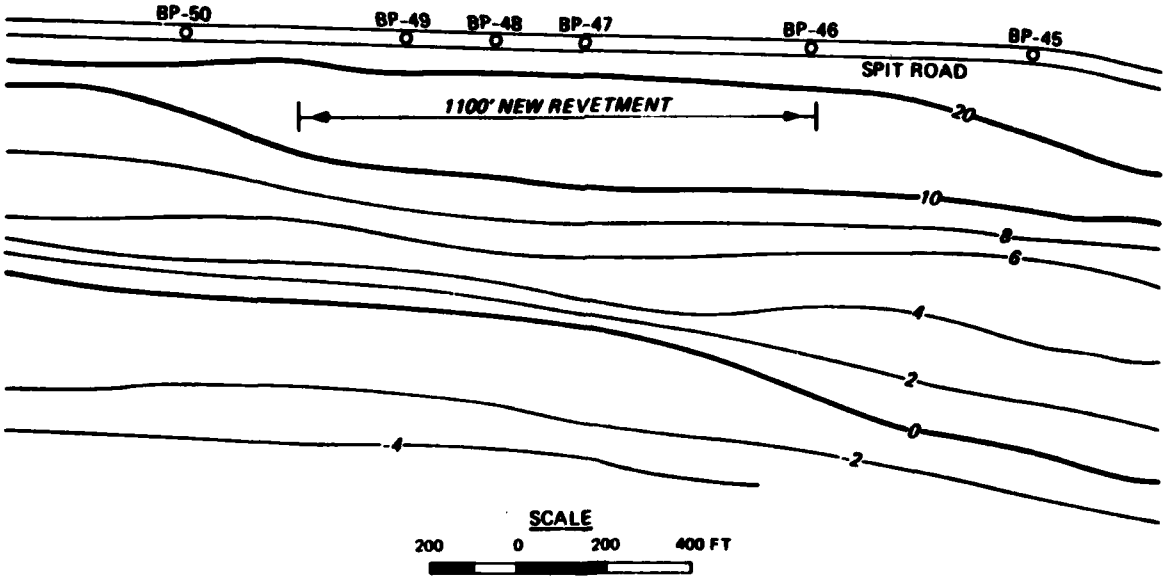

Figure 19. Bathymetry at the project site after beach fill, Homer Spit, Alaska

PART VIII: CONCLUSIONS AND RECOMMENDATIONS

24. The following conclusions and recommendations result from CERC's engineering analysis of the erosion problem at Homer Spit, Alaska:

a. The sediment transport dominated by wind wave action is toward the tip of the Spit. Relatively minor beach erosion occurred at the project area prior to the 1964 Alaska earthquake. This erosion process has accelerated since the earthquake and has been at a much higher rate than before the earthquake. It is unclear whether the eroded beach has been stabilized because of the highly active littoral transport at the Spit. The 2-year beach survey does suggest that beach erosion at the project area may have slowed recently, although the high water levels and wave overtopping continue to be a major threat to roadway safety during storms. Nevertheless, it is recommended that the beach survey program be continued during August to establish a long-term data base for appraising beach processes at Homer Spit.

b. The revetment extension option is not an effective means for erosion control at Homer Spit. However, it could provide protection to the roadway if it is properly designed. Since erosion of the beach will continue, the revetment may need further extension in future years.

c. Placement of a rubble revetment is recommended in front of the existing sheet-pile seawall. This revetment will protect the seawall from collapse, reduce wave overtopping by dissipating wave energy, and protect the roadway from flooding during periods of high tide and storms. This revetment should extend 1,100 ft from the existing rubble revetment toward the tip of the Spit.

d. Beach fill is recommended to nourish the severely eroded beach at the project area, to form a protective beach inducing early wave breaking, and to reduce wave loading on the protective structure at the shore. A volume of 150,000 cu yd of borrow material is needed for the initial nourishment. Renourishment may be required in future time intervals.

REFERENCES

Ebersole, B., Cialone, M., and Prater, M. 1986. "Regional Coastal Processes Numerical Modeling System; Report 1, RCPWAVE - A Linear Wave Propagation Model for Field Use," Technical Report CERC-86-4, US Army Engineer Waterways Experiment Station, Vicksburg, Miss.

Gronewald, G., and Duncan, W. 1965. "Study of Erosion Along Homer Spit and Vicinity, Kachemak Bay, Alaska," Proceedings, Coastal Engineering Conference, American Society of Civil Engineers, New York, N.Y., pp 673-682.

Hanson, H., and Kraus, N. C. 1986. "Seawall Boundary Condition in Numerical Models of Shoreline Evolution," Technical Report CERC-86-3, US Army Engineer Waterways Experiment Station, Vicksburg, Miss.

_____. In preparation. "Generalized Shoreline Simulation System: Report 1, GENESIS - A shoreline Change Numerical Simulation Model for Engineering Use," Technical Report, US Army Engineer Waterways Experiment Station, Vicksburg, Miss.

Kawahara, M. 1978. "Two Step Explicit Finite Element Method for Tsunami Wave Propagation Analysis," International Journal of Numerical Mathematic Engineering, Vol 12, No. 2, pp 331-351.

_____. 1983(Jun). "Multiple Level Finite Element Analysis and Its Application to Tidal Current Flow in Tokyo Bay," Applied Mathematical Modeling, Vol 7, pp 197-211.

Kraus, N. C. 1983. "Applications of a Shoreline Prediction Model," Proceedings of Coastal Structures '83, American Society of Civil Engineers, pp 632-645.

Kraus, N. C., et al. In preparation. "Coastal Processes at Sea Bright to Ocean Township, New Jersey," Miscellaneous Paper, US Army Engineer Waterways Experiment Station, Vicksburg, Miss.

Kraus, N. C., Hanson, H., and Harikai, S. 1985. "Shoreline Change at Oarai Beach: Past, Present and Future," Proceedings of the 19th Coastal Engineering Conference, American Society of Civil Engineers, pp 2107-2123.

Kraus, N. C., and Harikai, S. 1983. "Numerical Model of the Shoreline Change at Oarai Beach," Coastal Engineering, Vol 7, No. 1, pp 1-28.

Le Méhauté, B., and Soldate, M. 1980. "A Numerical Model for Predicting Beach Changes," CERC Miscellaneous Report No. 80(6), US Army Engineer Waterways Experiment Station, Vicksburg, Miss.

Motyka, J. M., and Willis, D. H. 1975. "The Effect of Wave Refraction Over Dredged Holes," Proceedings of the 14th Coastal Engineering Conference, American Society of Civil Engineers, pp 615-625.

Nottingham, D., Drage, B., and Gilman, J. 1982. "Littoral Drift and Spit Degradation of Homer Spit, Alaska," prepared for Alaska Department of Transportation and Public Facilities, Interior Region Research Section, Anchorage, Alaska.

Ozasa, H., and Brampton, A. H. 1980. "Mathematical Modeling of Beaches Backed by Seawalls," Coastal Engineering, Vol 4, No. 1, pp 47-64.

Perlin, M., and Dean, R. G. 1979. "Prediction of Beach Planforms with Littoral Controls," Proceedings of the 16th Coastal Engineering Conference, American Society of Civil Engineers, pp 1818-1838.

_____. 1983. "A Numerical Model to Simulate Sediment Transport in the Vicinity of Structures," CERC Miscellaneous Report No. 83-10, US Army Engineer Waterways Experiment Station, Coastal Engineering Research Center, p 119.

Price, W. A., Tomlinson, K. W., and Willis, D. H. 1973. "Predicting the Change in Plan shape of Beaches," Proceedings, 13th Coastal Engineering Conference, American Society of Civil Engineers, pp 1321-1329.

Sasaki, T. 1975. "Simulation of Shoreline and Nearshore Current," Proceedings of Civil Engineering in the Oceans III, American Society of Civil Engineers, pp 179-196.

Sasaki, T. O., and Sakuromoto, H. 1978. "Field Verification of a Shoreline Numerical Model," Proceedings of the International Conference of Water Resources Engineering, International Association of Hydraulic Research, pp 501-518.

Shore Protection Manual. 1984. 4th ed., 2 vols, US Army Engineer Waterways Experiment Station, Coastal Engineering Research Center, US Government Printing Office, Washington, DC.

Smith, O. P., Smith, J. M., Cialone, M. A., Pope, J., and Walton, T. L. 1985. "Engineering Analysis of Beach Erosion at Homer Spit, Alaska," Miscellaneous Paper CERC-85-13, US Army Engineer Waterways Experiment Station, Coastal Engineering Research Center, Vicksburg, Miss.

Stanley, K. 1966. "Beach Changes on the Homer Spit," Geological Survey Professional Paper 542-D, US Government Printing Office, Washington, DC.

US Department of Commerce. 1984. "Tide Tables, 1984 - West Coast of North and South America, Including the Hawaiian Islands," National Oceanic and Atmospheric Administration, National Ocean Service, Rockville, Md.

_____. 1984. "Tidal Current Tables 1984 - Pacific Coast of North America and Asia," National Oceanic and Atmospheric Administration, National Ocean Service, Rockville, Md.

Waller, R. 1966. "Effects of the Earthquake of March 27, 1964 in the Homer Area, Alaska," Geological Survey Professional Paper 542-D, US Government Printing Office, Washington, DC.

Wang, S. S. Y. 1986. "Finite Element Modeling of Coastal Flows," Technical Report, Center for Computational Hydroscience and Engineering, School of Engineering, The University of Mississippi, Oxford, Miss.

Willis, D. H., and Price, W. A. 1975. "Trends in the Application of Research to Solve Coastal Engineering Problems," in J. Hails and A. Carr, eds., Nearshore Sediment Dynamics and Sedimentation, Wiley, New York, pp 111-141.

Woodward-Clyde Consultants. 1980. "Homer Spit Littoral Drift Studies," US Army Engineer District, Alaska, Anchorage, Ak.

APPENDIX A: WIND AND DEEPWATER WAVE ANALYSIS

Introduction

1. Long-term measurements of wave conditions at Kachemak Bay off Homer Spit, Alaska, do not exist. This appendix describes the method used to hindcast deepwater waves from wind summaries using a fetch-limited wave generation model. The analysis of measured wind frequency, duration, and direction is discussed also.

Measured Wind Data

2. Wind data were available from three sources: (a) an anemometer on Homer Spit located at the harbor master's office near the end of the Spit, (b) a National Weather Service anemometer located at Homer Airport (north of Homer Spit) and (c) a National Data Buoy Office (NDBO) buoy (EB-46007) located in Lower Cook Inlet. Smith et al. (1985)* made a detailed comparison of data from the three sources. It was concluded from the results of these comparisons plus subsequent observations that the Spit wind data are representative of the winds in the area of interest.

3. The airport and Spit data were very similar in directional distribution, but wind speeds recorded at the airport were lower. Smith et al. (1985) gave two possible explanations for the differences:

a. The airport anemometer is sheltered, and it responds to localized topographical and thermal effects.

b. The Spit anemometer gives inconsistent results. Large gaps in the data indicate poor maintenance.

Since fall 1983, the US Army Engineer District, Alaska, has made periodic checks of the Spit anemometer and found it functioning properly. Also, in July 1986 Dr. Yen-hsi Chu of the Coastal Engineering Research Center reported that the airport anemometer is sheltered by nearby mountains. These two observations indicate that the wind data collected at the Spit are superior to the airport data for the purpose of estimating the wind climate over outer Kachemak Bay (seaward of the Spit).

---

* References cited in the Appendixes can be found in the References at the end of the main text.

4. The NDBO buoy was positioned in Lower Cook Inlet, so it was strongly affected by major wind patterns in the Inlet (Cook Inlet to Shelikof Strait, and Kennedy and Stevenson entrances to Kamishak Gap) instead of the local wind patterns of Kachemak Bay (as was the Spit anemometer). Smith et al. (1985) found no statistical correlation between the buoy winds and the Spit (or airport) winds. This occurrence is not surprising because the katabatic effects and differences in orographic funneling in Kachemak Bay would not affect the buoy. Therefore, the wind conditions at the buoy do not represent what is happening in Kachemak Bay.

5. Ideally, an array of meteorological stations in outer Kachemak Bay and Lower Cook Inlet opposite Homer Spit would be used to define the complex wind field in the area. Since these additional data are not available, the Spit wind data are the best available to describe winds in outer Kachemak Bay.

6. The anemometer at Homer Spit is at an elevation of approximately 25 ft above the land surface. Hourly averages, readings taken once a second and averaged over 1 hr, from February 1965 through January 1982 and September 1983 through February 1986, are available. The data from August 1973 through January 1982 are not usable because a 20-mph threshold was applied when the data were digitized, so wind speeds less than 20 mph were excluded from the wind record. The data from September 1983 through March 1984 are also unusable. During this period, only wind from northwest and west-northwest directions were recorded. The data are apparently incorrect because of the lack of variation in direction and, historically, because winds are predominantly from the northeast in the winter at the Spit. In the data from 1965-73, 53 percent of the data was missing, leaving 32,025 data points (including calm values). In the data from 1984-86, 44 percent of the data was missing, leaving 9,378 data points (including calm values). The combination of wind data from these two periods (1965-73 and 1984-86) are used for characterizing the wind pattern of the study area.

7. The wind data were adjusted using the method presented in the Shore Protection Manual (SPM) (1984). The adjustments included:

a. Correction to 10-m level.

b. Correction for instability resulting from air-sea temperature differences for directions where the fetch is greater than 10 miles. (An unstable condition was assumed, since no temperature data were available.)

c. Correction for nonconstant coefficient of drag.

These corrections were made so that the wind data could be applied directly to wave forecasting curves. The adjusted data should not be considered actual wind speeds, but rather "wind stress factors," since the adjustment for non-constant coefficient of drag is included.

8. The distributions of the hourly winds with respect to direction for each season (winter, spring, summer, and fall) are shown as wind roses in Figures A1 through A4. The wind roses show the distribution of winds in 16 directional sectors as a percent of all winds. The bars in each direction are divided into 10-mph intervals. Slightly more of the total wind data was collected in the winter (27.4 percent) than in the spring (25.3 percent) and fall (25.7 percent), and slightly less data were collected in the summer (21.6 percent). To avoid a seasonal bias in the total wind data, weighting factors were applied to the observations in each season so that each season accounted for 25 percent of the total data set. The wind rose for the entire data set (with seasonal weighting applied) is given in Figure A5.

Wind Hindcast Data

9. A simplified technique was used to calculate gross estimates of wave height, period, and direction from the single point source of wind data at Homer Spit. It was assumed that wind conditions existing at Homer Spit were present in the entire region of Lower Cook Inlet and outer Kachemak Bay. This approach was expected to overestimate existing wave conditions since the winds well offshore from Homer are generally not blowing toward Homer Spit.

10. Spectrally-based deepwater wave heights, peak spectral periods, and peak directions were calculated from the Spit wind distribution based on 6-hr wind averages using the fetch-limited Joint North Sea Wave Project (JONSWAP) equation from the SPM (1984). Six-hour averages were used because approximately a 6-hr duration is needed to reach fetch-limited conditions for higher wind speeds. In the preliminary study (Smith et al. 1985), 1-hr averages were used which contributed to overestimation of wave heights because fetch-limited conditions may not have been obtained in 1 hr. The fetch lengths are given in Table A1. Results of the wave hindcast, wave height H_{mo}, and wave period T, including their cumulative probability distributions, are given in Table A2.

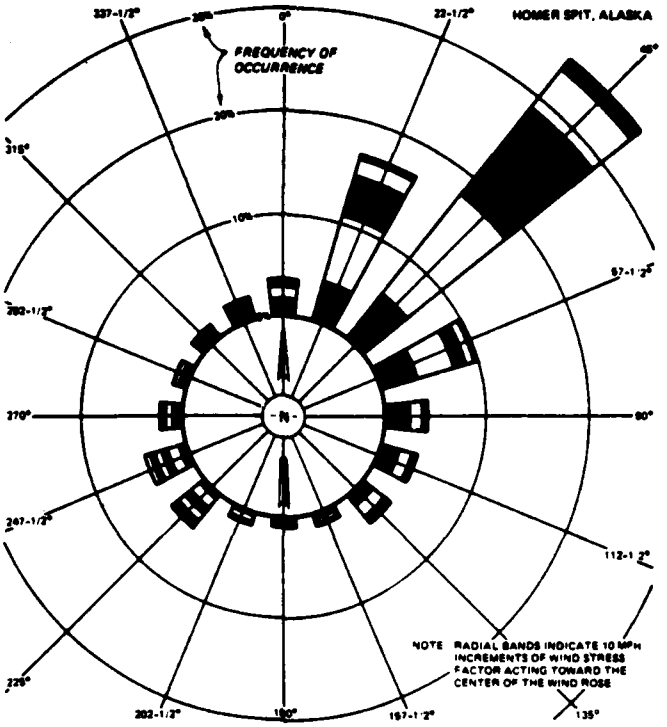

Figure A1. Winter wind rose Homer Spit, Alaska

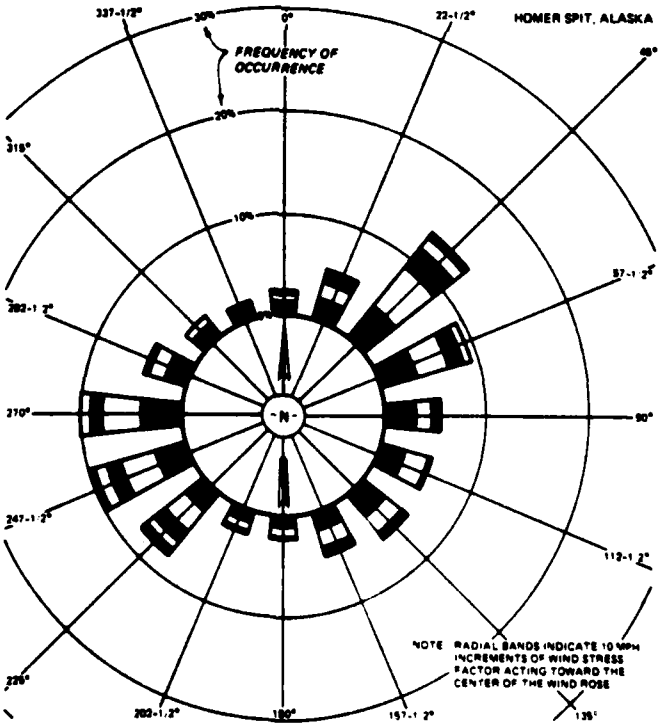

Figure A2. Spring wind rose Homer Spit, Alaska

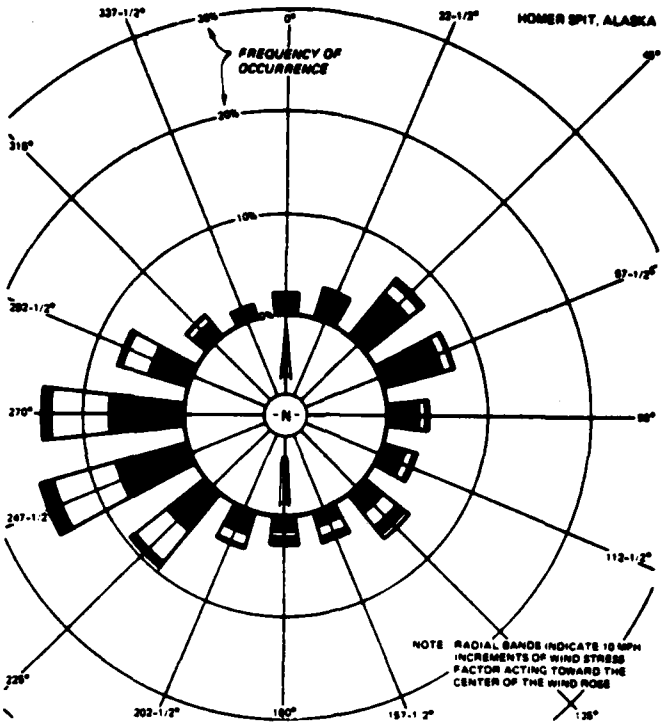

Figure A3. Summer wind rose
Homer Spit, Alaska

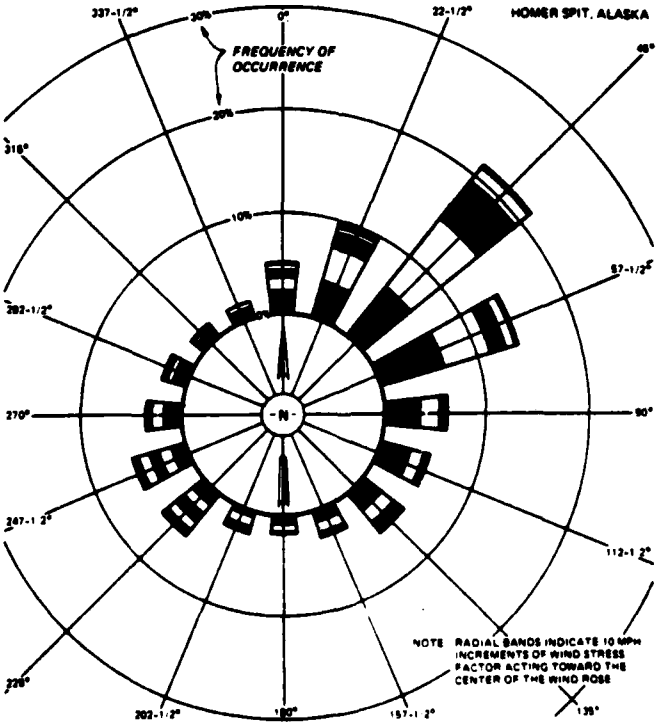

Figure A4. Fall wind rose
Homer Spit, Alaska

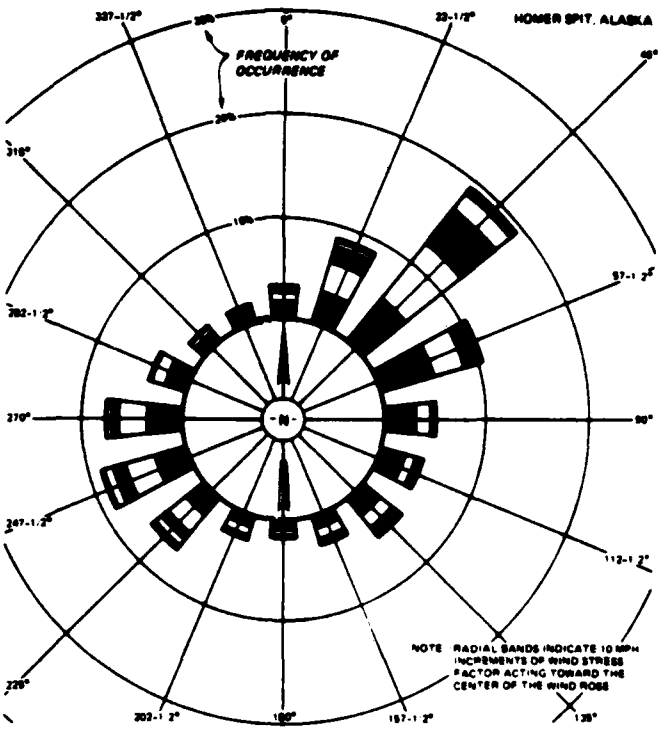

Figure A5. Wind rose for all seasons
Homer Spit, Alaska

Table A1

Fetch Lengths

Direction deg	Fetch miles
281.25-303.75	46.7
258.75-281.25	61.9
236.25-258.75	77.7

11. Measured wave data from Kachemak Bay and concurrent wind data from Homer Spit for July 1984 through February 1986 were available to test this method. Wind data were available hourly from the Spit anemometer. Wave data measured by an accelerometer were obtained every 3 hr from a Waverider buoy in Kachemak Bay (59° 36.36' N, 151° 32.39' W). Wind data were averaged over a 6-hr period prior to every other wave gage measurement. Wave heights and periods were calculated from the average wind speeds and directions

Table A2

Deepwater Wave Statistics Versus Cumulative Probabilities

Wind Stress Factor, mph	Wave Height ft	Wave Period sec	Cumulative Probabilities occurrence per year
	Wave angle = -35.5 deg (relative to grid x-axis)		
2.5	0.10	0.93	0.1008
7.5	0.91	2.78	0.0833
12.5	2.54	4.63	0.0535
17.5	4.64	6.19	0.0306
22.5	5.97	6.73	0.0183
27.5	7.30	7.20	0.0136
32.5	8.62	7.61	0.0085
37.5	9.95	7.98	0.0055
42.5	11.28	8.32	0.0036
47.5	12.60	8.64	0.0020
52.5	13.93	8.93	0.00095
57.5	15.26	9.21	0.00014
	Wave angle = -58.0 deg (relative to grid x-axis)		
2.5	0.10	0.93	0.0559
7.5	0.91	2.78	0.0424
12.5	2.54	4.63	0.0244
17.5	4.14	5.74	0.0121
22.5	5.33	6.24	0.0057
27.5	6.51	6.67	0.0034
32.5	7.70	7.06	0.0023
37.5	8.88	7.40	0.0011
42.5	10.06	7.72	0.00085
47.5	11.25	8.01	0.00071
52.5	12.43	8.28	0.00043
57.5	13.62	8.53	0.00030
	Wave angle = -69.25 deg (relative to the grid x-axis)		
2.5	0.10	0.93	0.0267
7.5	0.91	2.78	0.0189
12.5	2.54	4.63	0.0091
17.5	3.60	5.23	0.0054
22.5	4.63	5.68	0.0025
27.5	5.66	6.08	0.0014
32.5	6.69	6.42	0.00081
37.5	7.71	6.74	0.00054
42.5	8.74	7.03	0.00013

approaching Homer Spit from Cook Inlet. These calculated wave heights and periods were compared with the wave heights and periods measured at the Waverider buoy at the end of each averaging period. A scatter plot of the calculated versus observed wave heights is shown in Figure A6. The mean wave heights for July 1984 to February 1986 are:

	Mean	Standard Deviation
Calculated wave height, ft	2.73	2.17
Observed wave height, ft	2.63	2.72

A linear regression analysis with the observed wave height as the independent variable X and the calculated wave height as the dependent variable Y gave the following results:

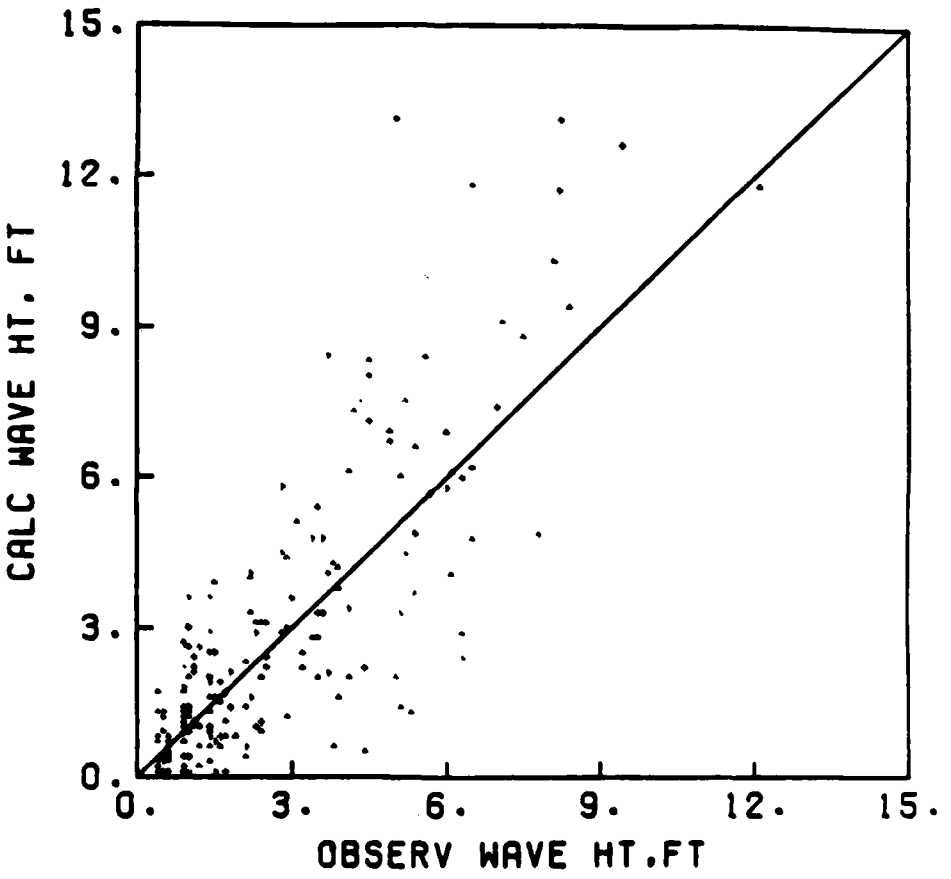

Figure A6. Scatter plot of calculated versus measured wave heights

$$A = 0.005$$

$$B = 0.965$$

$$\text{where } Y = A + BX$$

$$\text{correlation coefficient} = 0.771$$

The calculated wave height estimates the observed wave height well. The mean wave periods are:

	Mean	Standard Deviation
Calculated wave period, sec	4.86	1.85
Observed wave period, sec	4.38	1.59

A linear regression analysis comparing wave periods (with observed wave period as the independent variable and calculated period as the dependent variable) gave no correlation. Differences in wave periods result partially from definitions; i.e., the measured wave period is the average zero-crossing period over the entire record, and the calculated period is the peak spectral period. Overall comparison between the calculated and measured wave heights is reasonably good considering the assumptions involved. Thus, the wave hindcast technique is reasonable. A slight overestimation of wave height and period is expected because of overestimation of the fetch length. A sample of spectral data examined after the completion of this study indicates that the energy contained in low frequencies is not significant, supporting, therefore, the assumption of locally generated waves.

Extremal Analysis

12. The purpose of the extremal analysis is to predict extreme deepwater waves associated with return periods of 5, 10, 25, 50, and 100 years. The extremal analysis was performed using unadjusted wind data exceeding 30 mph. Three frequently used probability distributions for describing extremal statistics were fit by the method of least squares. The three distributions used were (a) Extremal Type I, (b) Weibull, and (c) Log-Extremal. The Log-Extremal distribution gave the best fit with a correlation coefficient of 0.979. The unadjusted extreme wind speeds were adjusted to wind stress factors as discussed earlier. The associated deepwater waves were

calculated using the fetch-limited JONSWAP equation. The majority of unadjusted wind events over 30 mph were from the directional sector 236.25 to 258.75 deg, so the fetch associated with this sector, 77.7 miles, was used in the wave calculation. Table A3 gives the results of the extremal analysis. Caution should be used interpreting these results, especially the longer return periods, because of the short period of record of the input wind data. This short period of record increases the probability of bias in the data.

Table A3

Extremal Results

Return Period yr	Unadjusted Wind Speed mph	Wind Stress Factor mph	Wave Height ft	Wave Period sec
5	46	79	21	10.2
10	50	87	23	10.6
25	56	99	26	11.0
50	61	109	29	11.4
100	66	121	32	11.8

Summary and Conclusions

13. Measured wind data from the Homer Spit anemometer were chosen to represent the wind climate over outer Kachemak Bay. The wind data were adjusted so direct application of wave forecasting equations could be made. The adjusted data should not be considered wind speeds because the adjustment for nonconstant coefficient of drag is included. The wind data were used to calculate deepwater spectrally-based wave height, peak spectral period, peak direction, and the associated probability of occurrence. Constant wind speed and direction across outer Kachemak Bay and fetch-limited wave growth were assumed. Comparisons between measured wave heights and calculated wave heights were made to test the wave calculation technique. The results showed good correlation. An extremal analysis was made with the wind data to predict extreme events for 5-, 10-, 25-, 50-, and 100-year return periods. The

deepwater hindcast wave data are used for developing nearshore wave information (see Appendix B).

APPENDIX B: WAVE TRANSFORMATION ANALYSIS

Introduction

1. Deepwater wave conditions in outer Kachemak Bay were estimated using the fetch-limited Joint North Sea Wave Project (JONSWAP) equation from the Shore Protection Manual (SPM) (1984) with measured wind conditions from Homer Spit and measured fetch lengths (see Appendix A). This appendix describes the methods used to transform deepwater wave conditions to nearshore conditions to study longshore sediment transport.

2. Two approaches were used to estimate the sediment transport rate. Rough estimates of sediment transport were calculated by transforming typical deepwater wave conditions to breaking conditions and calculating the longshore sediment transport from longshore wave energy flux using the SPM equation. An average yearly transport rate was estimated by assigning probabilities to typical wave conditions. The second approach estimated longshore sediment transport with a numerical shoreline change model. As input to the shoreline change model, a typical 1-year time-history of deepwater wave conditions was transformed to prebreaking conditions.

Wave Transformation Model

3. The Regional Coastal Processes Wave (RCPWAVE) model (Ebersole, Cialone, and Prater 1986) was used to transform deepwater waves over the outer Kachemak Bay bathymetry to breaking for the typical wave approach and prebreaking for the time-history approach. The model employs an iterative, finite difference scheme including full refraction and diffraction effects produced by the sea bottom, assuming

a. Mild bottom slopes.

b. Linear, monochromatic, and irrotational waves.

c. Negligible wave reflection.

d. Negligible energy loss resulting from bottom friction and wave breaking outside the surf zone.

Typical Wave Approach

4. A stretched rectangular grid of 76 cells in the offshore or x-direction by 72 cells in the longshore or y-direction covering an area of 22,500 × 60,000 ft was applied, as shown in Figure B1. The grid spacing was fine in the nearshore and coarse offshore along the x-axis, and the spacing was constant along the y-axis. Stretched grids minimize computer time by minimizing the number of grid cells. The grid was oriented to minimize the number of land cells and to accommodate a maximum incident wave angle of 70 deg relative to the grid's x-direction. The grid's y-axis runs from Bluff Point, Alaska, southeastward to the tip of Homer Spit (Figure B1). The x-axis extends seaward to a depth of approximately 20 to 30 fathoms.

5. The grid was overlaid on the National Ocean Survey (NOS) bathymetric chart to assign an average depth to each grid cell relative to mean lower low water (MLLW) (Smith et al. 1985). The bathymetry near the Spit was updated with survey data from August 1984. The new survey included detailed data above MLLW; whereas the NOS chart included only sparse data above MLLW. Since the grid lacked enough detail to resolve incipient breaking locations accurately, a modified version of RCPWAVE, developed in the previous study (Smith et al. 1985), was used to take the wave conditions one grid cell prior to breaking (SPM (1984) breaking criterion) and transform them to breaking conditions (breaking criterion of wave height = 0.78 × water depth). Wave conditions just prior to breaking include wave height, wave period, and wave angle relative to the local shoreline. From the breaking conditions, the longshore energy flux factor P_{ls} was calculated using

$$P_{ls} = \left(\frac{1}{16}\right) \rho g (H_b)^2 C_g (\sin 2\theta_b)$$

where

ρ = mass density of water

g = acceleration of gravity

H_b = wave height at breaking

C_g = group velocity of wave at breaking

θ_b = angle between the wave crest and shoreline breaking

6. Test runs of the model were made to verify the model was operating properly. It was noted that waves propagating nearly parallel to shore caused model instability because waves refracted offshore. Therefore, wave directions greater than -70 deg (Figure B2) could not be run. Two deepwater wave conditions were transformed to breaking conditions at three tide levels (MLLW, mean tide, and mean higher high water) with RCPWAVE to test the sensitivity of the P_{ls} values to the tide level. Figures B3 and B4 show the P_{ls} values calculated from the transformed wave conditions for each longshore grid cell. Figure B3 represents the following deepwater conditions: significant wave height H_o = 13.9 ft, wave period T = 8.2 sec, and θ_o = -69.25 (relative to the grid). Figure B4 represents the following deepwater conditions: H_o = 15.26 ft, T = 9.21 sec, and θ_o = -35.5 . The P_{ls} values for all three tide levels are included on each plot. The P_{ls} values for the three tide levels follow the same general trend longshore, while the longshore distributions differ greatly between the two deepwater wave conditions. For the

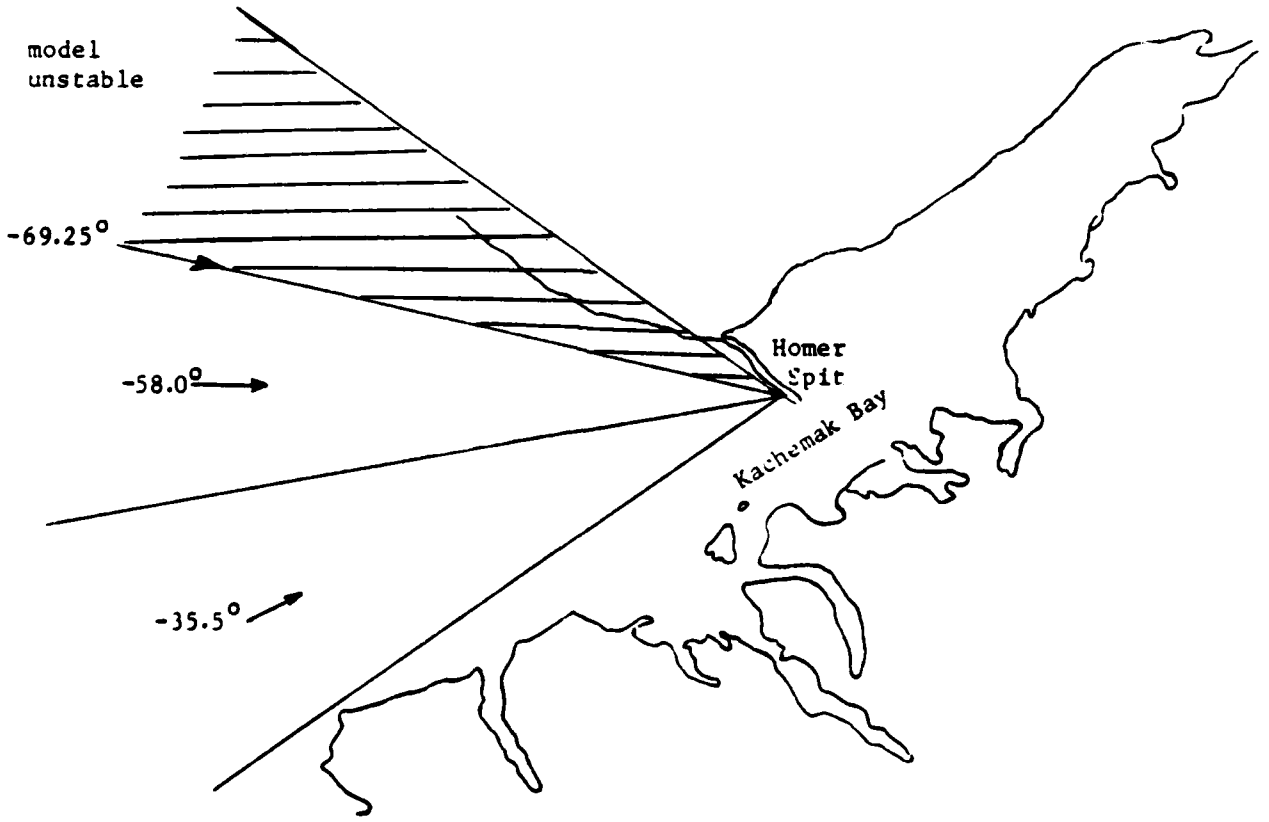

Figure B2. Wave direction bands relative to the transformation grid for typical wave approach

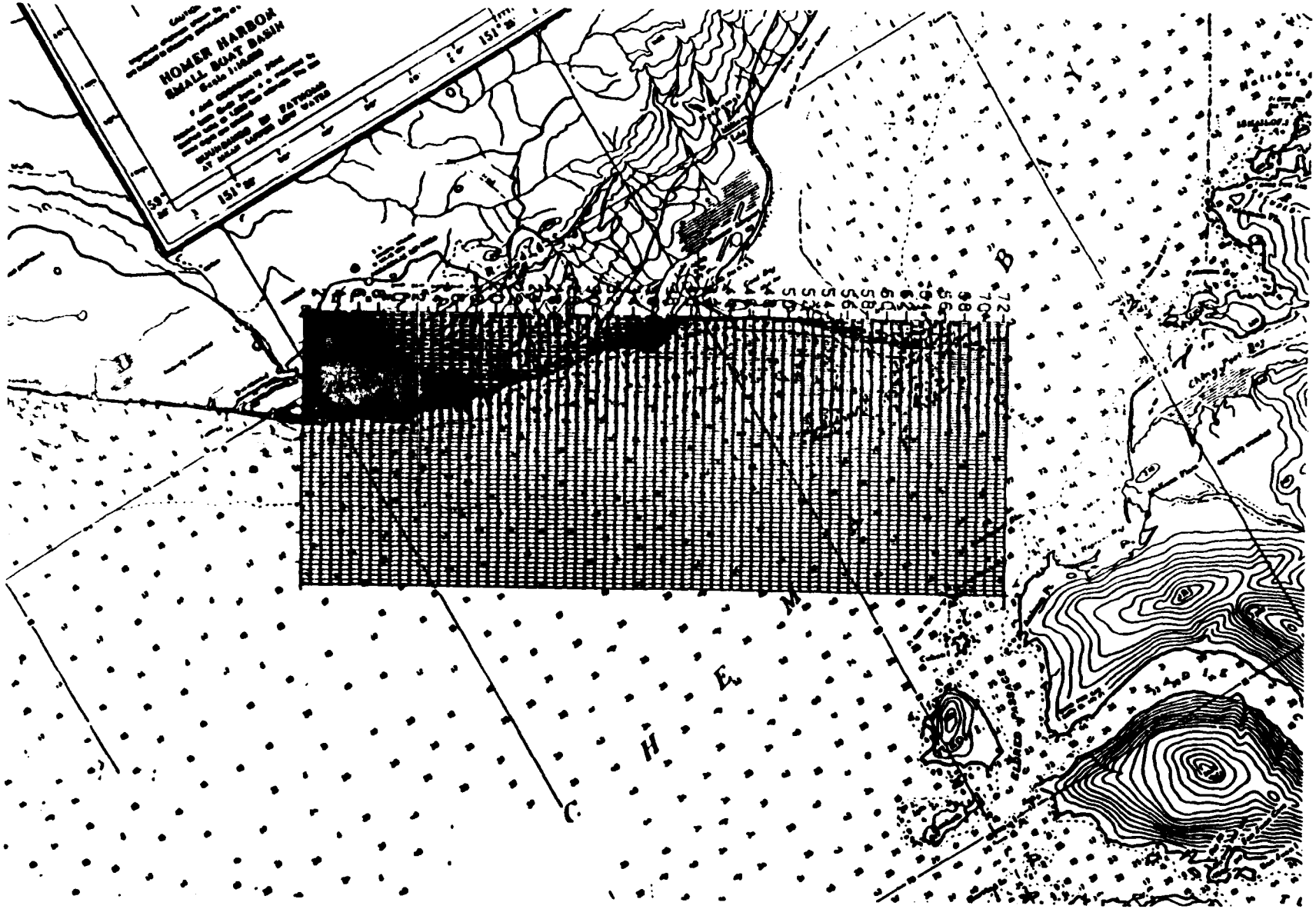

Figure B1. Numerical grid applied in wave transformation analysis superimposed on Homer Spit, Alaska

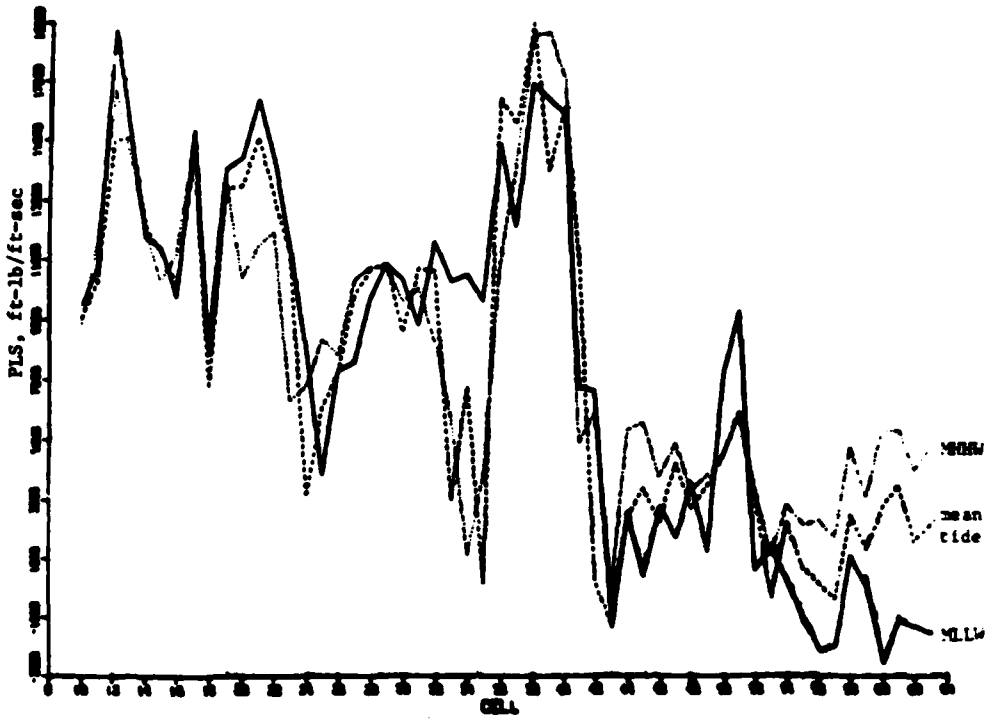

Figure B3. Longshore energy flux for H_o = 13.9 ft, T = 8.2 sec, and θ_o = -69.25 at three tide levels

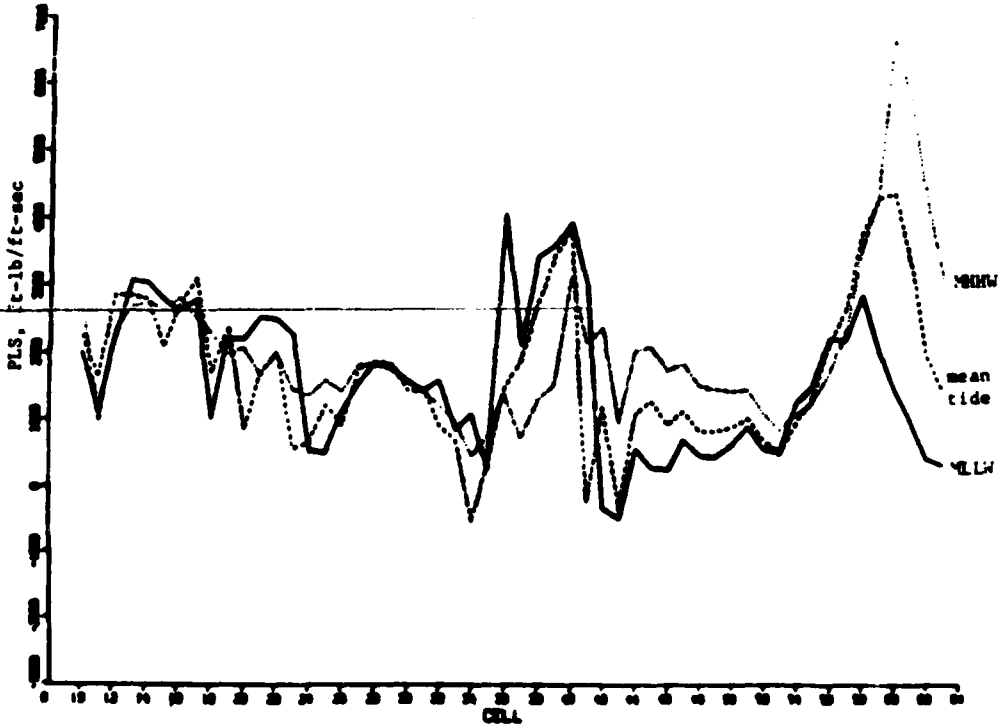

Figure B4. Longshore energy flux for H_o = 15.26 ft, T = 9.21 sec, and θ_o = -35.5 at three tide levels

accuracy of the typical wave approach, the difference in P_{ls} for the three tide levels is not significant; therefore, for this approach, the mean tide level was used for all wave conditions.

7. The modified RCPWAVE model was run for each deepwater wave condition given in Table A2 (Appendix A) as previously calculated from the wind analysis. It should be noted that the wind analysis output wave height is energy-based significant wave height, and the period is the peak spectral period which the wave model treats as monochromatic. A P_{ls} value was calculated at each of the 72 shoreline grid cells for each deepwater wave condition, and each value was weighted by the probability of occurrence associated with the corresponding deepwater wave condition. The probabilities for each wave condition are obtained by subtracting successive cumulative probabilities in Table A2. The weighted P_{ls} values were computed as $P_{ls} \times w$, where w is the weighting factor. At each shoreline grid cell, the P_{ls} values for all wave conditions run were summed

$$(P_{ls})_j = \sum_{i=1}^{n} (P_{ls})_{ji} \times w$$

where

$(P_{ls})_j$ = expected annual P_{ls} for j

n = number of wave condition

$(P_{ls})_{ji}$ = longshore energy flux factor at shoreline cell j for wave condition i

The calculated expected annual average P_{ls} values for each shoreline cell are provided in (Table B1 and Figure B5).

8. Longshore sediment transport rate Q was estimated directly from P_{ls} using Equation 4-49 in the SPM (1984) as follows:

$$Q = \frac{K}{g a' (\rho_s - \rho_w)} P_{ls}$$

where

$K = 0.265 \log(gH/V_f)^2 - 0.53$

g = acceleration of gravity

V_f = fall velocity of sediment

Table B1

Expected Annual P_{ls}

Cell	P_{ls}, ft-lb/ft-sec	Cell	P_{ls}, ft-lb/ft-sec
10	67.5	37	90.4
11	79.4	38	120.5
12	107.7	39	118.3
13	103.7	40	87.8
14	86.9	41	-19.6
15	70.7	42	-24.8
16	64.5	43	-33.2
17	103.3	44	19.5
18	46.9	45	26.9
19	96.4	46	14.9
20	28.7	47	20.8
21	73.9	48	17.9
22	56.9	49	21.6
23	-4.8	50	29.2
24	-5.8	51	39.5
25	20.5	52	24.0
26	25.7	53	10.4
27	57.2	54	24.6
28	68.3	55	28.8
29	69.9	56	37.7
30	46.4	57	34.8
31	55.6	58	53.1
32	16.5	59	67.2
33	18.7	60	92.0
34	-36.1	61	83.5
35	5.5	62	74.1
36	63.6	63	63.3

Note: Positive values indicate wave energy flux directed toward the end of Homer Spit; while negative values indicate the opposite direction.

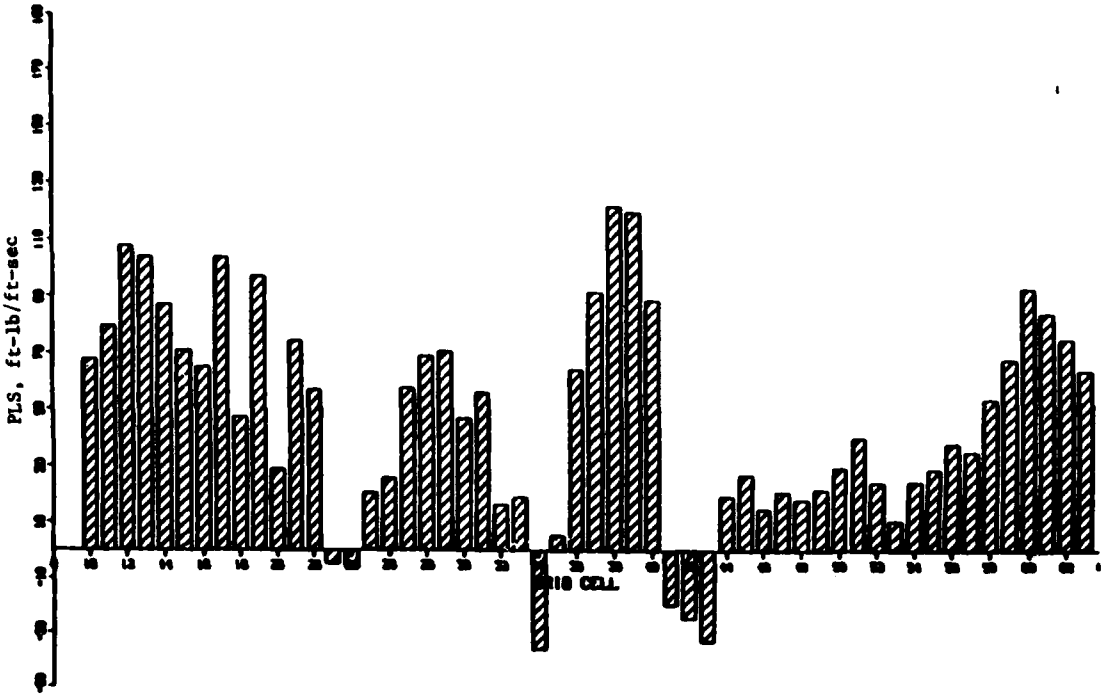

Figure B5. Longshore energy flux factor P_{ls}, Homer Spit, Alaska

a' = ratio of volume of solids to total volume (accounts for sediment porosity)

ρ_s = mass density of sediment

ρ_w = mass density of water

A K-value of 0.52 was computed for the 0.3-mm-diam sediment typical of the low tide regions of the Spit, assuming a conservative 5-ft significant wave height. It was assumed also that longshore transport at high tide is negligible because of the large sediment sizes typical on this part of the beach profiles (gravel and cobbles). An overall average K-value of 0.26 was estimated with the additional simplifying assumption of a step function tidal variation (versus the natural sinusodial variation). This procedure resulted in estimates of annual longshore transport (in cu yd/year) equal to 5,000 × P_{ls}. The SPM (1984) recommends using a larger constant of 7,500 in a similar expression for beaches with medium-to-fine sand; but this constant is meant as a first approximation based on more uniform conditions with much smaller tidal variation. Sediment transport along the shoreline is shown in Figure B6. Figure B7 shows changes in the sediment transport rate dQ along the shoreline S, or dQ/dS. A positive value of dQ/dS indicates an increasing transport

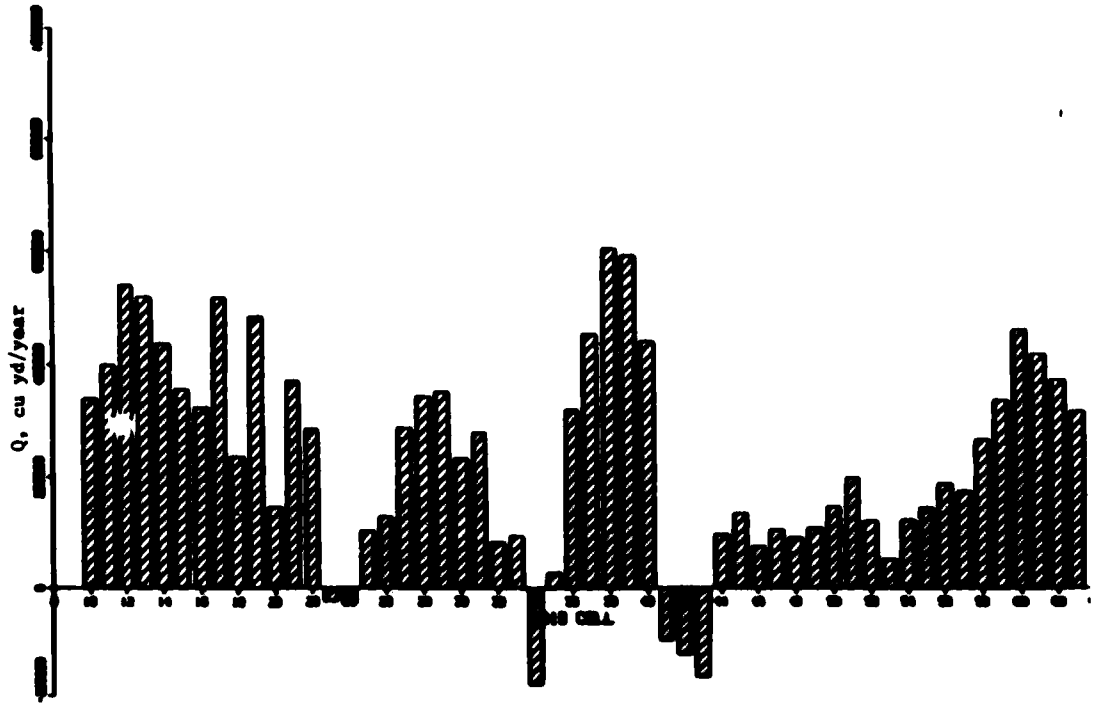

Figure B6. Longshore sediment transport Q Homer Spit, Alaska

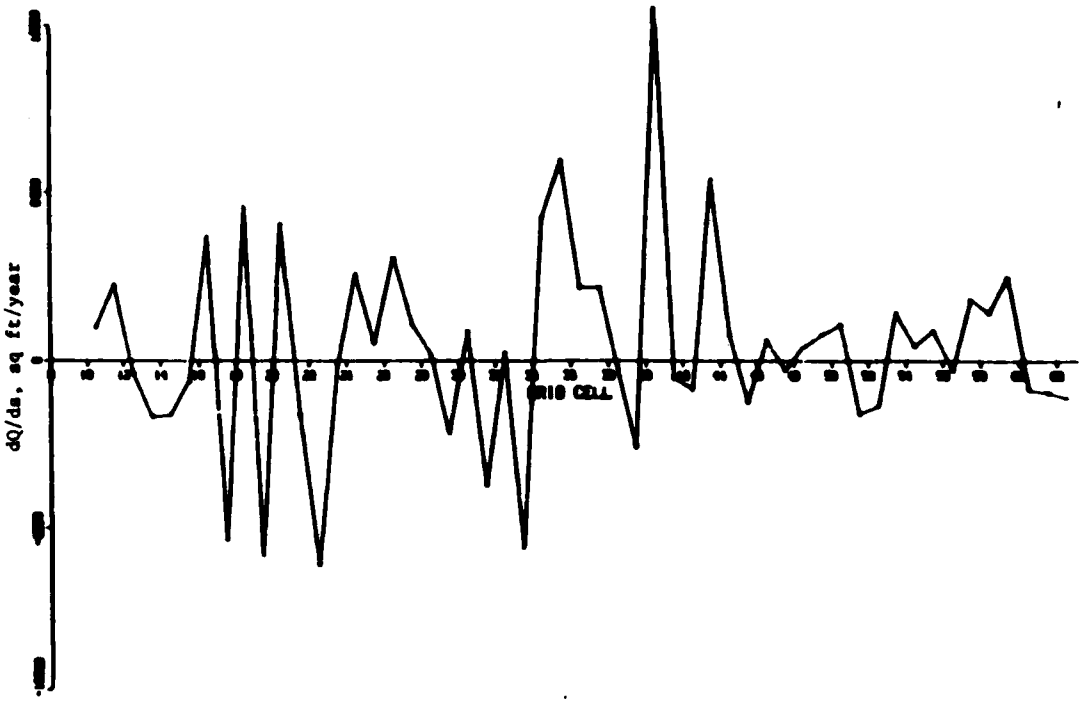

Figure B7. Changes in longshore sediment transport rate dQ/dS Homer Spit, Alaska

rate toward the end of the Spit, an indication of erosion. A negative value of dQ/dS indicates an area of local accretion.

Time-History Approach

9. The time-history of wind data from Homer Spit, described in Appendix A, was used to calculate the time-history of wave heights, periods, and directions. The fetch-limited JONSWAP equation was applied to each 6-hr average of wind speed and direction, producing a time-history of deepwater wave height, period, and direction. Table B2 is a summary of the deepwater wave time-history (February 1965 to January 1986) giving the average and maximum wave height and period for each month when data were available. The number of observations is the number of 6-hr averages for the month, not including bad or missing data. From this summary, typical months of data were chosen and combined to form a representative 1-year time-history of deepwater wave conditions. A typical month was chosen. One criterion for choosing representative months was that the month have few bad or missing data. Months and years chosen are given in Table B3.

10. The grid applied for the typical wave approach was altered in alignment and grid spacing to accommodate the shoreline modeling. (The shoreline change model is presented in Appendix C.) The grid was rotated to align the y-axis with the baseline of the shoreline change model, which is approximately parallel to Homer Spit. The y-axis was shortened, and the grid spacing was reduced in both directions. The resulting rectangular grid was 108 cells in the x-direction by 175 cells in the y-direction covering an area of 22,500 × 35,000 ft. The grid spacing in each direction was constant. The grid's y-axis extends from Homer, Alaska, southeastward to the tip of Homer Spit. The x-axis extends seaward to a depth of approximately 20 to 30 fathoms. The depths for each grid cell were interpolated from the grid used in the typical wave approach.

11. RCPWAVE was modified to store wave output at approximately the 3-m depth (prebreaking) for each longshore grid line. Test runs of the model were made to verify that the model was operating properly. It was noted that waves propagating nearly parallel to shore caused model instability because waves refracted offshore. Therefore, wave directions greater than 58 relative to the grid's x-axis (Figure B8) could not be run.

Table B2

Summary of Wave Time-History

		JAN	FEB	MAR	APR	MAY	JUN	JUL	AUG	SEP	OCT	NOV	DEC
65	HAVE	0.000-	1.267	0.694	1.640	1.837	1.059	1.435	1.099	0.728	0.720	0.421	0.922
	TAVE	0.000	1.209	1.104	2.158	2.484	1.810	2.979	1.900	1.136	0.870	0.431	0.771
	HMAX	0.000	19.059	7.813	14.041	13.169	7.034	6.127	8.579	7.519	8.573	13.796	10.106
	TMAX	0.000	10.059	7.105	8.623	8.440	7.113	6.793	7.399	7.272	7.590	8.903	9.762
	OBS	0	69	124	120	110	86	76	74	100	124	117	124
66	HAVE	0.023	0.870	0.875	1.000	1.729	1.315	1.215	0.467	0.475	0.104	0.000	0.015
	TAVE	0.064	0.849	0.975	1.653	2.551	2.599	2.229	0.944	0.724	0.221	0.000	0.054
	HMAX	2.094	12.059	11.104	10.230	10.707	6.651	6.091	5.055	3.003	4.120	0.000	1.023
	TMAX	4.749	8.697	8.302	8.050	8.202	6.901	6.520	6.371	5.794	5.951	0.000	3.740
	OBS	124	112	124	120	124	120	117	120	8	57	0	69
67	HAVE	0.000	0.000	0.000	0.000	0.000	0.000	0.000	0.000	0.748	0.381	0.377	0.768
	TAVE	0.000	0.000	0.000	0.000	0.000	0.000	0.000	0.000	0.704	0.389	0.296	0.759
	HMAX	0.000	0.000	0.000	0.000	0.000	0.000	0.000	0.000	10.795	12.127	17.101	12.670
	TMAX	0.000	0.000	0.000	0.000	0.000	0.000	0.000	0.000	8.204	8.529	9.579	8.656
	OBS	0	0	0	0	0	0	0	0	41	124	69	124
68	HAVE	0.330	0.726	0.000	0.000	0.000	0.000	0.000	0.000	0.000	0.000	0.000	0.000
	TAVE	0.405	0.631	0.000	0.000	0.000	0.000	0.000	0.000	0.000	0.000	0.000	0.000
	HMAX	11.250	13.200	0.000	0.000	0.000	0.000	0.000	0.000	0.000	0.000	0.000	0.000
	TMAX	8.320	8.792	0.000	0.000	0.000	0.000	0.000	0.000	0.000	0.000	0.000	0.000
	OBS	112	116	4	0	0	0	0	0	0	0	0	0
69	HAVE	0.000	0.000	0.000	0.000	0.000	2.470	1.751	0.000	0.991	2.521	0.949	0.773
	TAVE	0.000	0.000	0.000	0.000	0.000	4.075	2.896	0.000	1.361	4.156	0.042	0.673
	HMAX	0.000	0.000	0.000	0.000	0.000	4.393	7.154	0.000	7.002	4.090	14.302	20.297
	TMAX	0.000	0.000	0.000	0.000	0.000	6.000	6.007	0.000	7.000	5.717	9.011	10.126
	OBS	0	0	0	0	0	5	58	0	62	5	114	114
70	HAVE	0.299	0.204	0.440	0.000	0.077	1.020	0.452	1.341	0.544	0.000	0.506	1.370
	TAVE	0.353	0.105	0.620	1.302	1.477	1.760	1.002	2.025	0.630	0.000	0.517	1.437
	HMAX	7.071	10.959	8.323	10.121	9.500	5.001	3.636	11.117	12.945	0.000	10.079	9.900
	TMAX	7.304	8.245	7.523	8.030	7.004	6.670	5.700	8.205	8.716	0.000	8.019	7.973
	OBS	121	110	123	112	119	120	46	58	116	0	99	33
71	HAVE	0.333	0.160	0.602	1.002	0.000	0.000	1.309	0.400	0.057	0.610	0.031	0.304
	TAVE	0.277	0.206	0.870	1.303	0.000	0.000	2.205	1.310	0.976	0.063	0.077	0.424
	HMAX	11.976	6.302	9.310	13.713	0.000	0.000	6.346	3.167	11.200	7.906	1.036	12.463
	TMAX	8.493	6.630	7.009	8.005	0.000	0.000	6.073	5.451	8.307	7.420	4.176	8.607
	OBS	54	75	124	120	5	0	67	60	104	114	107	113
72	HAVE	0.030	0.000	0.000	0.000	0.000	0.993	1.170	1.319	0.000	0.000	0.000	0.000
	TAVE	0.105	0.000	0.000	0.000	0.000	2.063	2.256	2.491	0.000	0.000	0.000	0.000
	HMAX	1.262	0.000	0.000	0.000	0.000	4.951	5.579	3.719	0.000	0.000	0.000	0.000
	TMAX	3.605	0.000	0.000	0.000	0.000	6.327	6.304	5.743	0.000	0.000	0.000	0.000
	OBS	67	0	0	0	0	65	117	16	0	0	0	0
73	HAVE	0.000	0.000	0.000	0.000	0.000	0.000	0.000	0.000	0.000	0.000	0.000	0.000
	TAVE	0.000	0.000	0.000	0.000	0.000	0.000	0.000	0.000	0.000	0.000	0.000	0.000
	HMAX	0.000	0.000	0.000	0.000	0.000	0.000	0.000	0.000	0.000	0.000	0.000	0.000
	TMAX	0.000	0.000	0.000	0.000	0.000	0.000	0.000	0.000	0.000	0.000	0.000	0.000
	OBS	1	0	0	0	0	0	0	0	0	0	0	0

(Continued)

Note: HAVE = monthly average significant wave height in feet.
HMAX = maximum monthly significant wave height in feet.
TAVE = monthly average wave period in seconds.
TMAX = maximum monthly wave period in seconds.
OBS = number of 6-hr observations in the month.

Table B2 (Concluded)

		JAN	FEB	MAR	APR	MAY	JUN	JUL	AUG	SEP	OCT	NOV	DEC
84	MAVE	0.000	0.000	0.072	0.455	0.544	0.527	0.470	0.944	0.322	0.229	0.498	0.505
	TAVE	0.000	0.000	0.360	0.972	1.751	1.370	1.412	1.419	0.982	0.453	0.590	0.743
	MMAX	0.000	0.000	1.127	6.599	2.249	3.065	4.463	13.157	4.433	4.330	7.257	10.621
	TMAX	0.000	0.000	3.063	6.963	4.864	5.192	6.112	8.438	5.968	6.051	7.187	9.160
	OBS	0	0	61	109	13	43	124	87	89	70	106	92
85	MAVE	0.000	0.691	0.721	1.221	1.725	0.992	0.616	0.340	0.363	0.452	0.047	0.090
	TAVE	0.000	0.724	0.931	1.558	2.455	1.605	1.943	0.982	0.773	0.723	0.187	0.190
	MMAX	0.000	11.741	11.154	13.284	10.539	2.089	3.539	3.364	9.473	7.900	3.127	4.837
	TMAX	0.000	8.437	7.906	8.792	8.153	5.238	5.447	5.562	7.854	7.393	5.420	6.270
	OBS	28	62	114	116	98	30	41	78	63	97	75	83
86	MAVE	0.034	0.000	0.000	0.000	0.000	0.000	0.000	0.000	0.000	0.000	0.000	0.000
	TAVE	0.058	0.000	0.000	0.000	0.000	0.000	0.000	0.000	0.000	0.000	0.000	0.000
	MMAX	2.085	0.000	0.000	0.000	0.000	0.000	0.000	0.000	0.000	0.000	0.000	0.000
	TMAX	4.742	0.000	0.000	0.000	0.000	0.000	0.000	0.000	0.000	0.000	0.000	0.000
	OBS	123	9	0	0	0	0	0	0	0	0	0	0

MAVE = 0.717 TOT OBS = 7212

Table B3

Representative Time-History

Month	Year
January	1986
February	1968
March	1971
April	1971
May	1966
June	1970
July	1984
August	1966
September	1970
October	1967
November	1965
December	1967

Figure B8. Wave direction bands relative to the transformation grid for time-history approach

12. Production wave model runs were made in an innovative way to eliminate the expense and time of making a run for each deepwater wave condition in the 1-year time-history. Instead, a total of 16 wave conditions representing expected combinations of deepwater wave period and direction were run (Table B4).

Table B4

Wave Conditions for Production Model Runs

Period sec	Direction deg, relative to the grid
4	-18.4
6	-29.6
8	-40.9
10	-52.1

Each of the 16 wave conditions was run at high, mean, and low tide for a total of 48 runs. It was necessary to include the effect of the tide for the shoreline change model. A unit (1-ft) wave height was used for each period, direction, and tide combination. Since the RCPWAVE model is based on linear wave theory, the transformed unit wave height is equivalent to the combined refraction, diffraction, and shoaling coefficients (transformation coefficient). The output from the production runs consisted of the transformation coefficient, wave period, and wave direction at approximately the 3-m depth for each of the 175 longshore grid lines. The information at 90 of these locations was saved because the locations coincide with the shoreline change model cells. The extra longshore cells were needed so that the boundary conditions of the RCPWAVE model would not influence transformation results. The results from all model runs were compiled into one random access file keyed on deepwater wave direction, wave period, and tide level.

13. A program was developed to link the 1-year time-history of deepwater conditions to the results of the wave model runs to create a time-history of wave height, period, and direction at the 3-m depth at each longshore grid line. The program reads one record of the deepwater time-history (wave height, period, and direction) and assigns a tide level,

assuming a progression of mean high to mean low for the four daily wave conditions. A key, defined based on the wave period, wave direction, and tide level, is used to enter the random access file and extract the transformed wave conditions. The transformed wave height is calculated by multiplying the input deepwater wave height by the transformation coefficient. Input deepwater wave results with a wave direction larger than -58 (unstable wave model condition) were processed with a wave direction of -52.1.

14. The final output is a sequential file containing a 1-year time history of wave heights, periods, and directions at 6-hr intervals at the 3-m depth for each of the 90 longshore grid lines needed for shoreline change modeling. The application of this information for estimating sediment transport using the shoreline change model is described in Appendix D.

Summary

15. Deepwater wave conditions were numerically transformed to breaking conditions for typical wave approach using the RCPWAVE model. Breaking conditions were used to estimate the expected annual longshore energy flux factor at each shoreline grid cell. The flux factor is directly related to sediment transport rate and direction. The predominant predicted sediment transport direction is toward the end of the Spit (southeast), but localized reversals in the longshore transport and related sediment deficits are predicted in the vicinity of the base of the Spit. RCPWAVE was used also to transform deepwater wave conditions to prebreaking conditions for the time-history approach. A 1-year typical time-history of prebreaking conditions was created for use in a numerical shoreline change model.

APPENDIX C: SHORELINE CHANGE MODEL AND ALTERNATIVES EVALUATION

Introduction

1. The central task of this study was to develop a numerical model for simulating long-term (5 to 10 years) shoreline change along the southwest coast of Homer Spit and to evaluate the relative merits of alternative plans for erosion control and storm damage reduction. A spit in coastal waters is an accretionary feature resulting from the transport of sediment longshore for which wave action is a major factor producing the sediment movement. Because of the typically regular pattern of sediment transport at a spit, shoreline change of such a morphological feature is expected to be amenable to quantitative analysis. The sediment budget analysis technique commonly used in coastal engineering is an arithmetic balance of beach volume changes with consideration of sediment flow into and out of the seaward, landward, and lateral boundaries of the study area. A numerical shoreline evolution model is a systemized and quantified implementation of the sediment budget analysis method in which the change in beach volume is calculated based on time-varying wave conditions. A numerical model of shoreline change for the study area, taking into account the large variation in sediment grain size across the profile and the relatively large (approximately 16-ft) mean range, will provide a useful tool for examining the effect of proposed erosion control alternatives at Homer Spit.

Shoreline Change Model

Background

2. Numerical modeling of shoreline change in applied coastal engineering began in the mid-1970's. Significant contributions to the development of these numerical models were made in England (Price, Tomlinson, and Willis 1973, Willis and Price 1975, Motyka and Willis 1975), Japan (Sasaki 1975, Sasaki and Sakuramoto 1978), and in the United States (Perlin and Dean 1979). Although the Corps of Engineers has sponsored development of numerical models of shoreline evolution (Le Méhauté and Soldate 1980, Perlin and Dean 1983), until recently this technology has had only limited use in district and division projects.

GENESIS

3. The numerical modeling effort for the present project was performed using a modified version of a shoreline evolution model called GENEralized model for SImulating Shoreline changes (GENESIS) recently developed at the Coastal Engineering Research Center (CERC) (Hanson and Kraus, in preparation). The model was modified for application to Homer Spit to account for the large tidal range and the significant differences in the average sediment grain size at low, mean, and high tides.

4. GENESIS is an integrated set of computer programs developed to calculate wave refraction and diffraction under simplified conditions, breaking wave height and direction, longshore sediment transport rates, and shoreline change. A wide range of boundary conditions, numbers and types of coastal structures, multiple beach fills, and other common situations influencing shoreline change can be simulated. It can also accept input of wave conditions from an external source (as from data obtained in the field or from a specialized computer program as done in the present study).

One-line model

5. The shoreline change portion of GENESIS is classified as a one-line model in which it is assumed that beach contours remain parallel over the course of the simulation period. Therefore, one line or contour, conveniently taken as the shoreline, can be used to characterize beach planform change. GENESIS is a generalized program derived from site-specific one-line models that have successfully described long-term shoreline change measured at long groins, detached breakwaters, and seawalls (Kraus 1983, Kraus and Harikai 1983, Kraus, Hanson, and Harikai 1985, Hanson and Kraus 1986), both in the field and in laboratory physical models. The first Corps of Engineers application of GENESIS was on the highly structured coast of northern New Jersey (Kraus et al. in preparation).

One-line theory
assumptions and equations

6. The fundamental assumptions of the one-line model are:

   a. Nearshore bottom contours move in parallel.

   b. A depth of closure exists beyond which longshore sediment transport does not take place.

   c. The volume of beach material is conserved.

d. Longshore sediment transport by wave action is the dominant factor controlling long-term shoreline change.

7. Comparisons of the available beach profiles for Homer Spit (August 1984 to August 1986) indicate that the slope of the profile along the project area is stable (Appendix D). Based on these data, assumption a. is considered to be satisfied. Visual inspection of the profile data in the study area show a depth of closure or "pinch-off" depth at approximately 19.5 ft (6 m) below mean tide level (assumption b.). Assumption c. is necessary for quantitative implementation of the budget analysis technique. Assumption d. is well satisfied for an accretionary geomorphological feature such as Homer Spit.

8. The basic equation of the one-line model is:

$$\frac{dy}{dt} + \frac{1}{(Db + Dc)} \frac{dQ}{dx} = 0 \qquad \text{(C1)}$$

where

y = shoreline position

t = time

Db = average berm height

Dc = depth of closure

Q = volume rate of longshore sediment transport

x = distance longshore

9. The predictive formula for the longshore sediment transport rate is taken to be

$$Q = \frac{Hb^2 \, Cgb}{16(S-1)(1-a)} \left[K1 \sin(2Zbs) - 2 \, K2 \frac{dHb}{dx} \cot(\beta) \cos(Zbs) \right] \qquad \text{(C2)}$$

where

Hb = breaking wave height

Cgb = wave group velocity at breaking

S = ratio of sediment density to water density (S = 2.65)

a = sediment porosity (a = 0.4)

Zbs = breaking wave angle to the shoreline

$\cot(\beta)$ = inverse of the beach slope

The quantities K1 and K2 are treated as parameters in order to calibrate the model.

10. The first term in Equation 2 corresponds to the CERC formula Shore Protection Manual (SPM) (1984, Chapter 4) and describes sediment transport produced by obliquely incident breaking waves. The second term describes transport produced by a longshore current resulting from a variation in the breaking wave height longshore. The first term is always dominant on an open coast, but the second term provides a significant correction if diffraction enters into the problem (Ozasa and Brampton 1980, Kraus 1983, Kraus and Harikai 1983). The SPM (1984) recommends a value of K1 equivalent to K1 = 0.77 , and the coefficient K2 has been empirically found to lie in the approximate range K2 = 0.5 K1 to 1.5 K1 (Kraus 1983).

Numerical solution scheme

11. GENESIS allows selection of either an explicit or implicit finite difference solution scheme. In order to minimize problems with numerical instability and to reduce execution time for production runs, the implicit solution scheme was chosen to be run at 6-hr intervals.

12. As stated in the introduction, the model GENESIS was modified to better describe shoreline change at the study site. The modification involved incorporation of a method of simulating the large tidal range and the observed variability in the median sediment grain size with depth along the profile. In the numerical model, longshore sediment transport rates and shoreline change were calculated with a simulated 6-hr time-step because the time series of the input wave data was prepared at 6-hr intervals. To be compatible with the shoreline change model, the tide level was simulated at successive time-steps in a cyclical fashion through four representative stages (mean tide, mean high, mean, and mean low). This procedure, in effect, results in a semi-diurnal representation of the tidal cycle. The tides at Homer Spit are semi-diurnal but do have a pronounced diurnal inequality (Smith et al. 1985). However, simulation of the tides in the stated manner is consistent with the accuracy of the shoreline change model. An average median sediment grain size for each of the three representative tide levels was calculated from grain size distribution curves received from the US Army Engineer District, Alaska. The result of this analysis is as follows: mean low tide, 0.25 mm; mean tide level, 10.23 mm; and mean high tide, 8.13 mm. These grain sizes then were used to estimate the transport parameter K1 in Equation 2, and the resultant

K1-values were implemented in the model based on the calculated tide level at the given time-step.

13. Calculation of the shoreline position was accomplished through the discretization of Equation 1; therefore, the inclusion of tidal changes required input of the average berm height at the various water levels. Consistent with the one-line theory of shoreline change, only one contour line was modeled (shoreline at mean tide elevation), but the longshore sediment transport rate and corresponding shoreline change were calculated at three tide levels based on the physical properties (transport parameter K1 and berm height) that exist at that elevation on the profile. The above-described modification of the numerical model was a major preparatory effort of the shoreline modeling task.

Grid and boundary conditions

14. The longshore axis was set parallel to the trend of the southwest shoreline of Homer Spit. The longshore axis of the original wave refraction grid was rotated to be compatible with the GENESIS longshore axis, as discussed in Appendix B. In shoreline modeling, the axis along the trend of the shore is customarily denoted as the "x-axis," and the axis orthogonal to it and pointing positive offshore is denoted as the "y-axis." This is the convention used in GENESIS and maintained in the shoreline modeling effort.

15. The longshore grid spacing in GENESIS was set at 200 ft. This spacing was sufficient for evaluating major alternative plans but still allowed economical computer execution times. The wave refraction grid was interpolated in the longshore direction from the original 833-ft spacing to 200-ft cell spacing for compatibility with the shoreline model.

16. The shoreline model grid was extended beyond the project area on both sides to obtain termination points that would provide appropriate boundary conditions. The southeast (tip of spit) model boundary was placed midway between beach profile BP-34 and BP-36 (Figure C1). The northwest boundary was placed at the base of the Spit, off Beluga Lake.

17. Two surveys of Homer Spit were judged to be adequate for use in the shoreline modeling: Alaska Tideland Survey No. 612 (October 1968) and Homer Spit Erosion Study, Condition Survey No. 1 (August 1985) (Appendix D). From inspection of the available shoreline data it appeared that the shoreline position between BP-34 and BP-36 had moved very little over the past 17 years. Therefore, a fixed-beach boundary condition, in which the boundary shoreline

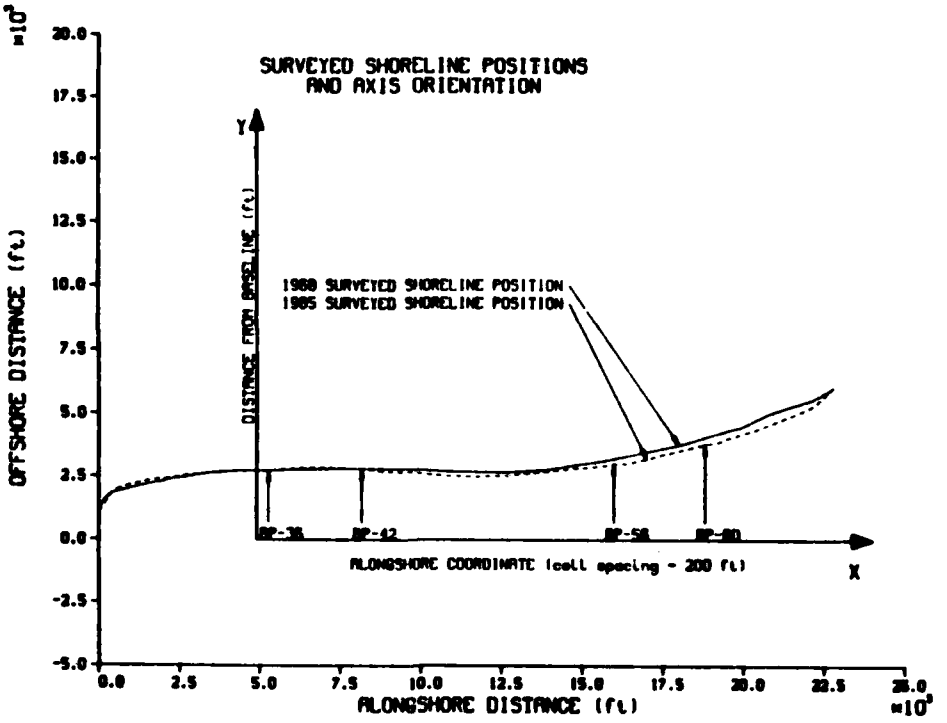

Figure C1. Surveyed shoreline positions and axis orientation

position is constrained not to move, was implemented on the southeast side. This type of boundary condition allows sediment to move across the boundary from either side. Again, from inspection of the shoreline data, the shoreline position at the northwest boundary was also found to be nearly stationary. The 1968 and 1985 surveyed shoreline positions are presented and discussed in Appendix E and shown in Figure C1. However, during trial runs of the model it was determined that a direct fixed-beach boundary condition would not allow adequate reproduction of the erosion occurring immediately downdrift of the boundary, as found in the shoreline position data. It was concluded that the northwest boundary condition required that the longshore sediment transport rate entering the grid from the northwest be limited, in addition to fixing the shoreline position, to reproduce the observed shoreline retreat.

18. In the one-line model, the magnitude of the longshore sediment transport rate and the associated shoreline change are controlled in part by the lateral boundary conditions. At Homer Spit, the principal direction of sediment transport is from the northwest to the southeast, i.e., toward the tip of the Spit. A series of simulations was performed to estimate the

quantity of littoral material transported onto the Spit. As a result, the longshore sediment transport rate at the northwest boundary was limited to 5 percent of the calculated potential rate (Equation C2) to reproduce the actual shoreline erosion occurring in the project area as obtained from the 1968 and 1985 surveys.

19. The condition set at the northwest boundary has various physical interpretations. Based on the shoreline position data, the region from the base of the Spit to BP-42 has been experiencing erosion (on the order of 11.5 ft per year) for the 17 years between 1968 and 1985. This trend indicates there is a lack of littoral material available for transport onto the Spit. Only speculative reasons for this apparent lack of littoral material can be given because of the absence of sediment transport and long-term beach profile data in the area west of and on Homer Spit. A number of reasons may be hypothesized for the lack of transportable material (see Appendix E). A further complicating factor which may have impact on the longshore sediment transport pattern at Homer Spit is the tidal current which, in combination with wave action, might produce net sediment transport toward the tip of the Spit, see Appendix B.

Structures Represented in the Model

20. GENESIS can be applied to simulate shoreline change in the vicinity of coastal structures and erosion control measures such as seawalls, revetments, groins, offshore breakwaters, and beach-fill projects. The application should, however, be done with caution.

Revetments and seawalls

21. A revetment or seawall is assumed by the model to prevent landward retreat of the shoreline. Therefore, a seawall introduces a constraint on the longshore sediment transport rate in addition to limiting the allowed position of the shoreline. The seawall constraint in GENESIS is imposed at the same level of approximation as the assumptions used to derive the one-line model. Wave reflection, scouring, and flanking are not simulated. This description is believed to be reasonable, provided the beach slope in front of the seawall does not appreciably deviate from that of the neighboring beach. This restriction is equivalent to assumption (a) of the one-line theory. Because

of the complexity of implementation of the seawall constraint in the model, the report by Hanson and Kraus (1986) should be consulted for further details.

Beach fills

22. Beach nourishment projects may easily be simulated in GENESIS. The beach-fill design parameters such as the berm width (after initial adjustments) and the length of the project, together with the beginning and ending dates of the beach-fill project, are required inputs into the shoreline model for simulation of beach fills. Several beach-fill locations and beginning and ending dates may be specified in one model run.

23. In summary, three kinds of information are required prior to the shoreline simulation: initial conditions, such as initial position of the shoreline, positions and characteristics of structures, duration of time to be modeled, grid spacing, etc.; wave conditions as a function of time to calculate the longshore sediment transport rate; and boundary conditions at the lateral ends of the study area. These were described previously for application to Homer Spit.

Model Calibration

24. The calibration procedure for GENESIS is to determine the transport parameters K1 and K2 of Equation 2 by reproducing measured shoreline change that occurred at the target site between two surveys. If sufficient shoreline survey and wave data are available, the calibrated model is then run to simulate observed shoreline change in a time interval not spanned by the calibration to verify that the calibration constants are independent of the time interval. Since wave data for these time intervals, which may cover several years, are virtually never available, it is common to use hindcast wave data. Details of the method used to hindcast the wave climate at Homer Spit are in Appendix A.

25. As discussed in the previous section, only two applicable surveys were available for Homer Spit. Hence, verification of the calibration could not be performed thereby necessitating scrutiny of the sensitivity of the calibrated model to quantify expected variations in predicted results.

26. The calibration was performed using the measured shorelines of 1968 and 1985. The simulation of shoreline change for this 17-year period was accomplished using the modified version of GENESIS, with the initial shoreline

position given by the 1968 measured shoreline. The calibration proceeded in the usual manner. The calibration constants K1 and K2 were systematically varied in successive runs of the model, and comparisons were made between the calculated shoreline position (from the 17-year model simulation) and the shoreline position surveyed in 1985. An additional calibration constant was introduced by the northwest boundary condition. This constant, defined as Pn , represents the percent of the calculated potential sediment transport rate allowed to cross the boundary. In the calibration, visual comparisons were made by plotting the calculated and measured shorelines. In addition, a measure of the calibration error, denoted as Yerr , was calculated to provide a more objective fitting criterion. The calibration error was defined as the sum of the absolute difference between the measured and calculated shoreline positions divided by the same quantity calculated from the 1968 and 1985 measured shoreline positions. The arithmetic expression of Yerr is

$$Yerr = \frac{(Ycalc - Ymeas85)}{(Ymeas68 - Ymeas85)} \qquad (C3)$$

where

Ycalc = calculated shoreline position

Ymeas85 = measured shoreline position from 1985 survey

Ymeas68 = measured shoreline position from 1968 survey

27. As Yerr approaches 0.0, the accuracy of the calibration increases. The quantity Yerr was calculated for the complete grid Yerr1 and for the project area Yerr2 between BP-42 and BP-56. The quantities Yerr1 and Yerr2 were used as numerical indicators of the relative accuracy of the calibration runs, thereby conveniently establishing the relative accuracy of the numerous (on the order of 100) calibration runs. Final determination of the suitability of the calibration should be made on the basis of a total integrated judgment by plotting the full two-dimensional features of the shoreline planform; i.e., the final judgment is based on inspection. The results of selected calibration runs are given in Table C1. These results show not only a satisfactory calibration but also the sensitivity of the model to the calibration parameters.

28. With reference to Table C1, model Run 4 was chosen as the best fit with respect to the calibration parameter K1 . Run 4 was selected through

Table C1

GENESIS Calibration Results

Model Run	K1 Low	K1 Mean	K1 High	K2	Pn	Measure of Accuracy Yerr1	Yerr2
			a. Optimization of K1				
1	0.77	0.77	0.77	0.15	2.5	0.880	0.342
2	0.77	0.55	0.65	0.15	2.5	0.639	0.165
3	0.77	0.50	0.60	0.15	2.5	0.594	0.159
4	0.77	0.50	0.55	0.15	2.5	0.582	0.161
5	0.77	0.45	0.55	0.15	2.5	0.560	0.179
6	0.77	0.30	0.50	0.15	2.5	0.553	0.299
			b. Optimization of K2				
7	0.77	0.50	0.55	0.05	2.5	0.583	0.186
8	0.77	0.50	0.55	0.10	2.5	0.578	0.161
9	0.77	0.50	0.55	0.15	2.5	0.582	0.161
10	0.77	0.50	0.55	0.20	2.5	0.594	0.181
11	0.77	0.50	0.55	0.25	2.5	0.622	0.237
			c. Optimization of Pn				
12	0.77	0.50	0.55	0.15	0.0	0.635	0.157
13	0.77	0.50	0.55	0.15	2.5	0.582	0.161
14	0.77	0.50	0.55	0.15	5.0	0.536	0.166
15	0.77	0.50	0.55	0.15	7.5	0.498	0.171
16	0.77	0.50	0.55	0.15	10.0	0.473	0.179
17	0.77	0.50	0.55	0.15	15.0	0.428	0.198
			d. Model sensitivity				
18	0.38	0.25	0.28	0.15	5.0	0.824	0.466
19	0.77	0.50	0.55	0.15	50.0	1.097	0.350
20	1.00	0.65	0.71	0.20	5.0	0.732	0.221

comparison of the accuracy balance between the overall grid and the project area. Run 9 was selected as giving the best fit for the calibration parameter K2 . The same value of Yerr2 was calculated for Runs 8 and 0. Inspection of the final shoreline position from plots of the results of model Runs 8 and 9 indicated that a better fit was obtained with the calibration parameters of Run 9 for the project area. For Pn , visual comparison of the calculated shoreline plots and evaluation of the accuracy balance between the whole grid and the project area led to the selection of model Run 14 to define the calibration parameters. The values of K1 , K2 , and Pn listed for Run 14 in Table C1 were used for all production runs with the model. Part d. of Table C1 illustrates the sensitivity of the model to variation in the calibration parameters and gives an example of the range of possible values for Yerr1 and Yerr2 . In model Run 19, Pn was set at 50, meaning that 50 percent of the calculated potential sediment transport rate was allowed to cross the northwest boundary. The large values of Yerr calculated for this run demonstrate the inaccuracy of allowing half of the calculated potential sediment transport rate to cross the northwest boundary. Similarly, model Run 18 was executed using K1-values of half the calibrated value of this parameter. A marked decrease in the accuracy is the result. In Run 20 both K1 and K2 were increased by 30 percent; the error for the whole grid Yerr1 increased over 100 percent; whereas, the error in the project area Yerr2 only increased about 25 percent.

29. A plot of the 1968 and 1985 surveyed shorelines and the calculated 1985 shoreline from a 17-year model simulation period using the calibration constants of model Run 14 in Table C1 is shown in Figure C2.

Representative Wave Conditions

30. Deepwater wave height, period, and direction were predicted from wind data obtained on Homer Spit (see Appendix A), and the input wave data used in GENESIS were assembled from this data set. Wind data were available for approximately 11 years, with the longest continuous record being only 7 months long. The entire data set was scanned to create a representative 1-year time series of wave conditions at 6-hr intervals from the available data. The criteria for creating the representative wave data were: (a) the

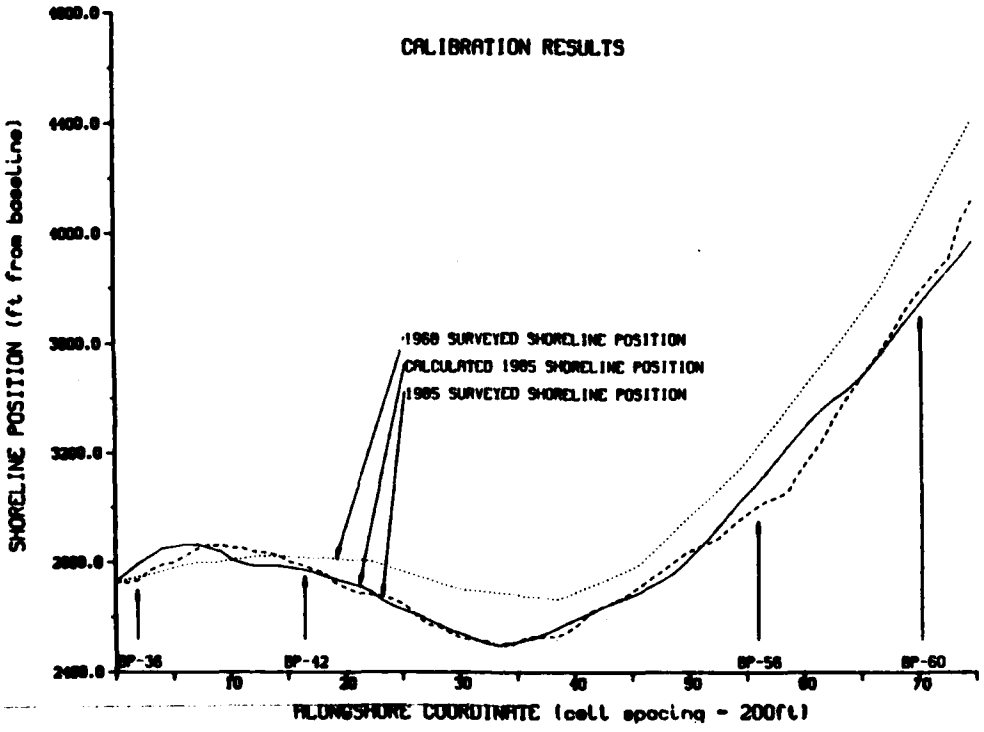

Figure C2. Results of shoreline model calibration

wind record used to predict the waves was continuous for the full month; and (b) the selected data were the most recent data meeting criterion (a) for the given month. The resulting time series was missing only eight 6-hr records (equivalent to 2 days). The eight missing records were generated by averaging adjacent records. A 1-year time series with fewer missing records could not have been selected from the available data. A comparison between the selected representative 1-year time series and the available data was made to determine if the selected wave conditions were indeed representative. The result of this comparison is shown in Table C2. For comparison purposes the analysis was made on a 3-month seasonal basis: winter - December, January, and February; spring - March, April, and May; summer - June, July, and August; and fall - September, October, and November.

31. The data in Table C2 show that the average wave height of the representative 1-year time series of wave conditions is slightly less than the average wave height of the total available data. On a seasonal basis, the average wave height is overestimated in the winter and spring and underestimated in the summer and fall. It is believed that the selected 1-year time

Table C2

Comparison of Selected Representative and Available Wave Conditions

Time Period	Average Wave Height, ft (Including Calm Events) Available	Selected	Wdiff* %
Winter	0.46	0.51	10.9
Spring	0.99	1.17	18.2
Summer	0.96	0.66	-31.3
Fall	0.56	0.42	-26.3
Spring/Summer	0.98	0.92	-6.1
Fall/Winter	0.51	0.46	-9.8
1 Year	0.72	0.69	-4.2

* Wdiff = (Slavg - Aavg)/Aavg × 100%.
SLavg = average wave height from selected data.
Aavg = average wave height from available data.

series adequately represents the existing wave climate at Homer Spit for use in GENESIS.

32. The sensitivity of the shoreline change model to the input wave conditions was investigated through the execution of 10 additional model runs. In these model runs the calibration parameters of model Run 14 in Table C1 were used, and the input wave conditions were varied to examine the sensitivity of the model to variation in input wave conditions. Incident wave height and direction were varied at the grid depths of the wave input to GENESIS (nominal depth of 10 ft; Appendix B). Wave height was varied by a percentage of the original input; whereas wave direction was varied by adding or subtracting a small angle from the input longshore. Since the adjustments are made at a shallow-water location, the small variation in wave angle nearshore corresponds to a large angle in deep water. Using Snell's law and assuming small angles, one may obtain a relationship between a given change $\Delta\theta_n$ in the nearshore wave angle θ_n and the corresponding change $\Delta\theta_o$ in the offshore angle θ_o. This relationship is as follows:

$$\Delta\theta_o = \frac{\tan \theta_o}{\tan \theta_n} \Delta\theta_n \qquad \text{(C4)}$$

From the above equation, an increase of 5.0 deg to a nearshore wave angle of 4.36 deg results in an increase of 11.8 deg in the offshore wave angle originally only 10.0 deg.

33. The model was run for the calibration period 1968-85, and the input wave height was increased and decreased by 5, 10, and 20 percent. In four other runs the incident wave angle was increased and decreased 2.5 and 5 deg. The quantity Yerr (Equation 3) was calculated for these model runs to give an indication of the relative error associated with the changes in the input wave conditions. The results of this investigation are shown in Table C3.

Table C3

Shoreline Model Sensitivity to Input Wave Conditions

Model Run	Change in Input Wave Data		Measure of Accuracy	
	Angle, deg	Height, %	Yerr1	Yerr2
1	none	+ 5	0.538	0.163
2	none	+ 10	0.722	0.203
3	none	+ 20	1.030	0.501
4	none	- 5	0.530	0.170
5	none	- 10	0.524	0.173
6	none	- 20	0.573	0.393
7	+ 2.5	none	0.601	0.609
8	+ 5.0	none	0.748	1.138
9	- 2.5	none	0.800	0.498
10	- 5.0	none	1.148	1.031

34. Values of the quantities Yerr1 and Yerr2 associated with the calibration model Run 14 of Table C1 were 0.536 and 0.166, respectively. Increasing or decreasing the wave height by 5 percent (Runs 1 and 4) changes the measure of accuracy (Yerr1 and Yerr2) by a maximum of 2 percent. An improved Yerr2 (measure of accuracy from BP-42 to BP-56) is noted for Run 1

(1.8 percent better); however, Yerr1 is slightly poorer. Run 1 was the only run which showed an improved Yerr2 in this investigation of sensitivity. For Run 2, 3, 5, and 6 Yerr2 progressively increases, indicating that the resulting shoreline position is farther from the surveyed shoreline position. Decreasing the incident wave heights by 5 and 10 percent resulted in an improved Yerr1 ; whereas decreasing the wave height by 20 percent increases Yerr1 by 6.9 percent, indicating a poorer reproduction of the measured shoreline change as compared to that of the calibrated model. Increasing the incident wave heights by 10 and 20 percent resulted in an increased value of Yerr1 of 35 and 92 percent, respectively. In summary, the shoreline model is only moderately sensitive to changes in the incident wave height. The shoreline model is somewhat more sensitive to changes in the nearshore incident wave angle (Runs 7 through 10 in Table C3). Increasing or decreasing the incident wave angle by 2.5 deg resulted in increasing the Yerr2 values by at least 200 percent; whereas Yerr1 values increased by 12 and 49 percent with respect to the calibrated model (Run 14 of Table C1). Changing the incident wave angle by plus or minus 5 deg resulted in a poor correlation to the surveyed shoreline position for the whole calculation grid (Yerr1), as well as between BP-42 and BP-56 (Yerr2). This exercise has shown that the model produces reasonable results given the uncertainty in the input wave data. Moderately different wave conditions would not affect the overall conclusions of shoreline evolution computed with a model.

Evaluation of Alternative Erosion Control Measures

35. This section addresses the results of GENESIS simulations of the alternative erosion control measures. Three generic alternatives were suggested to alleviate the chronic erosion problem at Homer Spit in a previous CERC report (Smith et al. 1985). All three alternatives included an extension of the existing revetment, one with a scour blanket, another in conjunction with a composite beach fill, and one in conjunction with a uniform beach fill. Two different designs were modeled from these suggested alternatives: one a revetment and the other a revetment in conjunction with a beach fill. Three additional designs were modeled for comparison and evaluation. One was the without-project option, which corresponds to shoreline change as resulting from the existing conditions. Another simulation incorporated an offshore

breakwater option. Finally, a beach-fill only option was simulated to complete a thorough investigation of typically utilized design concepts.

36. Several variations of these five modeled options were run for a total of 16 alternatives. A 20-year simulation was executed for each alternative, and shoreline position data were saved and plotted at the 5- and 10-year intervals. The initial shoreline position in the simulations was taken from the August 1985 survey. The plots of shoreline position given in this section are oriented such that the viewer is standing on Homer Spit and looking offshore with the base of the Spit at the right and the tip of the Spit at the left. There is an approximate 11 to 1 exaggeration of the shoreline position in the offshore direction with respect to the longshore direction in the given plots.

Option 1: without-project

37. The without-project option represents existing conditions at Homer Spit and corresponds to shoreline change assuming no remedial actions are taken. The net longshore sediment transport given by the model for Alternative 1A is directed toward the tip of the Spit. The magnitude of the net sediment transport rates increases from about 200,000 cu yd per year between BP-60 and BP-56 to approximately 280,000 cu yd per year near BP-36 (see Figure C3). Alternative 1A, shown in Figure C4, gives an indication of the planform changes that could be expected to occur in the next 10 years at Homer Spit. The results of this model simulation (Figure C4) show great potential for continued erosion downdrift (toward the end of the Spit) of the sheet-pile wall. The shoreline erosion is the result of the difference in the net sediment transport rates in and out (approximately 880,000 cu yd per year) of the project area. It is interesting to note that a distinct break in the 1985 surveyed shoreline position is evident just off the end of the existing sheet-pile wall. This trend is progressively magnified in the model simulation. However, the assumptions of the seawall boundary condition as implemented in the model must be considered in the interpretation of these results. For instance, in Figure C4, flanking of the revetment would very likely occur, impairing the structural integrity of the revetment and resulting in less downdrift shoreline recession. Furthermore, it is unrealistic to assume that the shoreline position would evolve to a right angle planform immediately downdrift of the revetment.

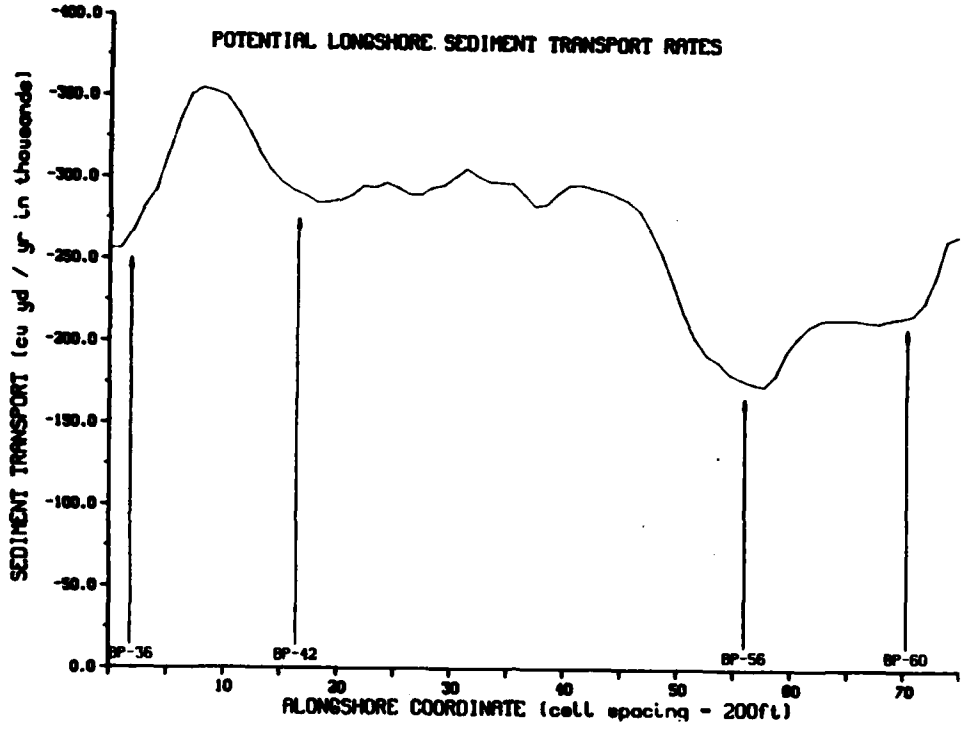

Figure C3. Calculated potential longshore sediment transport rates

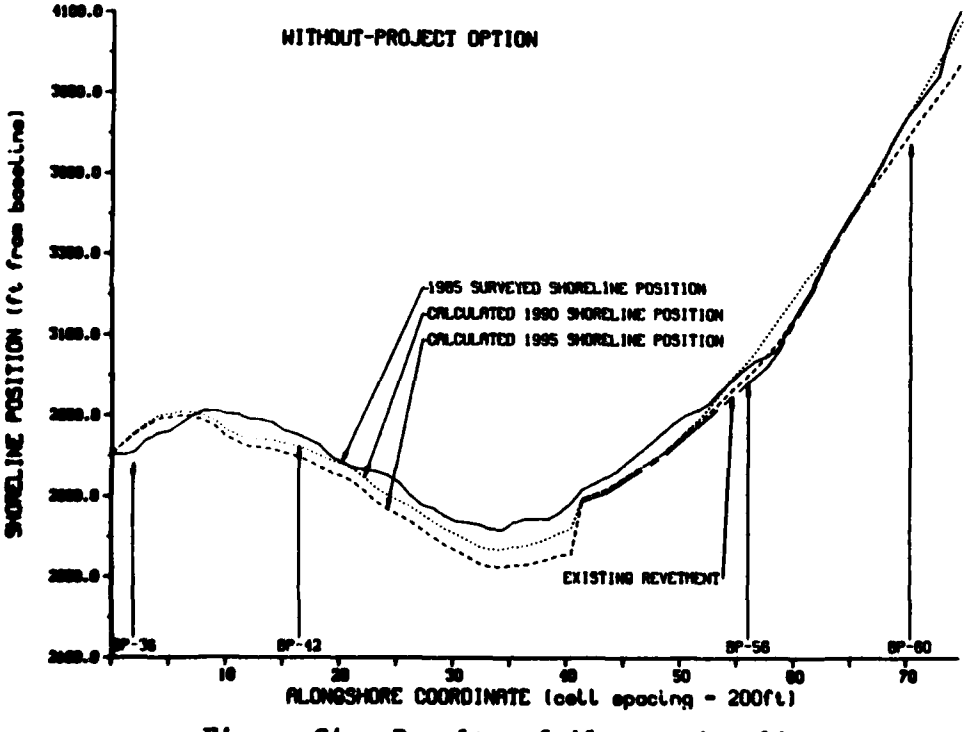

Figure C4. Results of Alternative 1A

Option 2: revetment extension

38. The revetment extension option was executed to show the effect of extending the existing revetment 2,000 ft longshore toward the tip of the Spit. The results of the model simulation of Alternative 2A, shown in Figure C5, indicate that the shoreline can be expected to continue to erode downdrift of the revetment. The interpretations given in the discussion of Alternative 1A are equally applicable to the results of Alternative 2A.

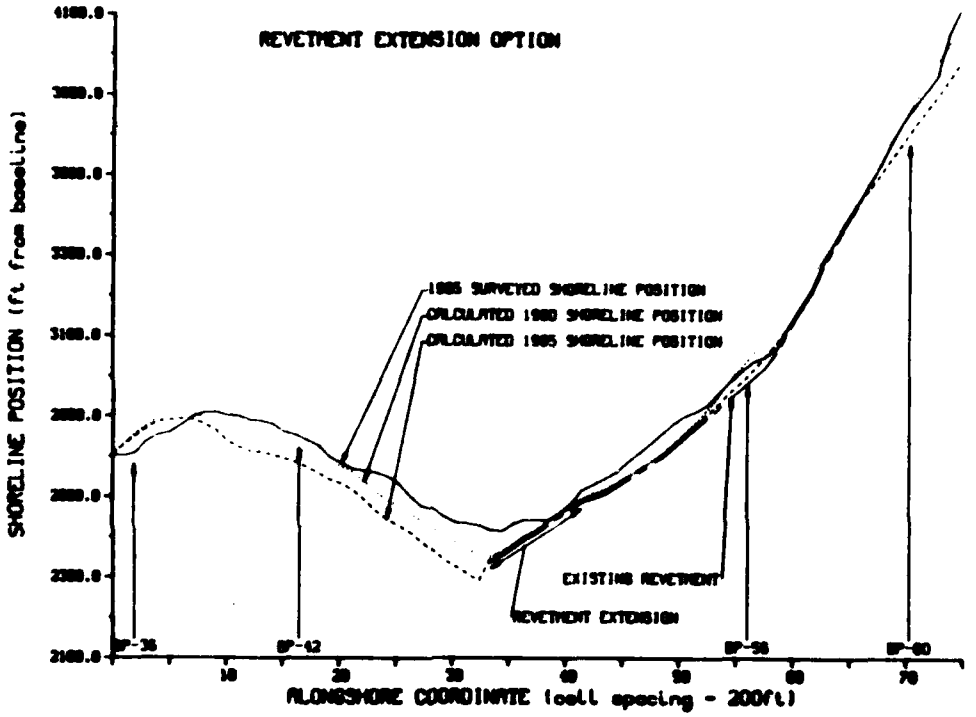

Figure C5. Results of Alternative 2A

Option 3: revetment extension with beach fill

39. The revetment with beach-fill option was executed for two different fill lengths and beach widths. The beach fills are specified to occur at 5-year intervals, and the plotted shoreline positions are those that exist just prior to renourishment. The results of the four alternatives evaluated for this option are shown in Figures C6 to C9. Alternatives 3A and 3B are identical to 3C and 3D except that the berm width of the beach fill is 50 ft in 3A and 3B; whereas in Alternatives 3C and 3D the beach-fill width is 100 ft. The location of the beach fill (between longshore coordinates 30 and 40 for Alternatives 3A and 3C and between longshore coordinates 25 and 35 for

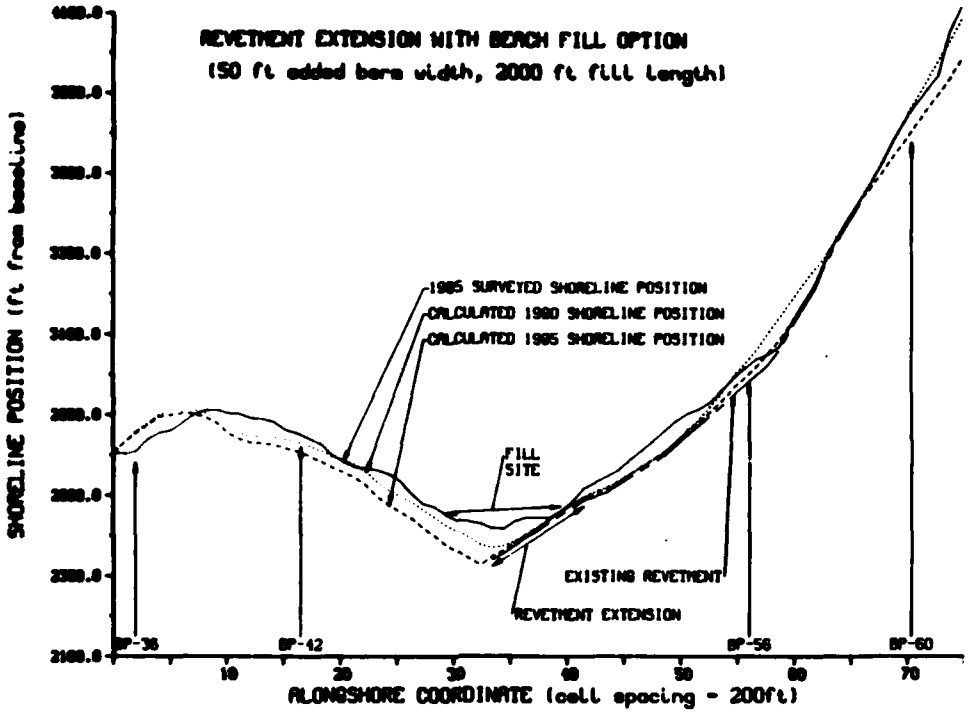

Figure C6. Results of Alternative 3A

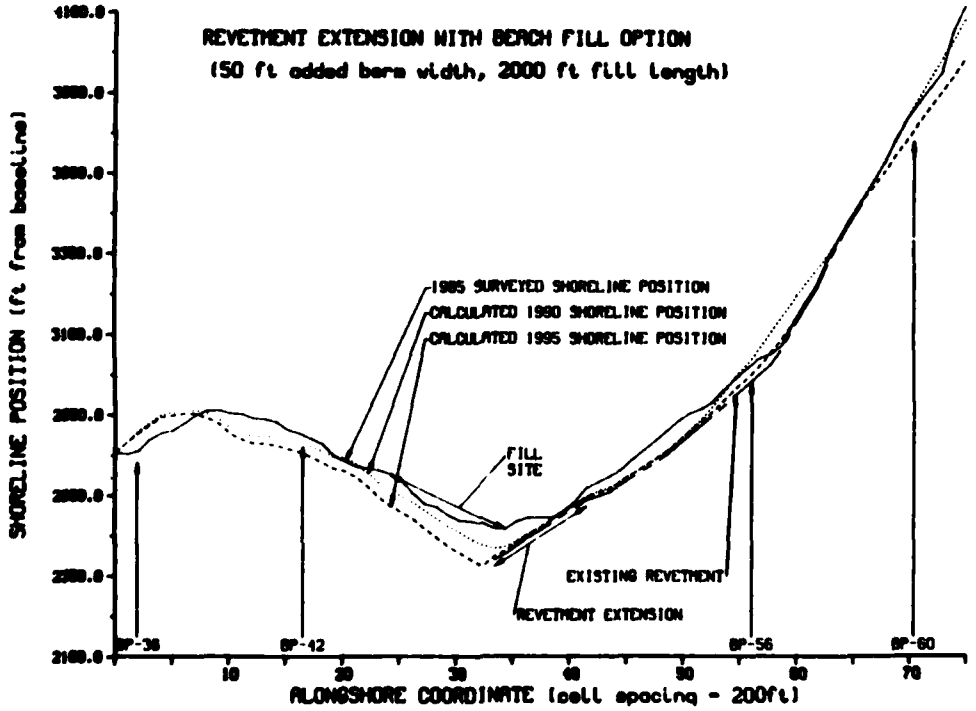

Figure C7. Results of Alternative 3B

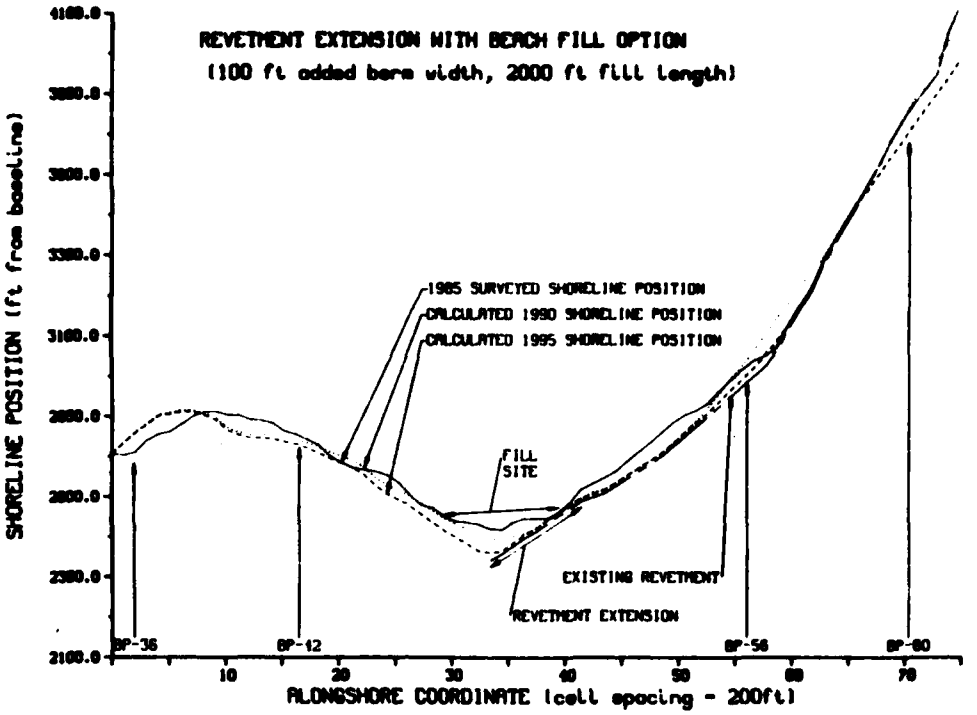

Figure C8. Results of Alternative 3C

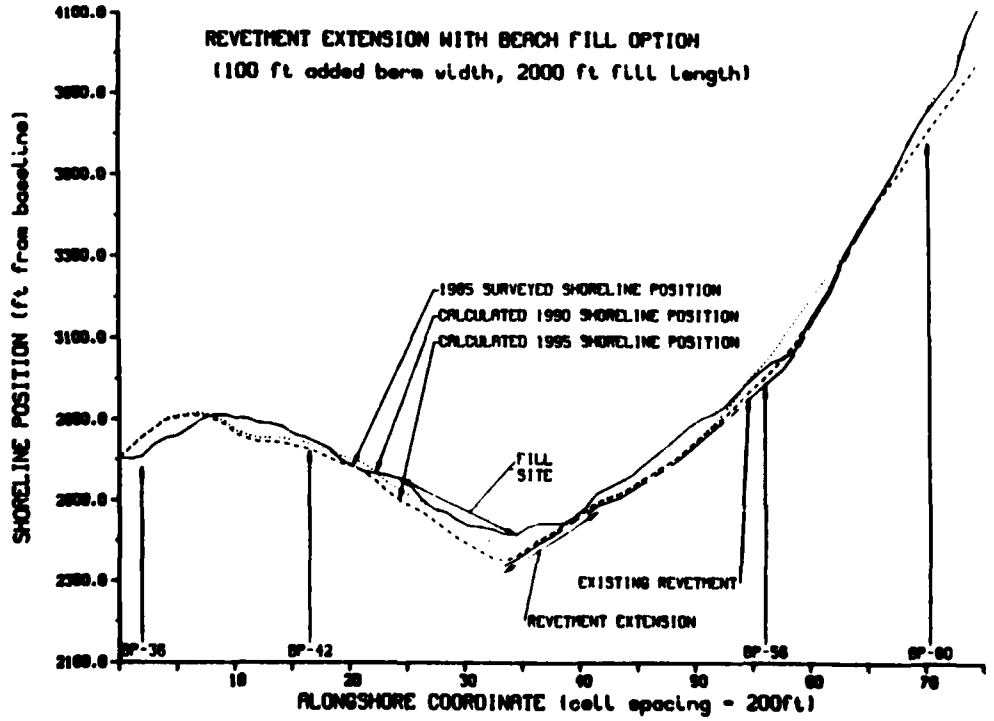

Figure C9. Results of Alternative 3D

Alternatives 3B and 3D) has essentially no impact on the resulting shoreline change. For Alternatives 3A and 3B, erosion downdrift of the revetment should be expected. Since this option calls for only 2,000 lin ft of beach fill, less shoreline erosion can be expected to occur if the length of the beach fill were increased. For instance, if the beach-fill length were increased to 7,600 ft or 3,800 ft, the predicted shoreline for Alternatives 3A and 3B would be similar to that for Alternatives 4A and 4B discussed below.

Option 4: beach fill

40. The beach-fill option was executed for four alternatives. The shorelines are plotted for the time corresponding to just prior to renourishment. The beach fills occur at 5-year intervals beginning in year one of the model of simulation. Alternative 4A, shown in Figure C10, is the result of the model simulation of the beach-fill option with an added berm width of 50 ft extending 7,600 ft longshore (between BP-42 and BP-56). Alternative 4B, shown in Figure C11, is identical to Alternative 4A except that the fill area has been reduced by half in length to 3,800 lin ft (between longshore coordinates 37 and 56). The results of this model simulation (Alternative 4B) show

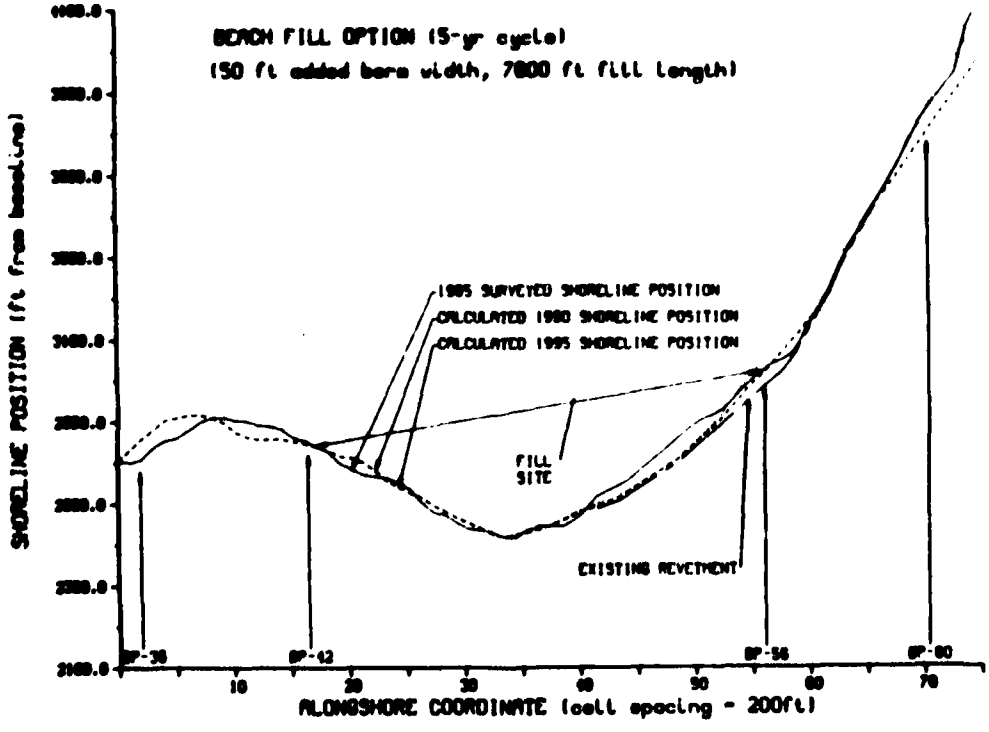

Figure C10. Results of Alternative 4A

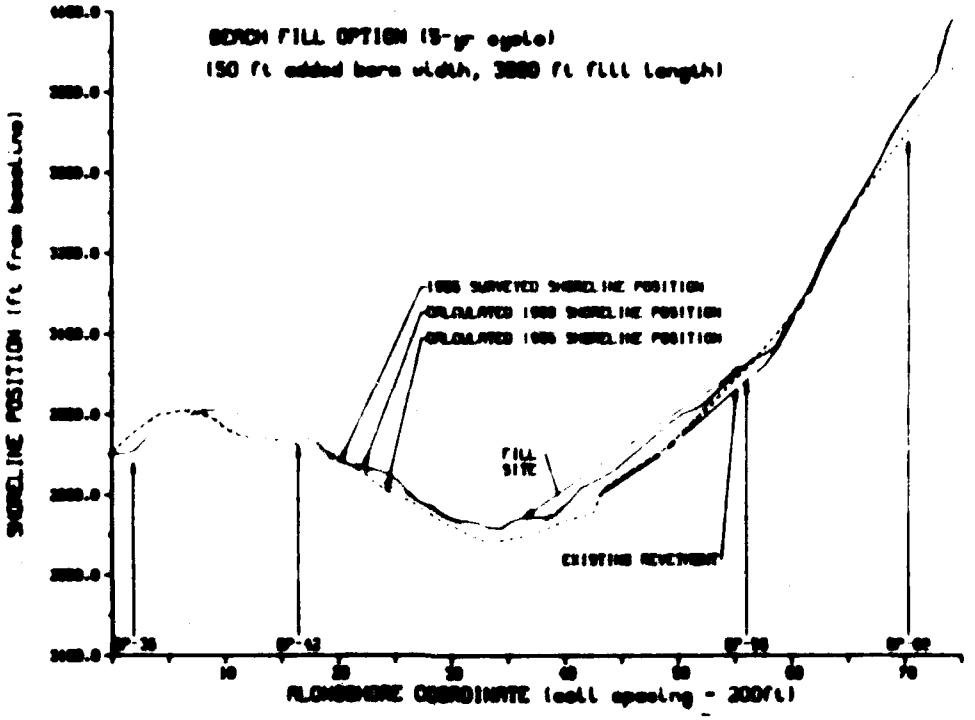

Figure C11. Results of Alternative 4B

that the average coastal erosion between BP-42 and BP-56 is greater than that in Alternative 4A, but it is noted that in both cases the shoreline in front of the revetment has receded to the revetment and is constrained at that location. Hence, the source of the littoral material (as determined from the wave conditions) moving toward the tip of the Spit is the downdrift side of the revetment, and the prescribed quantity of beach fill is no longer sufficient to maintain the shoreline in the vicinity of the 1985 surveyed shoreline position. Model simulations of Alternatives 4C and 4D, shown in Figures C12 and C13, respectively, indicate the effect of increasing the berm width of the beach fill from 50 to 75 ft. This specified increase in fill volume appears sufficient to maintain the shoreline close to its present location for the larger fill area specified in Alternative 4C (Figure C12). The smaller fill area simulated in Alternative 4D and shown in Figure C13 is not adequate to prevent erosion of the shoreline in front of the revetment.

Option 5: breakwater

41. The breakwater option was run for six alternatives, and its investigation required considerable additional effort. In order to obtain improved resolution of shoreline change in the vicinity of the breakwaters, the

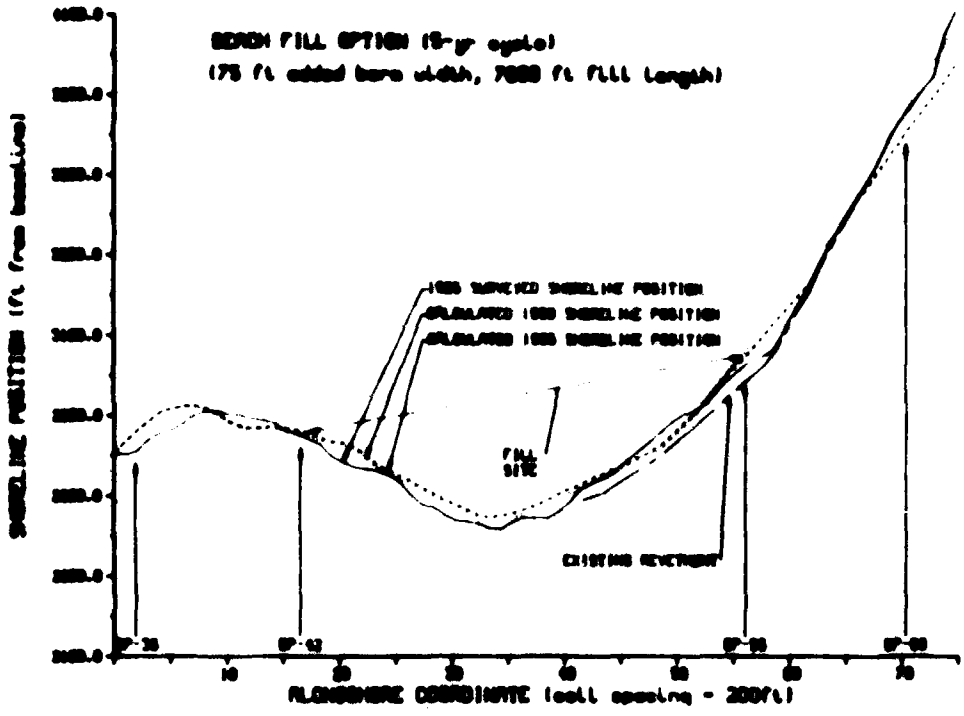

Figure C12. Results of Alternative 4C

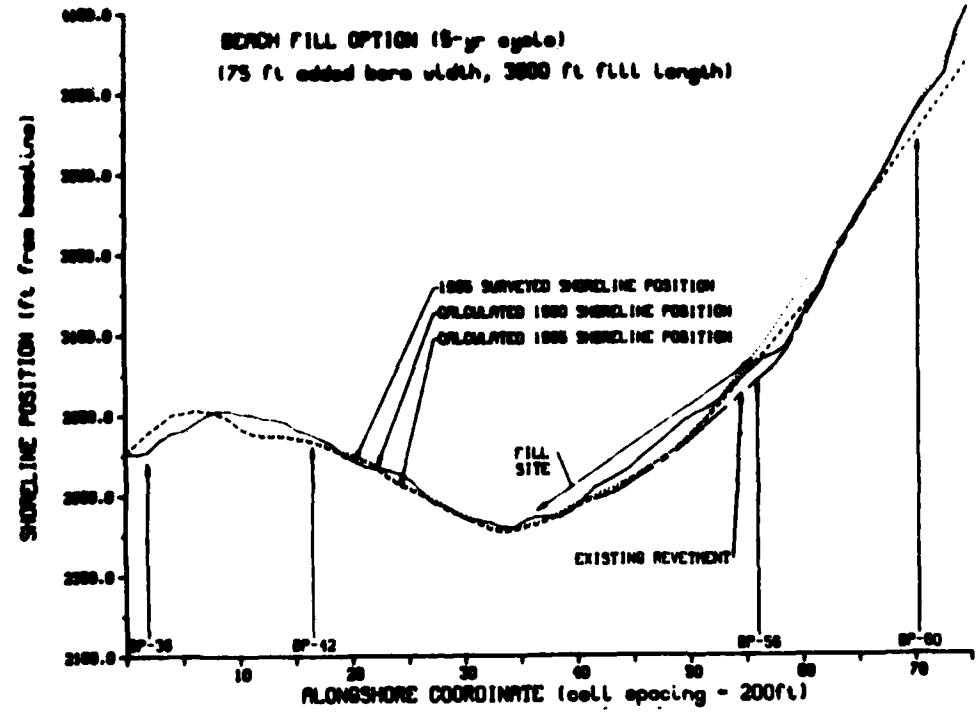

Figure C13. Results of Alternative 4D

longshore cell spacing was reduced from 200 to 100 ft. In addition, to maintain numerical accuracy with the reduced cell spacing, the time-step was decreased. The 100-ft longshore cell spacing provided a minimum of five calculation points per breakwater and was considered sufficient for an estimate of the effect a breakwater would have on shoreline change at Homer Spit. As a result of these changes, the execution time of the model for these alternatives tripled. The breakwaters were modeled to locate on the tidal flats. The elevation of their bases ranged between 1 and 4 ft above mean lower low water. The shoreline model is not capable of simulating a submerged breakwater; hence, the crest elevation was assumed to be greater than the high tide water level. It is assumed, however, that a breakwater with a crest elevation high enough that it would be exposed at mean tide but submerged at high tide would produce similar shoreline change. Alternatives 5A and 5B, shown in Figures C14 and C15, respectively, indicate that a breakwater positioned offshore of the end of the existing revetment would reduce the severe erosion expected immediately downdrift of the revetment. In both cases, however, the erosion is transferred or migrates toward the end of the

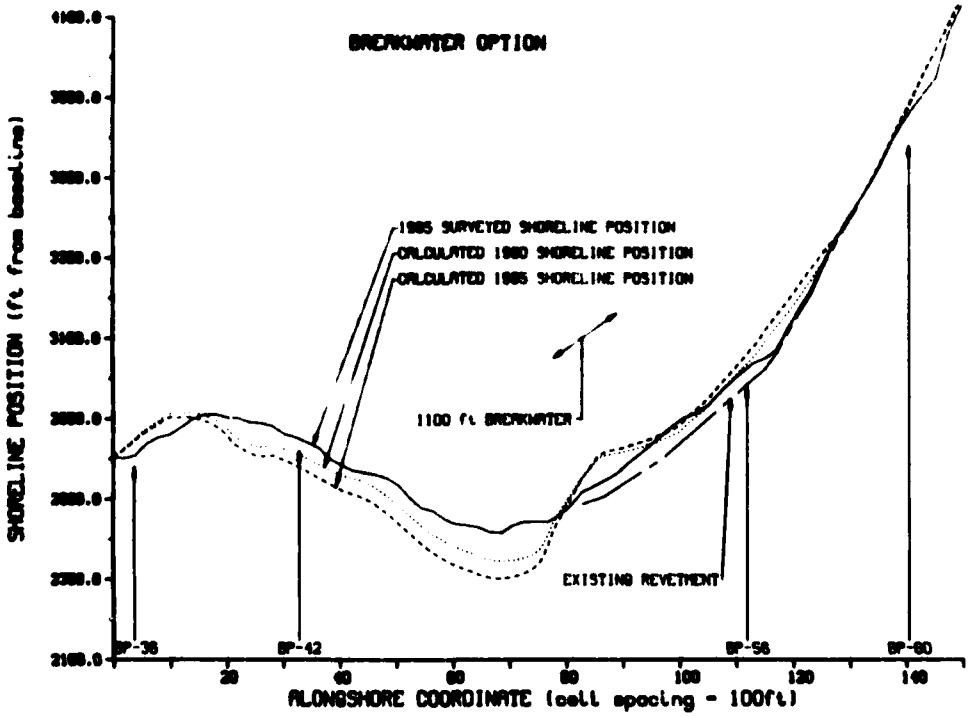

Figure C14. Results of Alternative 5A

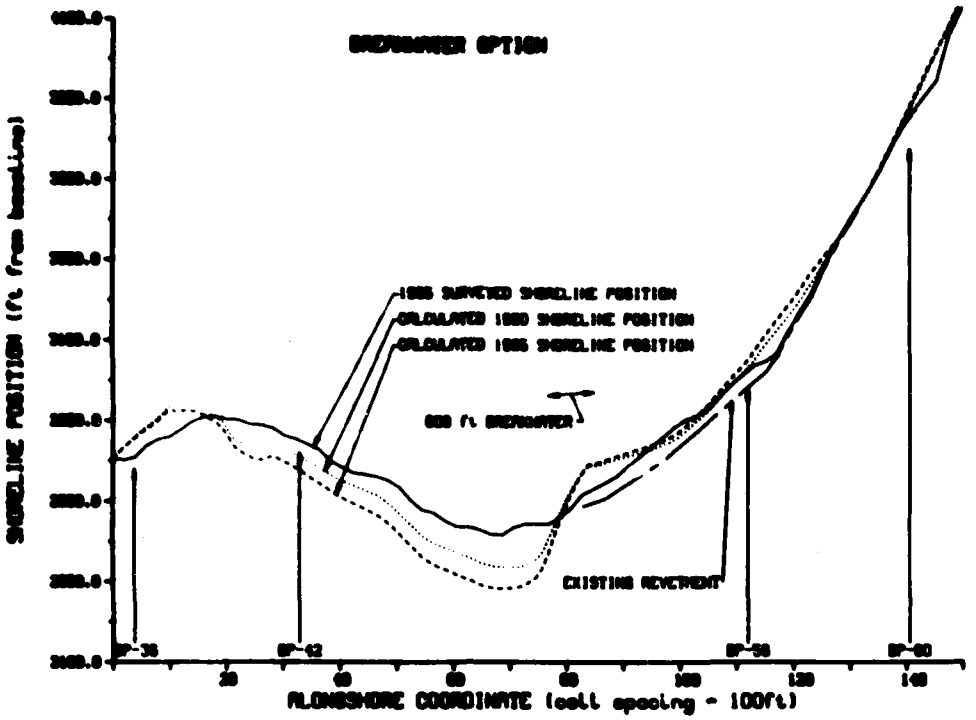

Figure C15. Results of Alternative 5B

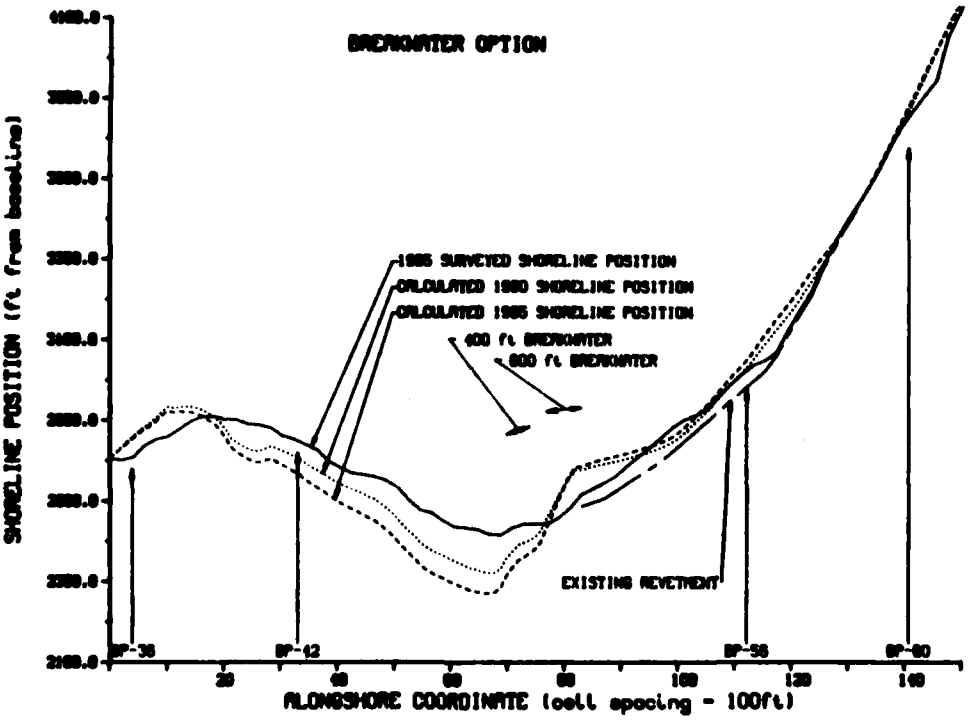

Figure C16. Results of Alternative 5C

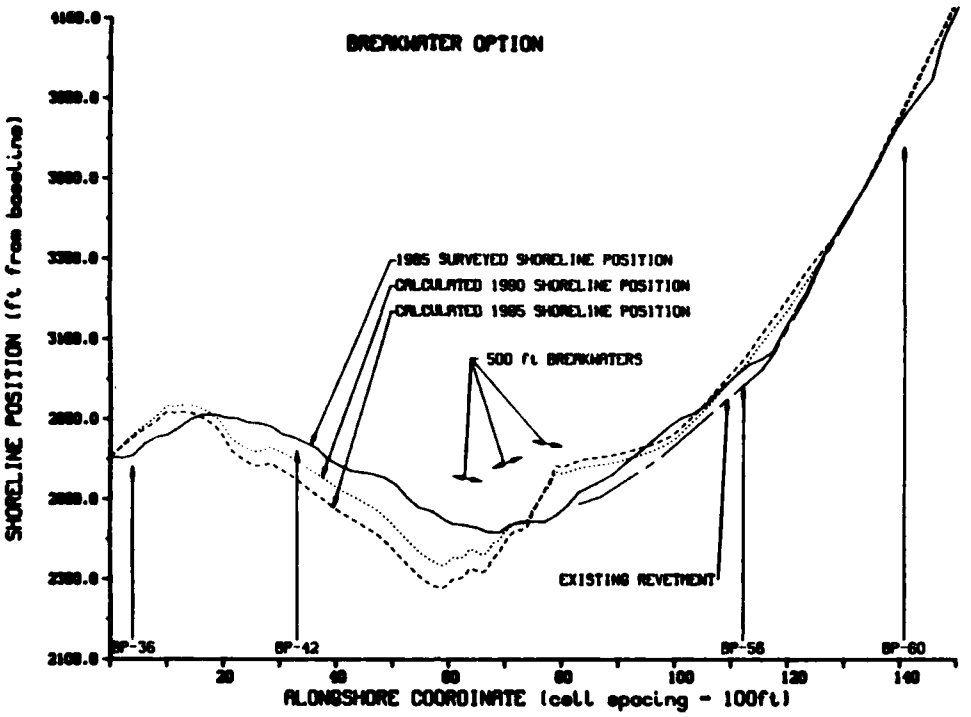

Figure C17. Results of Alternative 5D

Spit. Alternatives 5C through 5F, shown in Figures C16 through C19, represent several variations on the breakwater option in which an attempt was made to reduce the severity of the erosion at any one location. The configuration of the breakwaters as specified in Alternatives 5E and 5F, shown in Figures C18 and C19, respectively, resulted in minimizing the maximum erosion.

Summary and Conclusions

42. Comparison of the 16 alternative erosion control measures modeled in this study was accomplished by selecting one alternative from each of the general design options discussed above. The criterion for selection of the best alternative from the generic design option was that the shoreline position resulting from the model simulation after the given time interval remained closest to the 1985 surveyed shoreline position (that is, the alternative resulting in the least shoreline erosion over the given time interval). The selected alternatives were 1A, 2A, 3C, 4C, and 5F. A plot of the shoreline positions for each of the selected alternatives at the end of simulated 5- and 10-year intervals (of model simulation) is given in Figures C20 and

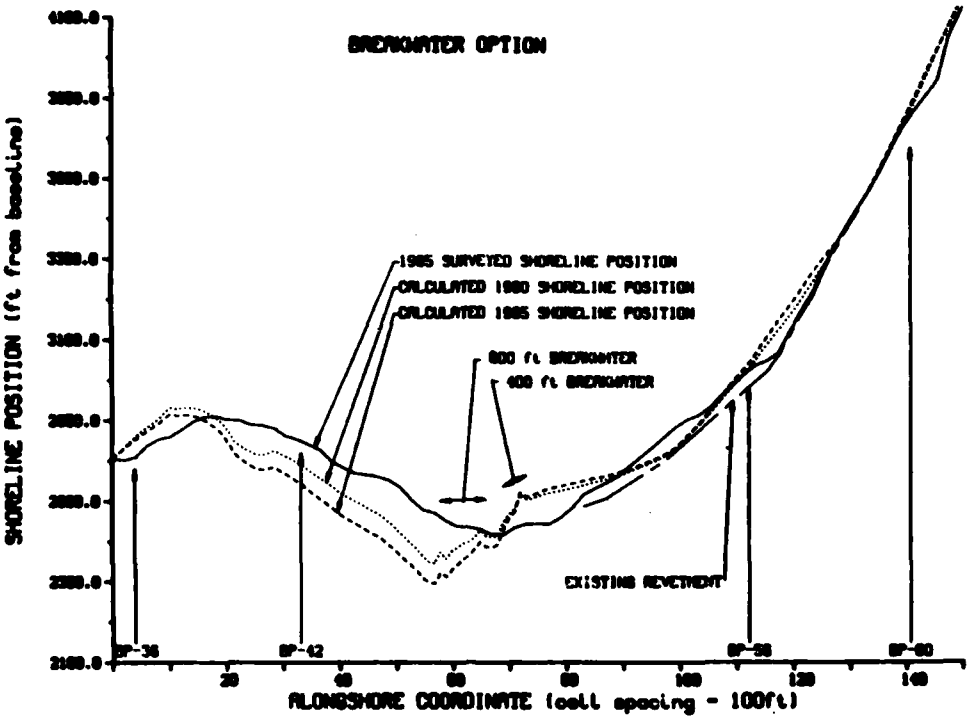

Figure C18. Results of Alternative 5E

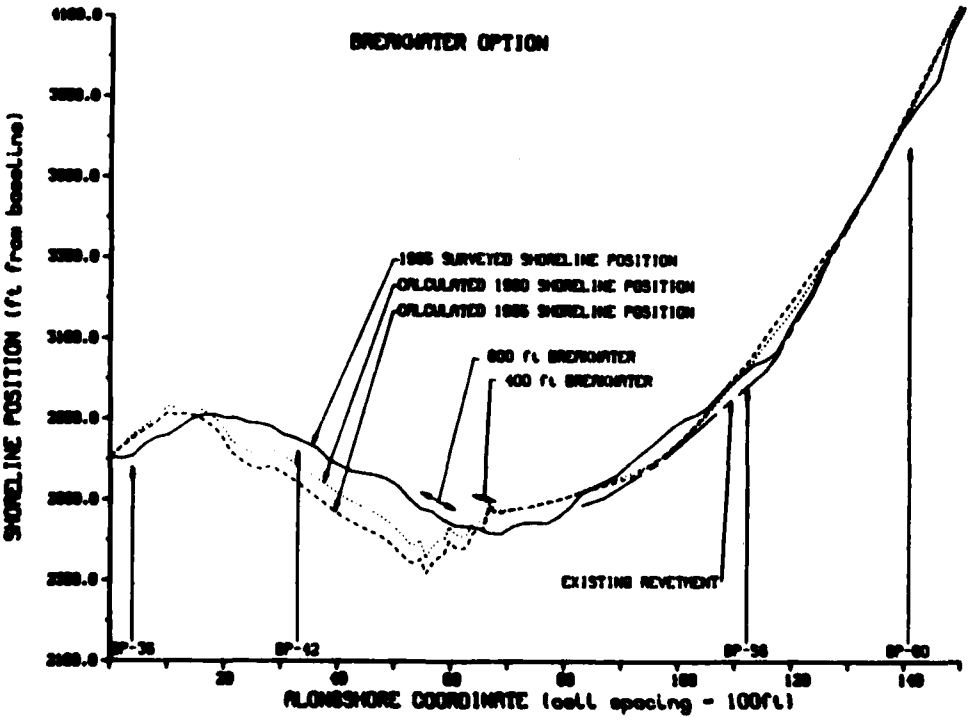

Figure 19. Results of Alternative 5F

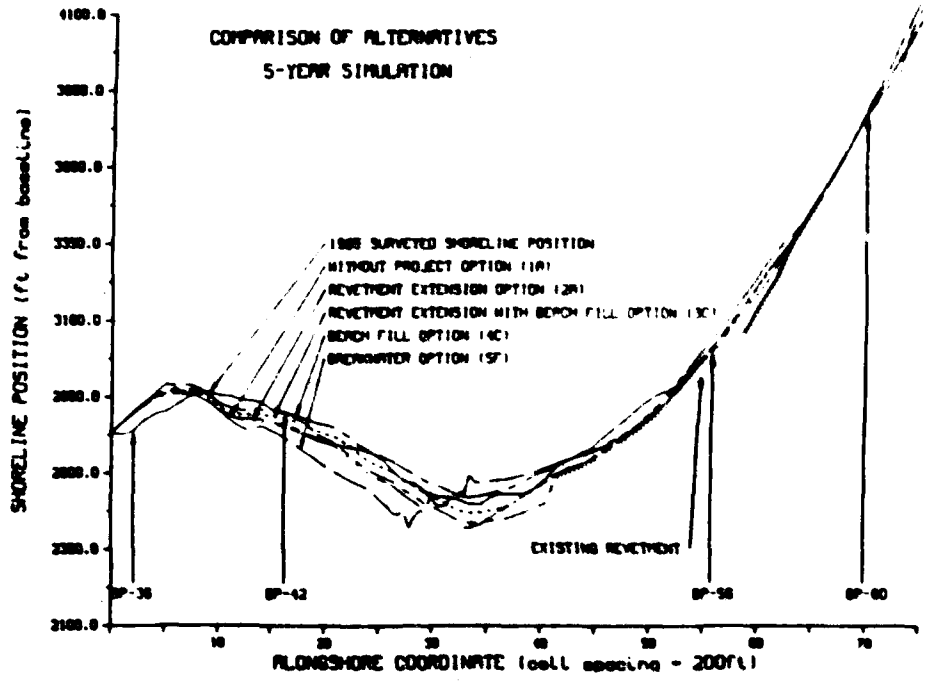

Figure C20. Comparison of alternatives, 5-year simulation

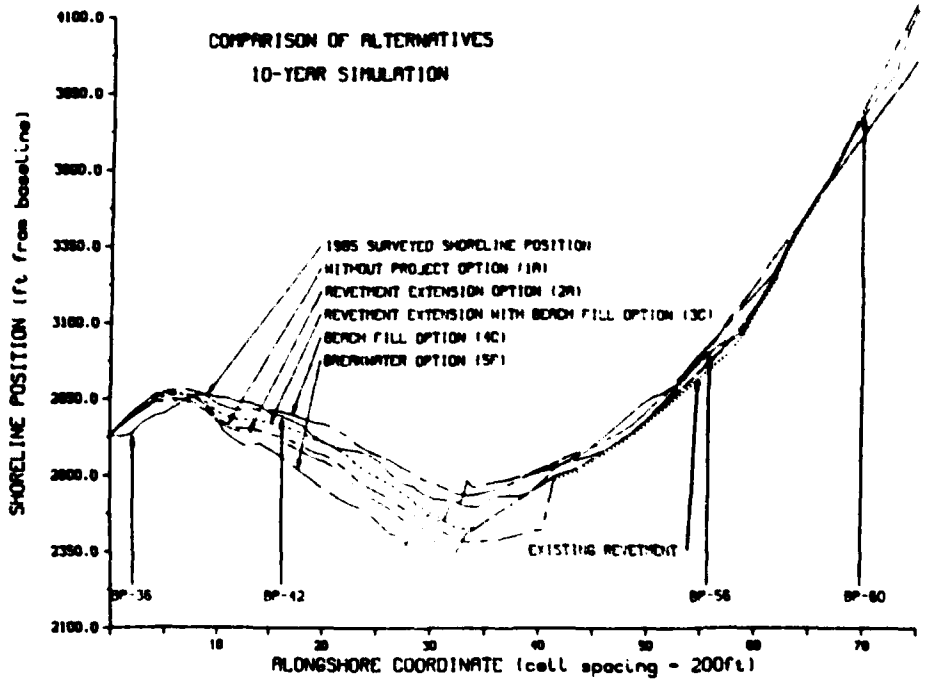

Figure C21. Comparison of alternatives, 10-year simulation

C21. Knowledge of the specific design parameters (e.g., the specified length and width of the beach fill) is necessary to properly differentiate among the given alternatives. Three of the alternatives shown indicate considerable erosion both at the 5- and 10-year interval and are not recommended for implementation at Homer Spit. These alternatives are the without-project option (1A), the revetment extension option (2A), and the breakwater option (5F). The remaining two alternatives are the revetment extension with beach-fill option (3C) and the beach-fill option (4C). It is difficult to determine which of these alternatives would best solve the coastal erosion problems at Homer Spit in that the extent of the specified beach fill will ultimately determine the shoreline position. However, the model simulations of shoreline evolution conducted in this study indicate that nourishment of the Spit is required to control the coastal erosion problems. A structural approach without beach nourishment may resolve a local problem, but the area of erosion will migrate to downdrift locations toward the distal end of the Spit.

APPENDIX D: BEACH SURVEYS

Introduction

1. During the period from 1984 to 1986 four field beach surveys (August 1984, August 1985, May 1986, and August 1986) were conducted at Homer Spit by the Alaska Department of Transportation and by the US Army Engineer District, Alaska. These surveys followed preestablished profile stations documented in Appendix C of Smith et al. (1985). More than 60 beach profiles were measured during each survey from the baseline to points approximately 10 ft below mean lower low water (MLLW) (1,600-1,800 ft offshore). Although the surveys were planned for establishing a data base for long-term beach erosion assessment, an interim evaluation of the obtained data was performed to assist the formulation of beach erosion protection plans and to assess volumetric profile changes in the vicinity of the sheet-pile seawall. This appendix summarizes the interim study results.

Spit Erosion

2. Beach profiles measured at the southwestern shoreline of the Spit were analyzed to determine the cross-sectional changes of the beach face. Profile comparisons were made by using data obtained from selected profiling stations with numbers from 1 to 60 (see Figure D1) for 1984-85, 1985-86, and 1984-86. Table D1 summarizes results of 22 profiles that were analyzed. Changes in cross-sectional areas are presented by "cut" and "fill" (Table D1) that represent, respectively, the erosionary and accretionary changes. Figures D2, D3, D4, and D5 illustrate the profile comparisons at beach profile BP-34, BP-47, BP-48, and BP-56, respectively. It should be noted that although both cut and fill may occur at the same beach cross section, a beach may appear to be erosionary if a smaller cut occurs at the upper beach or the high tide terrace and a larger fill occurs at the lower portion of the beach. BP-48 gives a typical example of upper beach erosion from 1984-85 (Figure D4).

3. From August 1984 to August 1985 the southwestern beach experienced an accretionary process. Except for BP-38, all the fill volumes listed in Table D1 were greater than cut volumes. This accretionary process was reversed during the 1985-86 period and the volumetric calculations indicate

AD-A187 016 BEACH EROSION CONTROL STUDY HOMER SPIT ALASKA(U) 2/2
COASTAL ENGINEERING RESEARCH CENTER VICKSBURG MS
Y CHU ET AL SEP 87 CERC-87-15

UNCLASSIFIED F/G 8/3 NL

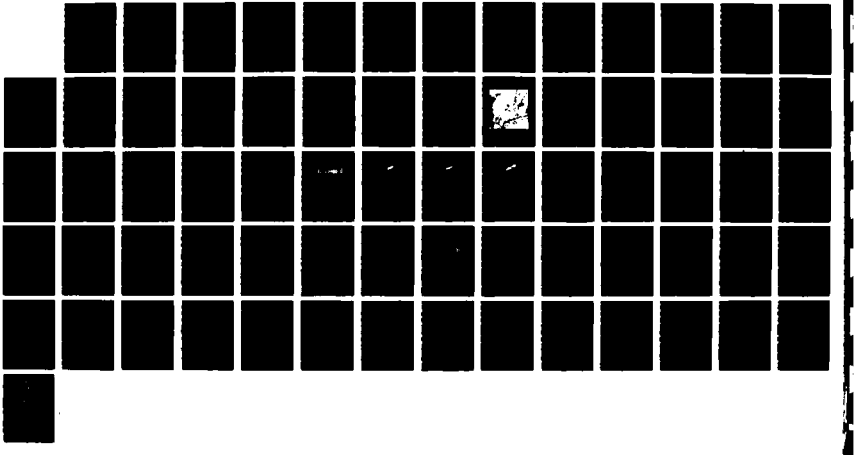

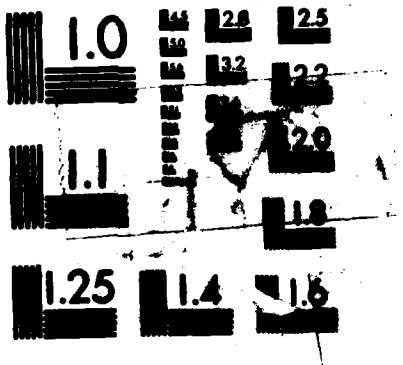

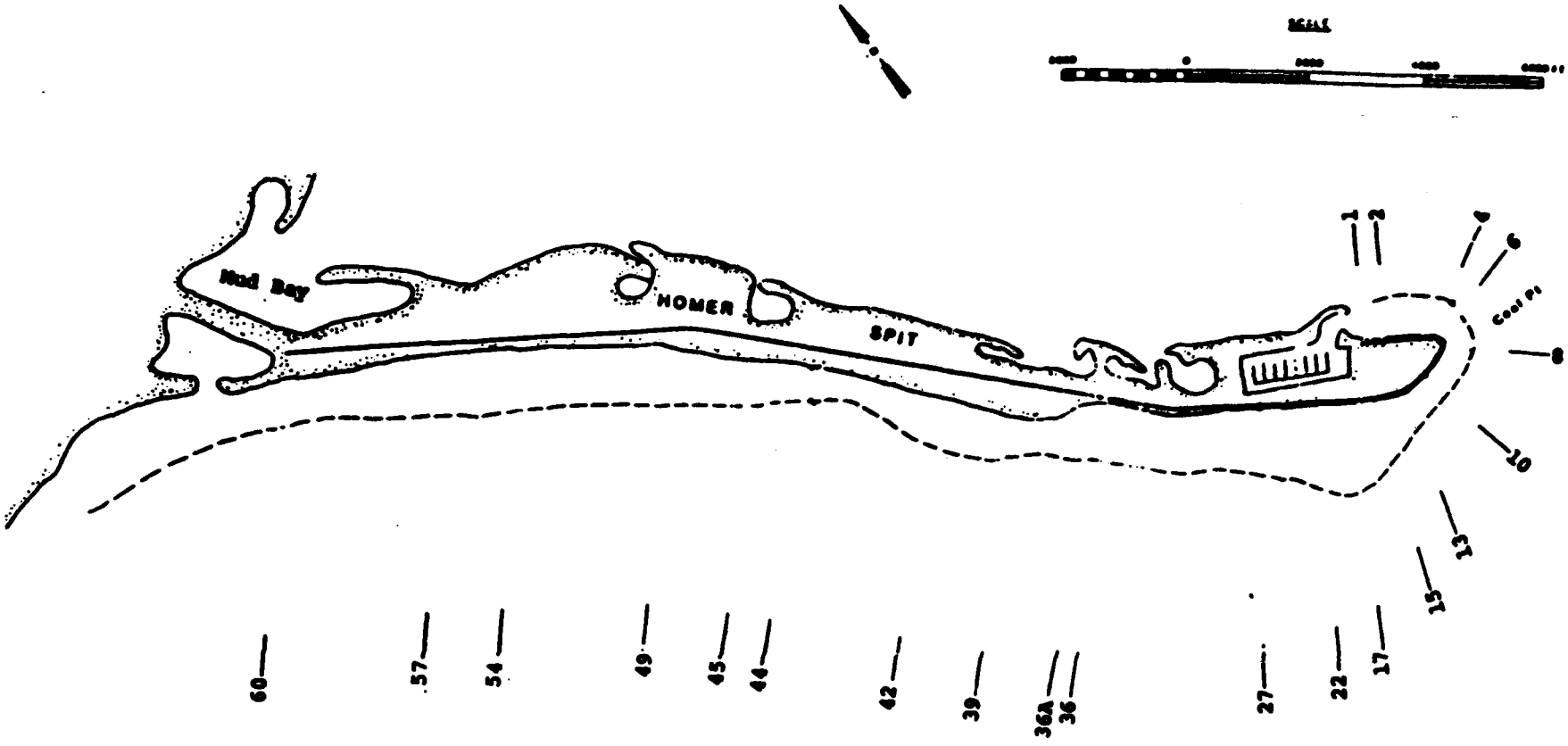

Figure D1. Beach profile locations for 1984-86

Table D1

Summary of Beach Profiles Comparison

Profile	Station No.	Quantity, cu ft/ft					
		1984-85		1985-86		1984-86	
		Cut	Fill	Cut	Fill	Cut	Fill
BP-20	13700.6	85	824	1,154	437	757	780
BP-25	14700.6	324	998	1,693	120	1,556	639
BP-31	15721.2	341	917	525	537	523	1,112
BP-34	16721.2	461	708	1,175	348	1,048	468
BP-38	18366.1	1,070	478	700	316	1,412	440
BP-40	19366.1	181	495	686	392	697	718
BP-42	20438.5	122	501	847	133	468	132
BP-43	21597.5	424	736	1,014	59	755	111
BP-44	22797.5	260	624	751	195	516	291
BP-46	23997.5	314	668	402	251	432	635
BP-47	24497.5	270	932	1,203	745	498	788
BP-48	24697.5	439	1,162	1,089	737	443	827
BP-49	24897.5	463	1,059	1,145	574	611	658
BP-50	25397.5	269	954	982	311	332	310
BP-51	25897.5	566	922	515	569	276	674
BP-52	26397.5	339	1,143	1,174	288	263	285
BP-53	26897.5	394	942	1,334	298	715	227
BP-54	27586.2	700	893	765	693	300	422
BP-56	28359.3	406	2,324	1,127	267	79	1,251
BP-58	29539.5	568	895	960	590	360	317
BP-59	30539.6	276	1,160	1,246	135	435	208
BP-60	31539.6	67	852	457	932	195	1,455

Note: All three surveys were conducted during the month of August. "Cut" and "fill" quantities are measured in cubic feet per foot of shore and are interpreted as erosion and accretion, respectively. Calculations of changes for each profile were made from base points to points approximately 1,400-1,800 ft offshore.

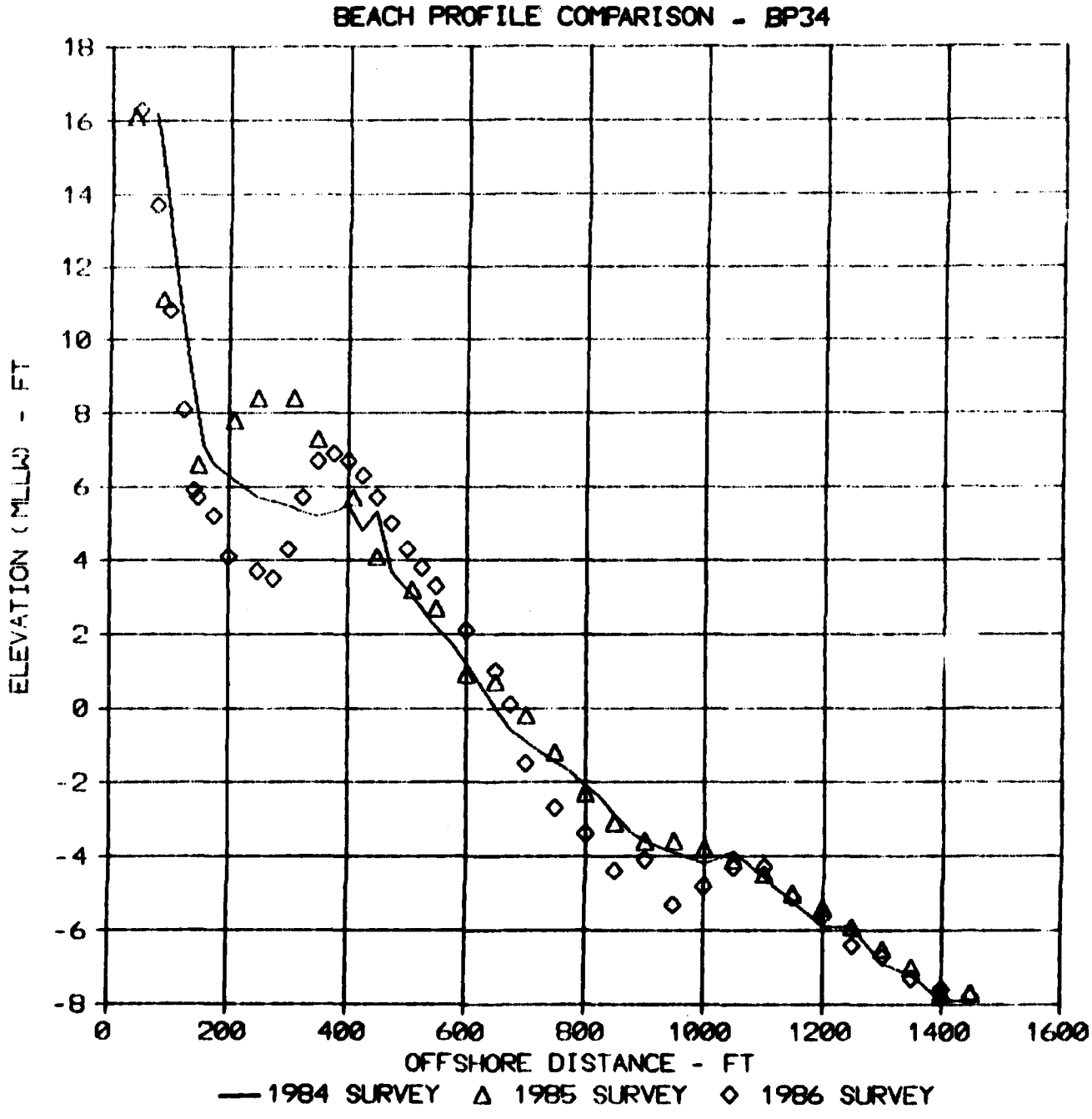

Figure D2. Comparison of August beach profiles, BP-34

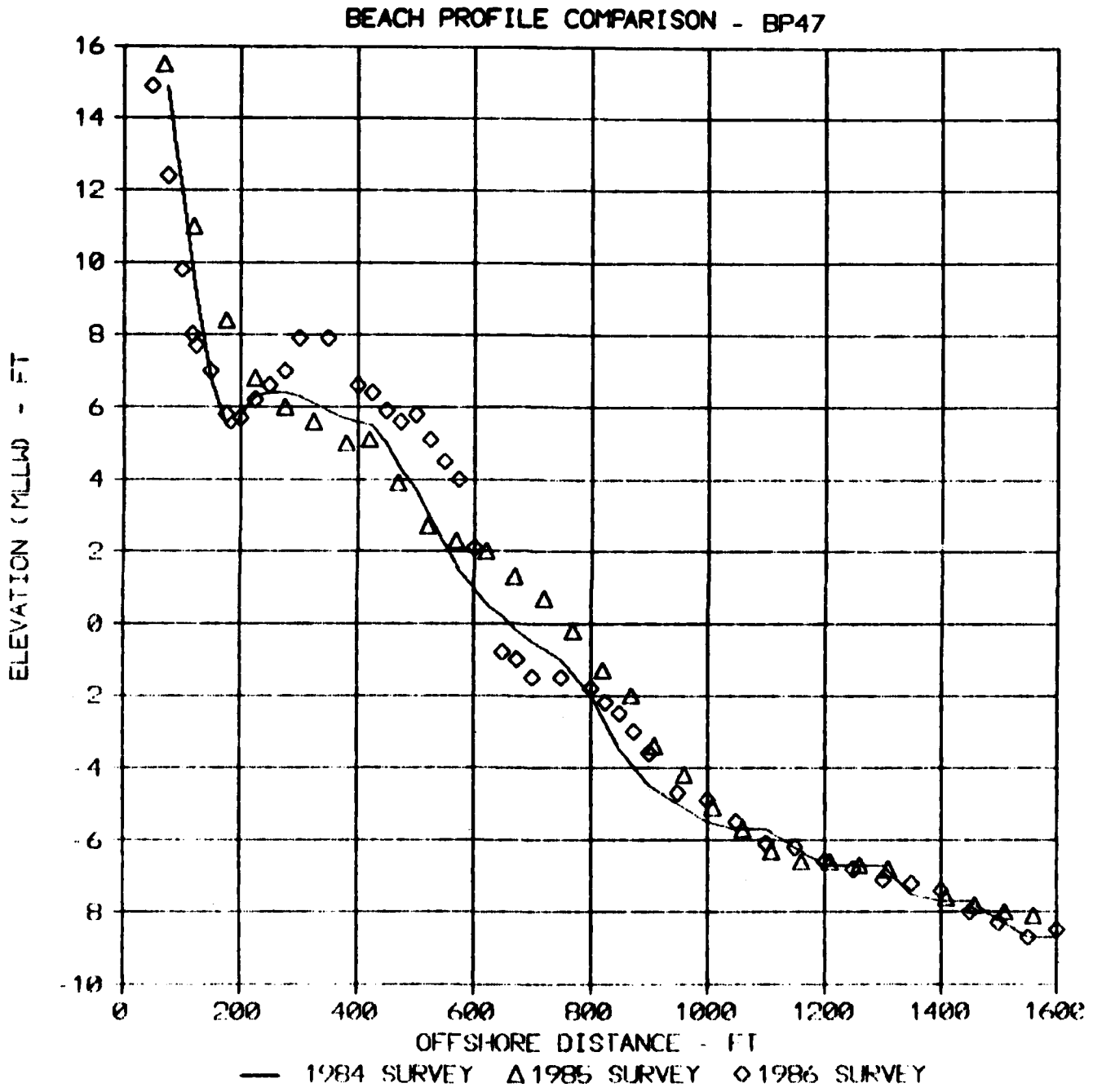

Figure D3. Comparison of August beach profiles, BP-47

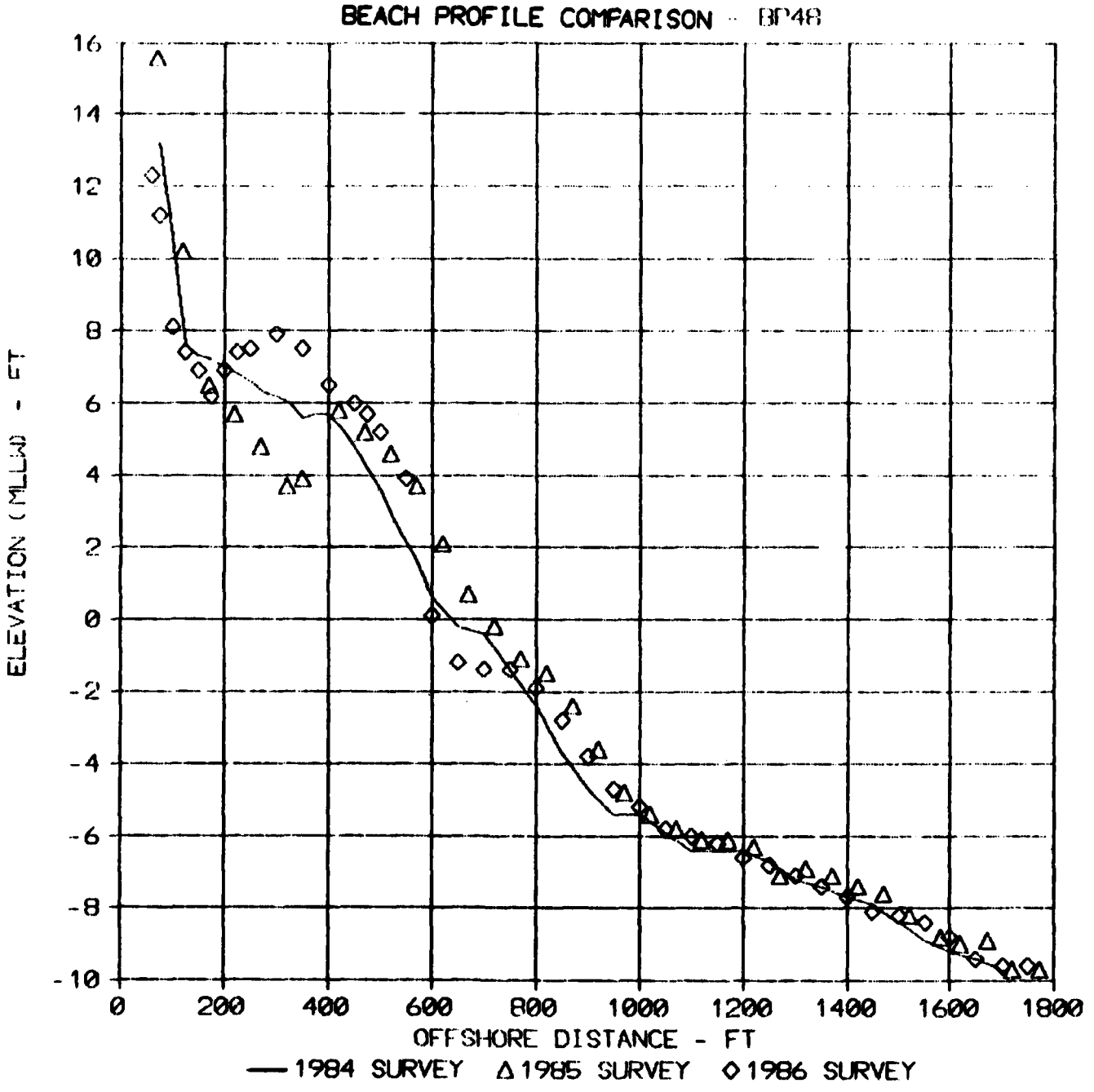

Figure D4. Comparison of August beach profiles, BP-48

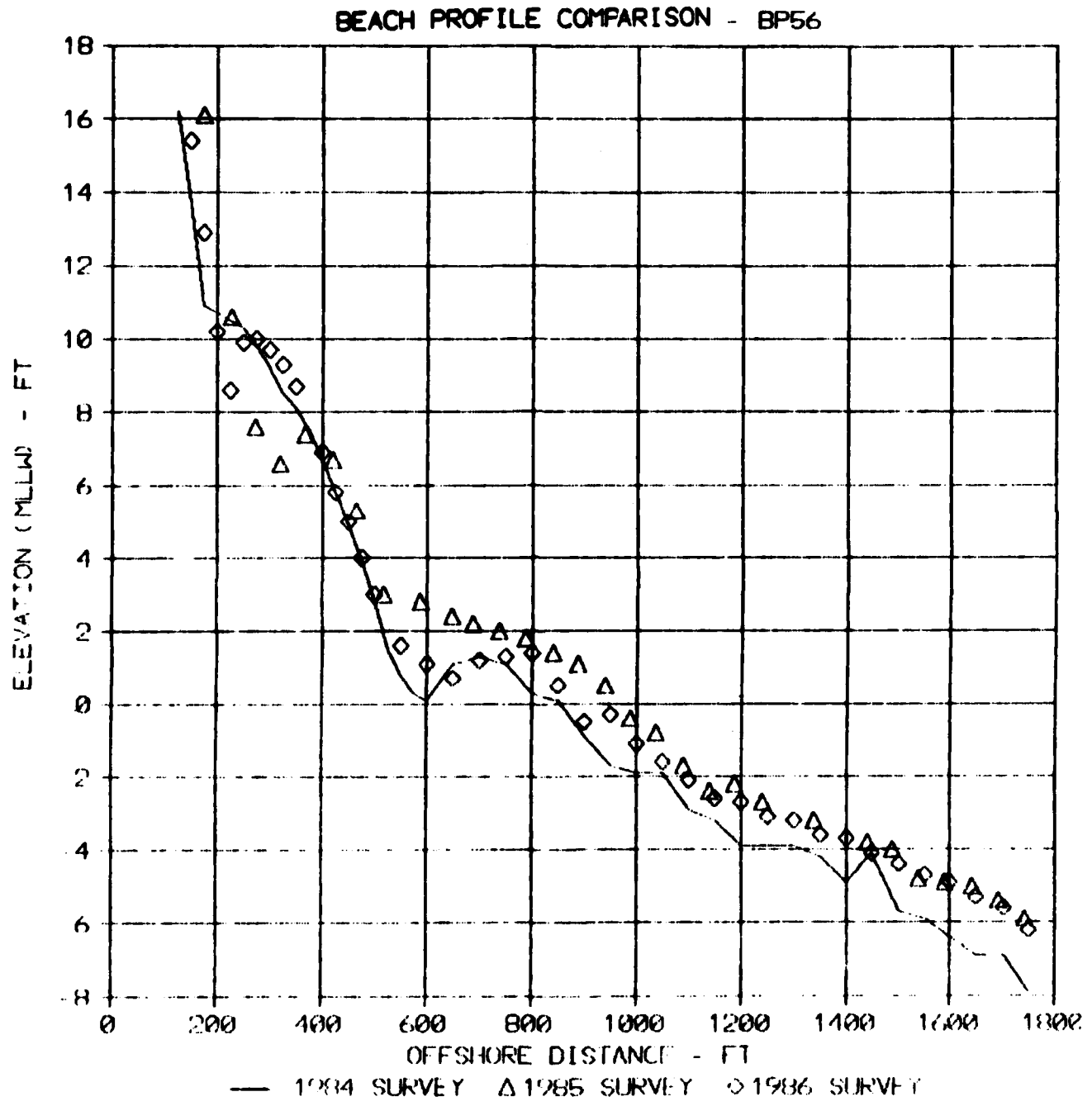

Figure D5. Comparison of August beach profiles, BP-56

that the Spit was in an erosionary phase. In view of the relatively short period of data record and the contributing erosion factors, such as the intensity of seasonal storms, the reversal of beach erosion processes does not seem physically significant. Figures D6 and D7 exhibit the nearshore bathymetry of the project area during August 1985 and 1986, respectively. These figures suggest the presence of standing waves in front of the sheet-pile seawall and rubble revetment. Standing waves are the results of partial reflection of incident wave energy caused by shoreline structures. The resulting higher wave amplitude and water particle velocities in front of the seawall will further aggravate the situation of wave overtopping, roadway flooding, and local scouring of beach material during storm events.

4. The distance between BP-20 and BP-60 is approximately 3.4 miles. Within this reach, a net accretion of the 1984-85 period was estimated to be 304,000 cu yd; whereas, a net erosion of the 1985-86 period was 390,000 cu yd, giving a net of 86,000 cu yd of profile erosion for the 2-year study period. Figure D8 shows the variation of accretion-erosion estimates along the southwestern shoreline. In this figure, erosion occurred along the lower half of the Spit near the distal end, while accretion occurred at the upper half near the Spit base.

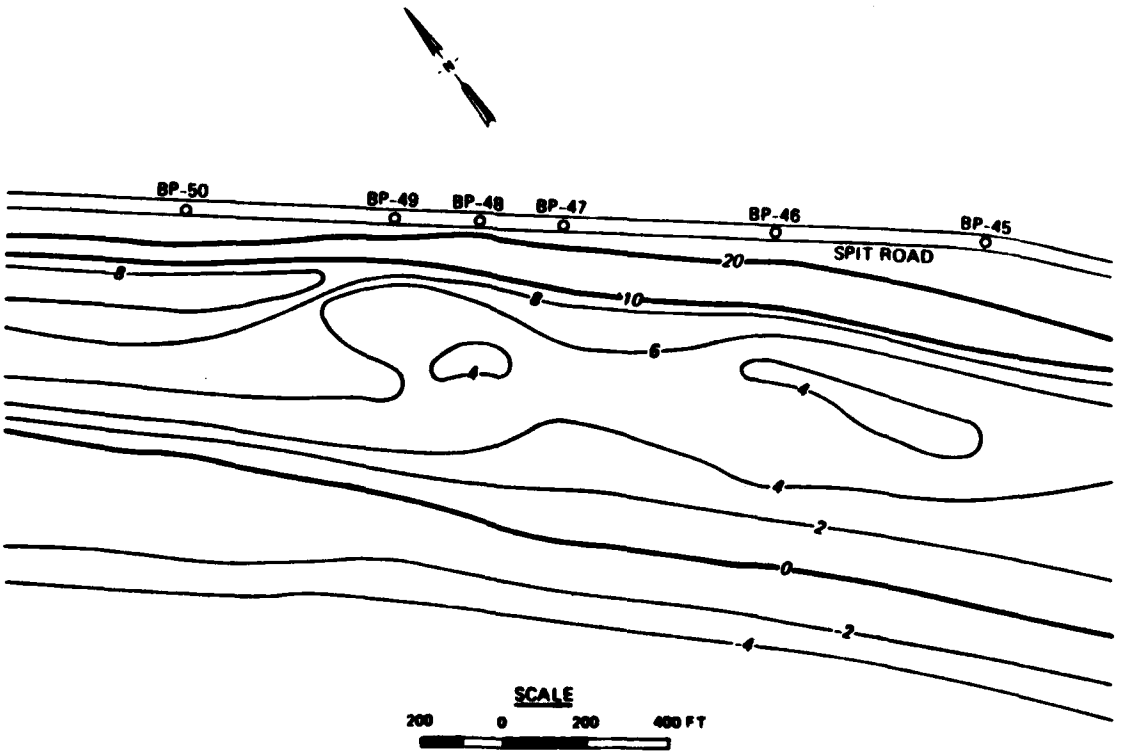

Figure D6. Nearshore bathymetry, August 1985

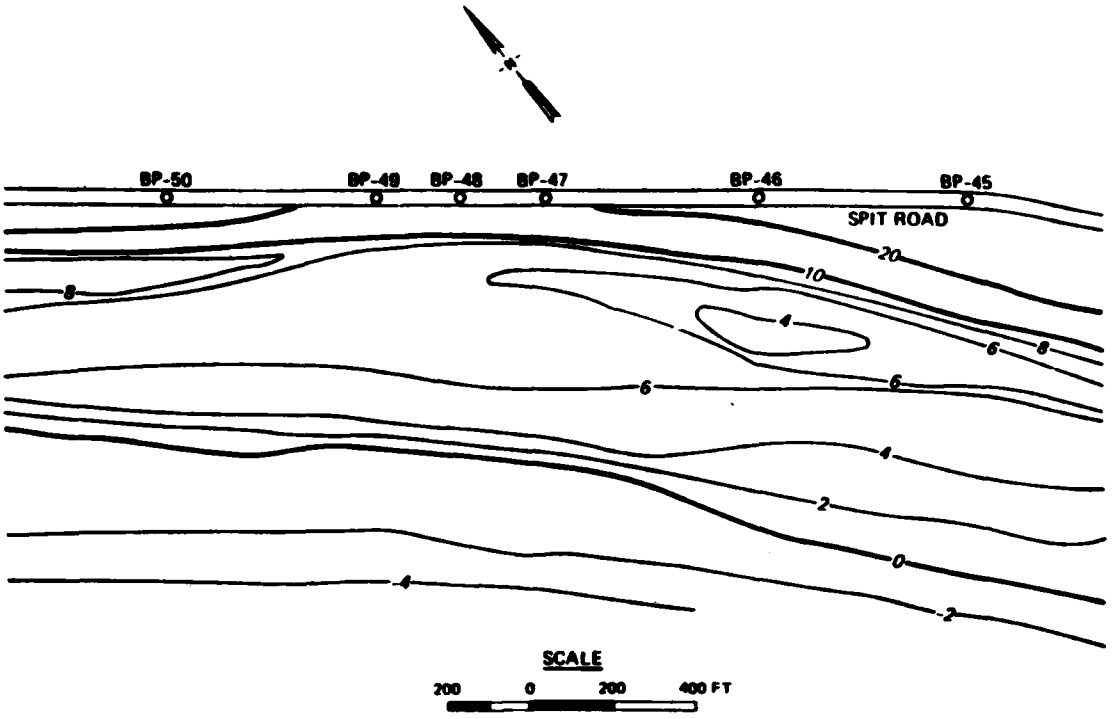

Figure D7. Nearshore bathymetry, August 1986

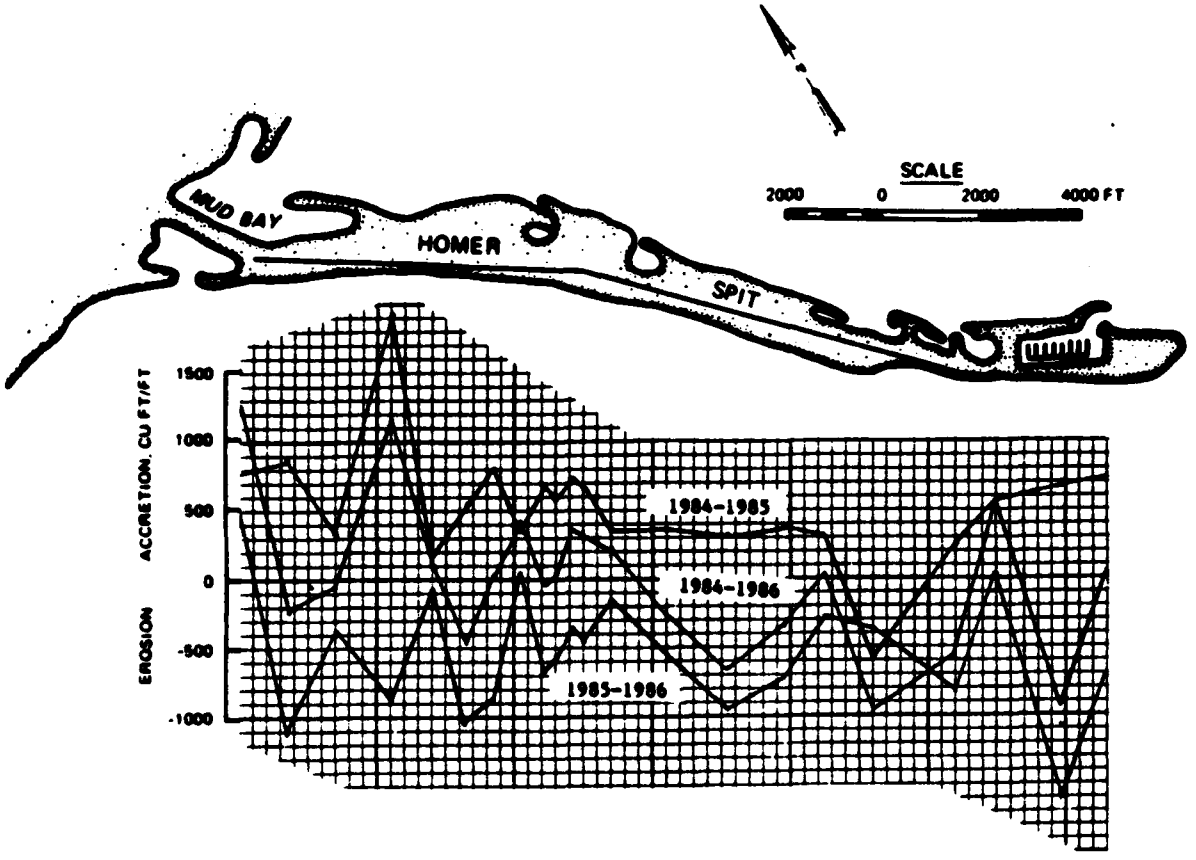

Figure D-8. Beach cross-sectional change, 1984-86

5. BP-47, BP-48, and BP-49 are located in front of the sheet-pile seawall. Beach profile data at these three stations was studied to compare the severity of erosion to that at other locations. Based on information presented in Table D1, erosion was not particularly severe for this reach during the study period. The present result does not imply that the severe erosion occurring at the seawall section has been revered. The duration of the 2-year data is too short to extrapolate a long-term trend. However, the data may suggest that the accelerated beach erosion process since the 1964 earthquake could have slowed down in recent years.

6. Figures D9, D10, and D11 illustrate comparisons between May 1986 beach profiles and August 1986 profiles at BP-34, BP-47, and BP-56, respectively. These three figures illustrate that beach profiles were reasonably stable during the summer of 1986. Winter storms can cause measurable profile alterations, as shown in Figures D12 and D13, the comparison of August 1985 and May 1986 beach profiles.

Conclusions

7. Repeated surveys of beach profiles at fixed profiling stations is the best way to define the accretionary-erosionary process. The annual summer survey program implemented at Homer Spit should be continued, preferably in August, to assess long-term beach erosion.

8. During the 2-year study period, erosion at the southwestern shore of Homer Spit was not excessive. Minor accretion occurred at the base of the Spit, including the segment where a steel sheet-pile seawall was erected. The formation of standing waves in front of the seawall contributes to wave overtopping, road flooding, and local scouring of beach material near the toe of the seawall.

9. There is a need for beach nourishment in front of the existing seawall to modify the local bathymetry and promote wave breaking during storm events. Based on obtained survey data, erosion at this segment was not excessive compared to that on the rest of the beach segment at the Spit. The deep bathymetry in the vicinity of the seawall, however, should be reduced for storm damage reduction and erosion control purposes.

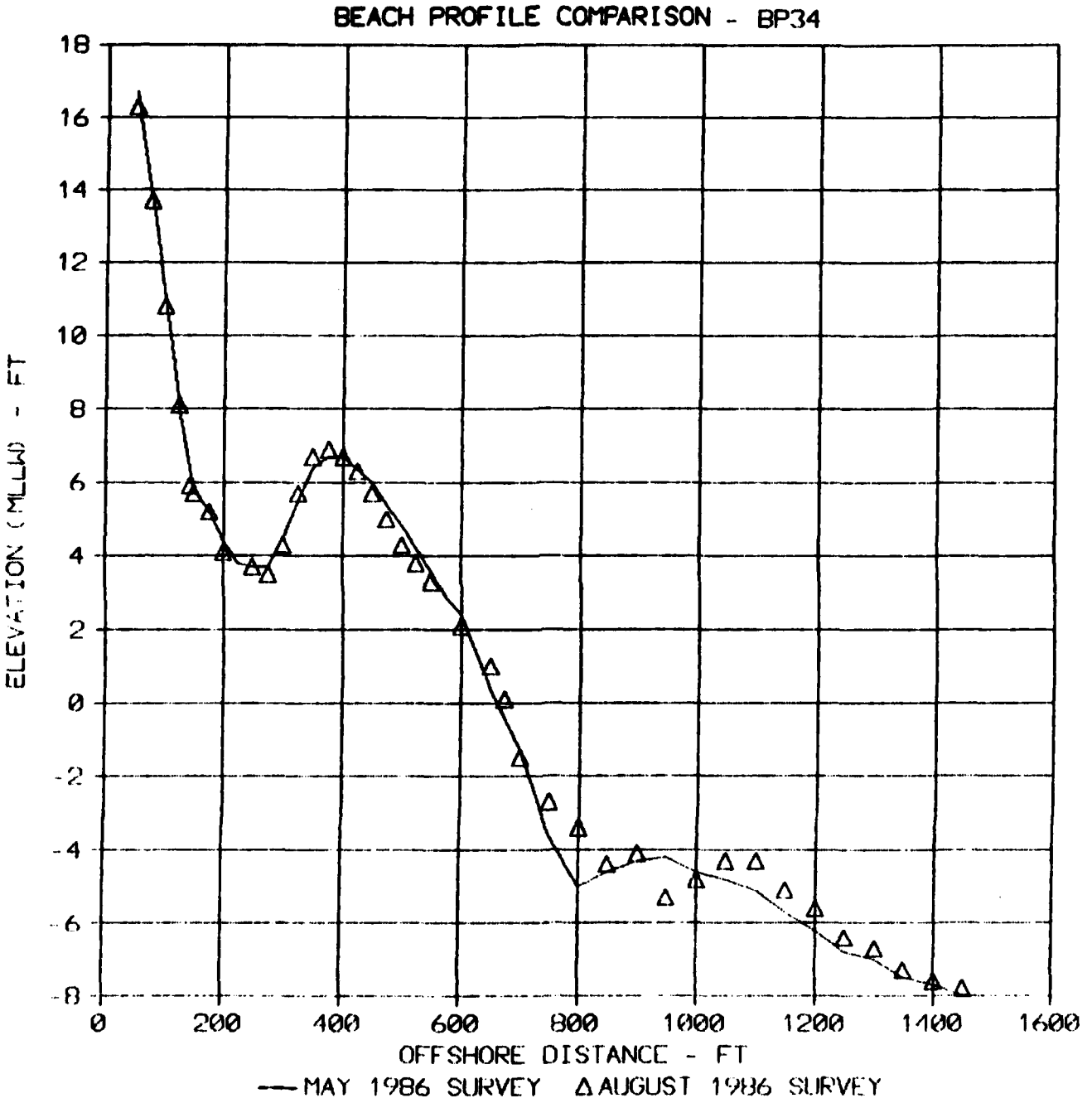

Figure D9. Comparison of beach profiles, BP-34

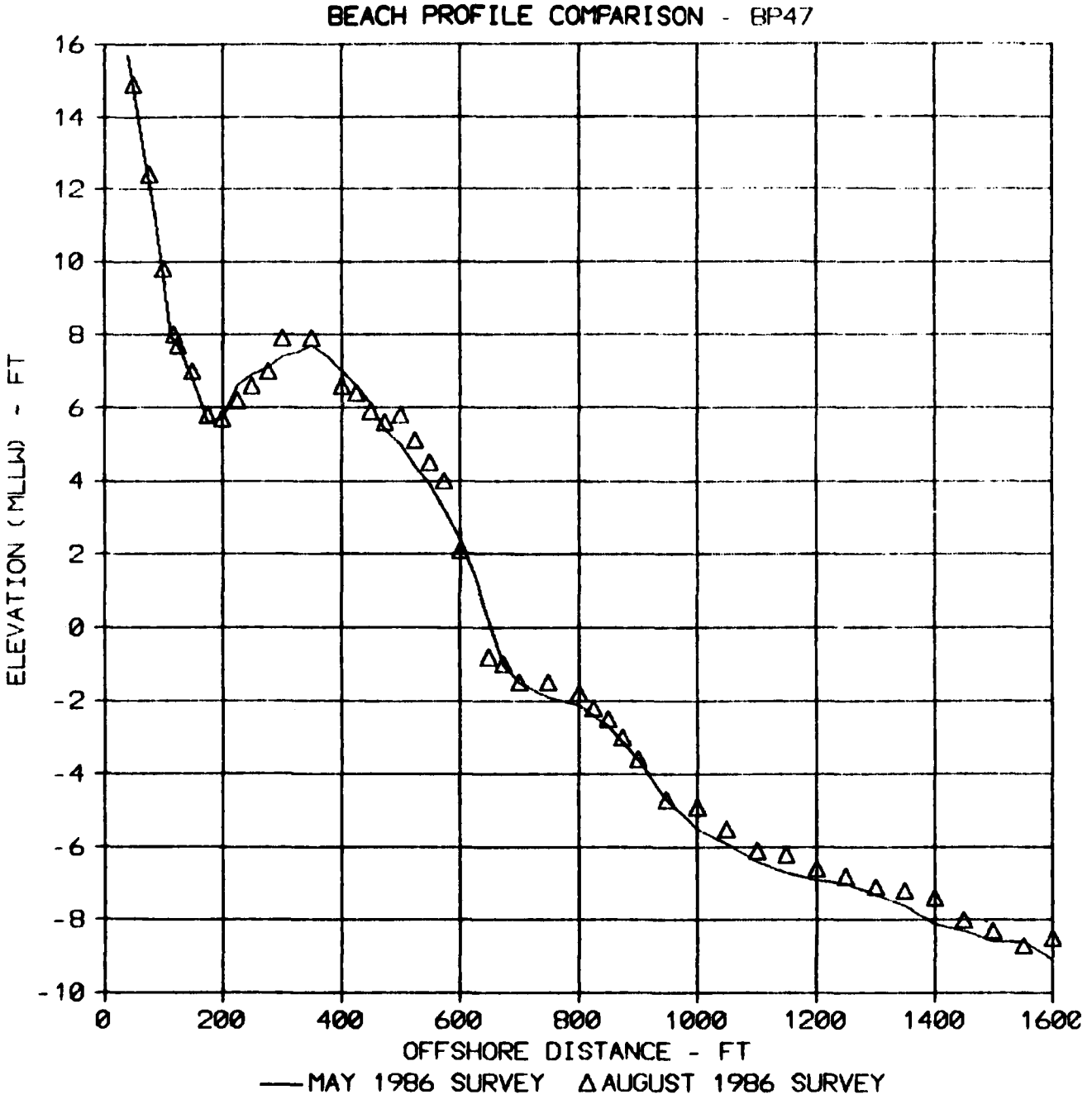

Figure D10. Comparison of beach profiles, BP-47

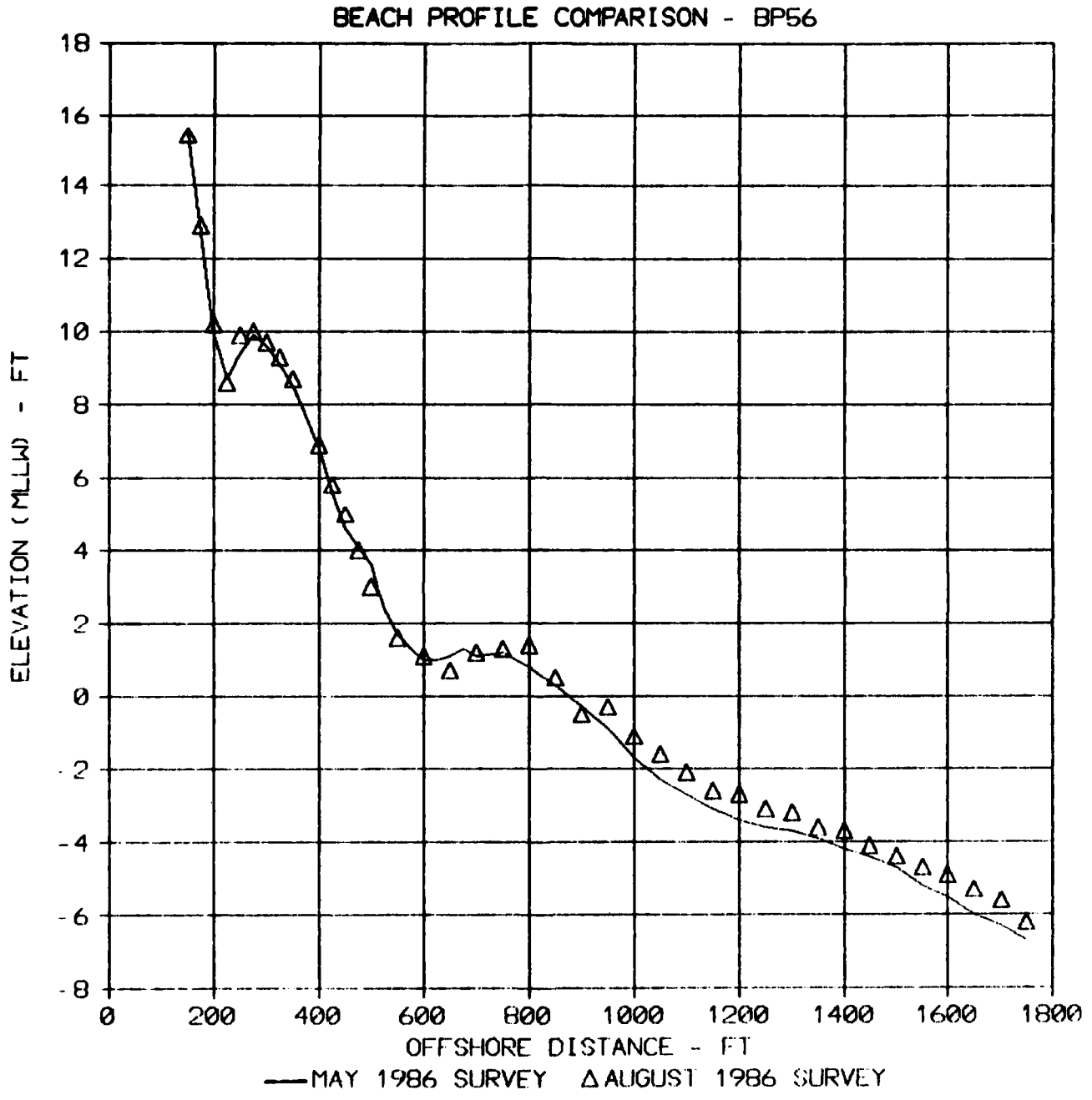

Figure D11. Comparison of beach profiles, BP-56

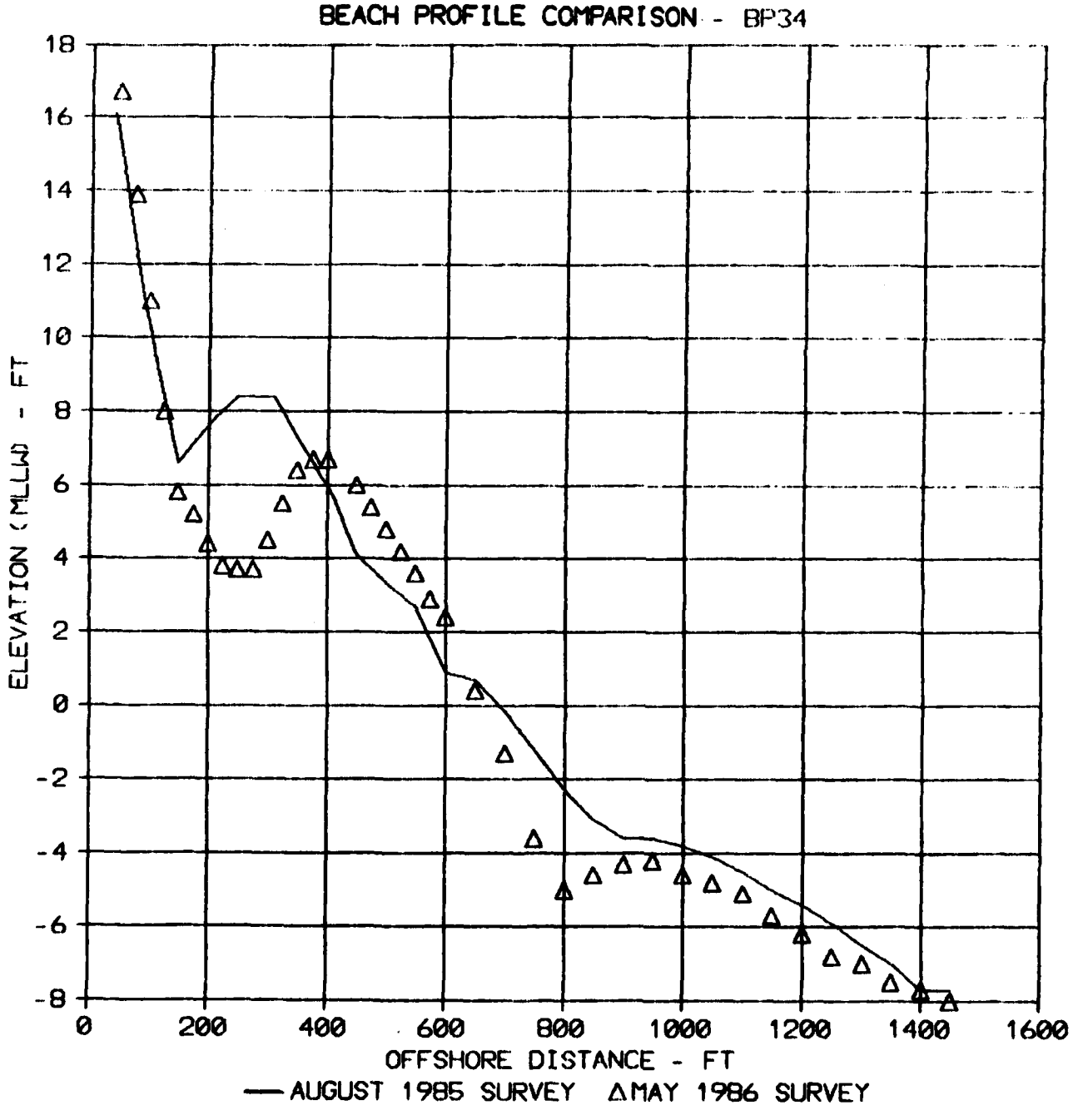

Figure D12. Comparison of beach profiles, BP-34

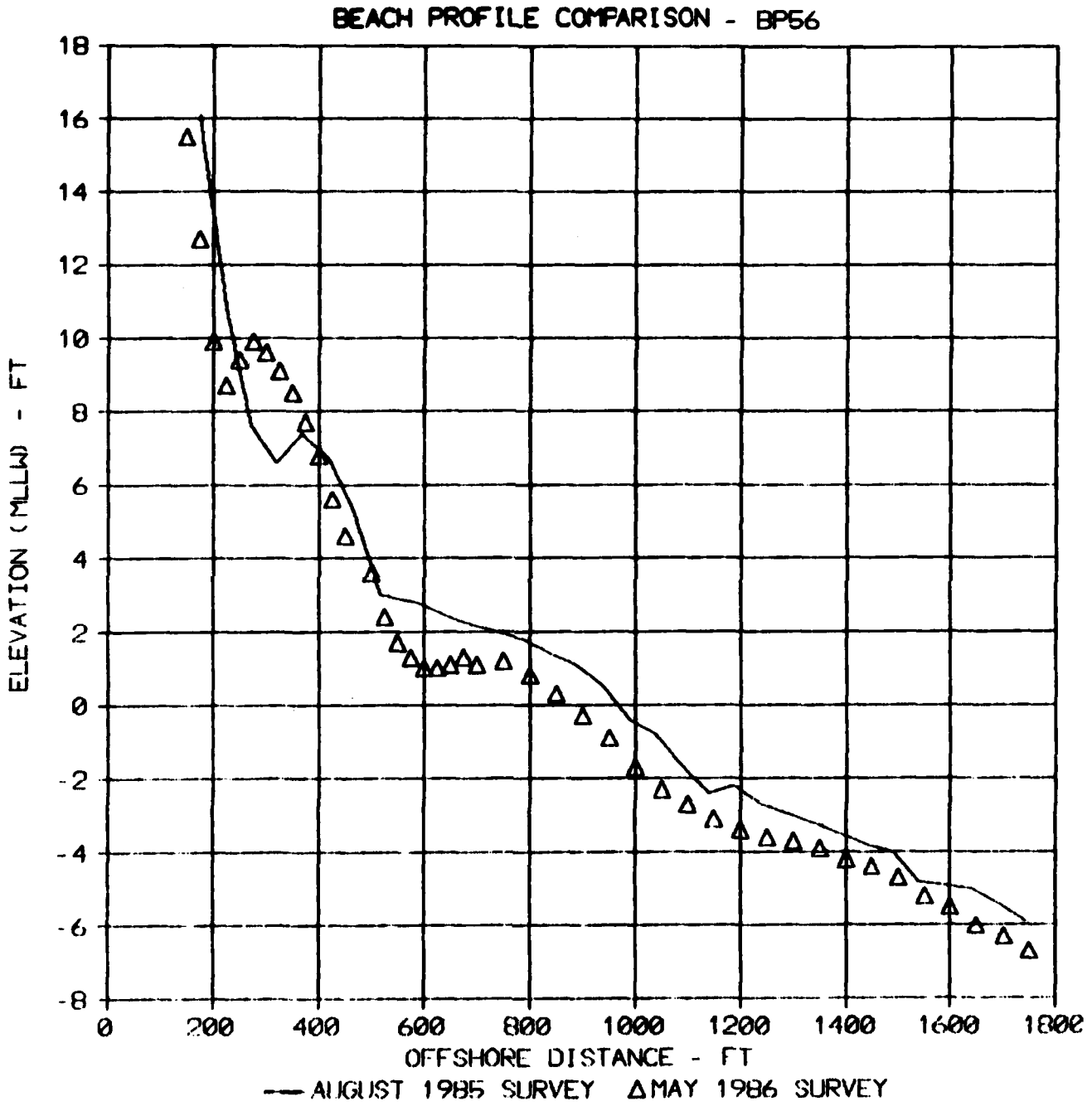

Figure D13. Comparison of beach profiles, BP-56

APPENDIX E: GEOMORPHOLOGICAL PROCESSES

Introduction

1. This appendix describes the geomorphic processes that affect the beach and nearshore zone of Homer Spit. In particular, shoreline trends over a historic time frame and the sedimentological relationships longshore and offshore of the Spit are emphasized. The following discussion builds on the previous work performed by CERC (Smith et al. 1985) for the US Army Engineer District, Alaska (CENPA). Appendix C presents the glacial history, origin of the Spit, and a description of relict beach morphological features.

2. This appendix is organized into two subtasks. The shoreline analysis subtask includes the evaluation of two shoreline data bases and a description of the morphodynamic processes affecting the coastline. The second subtask summarizes the sedimentological data collected by the CENPA in August 1985. Representative sediment size was evaluated for three water levels--high tide, mean tide, and low tide--and was plotted against the distance longshore. The sedimentary characteristics were also summarized in tabular form.

Shoreline Data Sources And Methodology

3. Shoreline trends for Homer Spit were analyzed using four historical and recent maps at two scales that date from 1918 through 1985. The shoreline data were evaluated as two separate data bases which included pre-1964 earthquake shorelines of 1918 and 1961 and post-1964 earthquake shorelines of 1968 and 1985. The dates, scales, and types of data sources used for the shoreline analysis are listed in Table E1. Several other maps of Homer Spit were acquired but could not be included in the shoreline data set because of a lack of reference points or questionable map accuracy.

4. Shoreline data were digitized and formatted in a Cartesian (X-Y) coordinate system. Shoreline positions were recorded at 100-ft intervals along the southwestern shoreline of the Spit. In order to manage and discuss the created data base, the project area was divided into four segments based on shoreline zones as listed in Table E2 and shown in Figure E1.

Table E1

Acquired Shoreline Maps And Surveys For The Project Area

Date	Scale	Map Source	Type
1918	1 in. = 1/2 mi	US Surveyors General Office	Topographic map
1961	1 in. = 1 mi	US Geological Survey	Topographic map
1968	1 in. = 200 ft	State of Alaska Dept. of Natural Resources	Tideland survey
1985	1 in. = 200 ft	CENPA	Survey map

Table E2

Shoreline Changes, Homer Spit

Segment No.	Location	1918-61 Mean Rate, ft/yr	1968-85 Mean Rate, ft/yr
1	Northeast of BP-60	+1.8	-11.8
2	BP-60 to BP-50	-0.7	-19.2
3	BP-50 to BP-38	-0.8	-7.4
4	BP-38 to BP-9	+1.1	+2.7

Discussion and Results

5. For regional shoreline analysis, the study area included the entire length of the Spit on the Cook Inlet side and the mainland of Kenai Lowlands northward to Beluga Lake. The shoreline for the study area which lies between BP-60 and BP-9 showed net erosion for both time intervals at a mean rate of -0.7 ft/yr (1918-61) and -7.7 ft/yr (1968-85). On a small time scale, however, the shoreline configuration was variable. Figure E2 (positive movements denotes accretion; negative movement denotes erosion) shows the average shoreline movement for the time interval 1918-61, and Figure E3 shows the corresponding shoreline movement for the second time interval of 1968-85. Several morphodynamic processes have modified the beach and nearshore zone at

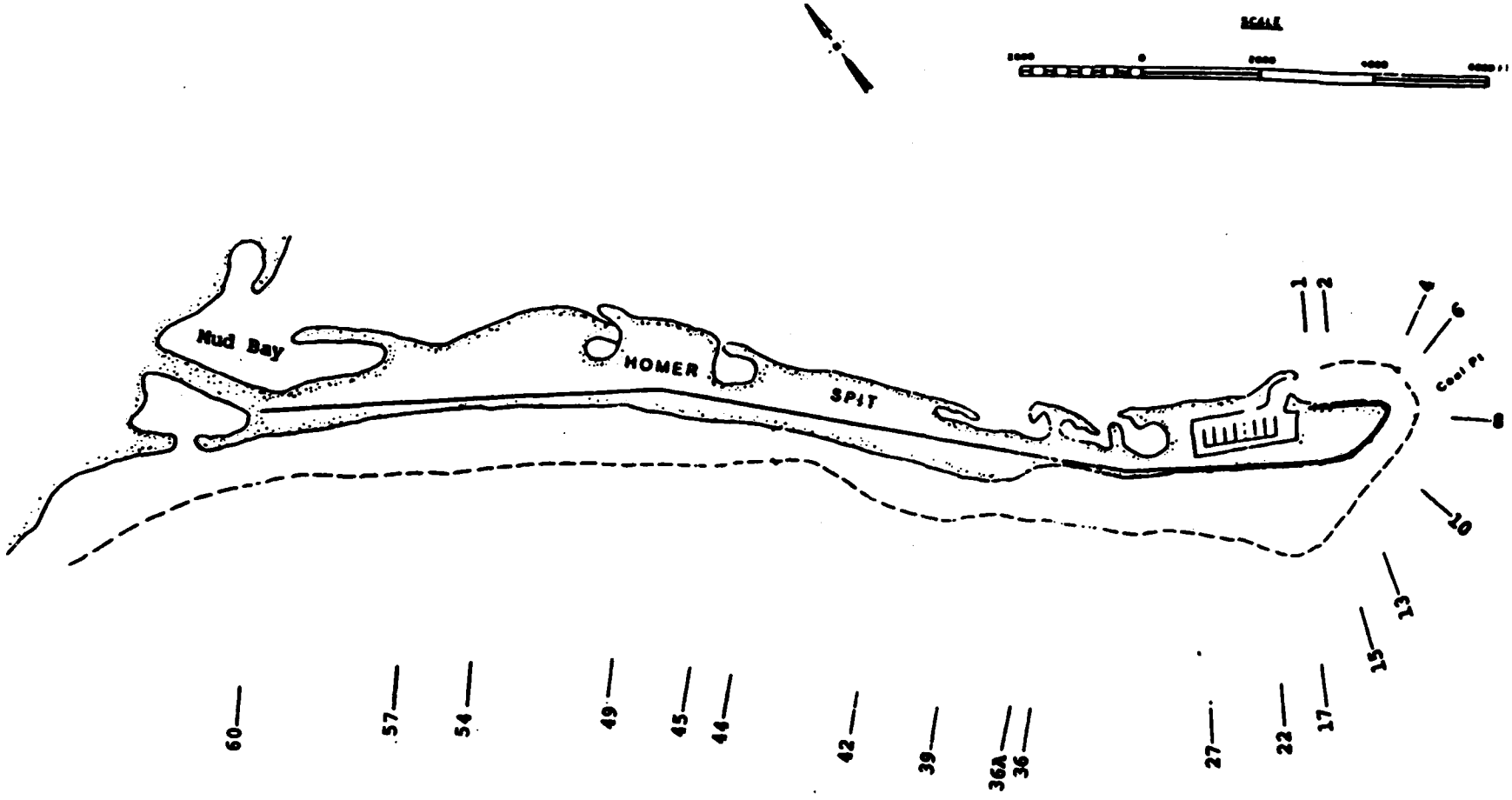

Figure E1. Beach profiles and shoreline segments of Homer Spit

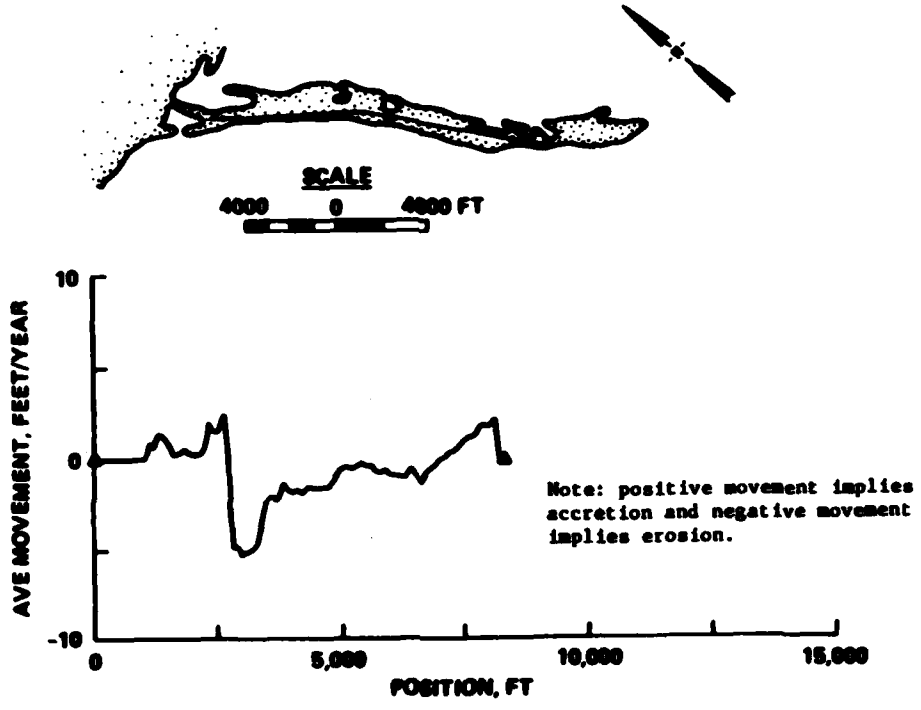

Figure E2. Shoreline movement, 1918-61, Homer Spit, Alaska

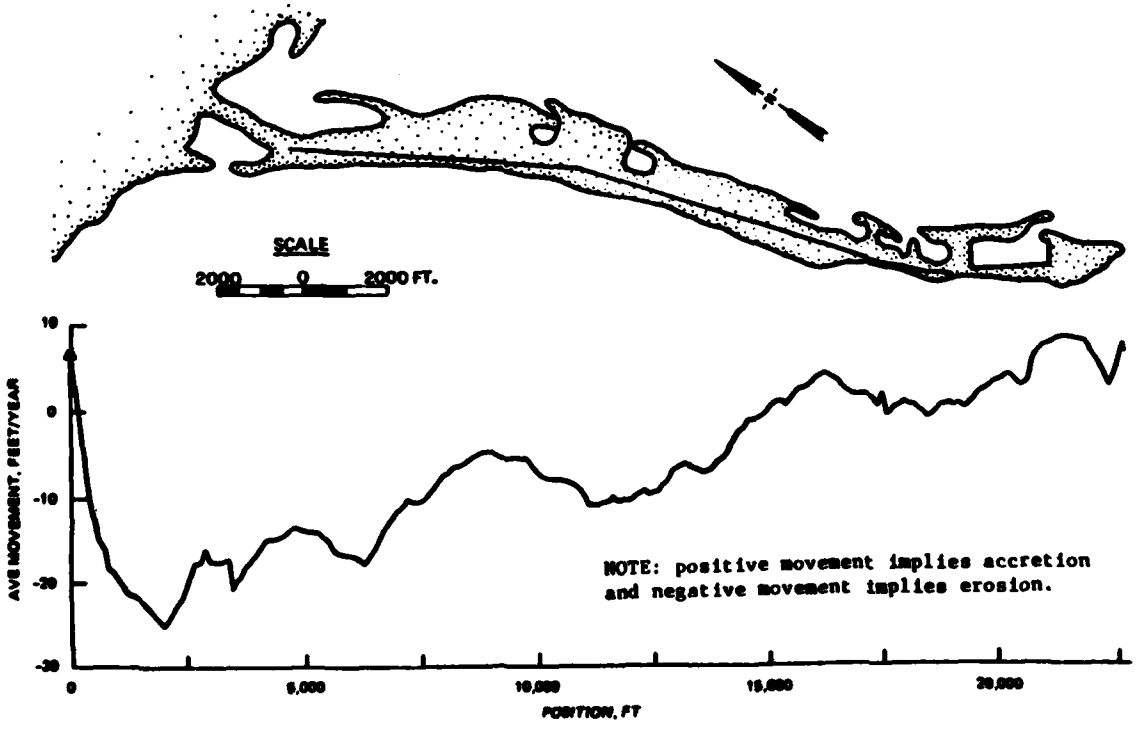

Figure E3. Shoreline movement, 1968-85, Homer Spit, Alaska

Homer Spit. Seasonal storms, wave-induced currents, longshore sediment transport, and tectonic activity have contributed to net shoreline position changes along the project area.

6. Shoreline change rates averaged over the two time intervals for the four segments are listed in Table E2. The preearthquake shoreline was relatively stable with an overall erosion rate of -0.6 ft per year. Minor erosion of -0.7 ft/yr and -0.8 ft/yr was recorded between BP-60 to BP-50 and BP-50 to BP-38, respectively. Net shoreline advance occurred at the tip (distal end) of the Spit (1.1 ft/yr) and the upper end of Homer Spit near the mainland (1.8 ft/yr).

7. Postearthquake shoreline change, however, showed a predominance of erosion with a rate of -19.2 ft/yr in Segment 2 (BP-60 to BP-50), referred to as the critical erosion area. Similar trends noted in the earlier time interval were recorded also for post-1964 earthquake shorelines but at accelerated rates. Segment 3 (BP-50 to BP-38) exhibited a net retreat of 7.4 ft/yr; whereas Segment 4 showed net accretion of 2.7 ft/yr at the tip of the Spit.

8. Shoreline trends at Homer Spit changed dramatically in recent decades based on a comparison of the two shoreline data bases. Historic maps show the coastline to be relatively stable with shoreline configuration remaining essentially the same. The 1964 Good Friday earthquake altered the Spit's geomorphology and littoral processes with massive slumping, subsidence, and soil liquefication. Several reports (Waller 1966, Stanley 1966, Woodward-Clyde 1964, Nottingham, Drage, and Gilman 1982, and Gronewald and Duncan 1965) documented high erosion rates and seismic evidence of massive slumping at the distal end of the Spit that occurred after the 1964 earthquake. Shoreline recession was estimated to be between 10-15 ft, with a maximum shoreline loss of about 60 ft, immediately after the earthquake (Stanley 1966).

9. In addition to the 1964 earthquake, another process that accelerated erosion by interrupting the west-east longshore transport is tidal inlet activity. Two inlet areas, an upper tidal inlet just above BP-60 and the inlet below Beluga Lake, were identified as regions where sediment is diverted away from the beach zone. The opening at the entrance to Beluga Lake has a deltaic feature covered with boulders and cobbles that is trapping sediments and preventing littoral drift from nourishing the downdrift beaches along the main body of the Spit (Smith et al. 1985). The second inlet feature, located just north of BP-60, is also acting as a sediment sink where sand and silt are

migrating into the tidal entrance. These overwash sediments have formed a distinct tidal flat on the landward side of the inlet as indicated in Figure E4. The inlet opening has not remained in the same position during the period 1959-85. Inlet migration and washover sedimentation have been attributed to seasonal storm activity and onshore waves that are nearly perpendicular to the shore. An unverified report by a local resident indicated that gravel mining took place in the early 1900's landward of this inlet. This activity might have led to the initial opening of the inlet and subsequent erosion in the vicinity of the inlet.

10. The bathymetry of Homer Spit indicated that an ebb-flood cycle has also influenced the sediment transport and shoreline configuration. The local flood-tidal cycle initially delivers sediment to the distal end but is interrupted by ebb currents. One indication of this trend is Archimandritof Shoals which is ebb-modified by currents flowing out of Kachemak Bay (Appendix F, Figure F8). If the ebb flow were weak or negligible, Archimandritof Shoals would probably be linear and parallel to the coastline. The lack of accretion and the steep profile at the tip of the Spit is further evidence that the ebb-flow is strong and a dominant force in maintaining the present position of the Spit.

Sediment Sources and Methodology

11. During the second phase of the beach erosion study, 96 samples were taken along established profiles at three water levels: mean high water (MHW), el* 17.3 ft; mean tide level (MTL), el 9.5 ft; and mean low water (MLW), el 1.6 ft. CENPA provided gradation analysis for each sample which is summarized in Table E3. Sediment statistics were also done for the sand and fines fraction of the sample to determine longshore transport Q (Appendixes B and C), as presented in Table E4.

---

* Elevations (el) cited herein are given relative to mean lower low water level, as referenced to National Geodetic Vertical Datum of 1929.

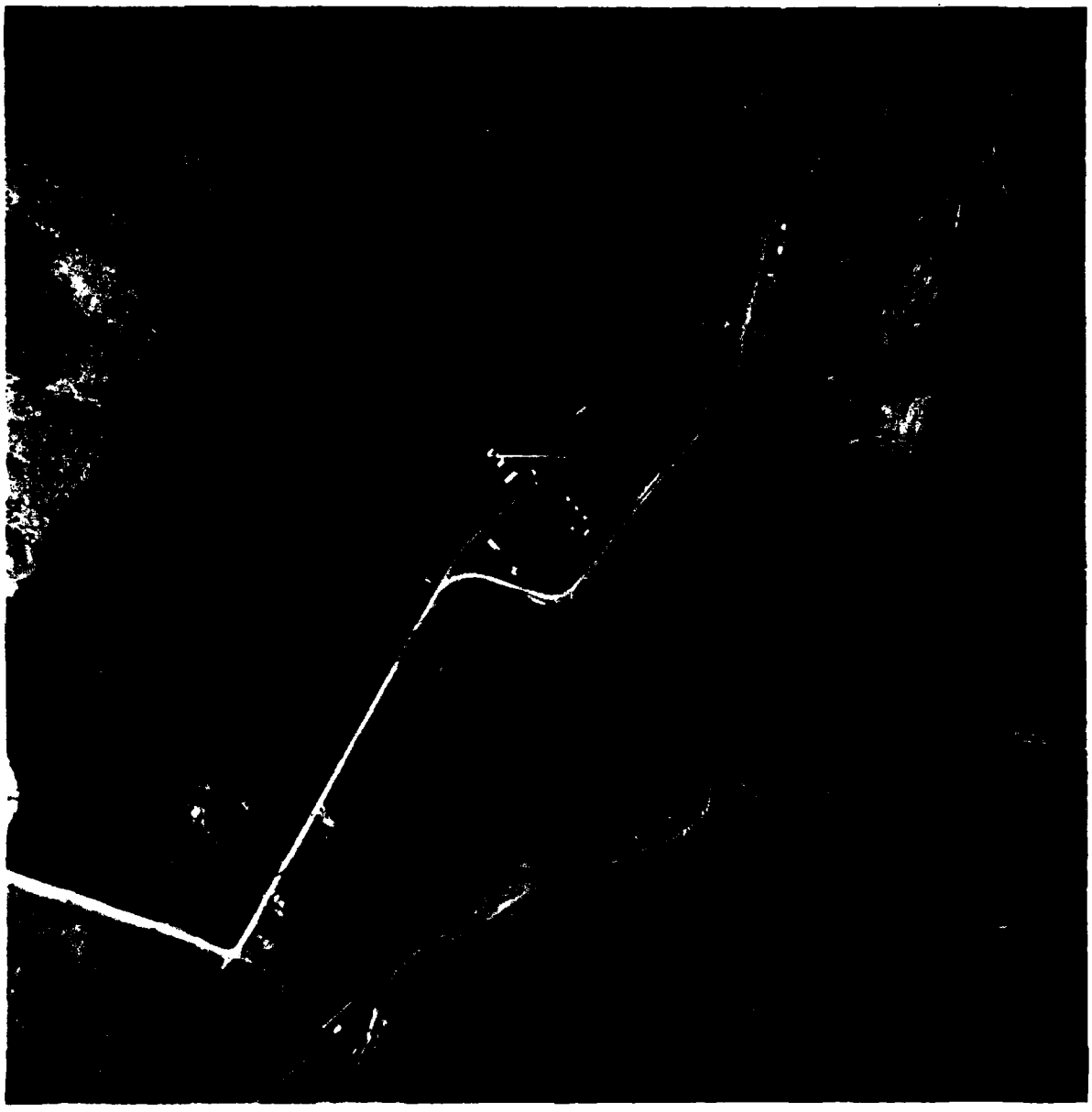

Figure E4. Overwash sediments trapped landward of tidal inlet located just north of BP-60

Table E3

Gradation Analysis for Homer Spit Erosion Study*

Sample	Gravel %	Sand %	Fines %	Soil Classification
BP025 MHW	44.6	53.1	0.2	SP
BP025 MTL	58.5	28.8	0.1	GP
BP025 MLW	0.9	98.8	0.3	SP
BP031 MHW	30.0	69.7	0.2	SP
BP031 MTL	39.7	60.0	0.2	SP
BP031 MLW	0.4	98.8	0.8	SP
BP034 MHW	56.5	43.4	0.1	GP
BP034 MTL	73.1	23.5	0.5	GW
BP034 MLW	1.0	98.5	0.5	SP
BP036 MHW	44.2	55.3	0.5	SP
BP036 MTL	6.3	93.4	0.3	SP
SP036 MLW	0.7	98.7	0.6	SP
BP038 MHW	34.4	65.2	0.4	SP
BP038 MTL	10.4	89.4	0.2	SP
BP038 MLW	1.5	98.0	0.5	SP
BP040 MHW	61.5	38.4	0.0	GP
BP040 MTL	30.6	53.8	0.3	SW
BP040 MLW	8.5	82.0	9.5	SP-S
BP040 MLW	3.4	9.5	87.1	??
BP041 MHW	51.8	48.1	0.1	GP
BP041 MTL	41.4	58.5	0.1	SW
BP041 MLW	25.9	73.5	0.6	SP
BP042 MHW	57.7	38.8	0.4	GP
BP042 MTL	40.6	59.0	0.1	SW
BP042 MLW	28.4	11.1	0.5	GP
BP043 MHW	62.1	37.5	0.3	GP
BP043 MTL	44.5	55.5	0.0	SW
BP043 MLW	0.5	99.0	0.5	SP
BP044 MHW	57.8	42.2	0.0	GP
BP044 MTL	60.5	39.3	0.2	GW
BP044 MLW	1.6	97.5	0.9	SP
BP05 MHW	77.7	22.3	0.0	GP
BP05 MTL	51.7	48.1	0.2	GW
BP05 MLW	1.3	98.2	0.5	SP
BP045 MHW	58.8	41.1	0.1	GP
BP045 MTL	54.7	45.1	0.1	GW
BP045 MLW	2.4	97.2	0.4	SP
BP046 MHW	67.1	32.9	0.0	
BP046 MTL	49.9	49.8	0.1	GW
BP046 MLW	1.0	98.1	0.9	SP
BP046AMHW	63.3	36.6	0.1	GW
BP046AMTL	52.8	24.8	0.3	GW
BP046AMLW	0.3	99.5	0.2	SP
BP047 MHW	44.1	55.8	0.1	SP
BP047 MTL	57.3	42.5	0.2	GW
BP047 MLW	0.8	98.8	0.4	SP
BP048 MHW	70.0	29.9	0.1	GP
BP048 MTL	57.4	36.5	6.1	GW-G?
BP048 MLW	1.3	97.8	0.9	SP
BP049 MHW	83.7	16.3	0.0	GW
BP049 MTL	56.2	43.7	0.1	GW
BP049 MLW	1.7	97.7	0.6	SP

(Continued)

* Sediment samples collected July 1986.

Table E3 (Concluded)

Sample	Gravel %	Sand %	Fines %	Soil Classification
BP#50 MHW	77.1	22.9	0.0	GP
BP#50 MTL	50.9	48.9	0.1	GM
BP#50 MLW	6.7	92.1	1.2	SP
BP#51 MHW	86.5	13.5	0.0	GP
BP#51 MTL	45.9	51.5	0.1	SM
BP#51 MLW	0.4	98.6	1.0	SP
BP#52 MHW	80.6	19.4	0.0	GP
BP#52 MTL	49.2	39.6	0.0	GP
BP#52 MLW	4.6	94.5	0.9	SP
BP#53 MHW	28.4	11.6	0.0	GP
BP#53 MTL	58.1	20.6	0.1	GM
BP#53 MLW	1.9	97.5	0.6	SP
BP#53AMHW	48.4	49.0	2.6	SM
BP#53AMTL	52.4	36.1	0.3	GP
BP#53AMLW	1.0	97.9	1.1	SP
BP#54 MHW	92.7	7.2	0.0	GP
BP#54 MTL	64.5	34.9	0.3	GP
BP#54 MLW	1.2	97.8	1.0	SP
BP#55 MHW	46.1	53.2	0.7	SP
BP#55 MTL	66.3	33.7	0.1	GP
BP#55 MLW	0.6	98.5	0.9	SP
BP#56 MHW	33.1	66.8	0.1	SP
BP#56 MTL	0.4	99.0	0.6	SP
BP#56 MLW	0.2	98.5	1.3	SP
BP#57 MHW	64.0	27.5	0.2	GP
BP#57 MTL	5.5	94.0	0.5	SP
BP#57 MLW	12.2	86.8	1.0	SP
BP#58 MHW	65.2	15.7	0.7	GP
BP#58 MTL	24.9	65.7	0.3	SP
BP#58 MLW	15.2	83.2	1.4	SP
BP#59 MHW	32.4	67.0	0.2	SP
BP#59 MTL	49.0	19.1	0.1	GP
BP#59 MLW	63.0	34.0	0.2	GP
BP#60 MHW	41.3	58.6	0.1	SP
BP#60 MTL	45.0	23.3	0.1	GP
BP#60 MLW	53.7	37.8	0.0	GP

Table E4

Sediment Statistics for Homer Spit Erosion Study*

Sample	Mean	Std. Dev.	Skew-ness	Kur-tosis
BP025 MHW	.42	.94	-.42	.69
BP025 MTL	-.42	1.40	.24	-1.06
BP025 MLW	1.50	.56	-1.28	12.96
BP031 MHW	.72	.91	-.65	1.61
BP031 MTL	.20	1.32	-.19	-1.14
BP031 MLW	1.40	.55	-.53	7.20
BP034 MHW	.35	1.06	-.40	-.14
BP034 MTL	-.12	1.64	.17	-1.21
BP034 MLW	1.35	.63	-.83	6.97
BP036 MHW	.24	1.23	-.23	-.69
BP036 MTL	.90	.98	-.71	1.81
BP036 MLW	1.37	.56	-.80	8.90
BP038 MHW	.22	1.18	-.18	-.70
BP038 MTL	1.05	.91	-.85	3.20
BP038 MLW	.93	1.04	-.53	.89
BP040 MHW	.22	1.31	-.23	-1.17
BP040 MTL	.10	1.57	-.09	-1.55
BP040 MLW				
BP040 MLW				
BP041 MHW	.50	1.11	-.52	.04
BP041 MTL	-.60	1.43	.33	-1.05
BP041 MLW	.60	1.33	-.38	-.51
BP042 MHW	.67	1.03	-.47	1.19
BP042 MTL	-.26	1.31	.13	-1.17
BP042 MLW	.36	1.61	-.00	-1.11
BP043 MHW	.63	.96	-.57	1.67
BP043 MTL	-.28	1.34	.10	-1.30
BP043 MLW	1.66	.54	-.87	9.37
BP044 MHW	.61	.79	-.54	1.98
BP044 MTL	.39	1.31	-.28	-.88
BP044 MLW	1.67	.56	-.88	11.11
BP05 MHW	.61	1.08	-.57	.32
BP05 MTL	.18	1.37	-.18	-1.27
BP05 MLW	1.47	.51	-.95	13.35
BP045 MHW	.75	.93	-.76	2.04
BP045 MTL	.32	1.38	-.28	-1.12
BP045 MLW	1.35	.60	-.91	8.20
BP046 MHW	.53	1.09	-.48	.04
BP046 MTL	-.12	1.37	.02	-1.41
BP046 MLW	1.45	.53	-.68	10.28
BP046AMTL				
BP046AMLW	1.40	.49	-.74	8.55
BP047 MHW	.18	1.30	-.24	-1.19
BP047 MTL	.27	1.42	-.16	-1.29
BP047 MLW	1.17	.82	-.69	3.02
BP048 MHW	.43	1.18	-.37	-.37
BP048 MTL				
BP048 MLW	1.34	.74	-.87	5.82
BP049 MHW	-.14	1.35	-.04	-1.30
BP049 MTL	-.32	1.43	.17	-1.34
BP049 MLW	1.35	.67	-.89	6.99
BP050 MHW	.27	1.34	-.34	-1.12

(Continued)

* Sediment samples were collected July 1986

Table E4 (Concluded)

Sample	Mean	Std. Dev.	Skew-ness	Kur-tosis
BP#50 MTL	.24	1.35	-.05	-1.57
BP#50 MLM	1.13	.94	-.73	2.98
BP#51 MMM				
BP#51 MTL	-.41	1.34	.18	-1.36
BP#51 MLM	1.45	.58	-.58	7.64
BP#52 MMM	-1.51	.72	1.31	9.88
BP#52 MTL	-.73	1.24	.43	-.46
BP#52 MLM	1.21	.90	-.78	3.48
BP#53 MMM	-.93	1.07	.48	.12
BP# MTL	-.13	1.46	.01	-1.51
BP#53 MLM	1.23	.85	-.82	3.89
BP#53AMMM	-.38	1.50	.46	.26
BP#53AMTL	-.77	1.27	.63	.84
BP#53AMLM	1.39	.71	-.84	6.80
BP#54 MMM	-1.66	.77	2.03	20.47
BP#54 MTL	-.66	1.40	.49	-.22
BP#54 MLM	1.41	.72	-1.02	8.33
BP#55 MMM	.36	1.14	-.25	.08
BP#55 MTL	-1.07	1.08	.81	2.55
BP#55 MLM	1.39	.63	-.77	6.68
BP#56 MMM	.67	.92	-.88	1.39
BP#56 MTL	1.31	.53	-.83	7.90
BP#56 MLM	1.43	.63	-.63	7.00
BP#57 MMM	.09	1.22	-.15	-.84
BP#57 MTL	1.17	.80	-1.03	5.74
BP#57 MLM	1.02	1.33	-.53	-.04
BP#58 MMM	-.08	1.28	-.01	-.95
BP#58 MTL	.74	1.21	-.54	.10
BP#58 MLM	1.17	.99	-.79	3.21
BP#59 MMM	1.21	.64	-1.08	8.63
BP#59 MTL	.61	1.22	-.39	-.34

Sediment Analysis

12. Sediment trends were evaluated offshore and longshore for similar characteristics. The median (D = 50 percent) grain size was used for the comparison of the samples between BP-60 and BP-34, as shown in Figures E5, E6, and E7. Generally, the sediment was coarse on the upper beach face at MHW, a mixture of all grain sizes was deposited at MTL, and fine sediments were found at MLW. These sediment results are similar to the gradation and grain size analyses summarized in the report by Smith et al. (1985).

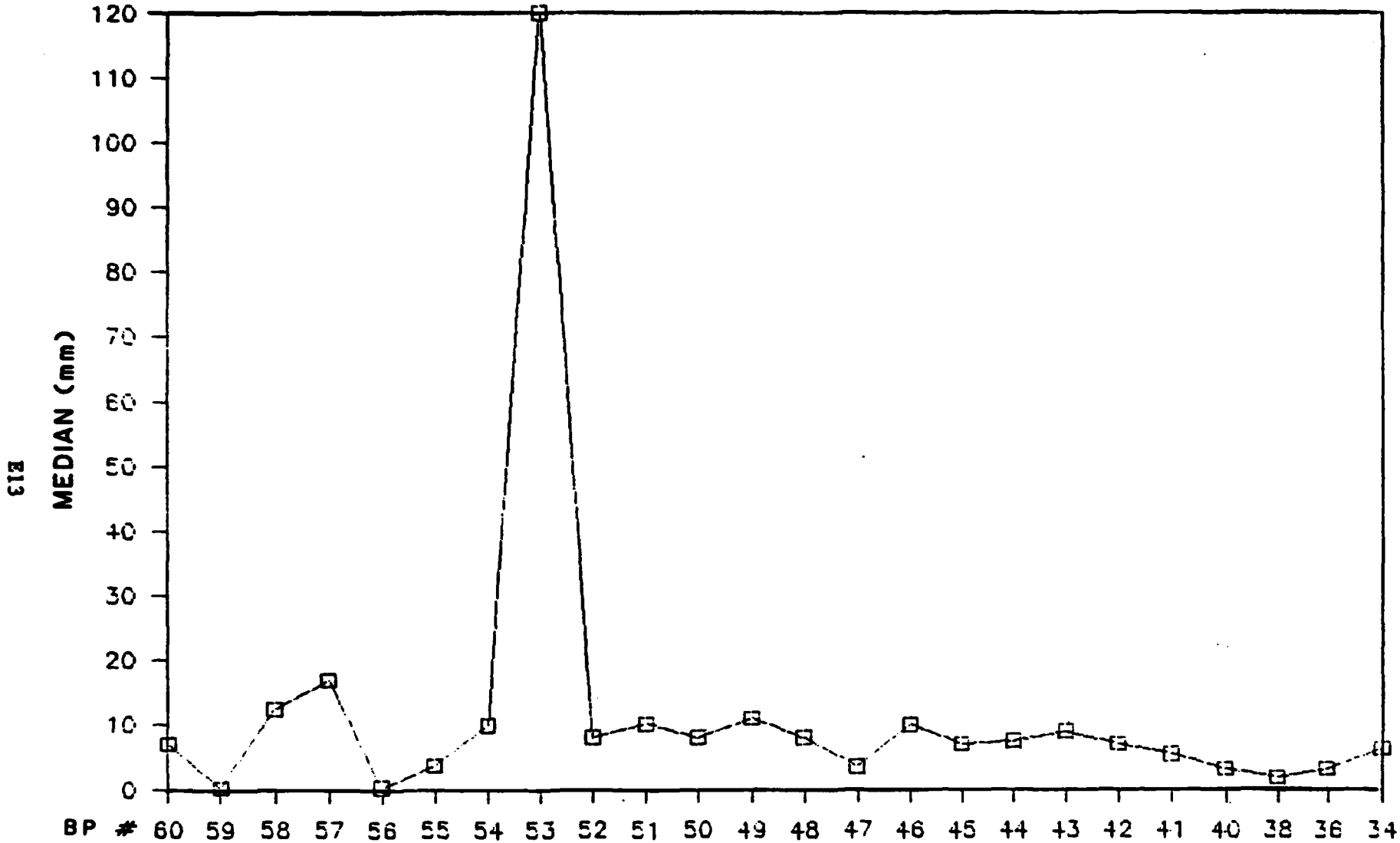

Figure E5. A comparison of median grain size longshore at MHW

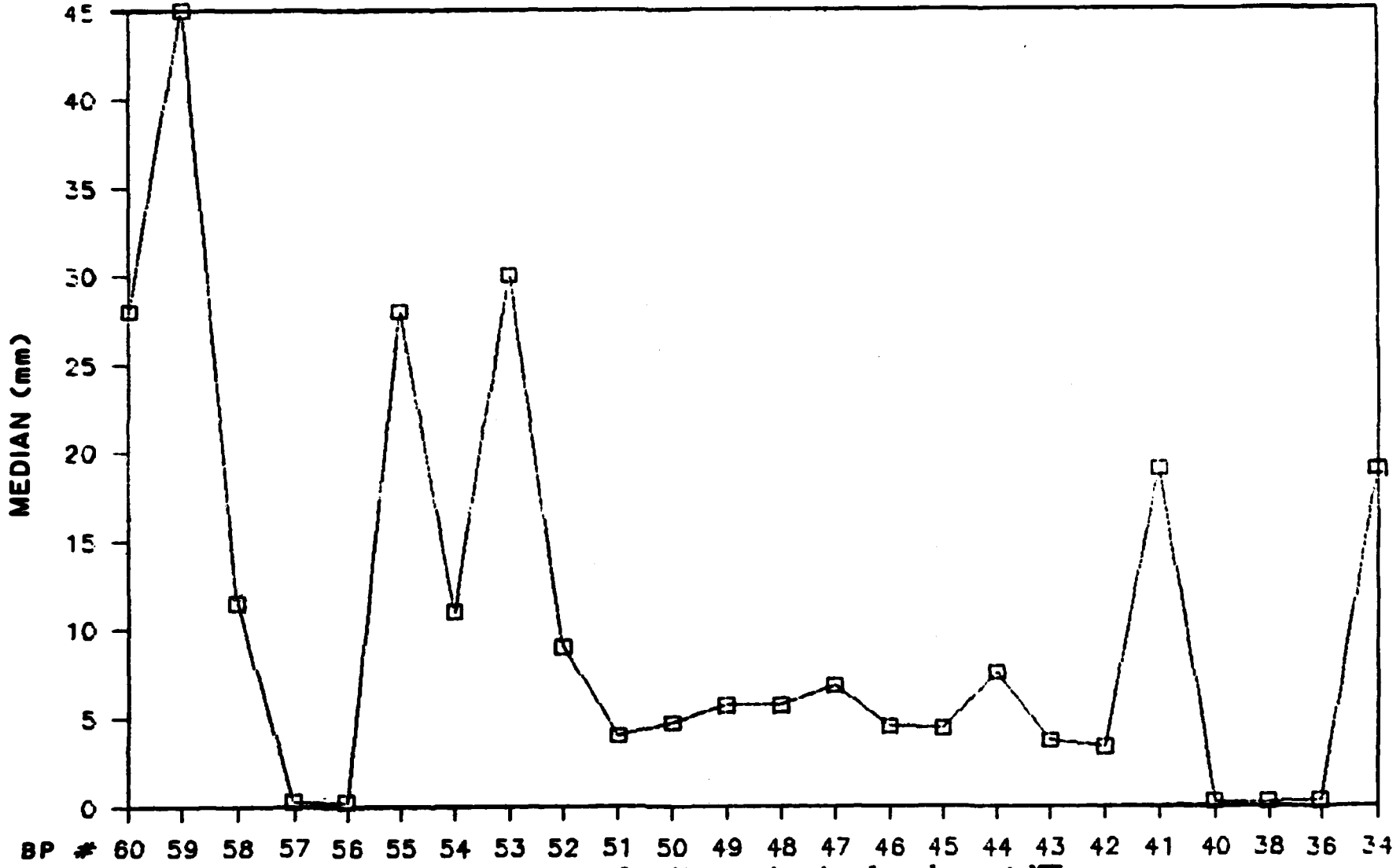

Figure E6. A comparison of median grain size longshore at MTL

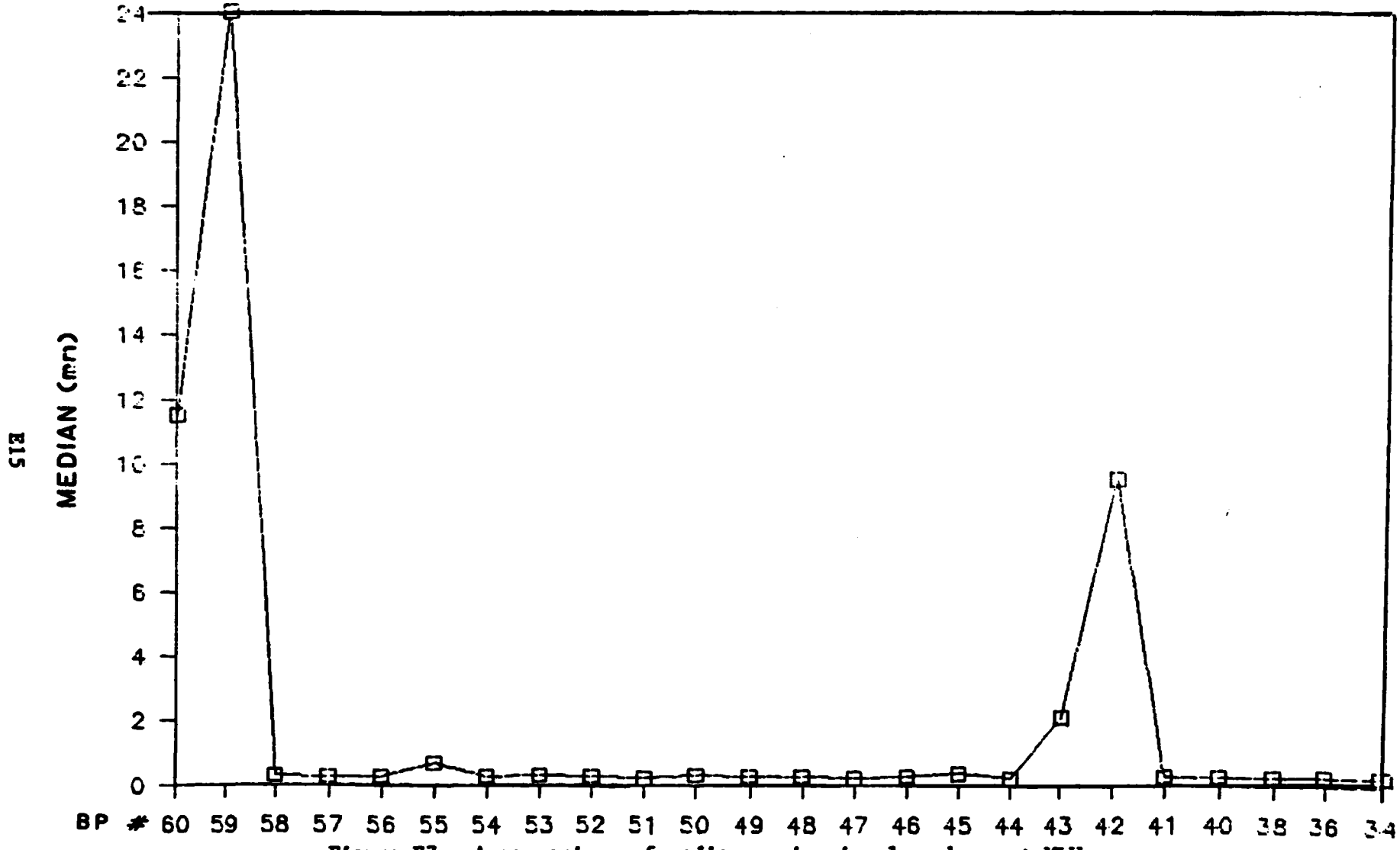

Figure E7. A comparison of median grain size longshore at MLW

APPENDIX F: TIDAL ELEVATION AND CURRENTS

Introduction

1. Homer Spit, extending approximately 4-1/2 miles from the lower Kenai Peninsula into the Kachemak Bay, creates an upper bay area of 116.5 square miles. The relatively large tidal range at this region results in an average tidal prism of 51 billion cubic feet passing twice a day through the constricted section formed by the Spit. During the flood phase, tidal water moves into the upper bay area in all directions from the lower bay area. When the tidal water exits from the constriction, flow separation could potentially occur at the lower bay near the constriction section and form a large size eddy (gyre) off the lower half of the southwest Spit coast at the ebb tide. This eddy, if it exists, could be a dominant factor to the erosion of the Spit shoreline and require special attention in the design of erosion control measures. Additionally, the magnitude and direction of tidal currents are important to the longshore transport of littoral material, particularly during the period of spring tides when the tidal prism is at its maximum level. The present study is planned for better understanding of the significance of tidal effects on spit erosion processes. The field data along with computer simulated water elevations and currents are presented. Results are provided in detail for the area along the southwest shore of Homer Spit.

Field Data on Tides

2. According to the Tide Tables (US Department of Commerce 1984), the tide data in Kachemak Bay are available at two permanent tide stations: Seldovia (on the south bank of the bay mouth) and Homer (near Homer Airport). The mean and diurnal tide ranges given in the Tide Tables are as follows:

	Ranges, ft	
Station	Mean	Diurnal
Seldovia	15.5	18.0
Homer	15.7	18.1

3. The tidal elevations at a station near the tip of Homer Spit were summarized by US Army Engineer District, Alaska (CENPA) (Smith et al. 1985), as follows:

Tide Level	Elevation, ft
Estimated Extreme High Water	23.3 MLLW
Mean Higher High Water (MHHW)	18.1 MLLW
Mean High Water	17.3 MLLW
Mean Tide Level	9.5 MLLW
Mean Low Water	1.6 MLLW
Mean Lower Low Water (MLLW)	0.0 (datum)
Estimated Extreme Low Water	-5.5 MLLW

4. In this project, three tide gages were deployed to three stations at Seldovia, Homer Spit (near the tip of Homer Spit), and Bluff Point during 4 August to 27 September 1984. Bluff Point is on the north bank of the bay mouth about midway between Anchor Point and Homer. The tide gage at Bluff Point was lost in the field and could not be retrieved. Therefore, no tide data are available at this station. The measured tides at Seldovia and Homer Spit are given in Figure F1.

5. In general, the tides in the bay are semidiurnal but have a pronounced diurnal inequality with elevations from 0.0 to 5.5 m (0.0 to 18.1 ft) for MLLW and MHHW, respectively. The extreme low and high water elevations are estimated to be -1.7 and 7.1 m (-5.5 and 23.3 ft), respectively.

Field Data on Tidal Currents

6. No current data in the bay are available from the Tidal Current Tables for 1984 (US Department of Commerce 1984). In the field study of this project, three ENDECO current meters were deployed to sta HS7 off the tip of Homer Spit to measure currents at three different depths during 8 to 12 August 1984. The current vectors and vector roses are shown in Figures F2 through F4. Figure F5 shows station locations.

7. To supply synoptic currents along the southwest shore of Homer Spit, six mooring stations were set up on 10 and 11 August 1984 for measuring tidal currents at three different depths from boats. The six mooring stations

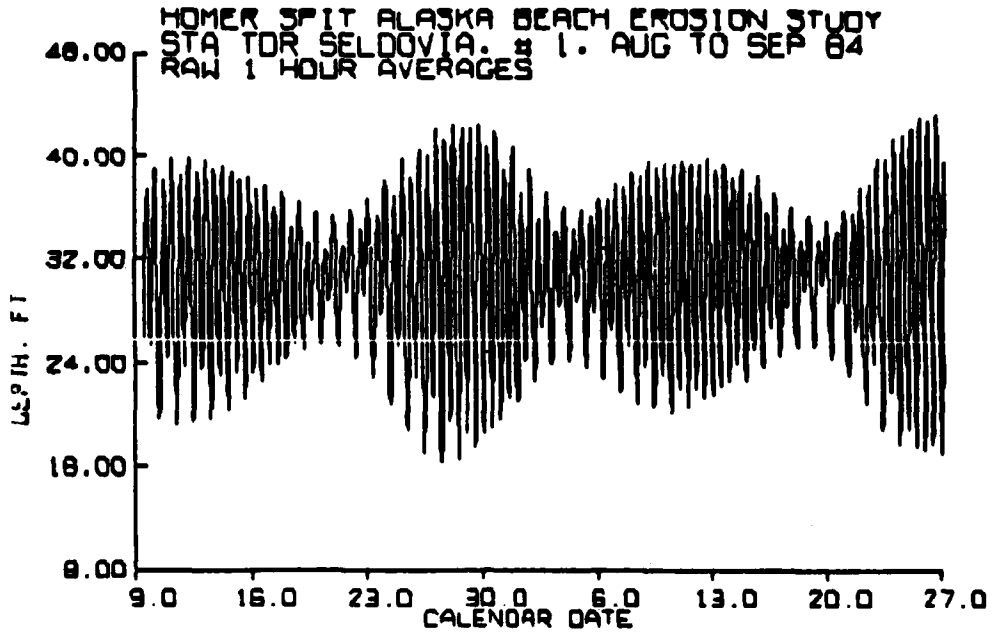

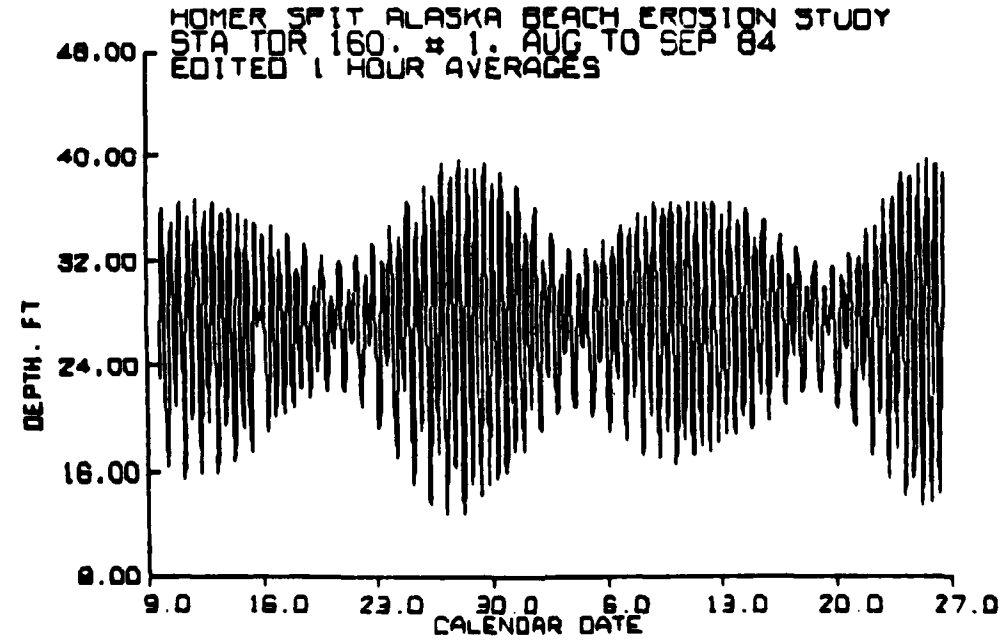

Figure F1. Tidal elevations at Seldovia and a station off the tip of Homer Spit

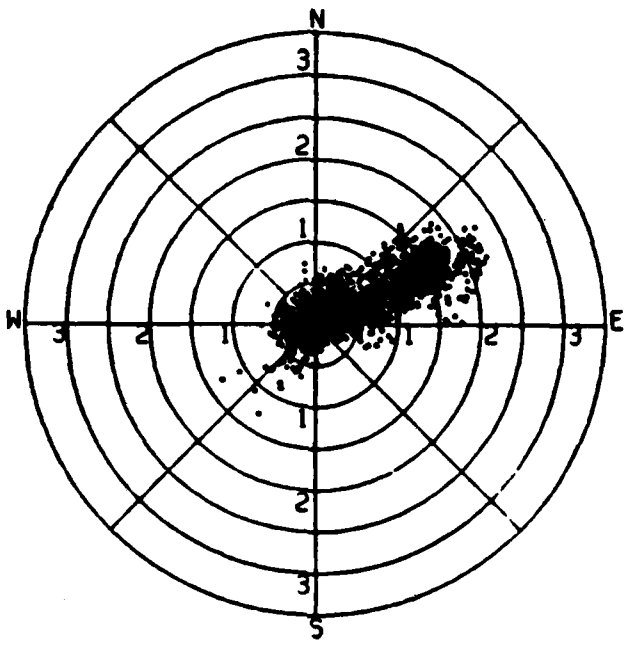

CURRENT VECTOR ROSE
HOMER SPIT, ALASKA
STATION HS7T, AUGUST 8-12 '84

CURRENT VECTOR PLOT
HOMER SPIT, ALASKA
STATION HS7T, AUGUST 8-12 '84

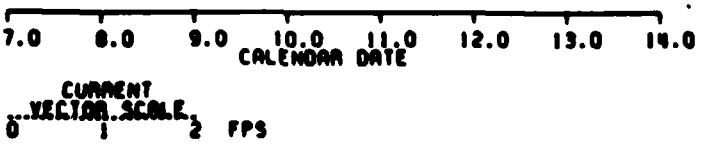

Figure F2. Current vector rose and plot near surface at sta HS7

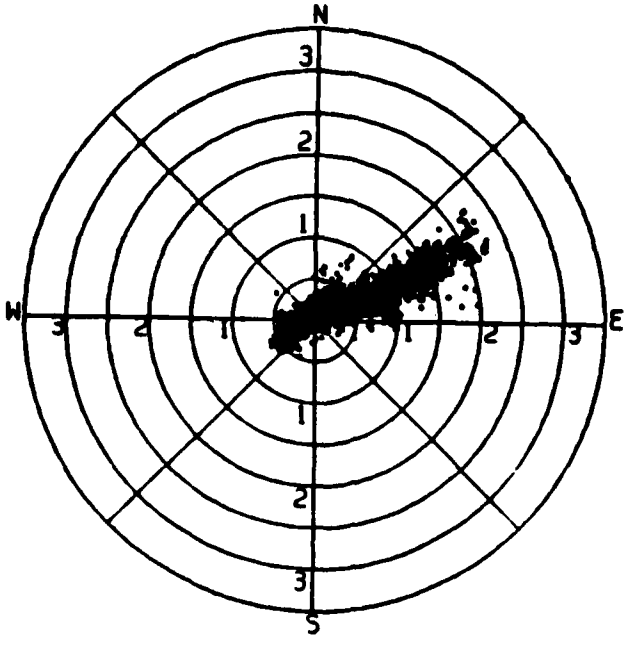

CURRENT VECTOR ROSE
HOMER SPIT, ALASKA
STATION HS7C, AUGUST 8-12 '84

CURRENT VECTOR PLOT
HOMER SPIT, ALASKA
STATION HS7C, AUGUST 8-12 '84

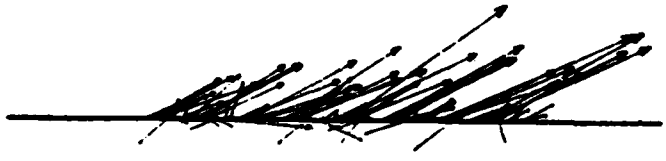

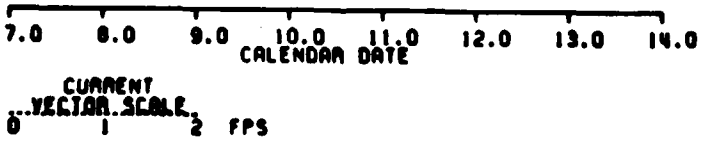

CURRENT
VECTOR SCALE
0 1 2 FPS

Figure F3. Current vector rose and plot near middle depth at sta HS7

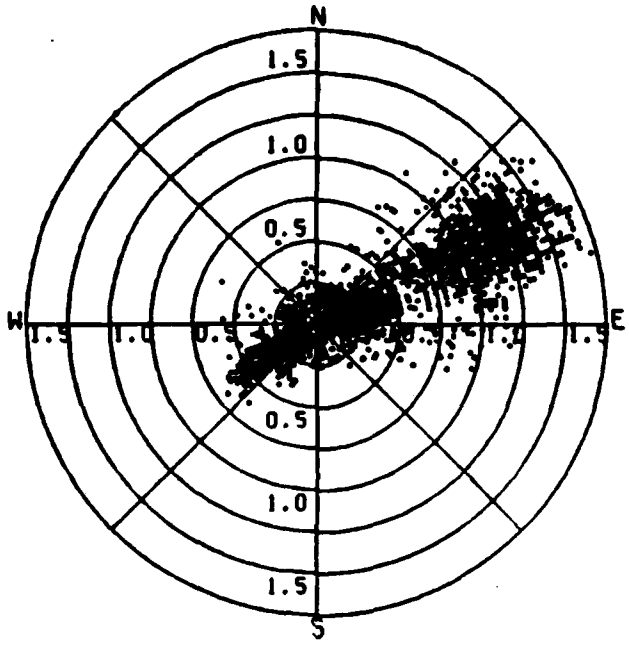

CURRENT VECTOR ROSE
HOMER SPIT, ALASKA
STATION HS7B, AUGUST 8-12 '84

CURRENT VECTOR PLOT
HOMER SPIT, ALASKA
STATION HS7B, AUGUST 8-12 '84

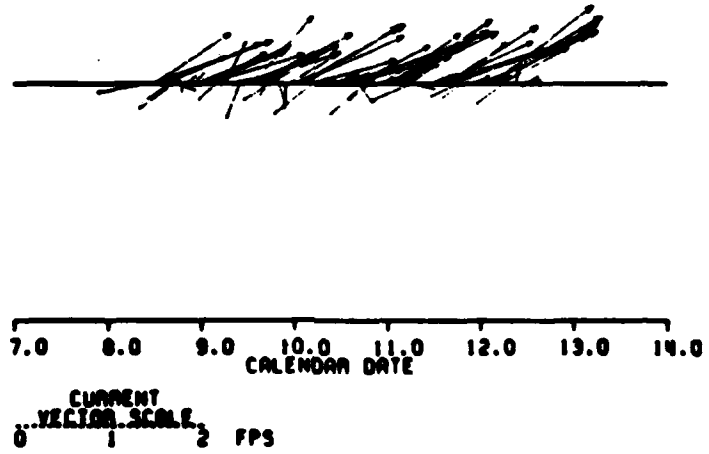

Figure F4. Current vector rose and plot near bottom at sta HS7

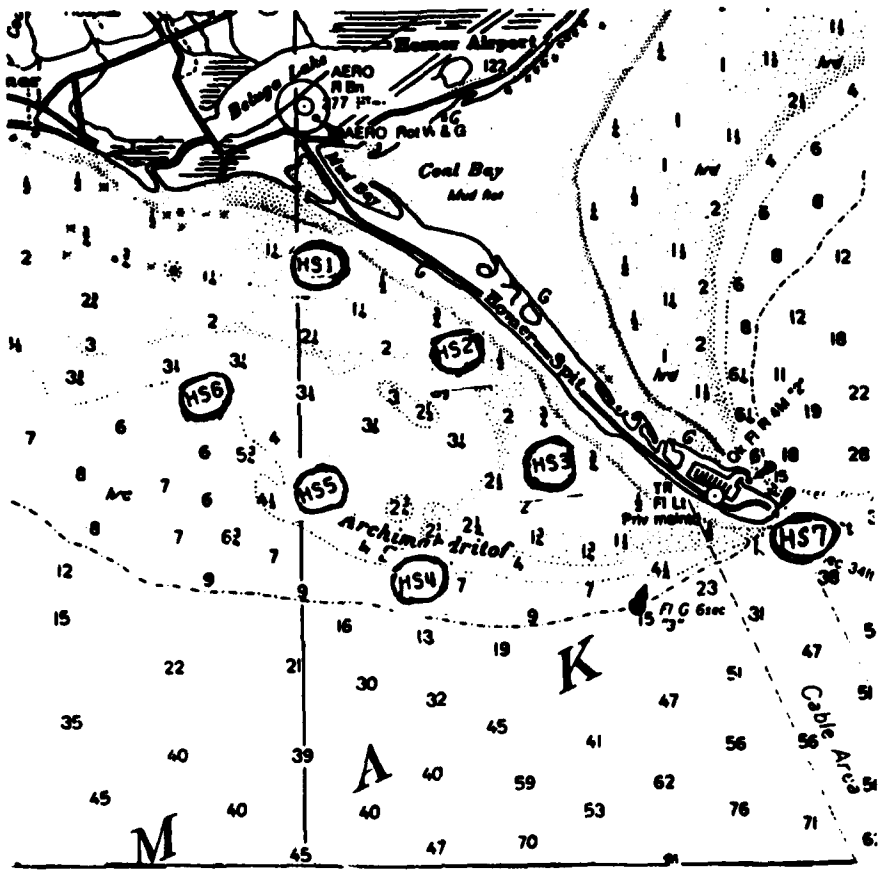

Figure F5. Locations of mooring sta HS1 through HS6 for current measurement

sta HS1 through HS6 are shown in Figure F5. The current vector histograms are shown in Figure F6. The accuracy of the current data is limited, particularly the current direction, as one can readily understand the difficulties in measuring the currents from a small boat. Nevertheless, the magnitudes of the currents from a small boat. Nevertheless, the magnitudes of the currents are still very useful for the study.

8. Notably, the currents were measured during 8 through 12 August 1984 when the tides were in the high tidal range, as shown in Figure F1. Therefore the tidal currents were strong, on the order of 2 fps at the ENDECO station and 1 fps at the mooring stations. However, in a lower tidal range one might expect the tidal currents to become weaker. Also, the maximum flood-tidal currents were larger than the maximum ebb-tidal currents at all the ENDECO and mooring stations.

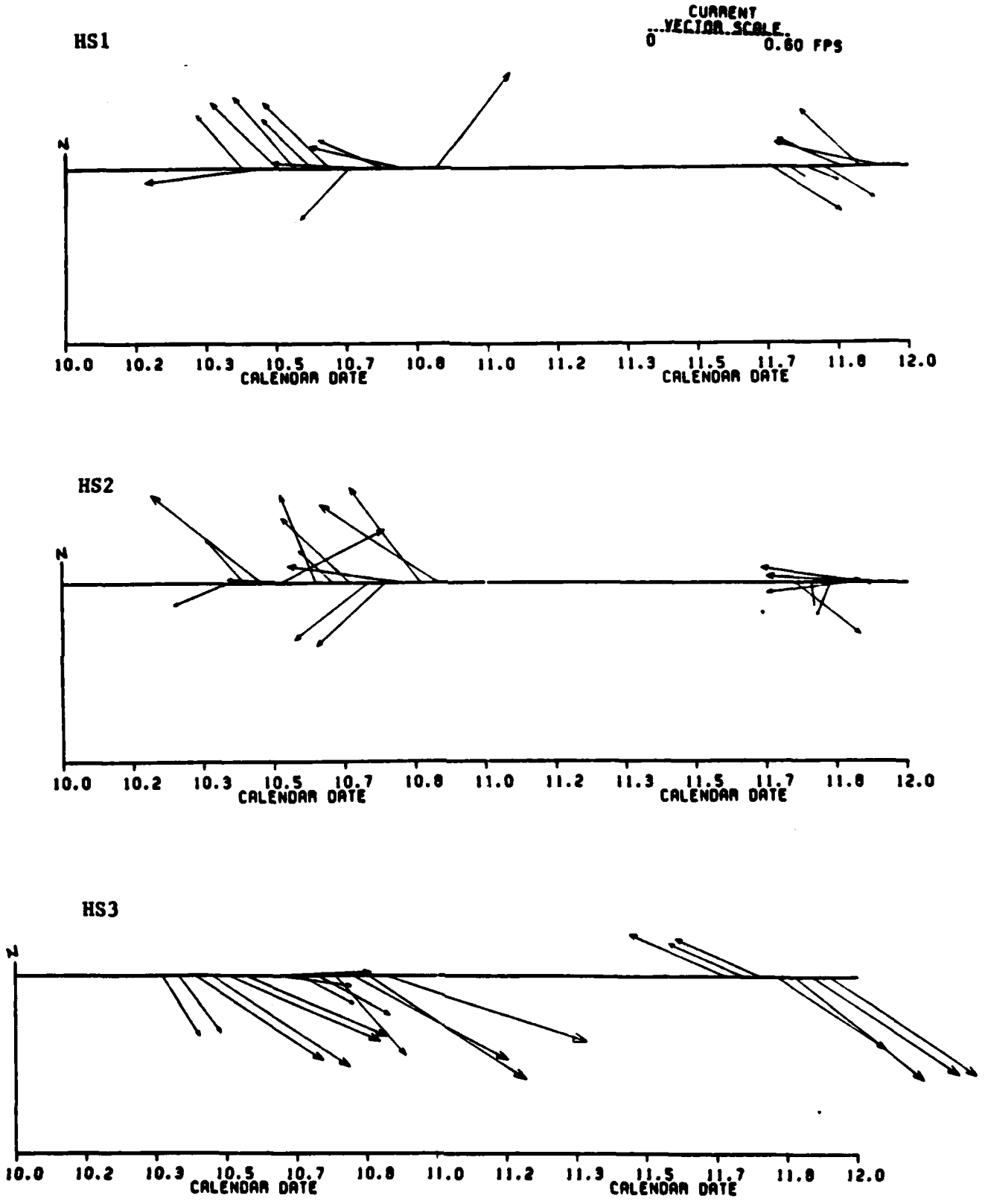

Figure F6. Current vector plots at mooring stations along southwest shore of Homer Spit, August 1984 (Continued)

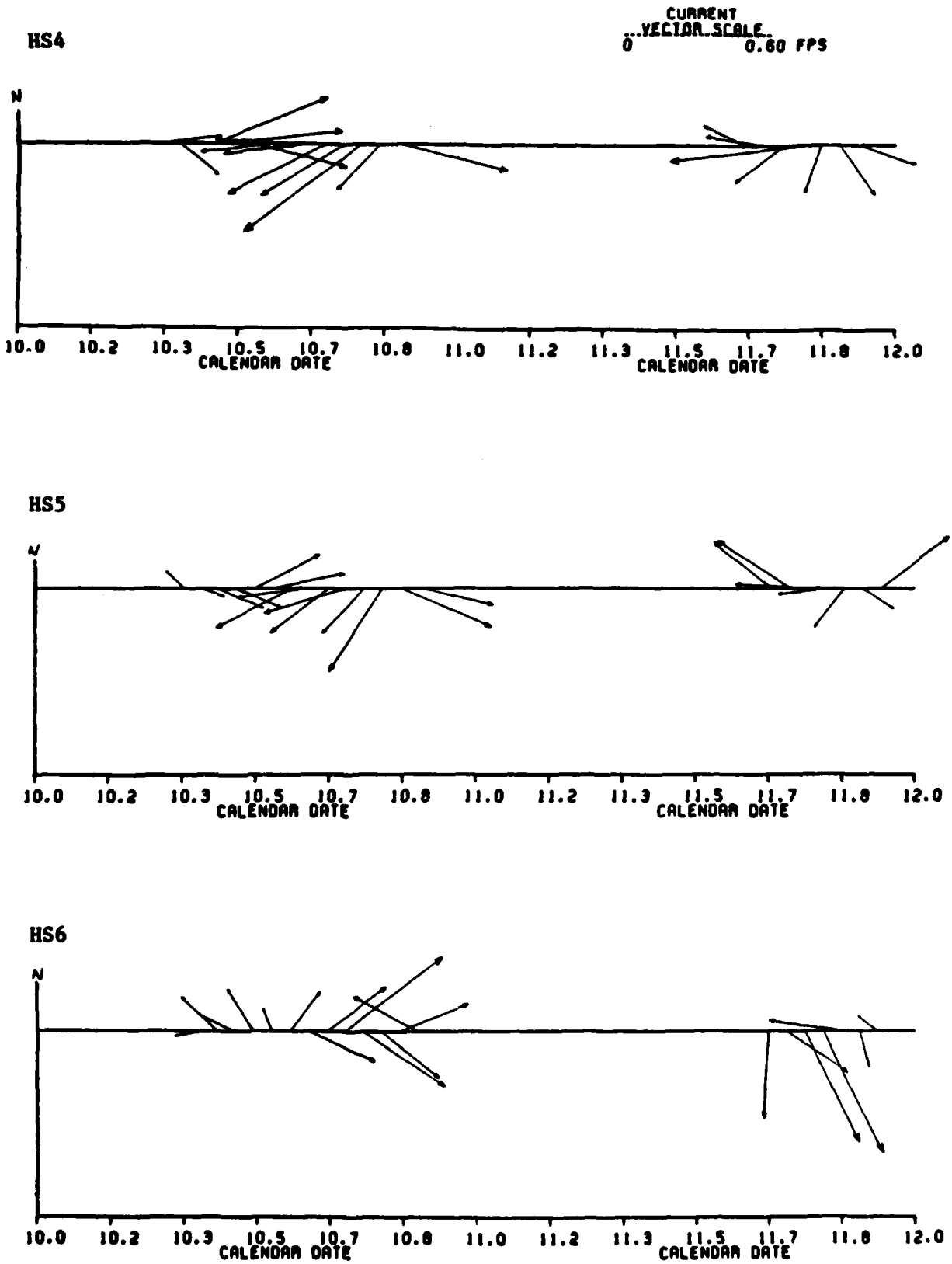

Figure F6. (Concluded)

9. In general, the high tidal range, high Coriolis force, and the inlet geometry cause strong currents during both flood and ebb tides. Tidal currents can reach as high as 2.5 fps near the bay constrictions.

Numerical Simulation of Tides and Tidal Currents

10. Numerical simulation of tides and tidal currents in the bay is an efficient and economic means to obtain hydrographic data to supplement the field data for the engineering project. A multilayer finite element model was originally developed by Kawahara (1978, 1983) and recently modified by Wang (1986). This model was employed to simulate tidal elevations and currents in the bay. Special attention was on the simulation of the project area along the southwest shore of Homer Spit. Dr. Wang and his group at the Center for Computational Hydroscience and Engineering at the University of Mississippi conducted the simulation calculation.

11. The model is based on the conservation equations of mass and momentum for fluid motion. The long wave theory is assumed, and the governing equations are depth-integrated for each layer. A lumped finite element technique, which uses Galerkin weighted residual formulation, is employed for numerical solution.

12. The bathymetry and geometric configuration of the bay for the simulation were taken from the National Ocean Service Nautical Charts. The four-layer finite element mesh system for modeling the bay is shown in Figure F7. There are 637 elements and 409 nodes. The elements along the southwest shore of Homer Spit have only one layer since those elements are in shallow water.

13. The tides at Seldovia shown in Figure F1 were selected as the tidal boundary condition on the south bank of the bay mouth. On the north bank the tidal boundary condition used the same tides at Seldovia but with a phase lag of 5 min. Since the tide gage at Bluff Point Station was lost, the tides on the north bank boundary were estimated from the tides of the nearby stations given in the Tide Table (US Department of Commerce 1984). The phase lag between Seldovia and Bluff Point is increased linearly along the open boundary. Three high, intermediate, and low tidal ranges, of 7.9, 4.5, and 1.1 m, respectively, and a sinusoidal function of 12 hr tidal period at Seldovia were

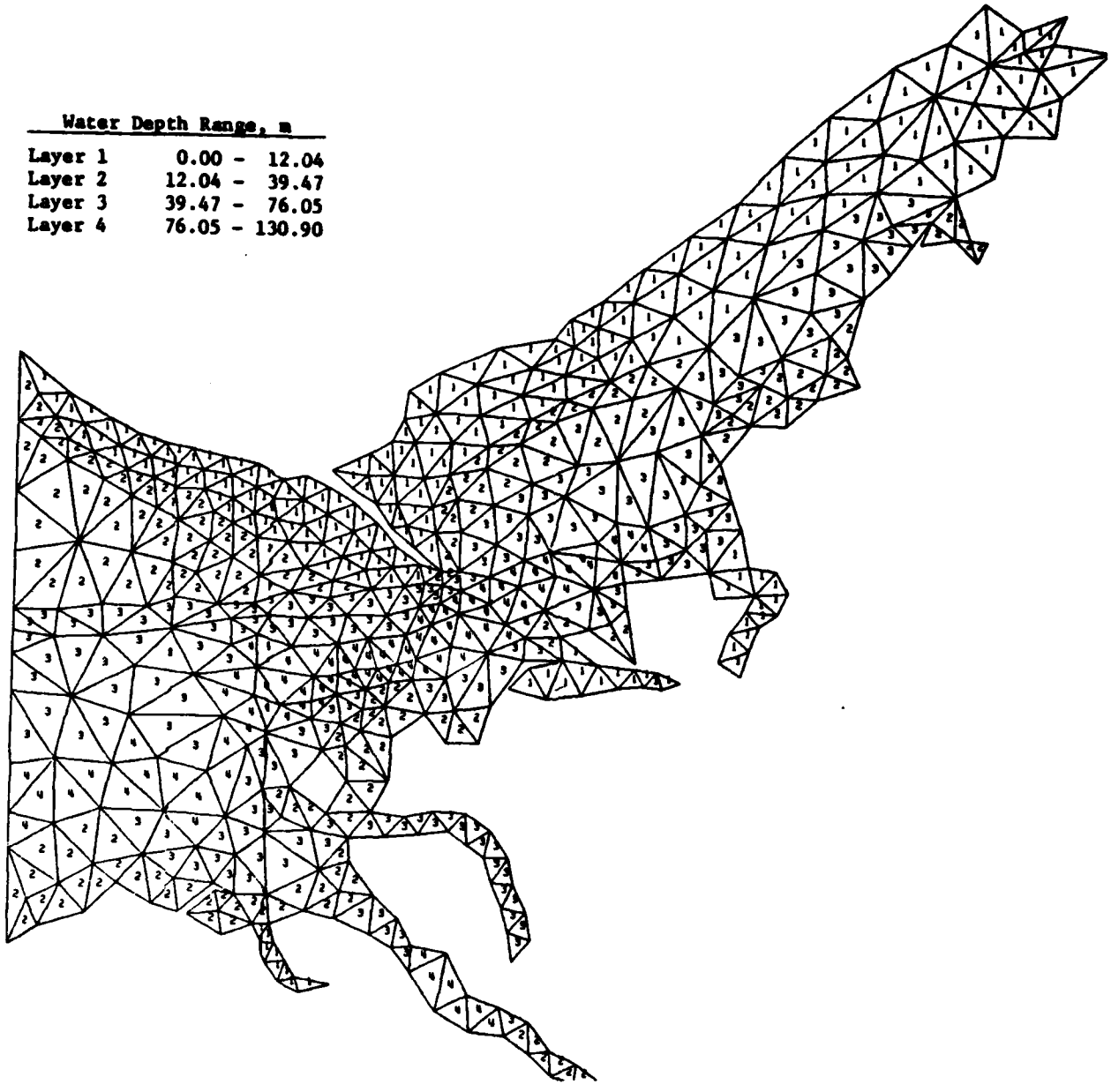

Figure F7. The four-layer finite element mesh system in Kachemak Bay (The number in an element indicates the number of layers of that element.)

used to investigate the effects on water elevations and currents in the bay, with special attention given to the southwest shore of Homer Spit.

14. The freshwater discharge of Bradley River of 86.93 m^3/sec was imposed as a boundary condition at the head of the bay. The slip boundary condition was used along the shorelines and nonslip condition on the bottom of

the bay. Stress boundary conditions were applied at the free surface and the bottom. Initial conditions used a cool start for water elevations and currents. The water elevations were set at the mean water level at the beginning of each simulation.

15. The following parameters were used in the simulation: water temperature was 12°C; water density was 1,024 kg/m^3; and water kinematic viscosity coefficient was 1×10^{-6} m^2/sec; the vertical and horizontal eddy viscosity coefficients were 0.05 and 0.5 m^2/sec, respectively; wind speed was 14 mph; wind direction was 130 deg; wind drag coefficient was 0.001; and the Chezy coefficient was 60.

Simulation Results

16. For each of the three tidal ranges at Seldovia given in paragraph 13, the tidal elevations and currents in the entire bay were continuously simulated until the results repeated themselves in the periods that followed, sometimes up to four tidal periods of computation. The results in the last period for each simulation were stored as output.

17. The horizontal flow circulation in the entire bay subject to the high tidal range of 7.9 m is typically shown in Figure F8 a through d and Figure F9 a through d. The figures represent the ebb and flood circulations. There are four figures in each circulation which show the flow velocity vectors of each of the four layers. These flow velocities are well in agreement with the observed data. In general, the flow accelerates when approaching the narrow passage of the main channel and decelerates after it is passed. Notably the water depth is large along the main channel, and the steepest bottom slope exists along the main channel. Therefore, the maximum velocities do not necessarily occur in the uppermost layer of the narrow passage, but in fact occur in the lower layers. The results also indicate that there is a longshore current along the Homer Spit coastline during most of the tidal period.

18. The vertical components of these flow velocities are at least one order of magnitude smaller than the horizontal components. They are shown in Figure F10. In the figure the vertical dimension and vertical velocity components have been exaggerated to make them more perceptible to the naked eye. The location of the vertical plane selected for projection of the velocity field follows through the main channel of the bay and is shown in Figure F11.

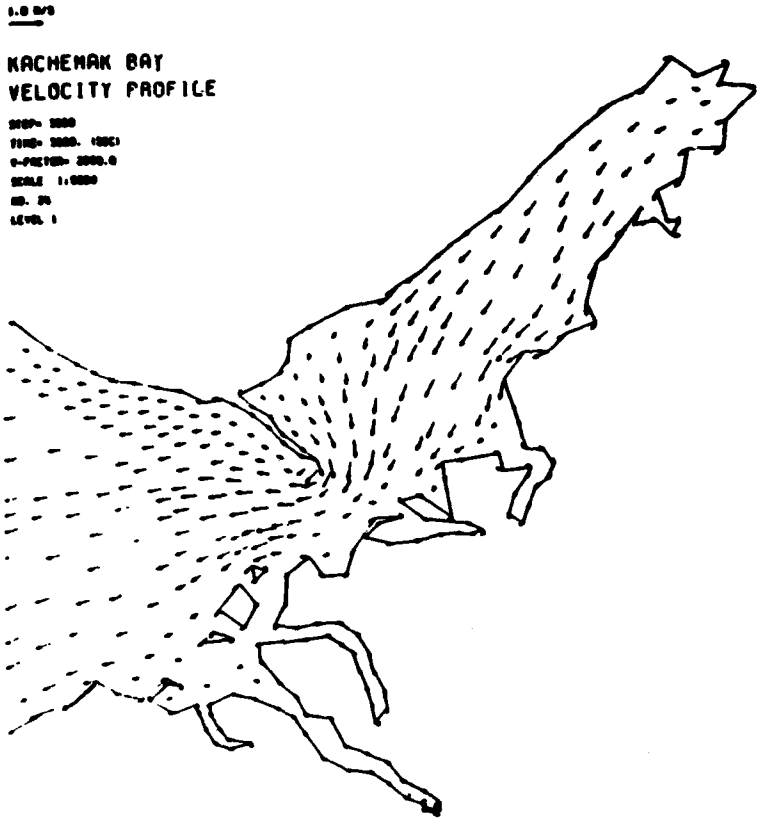

a. Layer 1

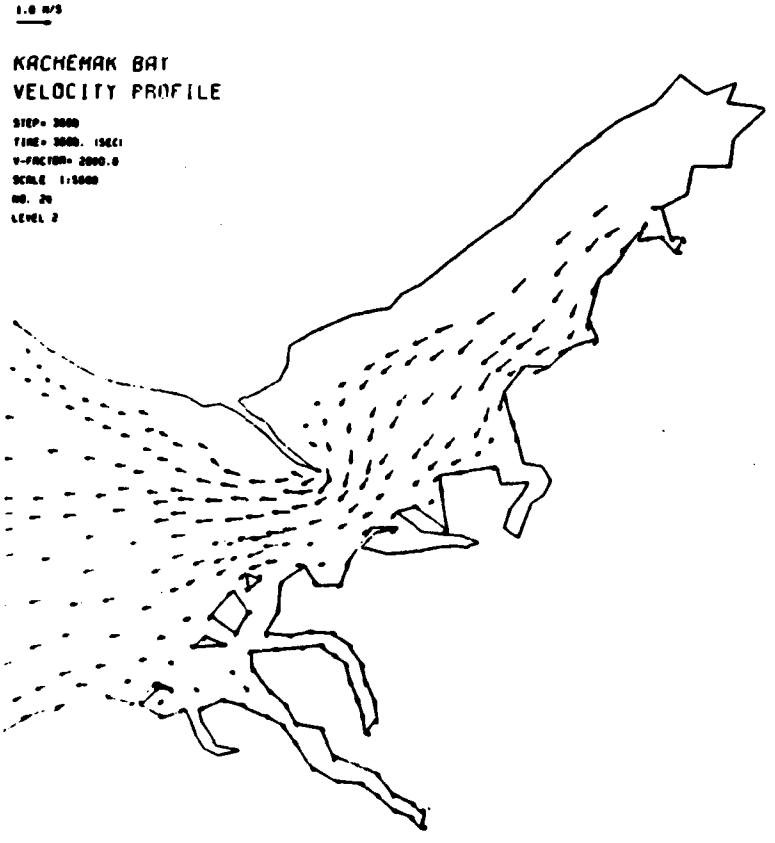

b. Layer 2

Figure F8. Ebb-tidal circulation, tidal range = 7.9 m (Continued)

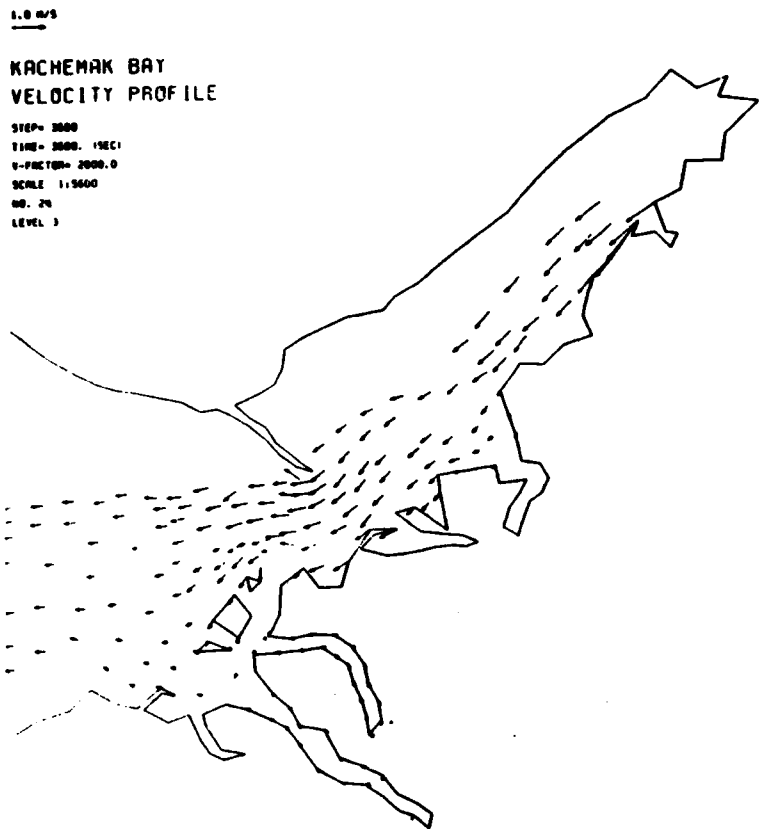

c. Layer 3

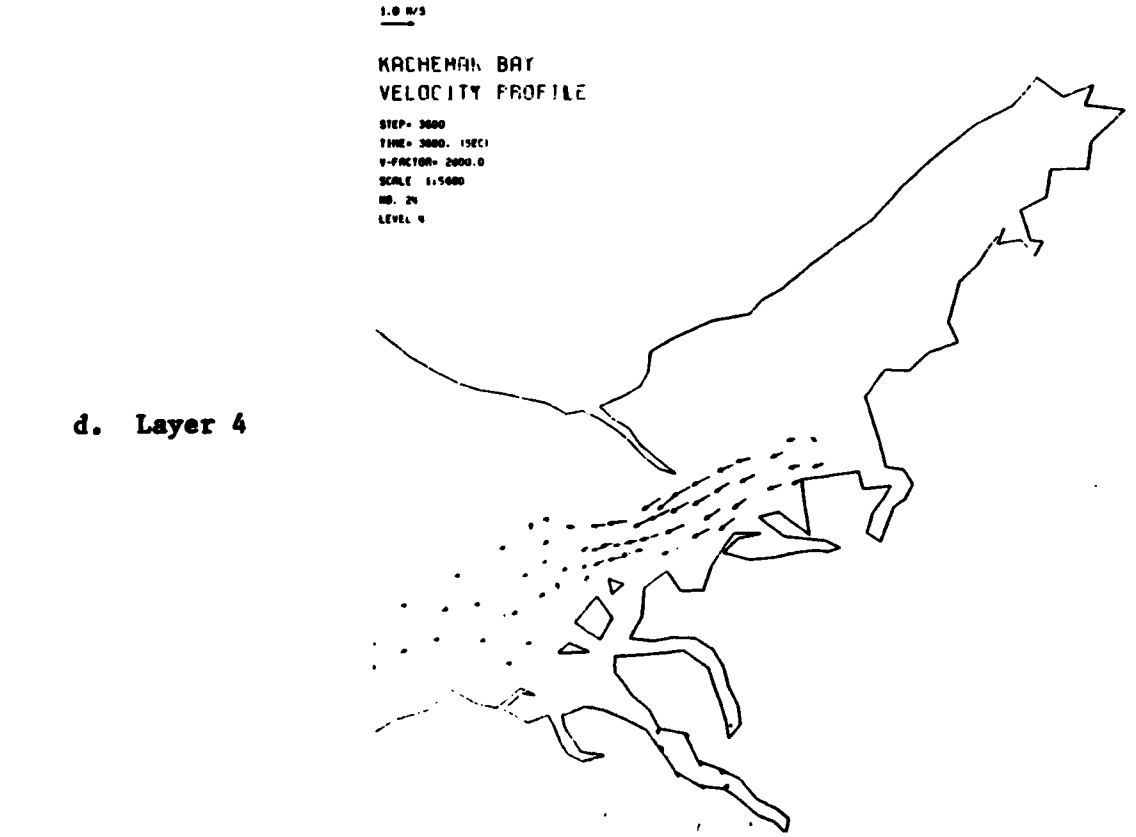

d. Layer 4

Figure F8. (Concluded)

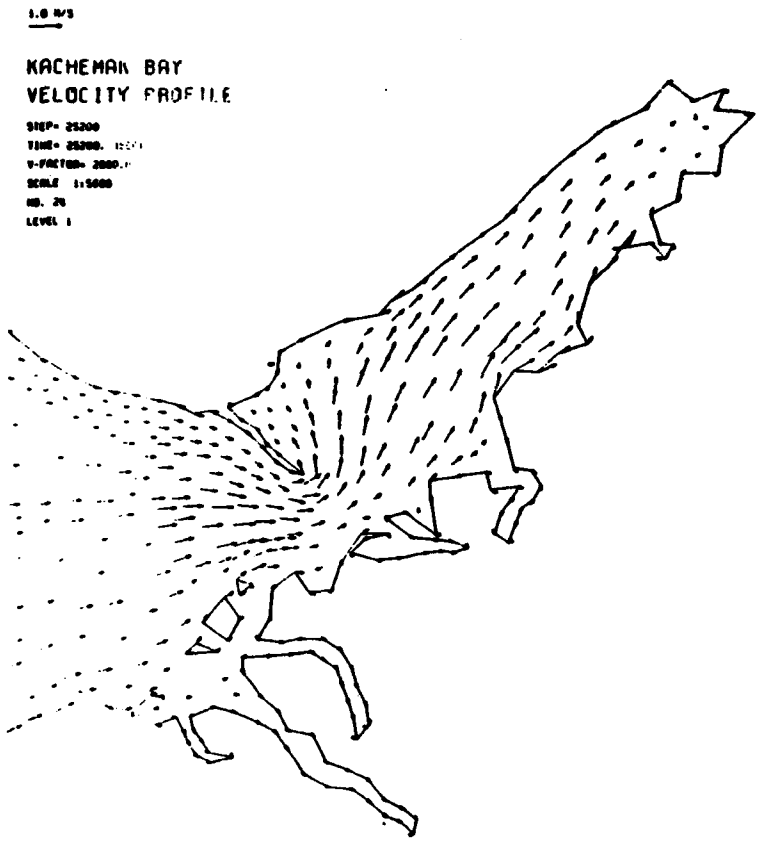

a. Layer 1

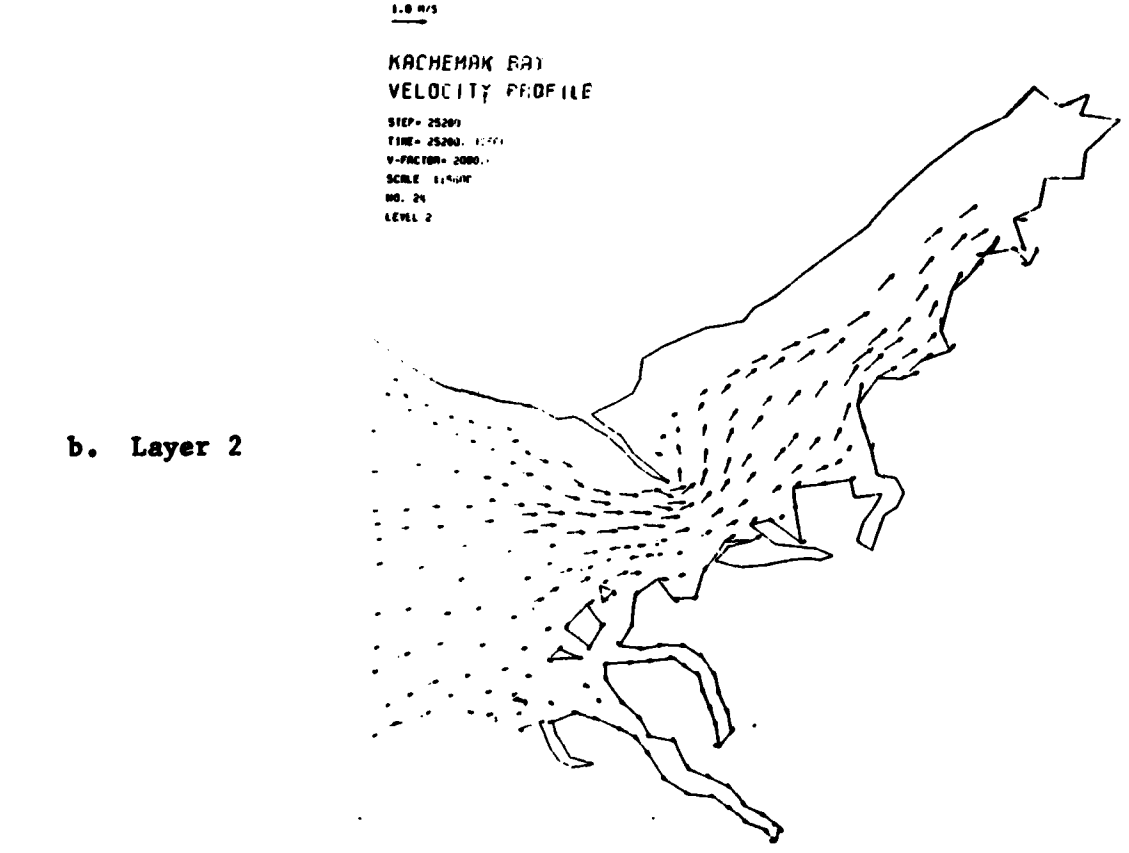

b. Layer 2

Figure F9. Flood-tidal circulation, tidal range = 7.9 m (Continued)

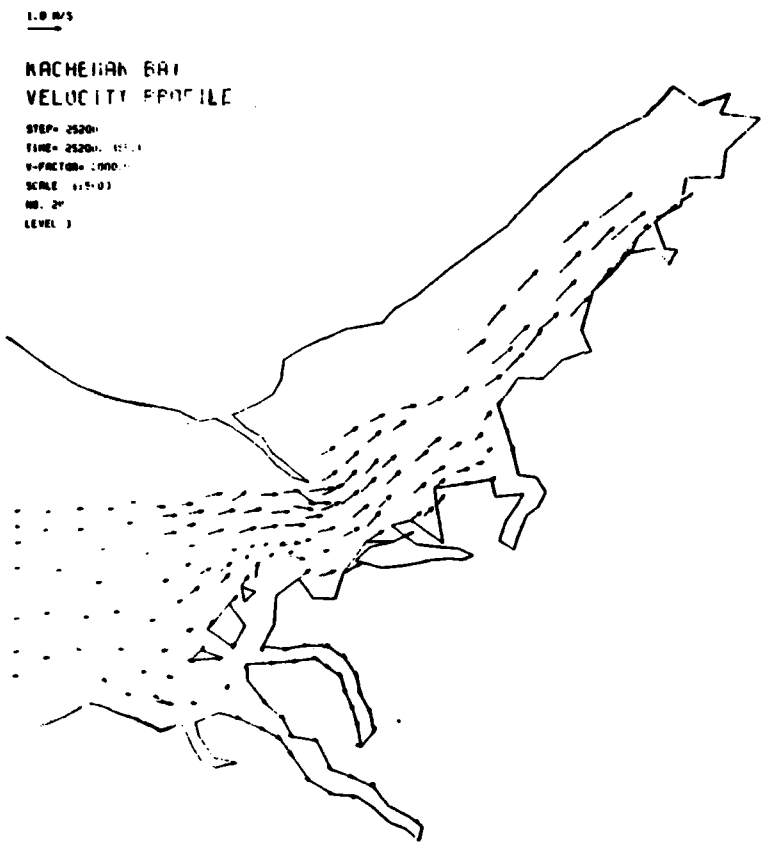

c. Layer 3

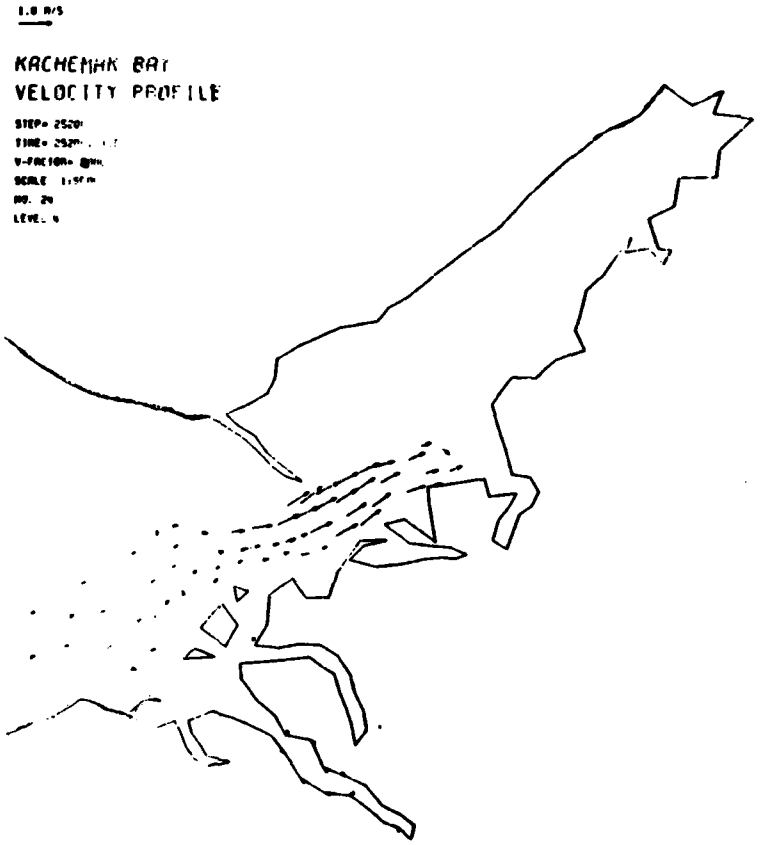

d. Layer 4

Figure F9. (Concluded)

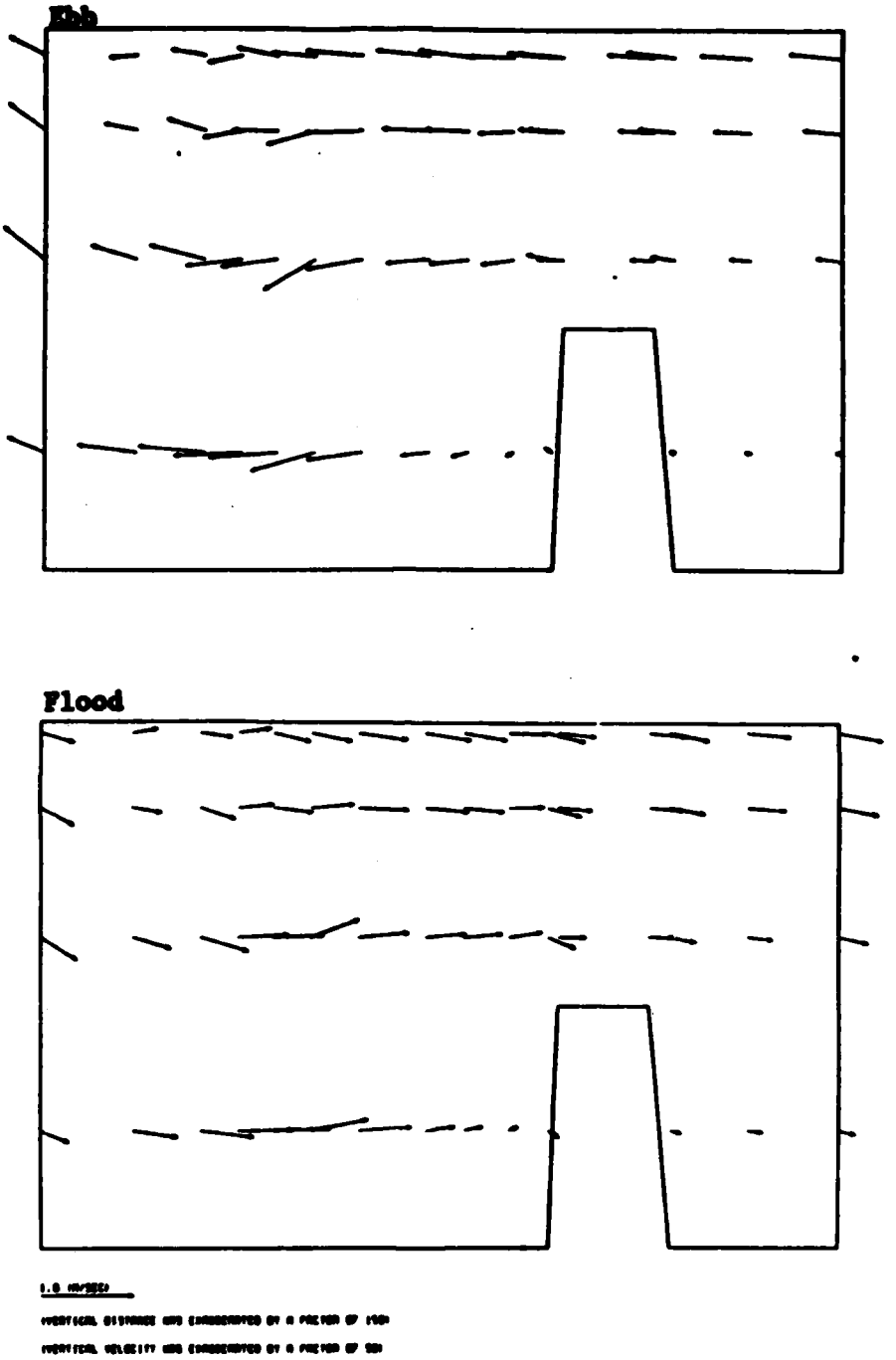

Figure F10. Ebb and flood velocity vectors projected on a vertical plane

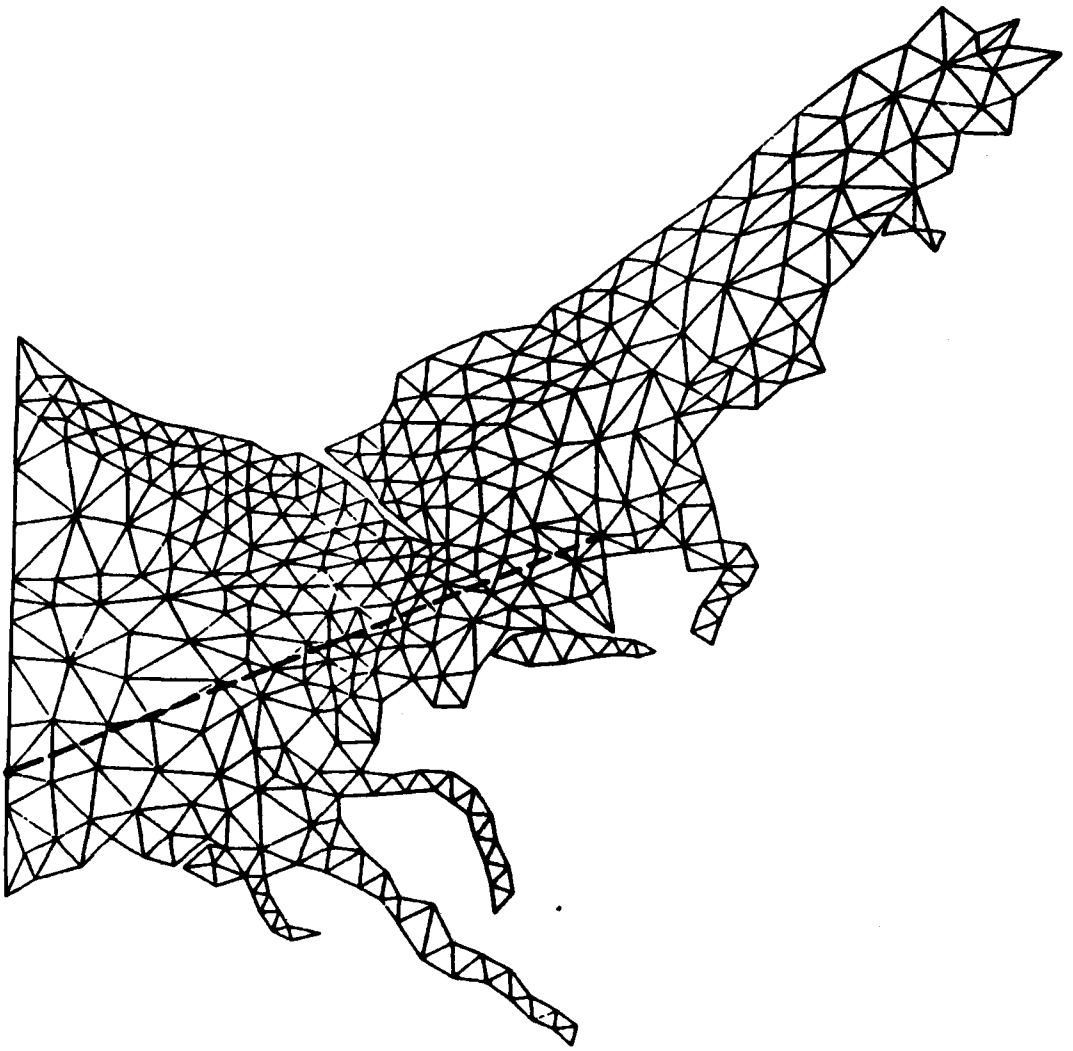

Figure F11. Location of the vertical plane selected for projection of the velocity field

19. The water elevation histograms at three selected nodes, for the case of the intermediate tidal range of 4.5 m at Seldovia, are shown in Figure F12. The tidal ranges at these three nodes are similar to those at Seldovia.

20. Since the critical area in this study is in the vicinity of the southwest shore of Homer Spit, more detailed results are given at nodes in this area. An enlarged finite element of the locations of these nodes is shown in Figure F13. The project area is near node 12. The results of water elevations and velocity vectors for the case of the high tidal range 7.9 m are shown in Figure F14 a through r. The water elevations at the tip of Homer Spit are in agreement with the field observation. The results indicate

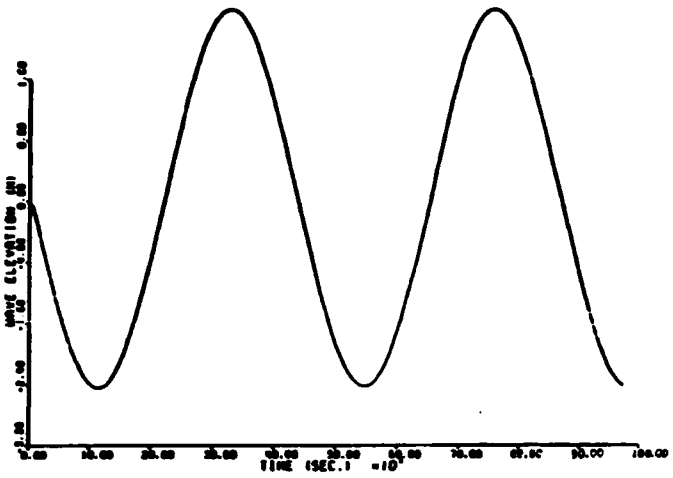

a. Kachemak Bay wave histogram at A

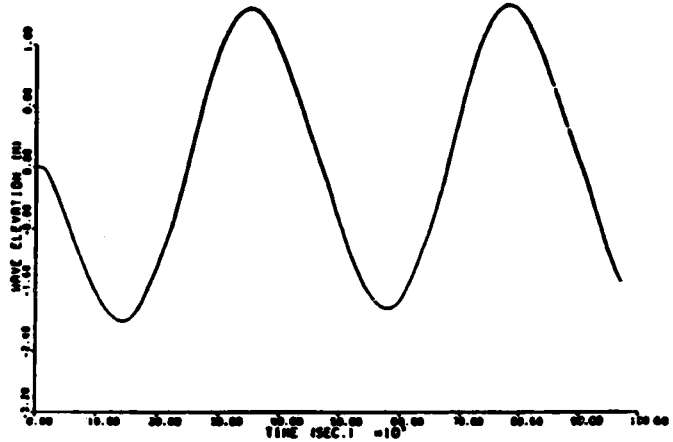

b. Kachemak Bay wave histogram at B

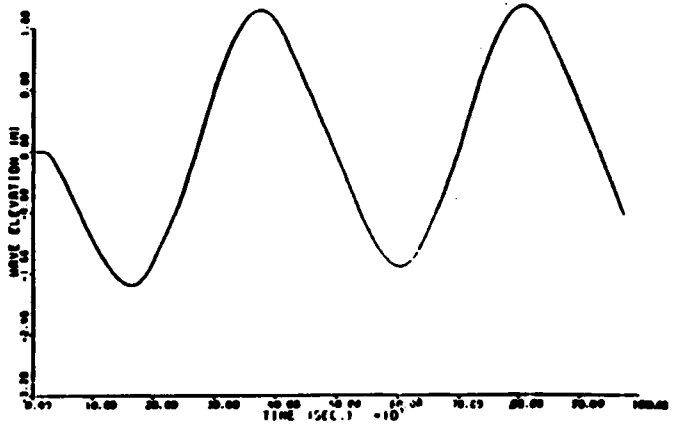

c. Kachemak Bay wave histogram at C

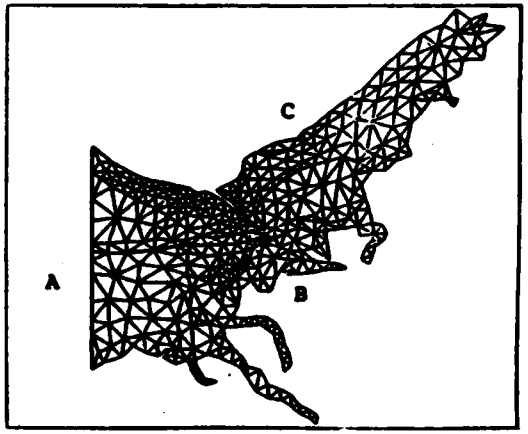

d. Locations of A, B, and C

Figure F12. Water elevation of Nodes A, B, and C; tidal range = 4.5 m

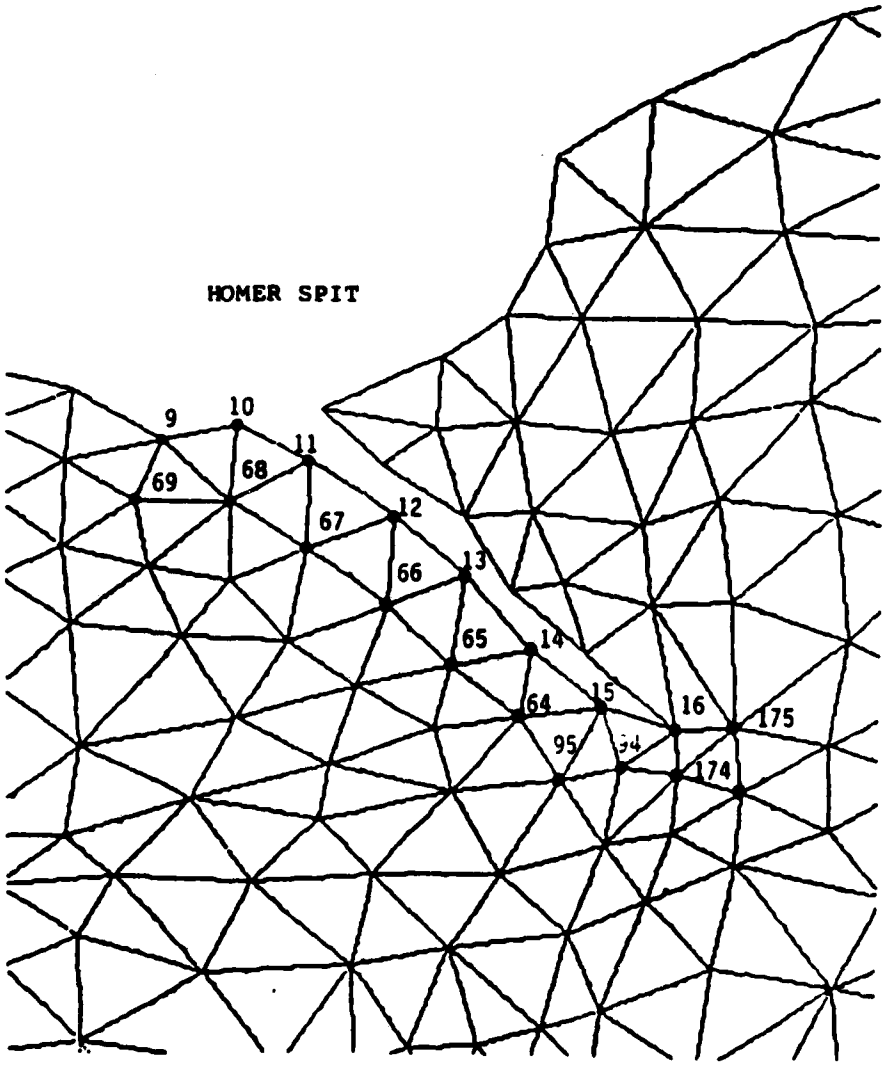

Figure F13. Nodal numbers of the selected nodes where detailed histograms of elevation and velocity are plotted

that the water elevations along the southwest shore of Homer Spit are almost identical to those at Seldovia, except for some phase difference on the order of minutes from Seldovia and among themselves.

21. The flow velocities also agree well with the field observation and are in the longshore directions. The maximum tidal currents near the project area are 0.262 m/sec at node 12 and 0.282 m/sec at node 66; maximums near the tip of Homer Spit are 0.644 m/sec at node 16 and 0.670 m/sec at node 175.

22. The simulations of the cases of the intermediate and low tidal ranges, 4.5 and 1.1 m, respectively, were conducted also. The results of the

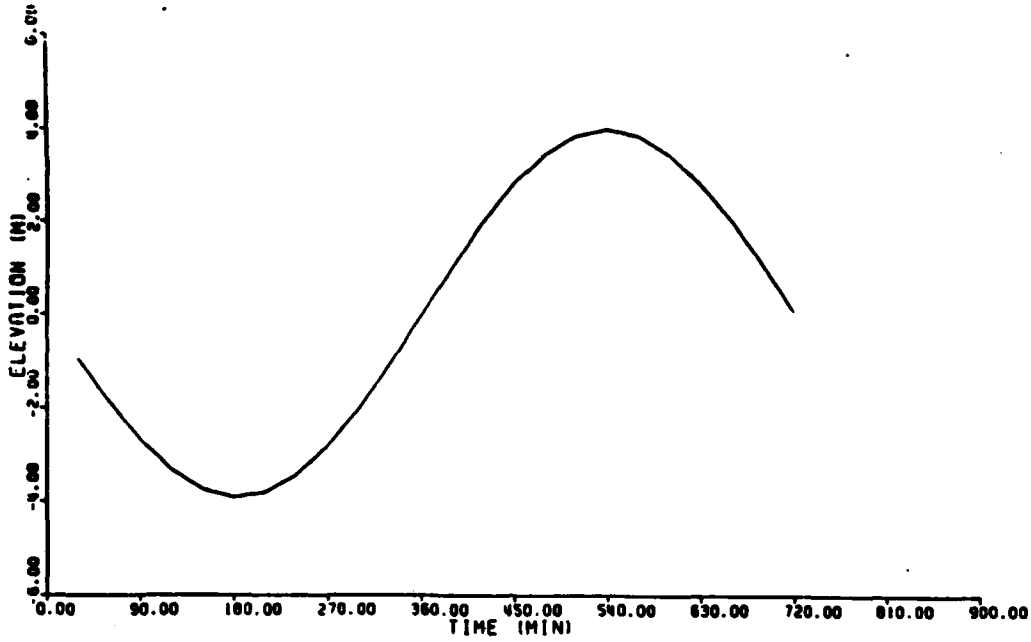

KACHEMAK BAY TIDAL ELEVATION HISTOGRAM

NODAL NUMBER 9 CASE NUMBER 24

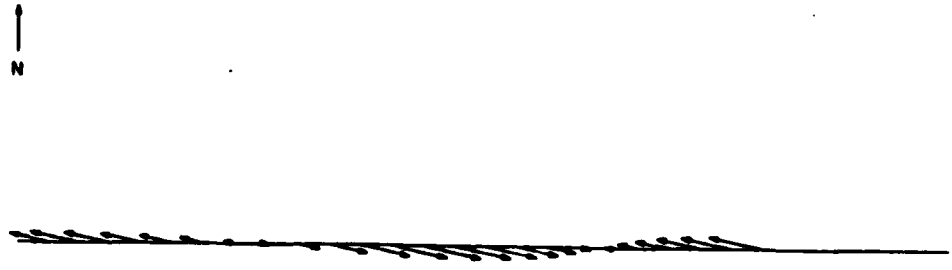

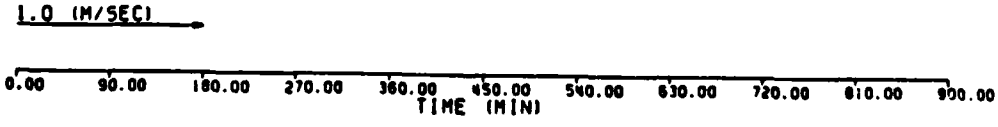

KACHEMAK BAY VELOCITY VECTORS

NODAL NUMBER 9 CASE NUMBER 24

a. Node 9

Figure F14. Water elevation and velocity, tidal range = 7.9 m (Sheet 1 of 18)

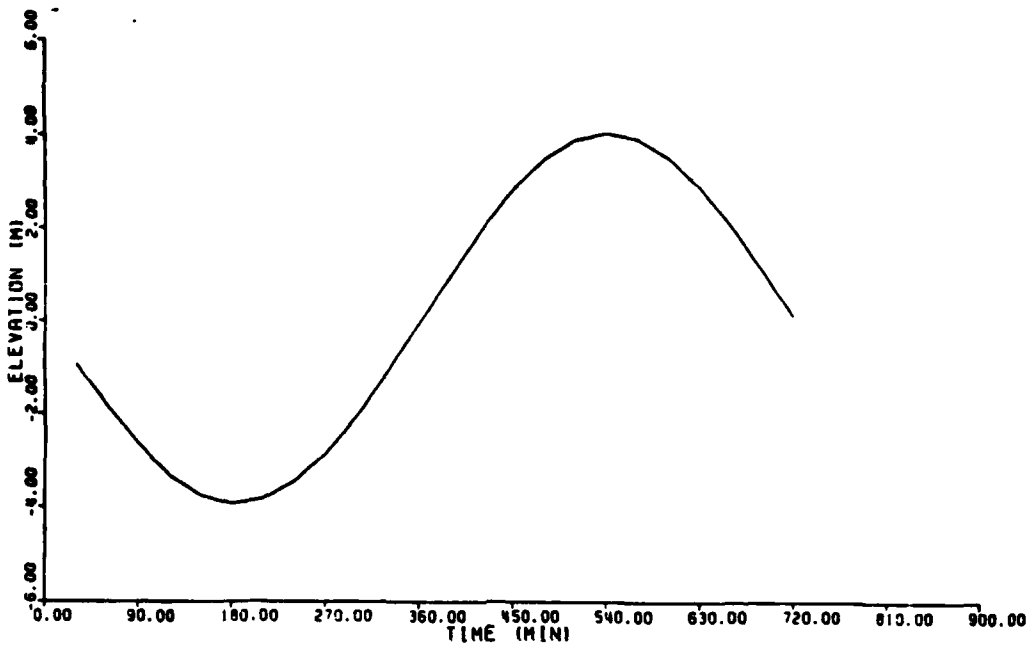

KACHEMAK BAY TIDAL ELEVATION HISTOGRAM

NODAL NUMBER 10 CASE NUMBER 24

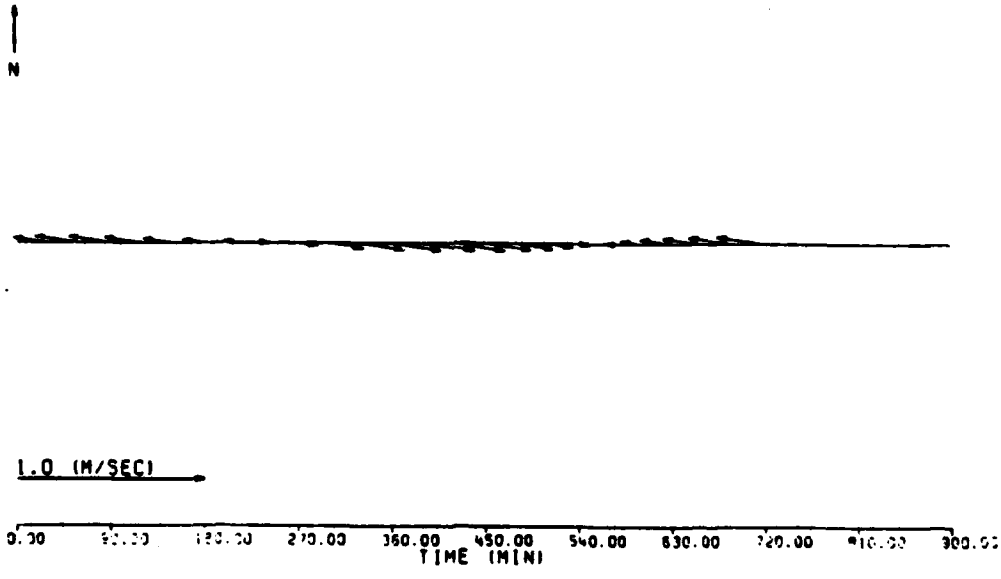

KACHEMAK BAY VELOCITY VECTORS

NODAL NUMBER 10 CASE NUMBER 24

b. Node 10

Figure F14. (Sheet 2 of 18)

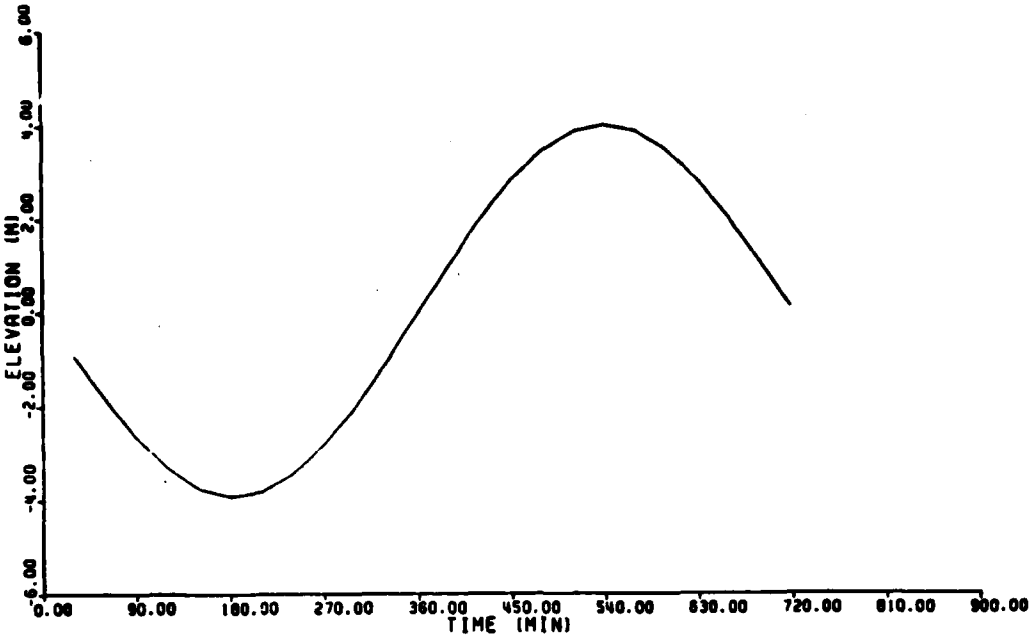

KACHEMAK BAY TIDAL ELEVATION HISTOGRAM

NODAL NUMBER 11 CASE NUMBER 24

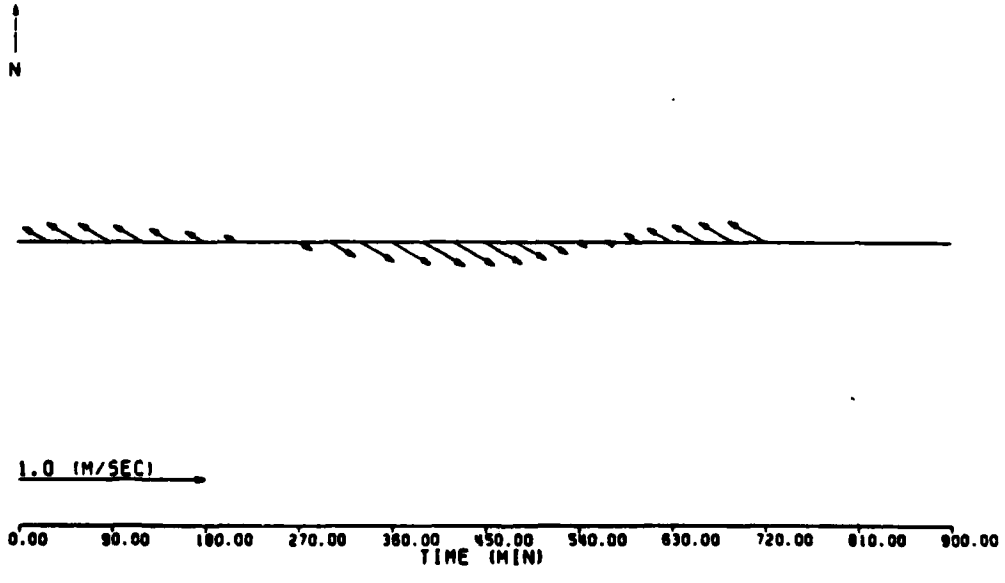

KACHEMAK BAY VELOCITY VECTORS

NODAL NUMBER 11 CASE NUMBER 24

c. Node 11

Figure 14. (Sheet 3 of 18)

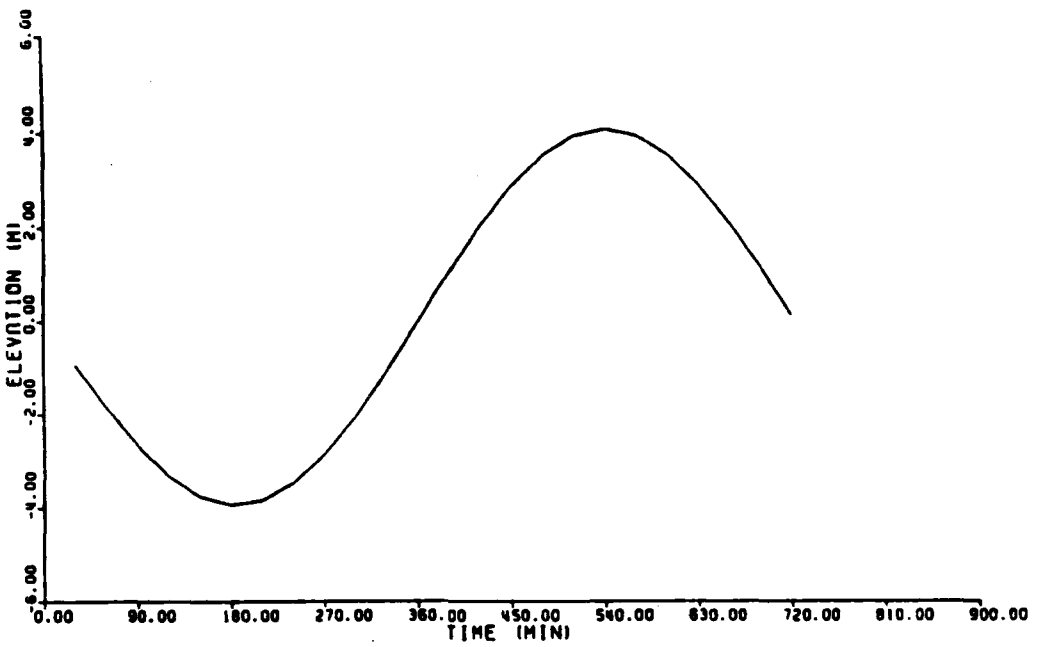

KACHEMAK BAY TIDAL ELEVATION HISTOGRAM

NODAL NUMBER 12 CASE NUMBER 24

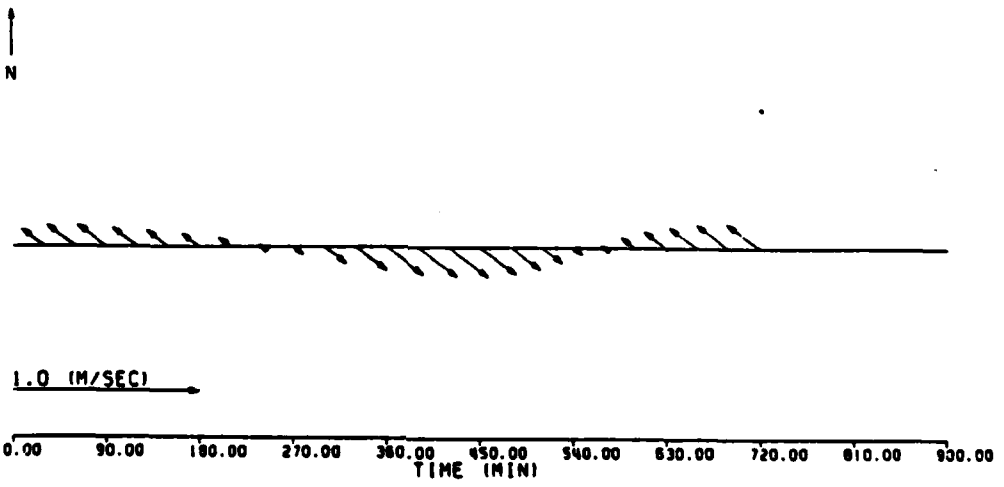

KACHEMAK BAY VELOCITY VECTORS

NODAL NUMBER 12 CASE NUMBER 24

d. Node 12

Figure F14. (Sheet 4 of 18)

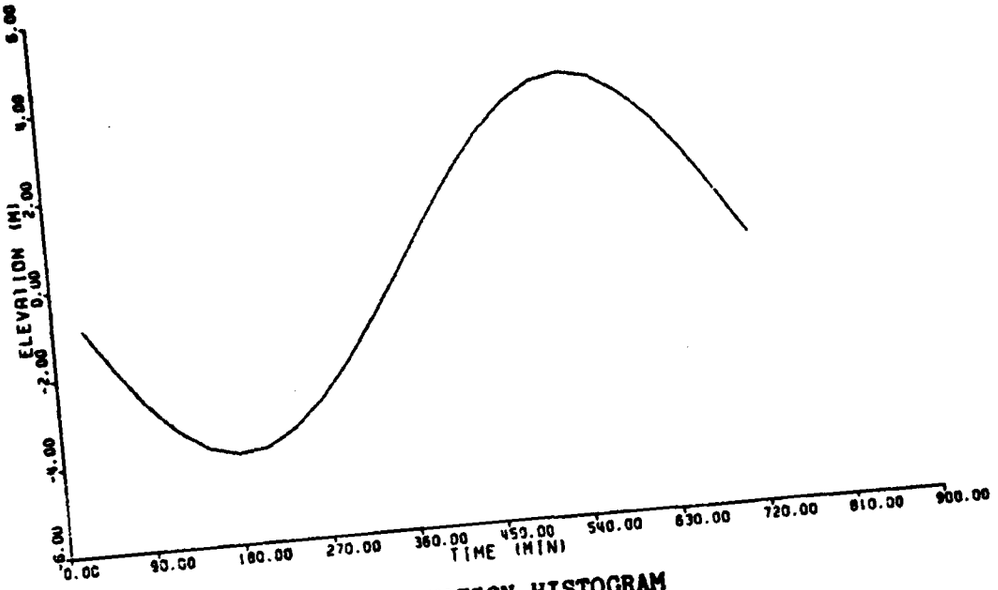

KACHEMAK BAY TIDAL ELEVATION HISTOGRAM

NODAL NUMBER 13 CASE NUMBER 24

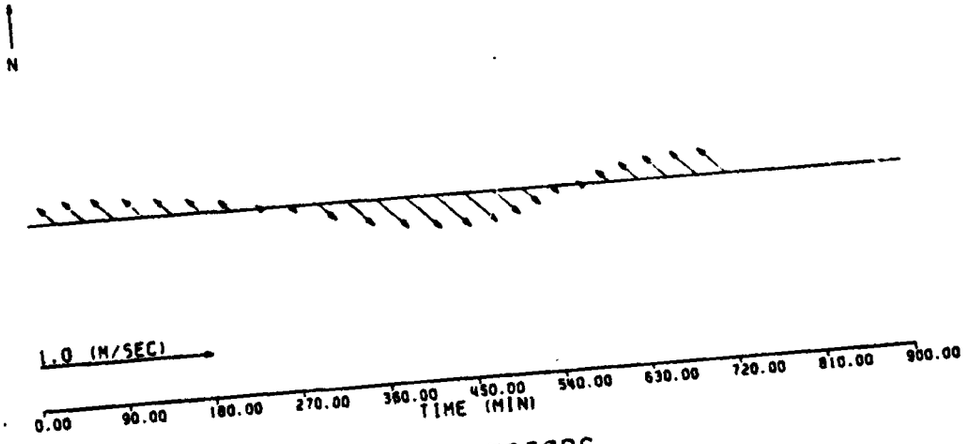

KACHEMAK BAY VELOCITY VECTORS

NODAL NUMBER 13 CASE NUMBER 24

e. Node 13

Figure 14. (Sheet 5 of 18)

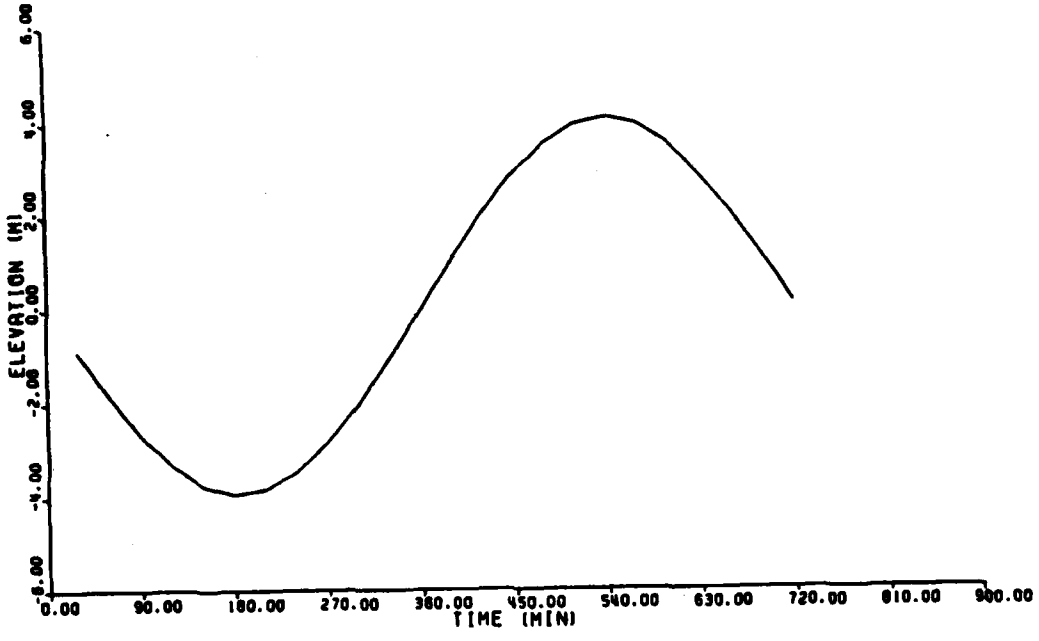

KACHEMAK BAY TIDAL ELEVATION HISTOGRAM

NODAL NUMBER 14 CASE NUMBER 24

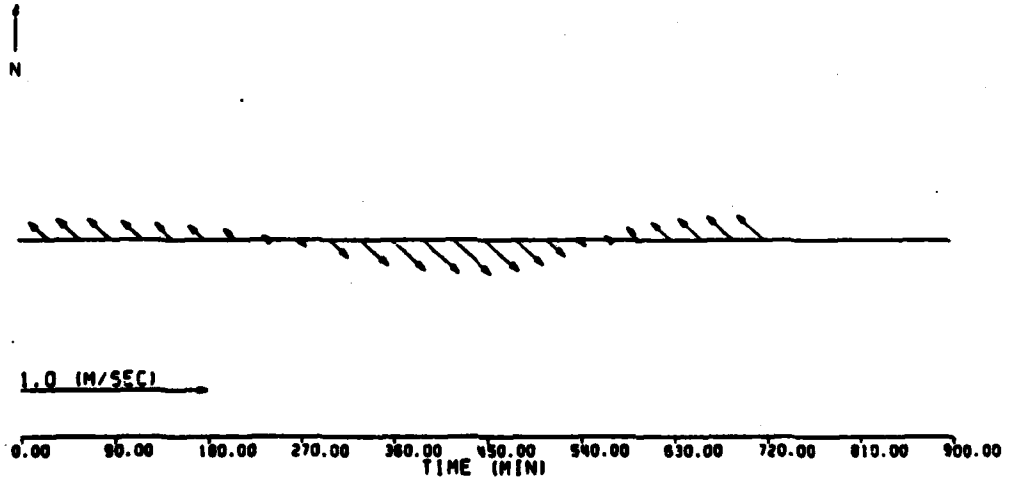

KACHEMAK BAY VELOCITY VECTORS

NODAL NUMBER 14 CASE NUMBER 24

f. Node 14

Figure 14. (Sheet 6 of 18)

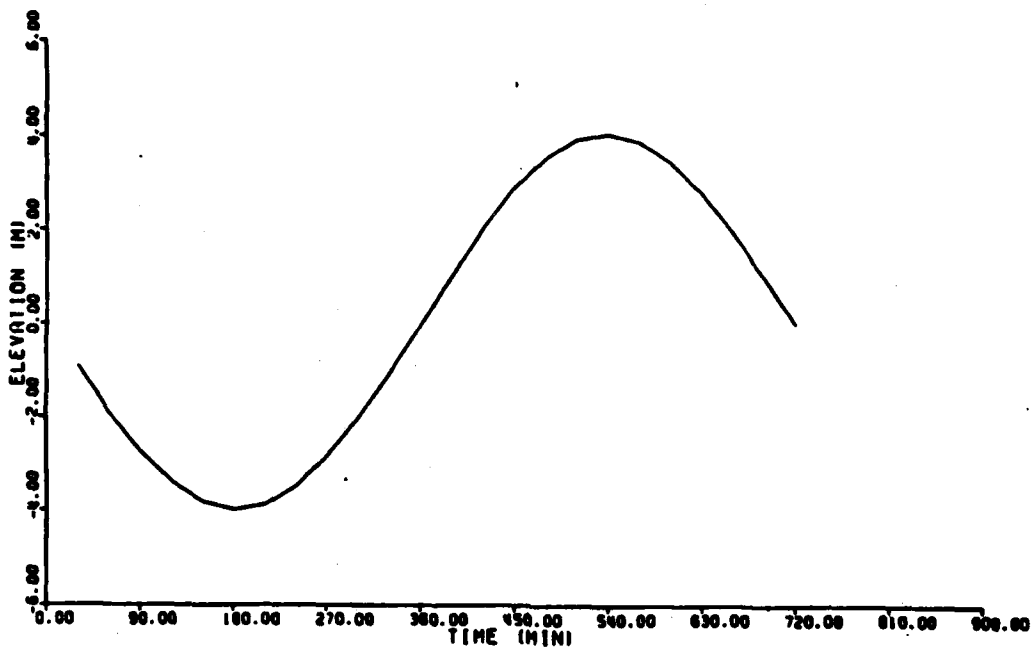

KACHEMAK BAY TIDAL ELEVATION HISTOGRAM

NODAL NUMBER 15 CASE NUMBER 24

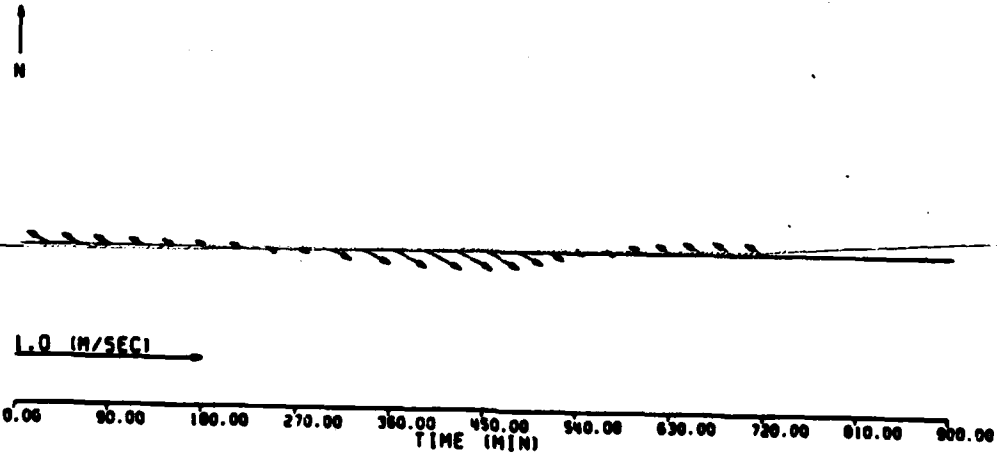

KACHEMAK BAY VELOCITY VECTORS

NODAL NUMBER 15 CASE NUMBER 24

g. Node 15

Figure F14. (Sheet 7 of 18)

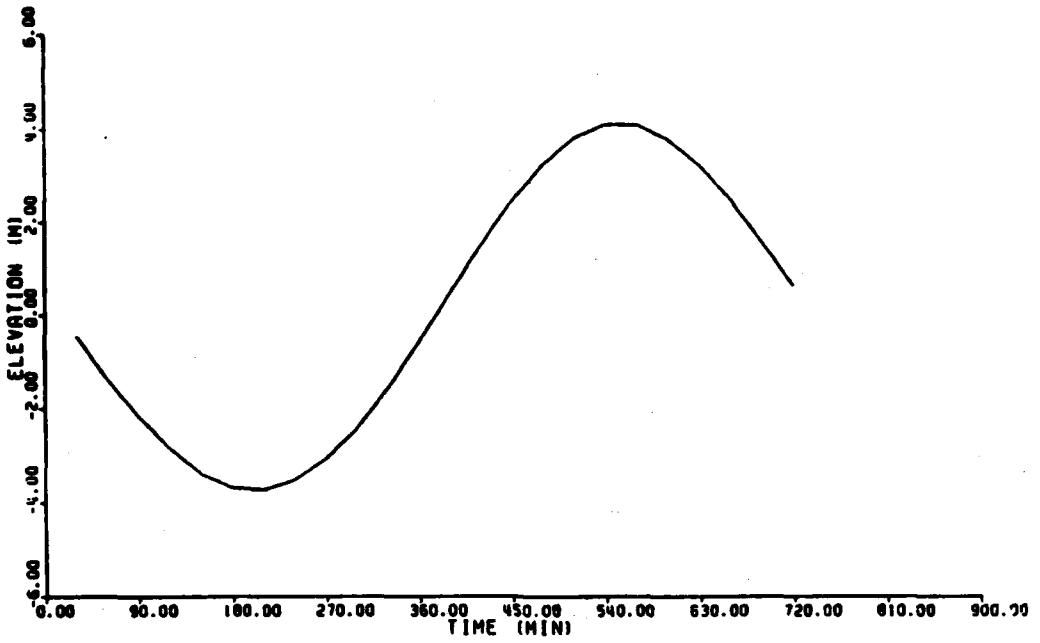

KACHEMAK BAY TIDAL ELEVATION HISTOGRAM

NODAL NUMBER 16 CASE NUMBER 24

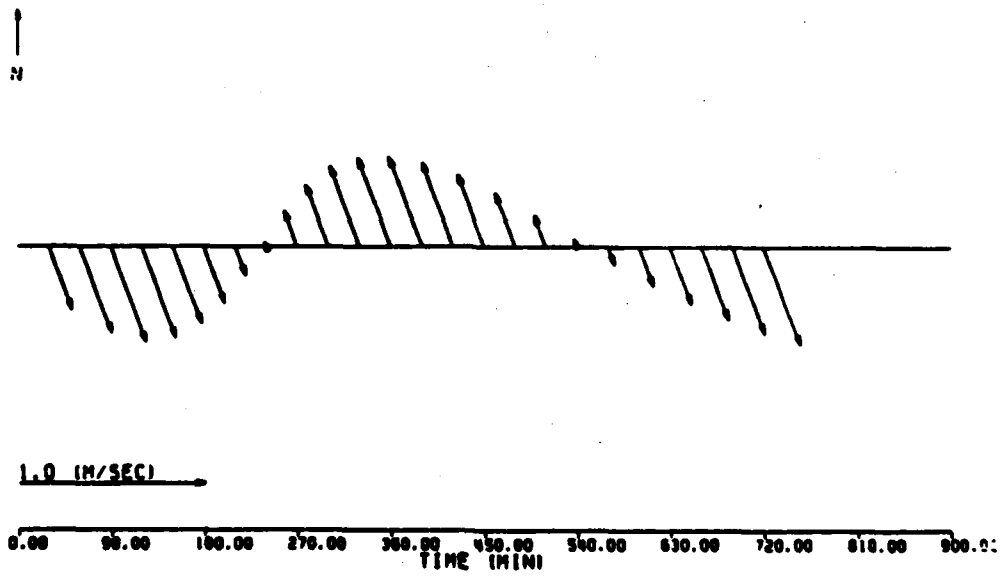

KACHEMAK BAY VELOCITY VECTORS

NODAL NUMBER 16 CASE NUMBER 24

h. Node 16

Figure 14. (Sheet 8 of 18)

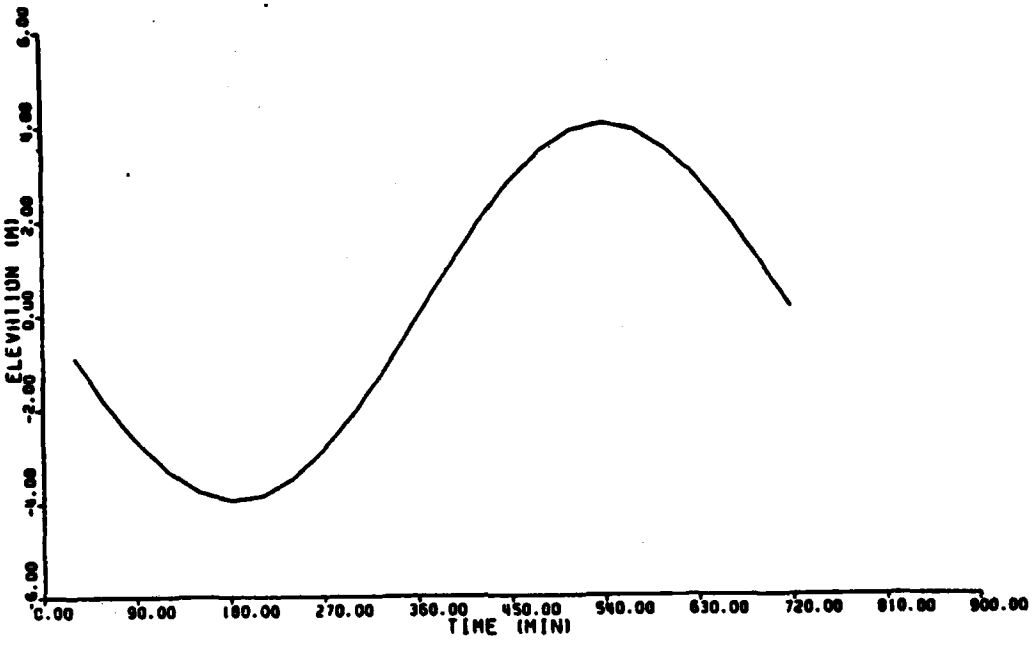

KACHEMAK BAY TIDAL ELEVATION HISTOGRAM

NODAL NUMBER 64 CASE NUMBER 24

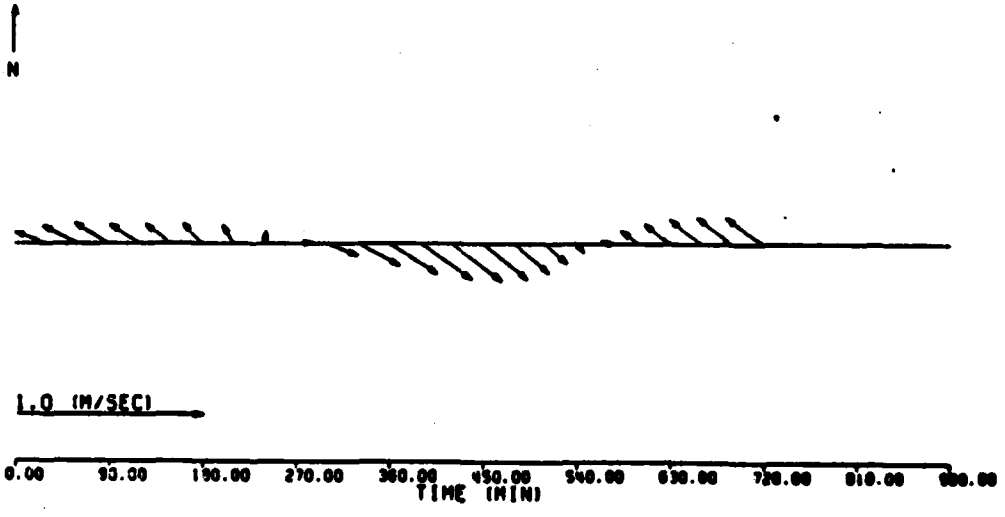

KACHEMAK BAY VELOCITY VECTORS

NODAL NUMBER 64 CASE NUMBER 24

1. Node 64

Figure F14. (Sheet 9 of 18)

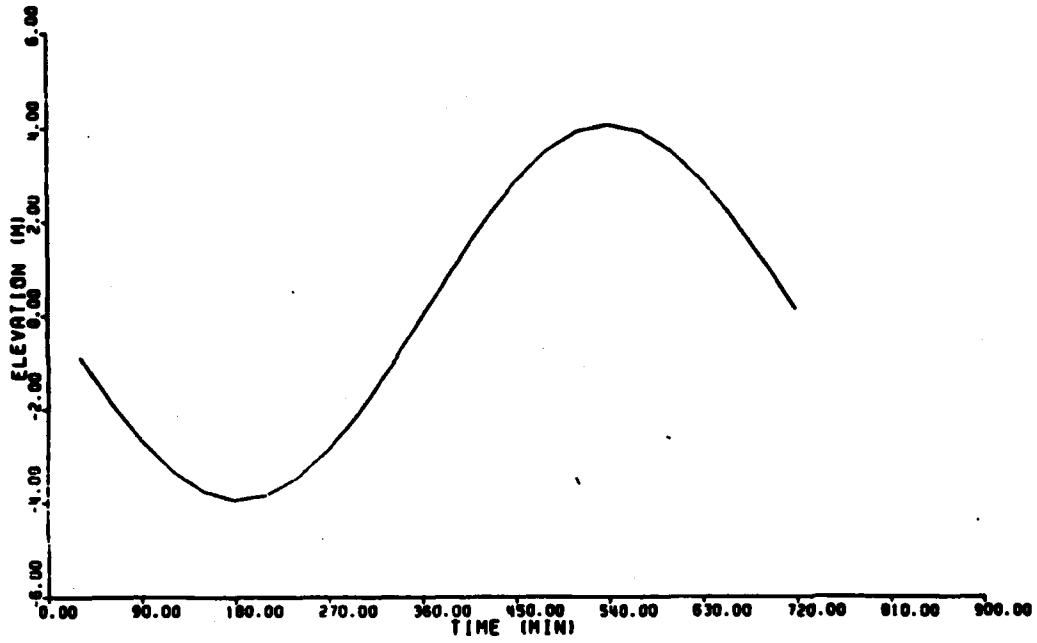

KACHEMAK BAY TIDAL ELEVATION HISTOGRAM

NODAL NUMBER 65 CASE NUMBER 24

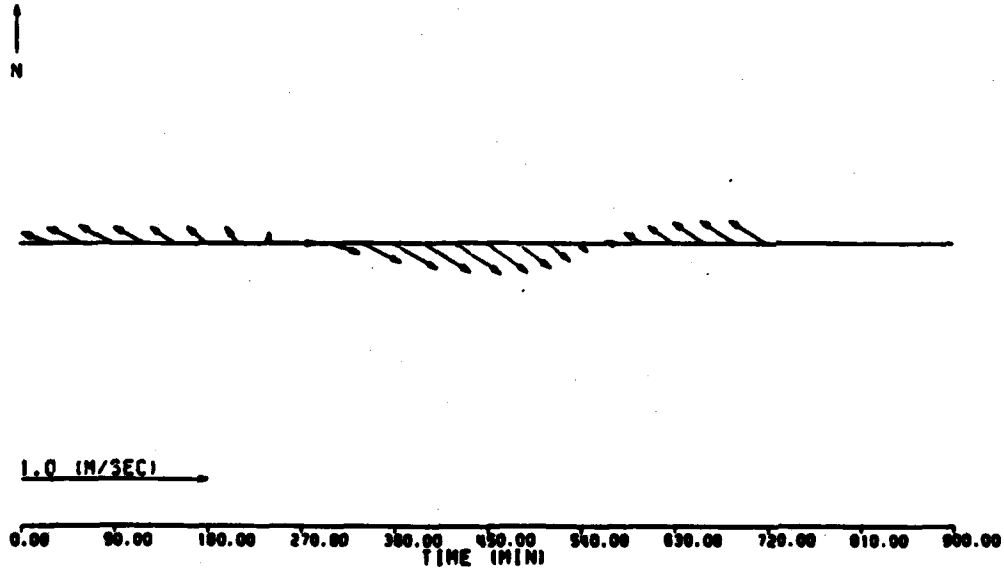

KACHEMAK BAY VELOCITY VECTORS

NODAL NUMBER 65 CASE NUMBER 24

j. Node 65

Figure F14. (Sheet 10 of 18)

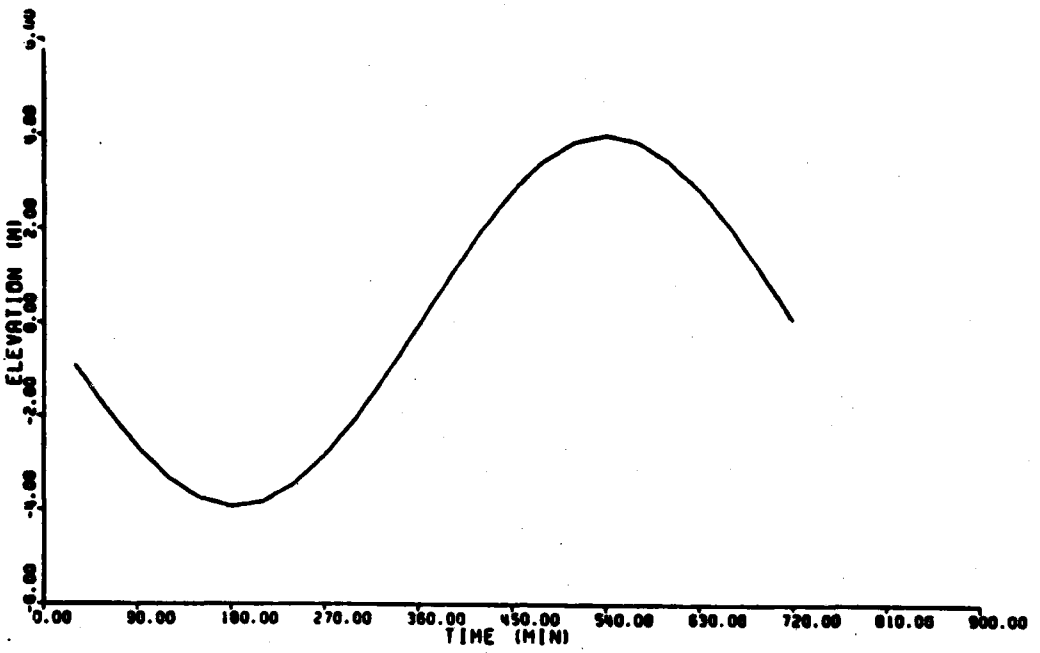

KACHEMAK BAY TIDAL ELEVATION HISTOGRAM

NODAL NUMBER 66 CASE NUMBER 24

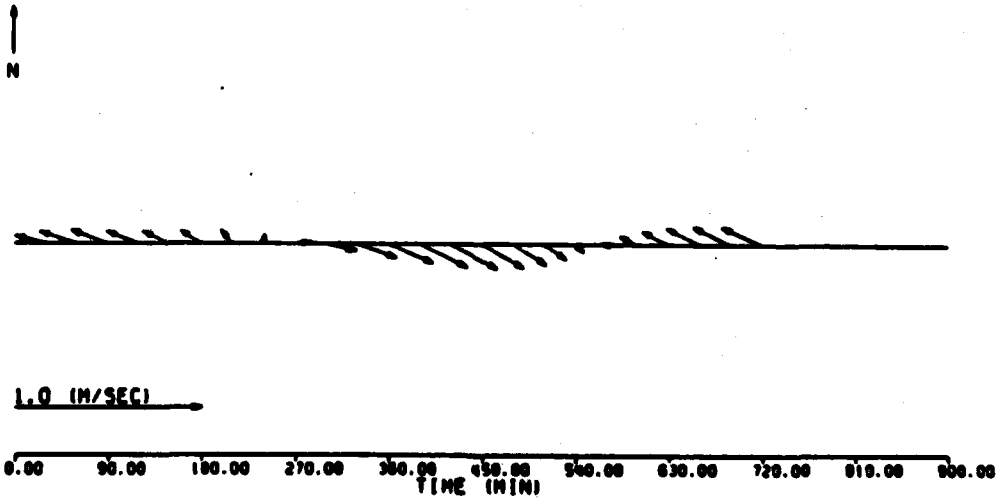

KACHEMAK BAY VELOCITY VECTORS

NODAL NUMBER 66 CASE NUMBER 24

k. Node 66

Figure 14. (Sheet 11 of 18)

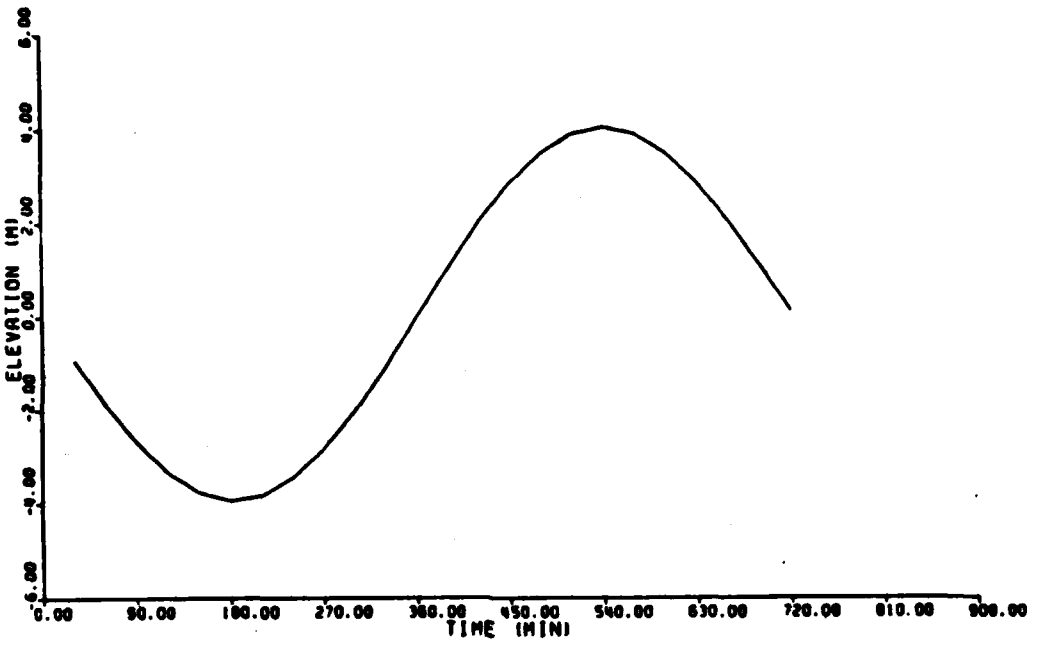

KACHEMAK BAY TIDAL ELEVATION HISTOGRAM

NODAL NUMBER 67 CASE NUMBER 24

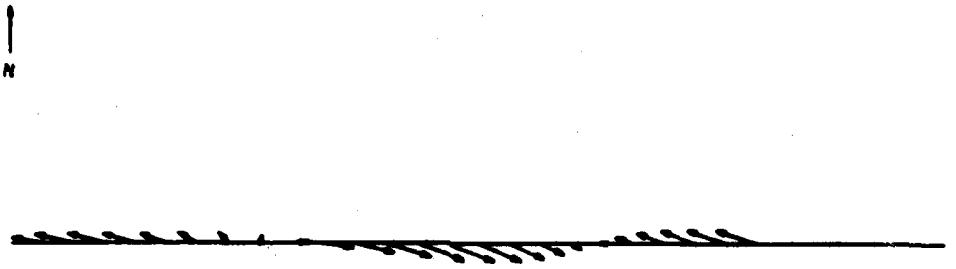

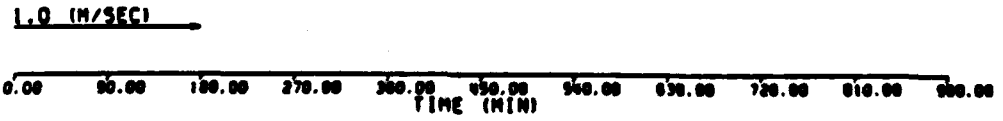

KACHEMAK BAY VELOCITY VECTORS

NODAL NUMBER 67 CASE NUMBER 24

1. Node 67

Figure F14. (Sheet 12 of 18)

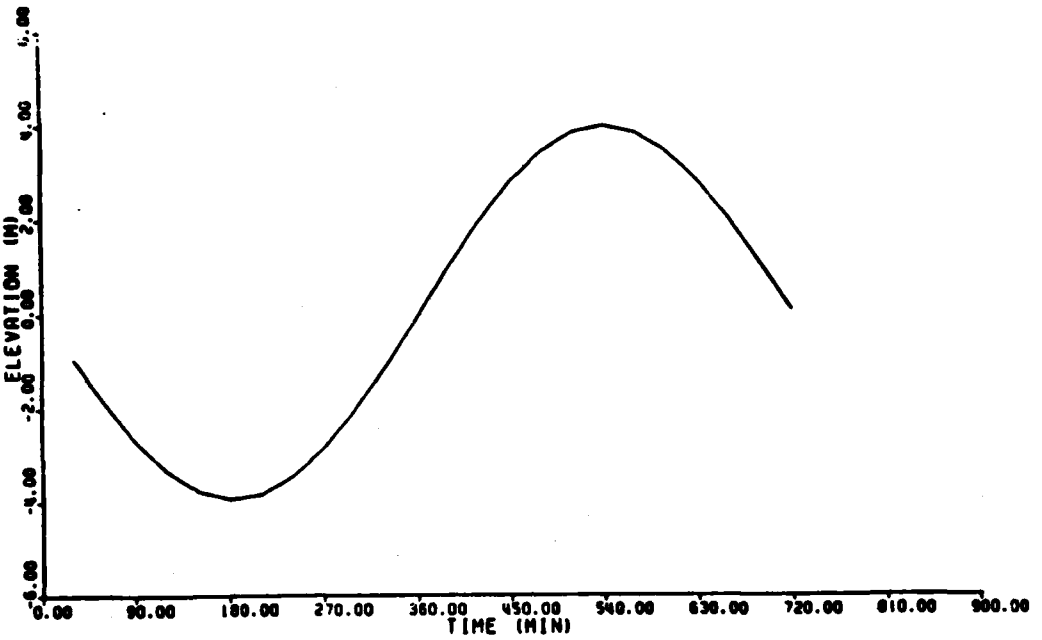

KACHEMAK BAY TIDAL ELEVATION HISTOGRAM

NODAL NUMBER 68 CASE NUMBER 24

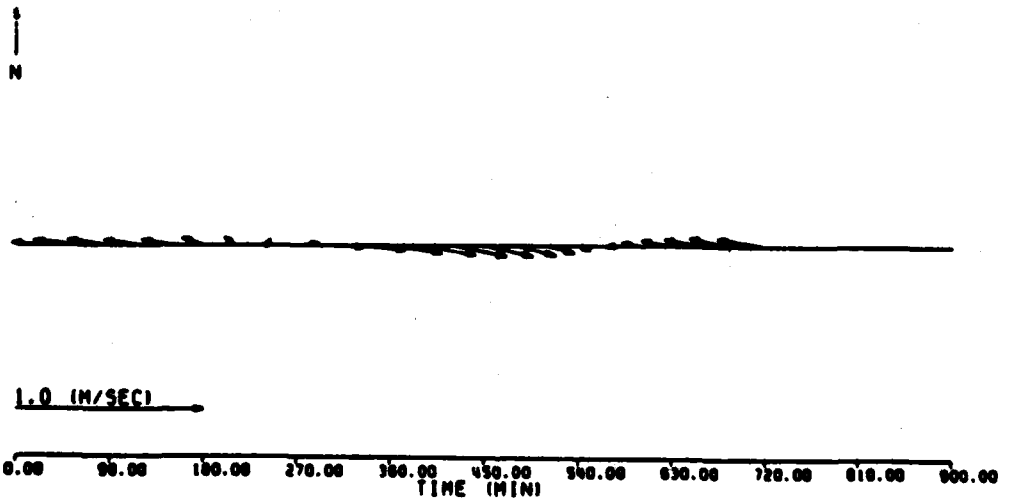

KACHEMAK BAY VELOCITY VECTORS

NODAL NUMBER 68 CASE NUMBER 24

m. Node 68

Figure F14. (Sheet 13 of 18)

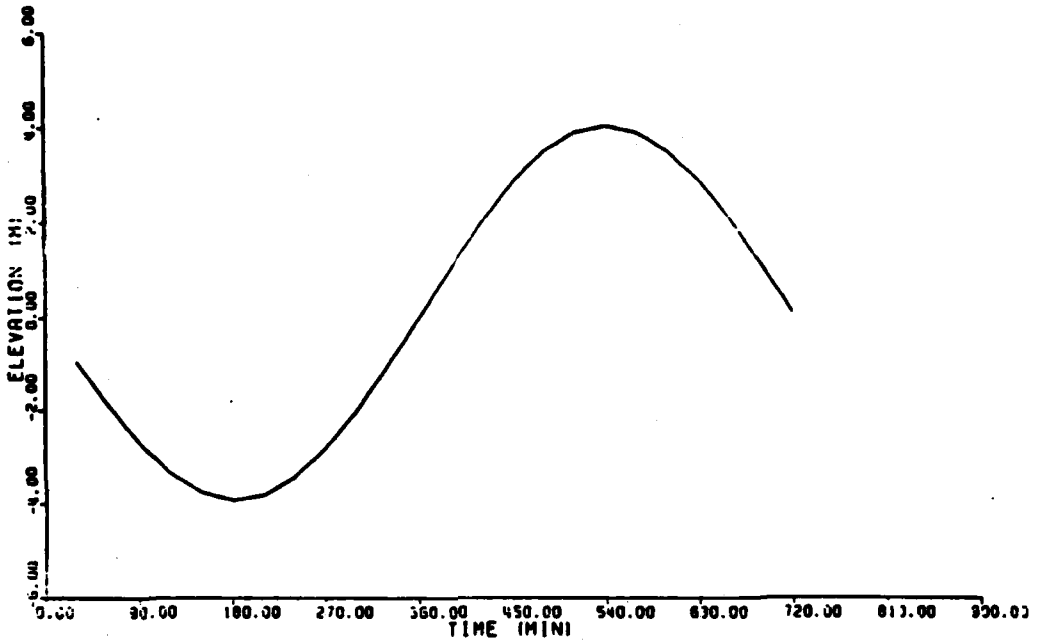

KACHEMAK BAY TIDAL ELEVATION HISTOGRAM

NODAL NUMBER 69 CASE NUMBER 24

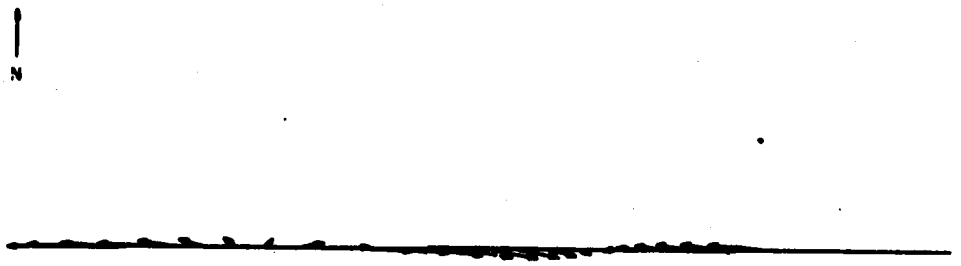

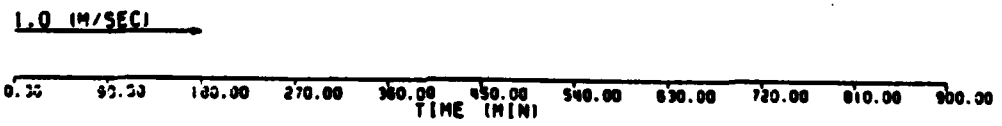

KACHEMAK BAY VELOCITY VECTORS

NODAL NUMBER 69 CASE NUMBER 24

n. Node 69

Figure F14. (Sheet 14 of 18)

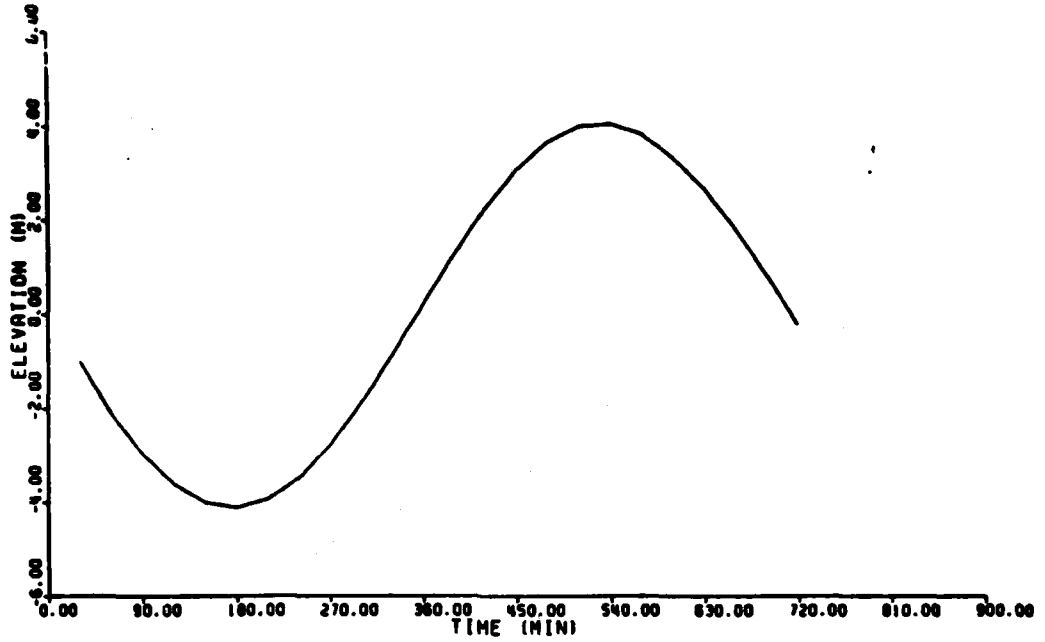

KACHEMAK BAY TIDAL ELEVATION HISTOGRAM

NODAL NUMBER 94 CASE NUMBER 24

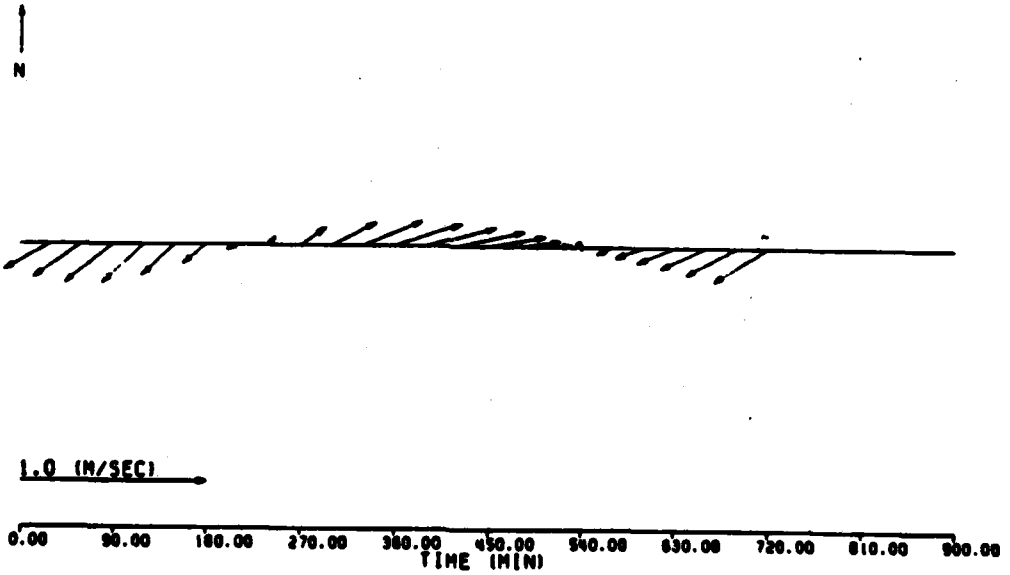

KACHEMAK BAY VELOCITY VECTORS

NODAL NUMBER 94 CASE NUMBER 24

o. Node 94

Figure 14. (Sheet 15 of 18)

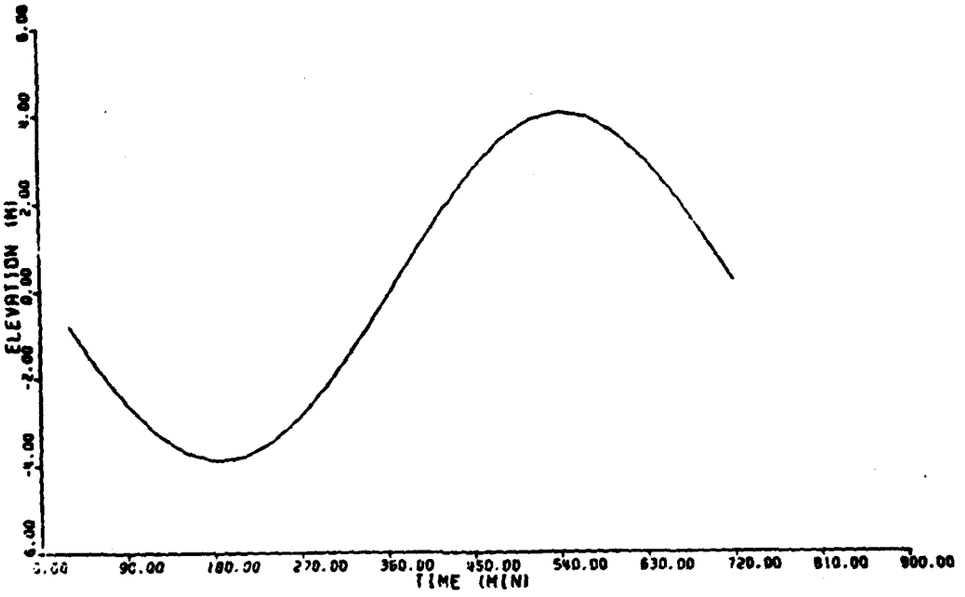

KACHEMAK BAY TIDAL ELEVATION HISTOGRAM

NODAL NUMBER 95 CASE NUMBER 24

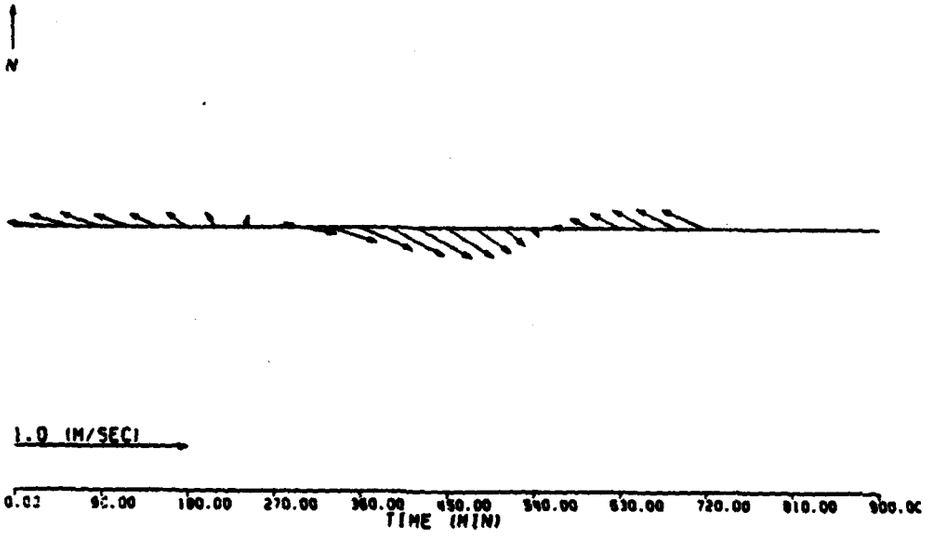

KACHEMAK BAY VELOCITY VECTORS

NODAL NUMBER 95 CASE NUMBER 24

p. Node 95

Figure F14. (Sheet 16 of 18)

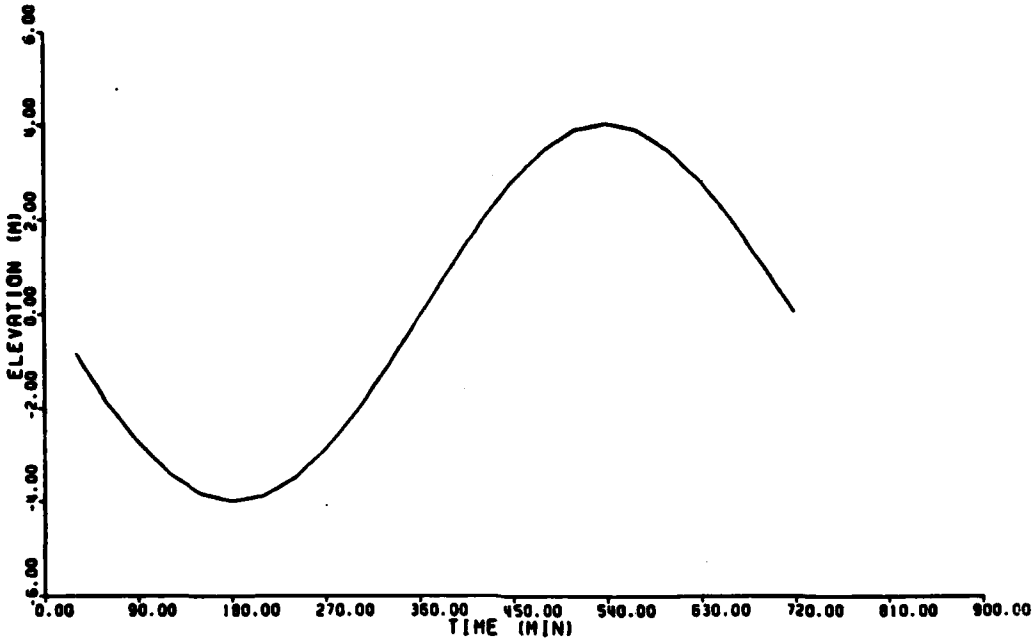

KACHEMAK BAY TIDAL ELEVATION HISTOGRAM

NODAL NUMBER 174 CASE NUMBER 24

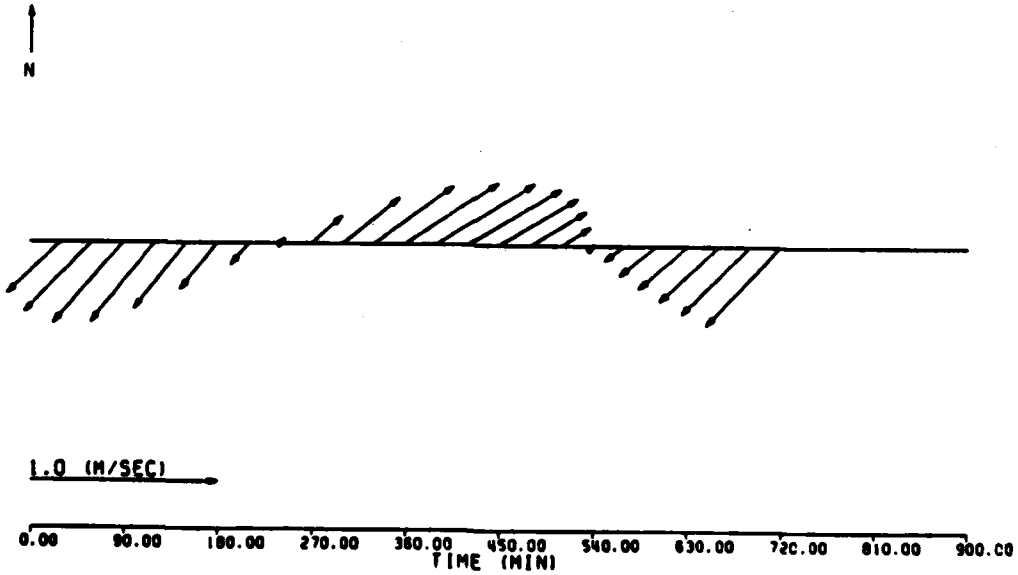

KACHEMAK BAY VELOCITY VECTORS

NODAL NUMBER 174 CASE NUMBER 24

q. Node 174

Figure F14. (Sheet 17 of 18)

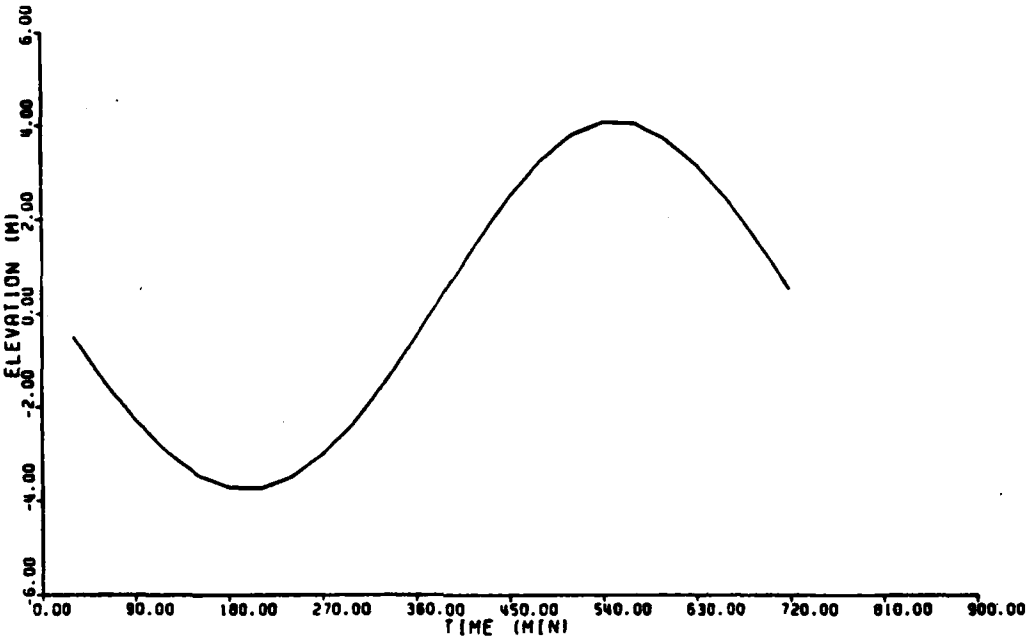

KACHEMAK BAY TIDAL ELEVATION HISTOGRAM

NODAL NUMBER 175 CASE NUMBER 24

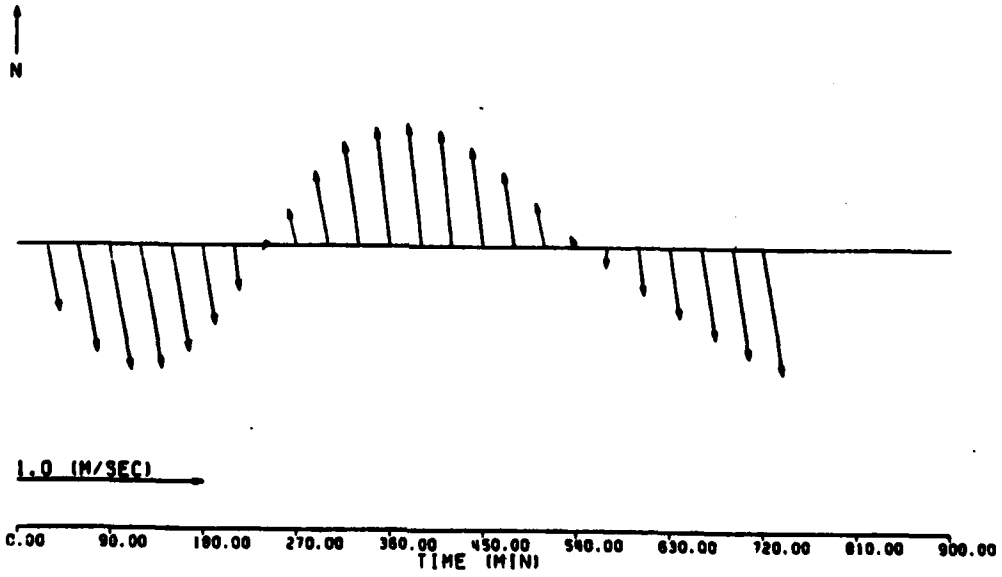

KACHEMAK BAY VELOCITY VECTORS

NODAL NUMBER 175 CASE NUMBER 24

r. Node 175

Figure F14. (Sheet 18 of 18)

water elevations and currents were examined and are of little difference from the case of the high tidal range, 7.9 m, except their magnitudes are reduced. The reductions are almost proportional to their tidal ranges at Seldovia. Therefore, the results of these two lower tidal ranges are not presented in this report.

Summary

23. The simulation of tidal currents in Kachemak Bay does not show the eddy formation off the southwest coast of the Spit during the period of ebb tides. It is quite possible that flow separation expected to occur at the tip of the Spit is small scale and cannot be simulated by the model. However, the model results indicate that longshore currents are strong, particularly during the spring tides. The maximum currents of either phase of tide exceed the threshold speeds of most sediments of the area. The model also shows that longshore currents during the flood tides are stronger than those of the ebb tides along the southwest shoreline of the Spit. This inequality in tidal currents could result in a net littoral transport toward the tip of the Spit. The maximum current speed is found to be reduced proportionally at the reduced tidal range.

END

FEB.

1988

DTIC